Investigating the Stress-Disease Connection:

Insights from Chronic Glucocorticoid Stimulation in Human Primary Fibroblasts

Maria Natalia Bobba Alves

Submitted in partial fulfillment of the
requirements for the degree of
Doctor of Philosophy
under the Executive Committee
of the Graduate School of Arts and Sciences

COLUMBIA UNIVERSITY

2024

Abstract

Investigating the stress-disease connection:

Insights from Chronic Glucocorticoid Stimulation in Human Primary Fibroblasts

Maria Natalia Bobba Alves

While the stress response represents an example of *allostasis* that enables the organism to cope with environmental and psychosocial challenges, its chronic activation imposes an *allostatic load* that contributes to the cumulative wear and tear of the system and induces negative mental and physical health outcomes. Nonetheless, the underlying basis of the stress-disease connection is still poorly understood and represents a gap in the knowledge that requires further research. We investigated the effects of chronic glucocorticoid stimulation in three independent human primary fibroblast lines, as an *in vitro* model of chronic psychosocial stress. By deploying a longitudinal, high-frequency, repeated-measures strategy across their entire lifespan, we were able to determine that chronically stressed cells present a significant increase in their total energy expenditure and that this stress-induced hypermetabolism is linked to an acceleration of their biological aging. Expanding from our results and placing emphasis on the energetic costs associated with the activation of the stress response, we proposed the "Energetic Model of Allostatic Load". This model proposes that chronic stress causes a redirection of the energetic resources towards allostatic responses and away from growth, maintenance, and repair processes, which in turn leads to the accumulation of damage that will further contribute to the development of disease and increased risk of mortality. Finally, we highlighted new avenues to quantify allostatic load and its link to health via the integration of systemic and cellular energy expenditure measurements together with classic biomarkers, that could contribute to further advances in the stress field.

Table of Contents

List of Tables and Figures

Chapter 2

Chapter 3

Acknowledgments

First, I would like to thank Dr. Martin Picard, for giving me the opportunity to join his lab in so extraordinary circumstances, such as running away from a mice allergy in the third year of a Ph.D. and the midst of a pandemic. For his constant support and encouragement to carry on with my work. For his time and effort to make sure it led to the best possible outcomes. For listening to my ideas and my questions. For his mentorship and his advice, and for agreeing to disagree. For making my graduation possible and enabling my pursuit of a scientific career.

I would also like to thank the Picard Lab members. A special thanks to Gabriel Sturm, for his amazing work that was the steppingstone of my Ph.D. To Anna Monzel, for the scientific discussions and reflections on data analysis and results. To Alex Sercel, for the constant brainstorming and bouncing of ideas and projects. To Mangesh Kurade, for making sure everything is in place and for dealing graciously with my last-minute orders. To Jeremy Michelson for standing side by side with me on the NMB PhD journey. To Janell Smith for being an incredibly supporting desk mate during this last stage of my Ph.D. To everyone with whom I had the pleasure to work with. You make the lab an amazing place to be in.

I would also like to thank Dr. Lori Zeltser, who officiated as my mentor during the first years of my Ph.D. and showed nothing but support during my departure from her lab. A truly special thanks to the people who made the Zeltser lab a great place, Olaya Fernández Gayol, Ángela Ramos Lobos, Danielle Neri, and Isabella Canal Delgado.

A sincere thanks to everyone in the Institute of Human Nutrition, including Debra Wolgemuth, Richard Deckelbaum, Sabrina Diano, Tony Ferrante, Zachary Corter, Sara Sternglass, Leslie de Pena, and Alex Sosa. And a special thanks to Estela Area Gomez, for her unconditional off-the-record support.

On a personal note, I would like to thank my Ph.D. fellows and closest friends Andrew Vandenberg, Marriah Green, Caroline Connors, Madeline Edwards, and Xinran Ma, as well as Maria Entonado Seco, Gabriel Seeman, and CJ Badenhausen. For the going-outs and staying-ins, for making this a great chapter of my life filled with cherished memories.

To *Los Marginales*, who are always close even from a distance. And to my family, which has always supported me wherever I am, whatever I'm doing. For the video calls and the visits to New York. And a special thanks to my mother, for flying over every time I needed her, for taking care of me - and of Ruffini. To Ruffini, for the unconditional love.

Chapter 1: Introduction

Alongside the mid-19th century, Claud Bernard postulated that maintaining the stability of the internal environment (or *"milieu intérieur"*) was a critical requirement for a living system to survive (*1*). In the early 20th century, Walter Cannon introduced the concept of *"homeostasis"* and proposed that the internal stability was achieved by keeping certain biological parameters at specific set-points within a narrow range, through the action of compensatory mechanisms (*2*). Fifty years later, Sterling and Eyer introduced the concept of *"allostasis"* and proposed that the internal stability was also achieved by allowing certain biological parameters to vary according to behavioral and environmental demands, through the action of anticipatory mechanisms (*3*). Building from this, McEwen and Stellar introduced the concept of *"allostatic load"*, arguing that the repeated activation of these anticipatory mechanisms imposed a strain on the system that led to its progressive wear and tear (*4*). McEwen also introduced the concept of *"allostatic states"* to refer to situations where the anticipatory mechanisms are either i) repeatedly activated, due to the repeated occurrence of the demand or due to the failure to habituate to it, ii) prolongedly activated, due to the failure to shut down the response, or iii) inadequately activated, due to the failure to initiating the response, and that these states constitute the bases of allostatic load (*5, 6*). Further extending the model, McEwen proposed that when sustained over time, allostatic load triggers recalibrations that cause progressive dysregulation among the organ systems and an increased risk for disease development and mortality, a state that he termed *"allostatic overload"* (*7, 8*).

A practical example to expose these phenomena is the regulation of human blood pressure. Human blood pressure normally hovers around 110/70 mmHg. However, if it suddenly increases, there is a rapid compensatory decrease in the heart rate, dilation of blood vessels, and excretion of salt and water by the kidneys that, by reducing the cardiac output, enlarging the vascular reservoir,

and decreasing blood volume, collectively contribute to restoring it to its normal mean value (*9*). This maintenance of a biological parameter at a specific set point represents the phenomenon of *homeostasis*. Nonetheless, if we look at a continuous record of blood pressure over 24 hours, we can identify different periods of the day that differ in their mean value. For example, blood pressure can remain below the mean at 90/60 mmHg throughout several hours while sleeping, rise above the mean to 130/80 mmHg in the first couple of hours after waking up, and then rise even more to 150/80 mmHg while doing exercise or going through a stressful situation (*10*). This maintenance of a biological parameter at different set points while under different behavioral and environmental demands represents the phenomenon of *allostasis*. Now, when an individual is under chronic stress, the persistent activation of the stress response induces a sustained elevation of blood pressure, and the newly established mean value corresponds to a hypertensive one (*11*). This maintenance of a biological parameter in a new set-point due to the repeated activation of an anticipatory response represents an *"allostatic state"* that imposes an *"allostatic load"* on the organism. Indeed, the newly established hypertension induces recalibrations in the heart and blood vessels that increase the risk of cardiovascular disease, stroke, and death (*12*), and therefore represents a state of *"allostatic overload"*.

The activation of the stress response is an example of allostasis, and its chronic activation imposes an allostatic load that can lead to allostatic overload. In the following pages, we will review the physiology of the stress response and the evidence that links its chronic activation to increased risk of morbidity and mortality. We will then go over the effects of stress on energetic demands and mitochondrial function, and how these can lead to an increase in damage that will result in accelerated aging and thus contribute to the development of disease. Finally, we will discuss the relevance of glucocorticoids in chronic stress and describe their mechanisms of action.

1.1. Stressors and the Stress Response

The study of stress started with Walter Cannon and his quest to define the mechanisms that maintained homeostasis. Cannon recognized that a wide variety of perturbations such as exposure to cold, pain, hypotension, hypoglycemia, and even emotional distress, all would induce the activation of the sympathetic nervous system and the adrenal gland medulla, which in turn initiated compensatory responses that enhanced the likelihood of survival, a phenomenon that he termed the *"fight or flight"* response (*2, 13, 14*). Nonetheless, it was Hans Selye who first introduced the word *"stress"* to define *"the nonspecific **response** of the body to any demand"* (*15*), trying to underscore that, regardless of the nature of the perturbation (i.e. what we now call *"stressor"*), the organism would always elicit the same response. He termed this response the *"General Adaptation Syndrome"* and proposed that it consisted of an initial *"stage of alarm"*, analogous to Cannon's *"fight or flight"* response, followed by a *"stage of adaptation"*, where the activation of the pituitary gland and the adrenal gland cortex would, in turn, elicit various mechanisms to reestablish homeostasis. Notably, he also pointed out that if the stressor persisted, the organism would enter a final *"stage of exhaustion"*, in which symptoms of dysfunction and disease would manifest (*15-17*). Our current understanding of *"stress"* is of a multidimensional process delineated by a stressor and a cognitive and affective appraisal of it, which elicits the actual stress response. This in turn involves neurological, neuroendocrine, and endocrine processes that lead to recalibrations on virtually all organ systems in the body and influence the future responses to the same or other stressors. Finally, it is also understood that its chronic activation has a negative impact on both mental and physical health that increases the risk of morbidity and mortality.

Stressors

Stressors can be categorized as biogenic and psychosocial (*18*). Biogenic stressors are those that induce the activation of the stress response without a cognitive appraisal and affective integration, and instead directly initiate neurological processes that trigger the rest of the stress response cascade. Among these stimuli are physical factors such as extreme cold, extreme heat, and pain, as well as various substances including caffeine, nicotine, and amphetamines, among others. Psychosocial stressors, on the other hand, are either real, imagined, anticipated, or recalled environmental events that are *interpreted as a threat* to the physiological and/or psychological integrity of the individual (*19, 20*). Among these stressors are adverse childhood experiences (such as psychological and physical abuse or the death of a parent), low socioeconomic status (living in a socioeconomically disadvantaged neighborhood or holding a low occupational position), major life events (divorce, job loss or the death of loved ones), catastrophic events (war, terrorist attacks or natural disasters) and chronic adversity (daily hassles, academic stress, work stress, caregiving stress, racial discrimination or social isolation) (*21*). The effect of each of these on the individual will directly depend on its cognitive appraisal and affective integration.

Cognitive appraisal and affective integration

Cognitive appraisal refers to the meaning we ascribe to the reality before us, and affective integration to the blending of felt emotions into the cognitive interpretation. These processes involve the action of the prefrontal cortex, hippocampus, and amygdala, among other limbic nuclei, and are strongly influenced by biological predispositions, personality patterns, life history, and available coping resources (*22*). Importantly, the resultant of these will determine whether an event is ultimately interpreted as a stressor or not, and therefore, whether the stress response is ultimately activated or not (*23*)

Stress response

Following the cognitive appraisal and affective integration processes, the interpretation of an event as a stressor results in neural impulses that activate the hypothalamic paraventricular nucleus (PVN) and various brainstem and limbic nuclei, which in turn leads to a psychological arousal characterized by enhanced alertness, vigilance, and focused attention (*24*). Additionally, it leads to the activation of the sympathetic adrenal medullary (SAM) and the hypothalamic-pituitary-adrenal (HPA) axes, which initiate the responses in the peripheric organs (*25, 26*).

The SAM axis begins with the activation of the preganglionic sympathetic neurons, which through cholinergic synapsis activate the postganglionic sympathetic neurons to release norepinephrine (NE) at their target organs. Additionally, a specific set of preganglionic neurons activate through cholinergic synapsis the chromaffin cells of the adrenal gland medulla, which in turn are activated to release epinephrine (E) and some NE into circulation. The cumulative action of the synaptic NE and the circulating NE and E leads to the activation of α-adrenergic and β-adrenergic receptors across the organ systems of the body, eliciting a response that manifests within seconds after the stressor is interpreted as such. This response involves major recalibrations in the cardiovascular system by increasing heart rate, cardiac output, and blood pressure (*27, 28*), and in the respiratory system by increasing breathing rate and bronchiolar dilation (*29*). It also exerts strong effects in metabolic tissues such as the liver, where it induces gluconeogenesis, and in adipose tissue, where it induces lipolysis, resulting in a steep increase in circulating levels of both glucose and fatty acids (*30*). Finally, there is a significant blood flow redistribution, with an increase towards the brain, cardiac muscle, and skeletal muscle and a concurrent decrease towards the kidneys, digestive system, gonads, and skin (*31*).

On the other hand, the HPA axis begins with projections of the PVN releasing corticotrophin-releasing hormone (CRH) and arginine vasopressin (AVP). CRH and AVP travel through the hypothalamo-hypophyseal portal vessels to the anterior pituitary, where they stimulate the release of adrenocorticotropic hormone (ACTH) into circulation. ACTH then activates the adrenal gland cortex to produce and release glucocorticoids (GC) into circulation (cortisol in humans, corticosterone in rodents), which peak 15-20 minutes after the stressor is interpreted as such. GC diffuses through the cell membranes and binds to cytosolic mineralocorticoid receptors (MR) and glucocorticoid receptors (GR) in the brain, and GR in the peripheric organs. In both cases, their activation induces changes in DNA transcription as well as other more rapid nongenomic effects (*26*). In the brain, GC negatively feedback on hypothalamic CRH and pituitary ACTH secretion, leading to a GR-mediated self-regulation, and it activates other brain regions that will promote food-seeking behavior (*32*). In the periphery, GC has effects on metabolic organs that add up to the ones exerted by the SAM axis (*33*). Specifically, they stimulate glycogenolysis and gluconeogenesis in the liver, inhibit the translocation to the membrane of the glucose transporter GLUT4 in both muscles and adipose tissues, and decrease insulin secretion by the pancreas, collectively contributing to an increase in the blood glucose levels (*34*). They also induce lipolysis in the adipose tissue, then contributing to the increase in circulating fatty acids (*35*).

While the stress response represents an adaptive process that enables the organism to rise to environmental challenges, its chronic activation can contribute to the cumulative wear and tear of the system and has a negative impact on both mental and physical health that increases the risk of morbidity and mortality. Not too long after being recognized for the first time as a public health concern, about 40 years ago (*36*), a vast number of studies have shown the role of chronic stress in the causation and/or exacerbation of diseases in most organ systems of the body (*37*, *38*).

1.2. Stress and disease

Consistently with the central role of brain regions such as the prefrontal cortex, hippocampus, amygdala, and hypothalamus, chronic stress is known to promote neurotoxicity and alter the function of these regions (*39-42*). This, in turn, induces detrimental effects on cognition, learning, and memory (*43, 44*), and can result in psychological disorders like generalized anxiety disorder, posttraumatic disorder, major depression disorder, bipolar disorder, and phobias (*45-47*).

In line with the actions of stress hormones in muscle, liver, and adipose tissue, chronic stress has significant effects on the organism metabolism (*48*) and has been associated with insulin resistance (*49*), higher blood glucose (*50*), and dyslipidemia (*51*). The clearest evidence of this phenomenon comes from a longitudinal study involving 3000 healthy participants aged 6-18 years and followed up for over 30 years, measuring life stress based on their socioeconomic status and performing biomedical examinations. While at baseline the entire cohort did not differ in their metabolic parameters, by early adulthood the individuals chronically exposed to high stress (in the form of socioeconomic disadvantage) showed decreased insulin sensitivity with a compensatory increase in insulin secretion, accompanied by hyperglycemia and hyperlipidemia. Furthermore, by age 33-48 years, these individuals were more likely to have obesity, type 2 diabetes, hepatic steatosis, and hypertension (*52*). Indeed, there are numerous studies linking chronic stress to abdominal obesity (*53-55*), type 2 diabetes (*56, 57*), hepatic steatosis (*58, 59*), and hypertension (*11*). Indeed, the above-mentioned metabolic dysregulation, along with the direct effects that the stress hormones have on the cardiovascular system, are consistent with chronic stress contributing to altered cardiac regulation, heart wall motion abnormalities, myocardial ischemia, myocardial infarction, and sudden death (*60, 61*).

Similarly, it is thought that both the metabolic changes and the direct effects of the stress hormones on the immune system are behind the compromising of its function. Chronic stress has been shown to suppress or dysregulate both innate and adaptive immune response by altering cytokine balance and generating low-grade chronic inflammation, as well as to suppress the number, traffic, and function of immunoprotective cells (*62, 63*). This in turn results in a decreased immunity for common viruses (*64, 65*), while inducing an increased immunity towards innocuous agents and then promoting allergic processes like asthma, eczema, and urticaria (*66-68*). In addition, chronic stress has also been implicated in the development and worsened progression of a variety of autoimmune diseases, including psoriasis, alopecia areata, rheumatoid arthritis, inflammatory bowel disease (*69-73*), and even malignancies (*74*).

Finally, both the behavioral and physiological consequences of chronic stress can also induce the development of unhealthy habits (*75*) such as disturbed sleep (*76, 77*), poor diet (*78, 79*), lack of exercise (*80, 81*), and substance abuse (*55, 82, 83*), which adds up to poorer health. Indeed, human studies have shown that perceived stress (*84, 85*) and a wide variety of stressors including adverse childhood experiences (*86*), bereavement (*87*), social isolation (*88*), low socioeconomic status (*89*), financial hardship (*90*) and work-related stress (*91, 92*) are associated with increased risks for morbidity and premature mortality.

The deleterious effects of stress on human health not only negatively affect the well-being of the population, but through increasing health care utilization and diminished work productivity, it also increases the economic costs to the society. Nonetheless, the underlying basis of the stress-disease connection is still poorly understood and represents a gap in the knowledge that requires further investigation. Notably, the literature points to a central role of the stress-induced metabolic recalibrations and the consequent effects on cellular energetic production and utilization.

1.2. Stress and hypermetabolism

The major metabolic recalibrations observed under the activation of both SAM and HPA axes serve to i) maintain effective blood supply to the organ systems in the body, primarily to the brain, cardiac, and skeletal muscle, ii) maintain continuous availability of the circulating oxygen and nutrient substrates, and iii) optimize their utilization by vital tissues at the expense of others (*93*). These recalibrations are critical because the mental and/or behavioral actions required to overcome the stressor impose a significant increase in the total body energy expenditure.

The evidence of stress leading to an increase in the total body energy expenditure, a.k.a. hypermetabolism, dates back to almost a century ago (*94, 95*). This has been shown in both human and animal models, most of the time relying on the technique known as indirect calorimetry, where oxygen consumption (ideally in parallel with carbon dioxide production) is measured from the expired breath (*96*). For obvious ethical reasons, experimental studies in humans can only study the effects of mild acute stressors, and they have mostly relied on some sort of acute cognitive challenge such as solving Raven matrixes, Stroop's color-world conflict tests, or mental arithmetic. For instance, solving Raven's matrixes, which involves a combination of detailed observation and abstract reasoning, induced up to a ~9% increase in energy expenditure (*97*), while performing mental arithmetic under time pressure induces an increase of ~13% (*97*) and by ~28% (*98*). Interestingly, performing mental arithmetic with rising time pressure and involving elements of competition (an observer taking scores, a leader board, a performance incentive), and elements of punishment (losing points, brief loud aversive sound when failing), induces an increase in energy expenditure of ~37-42% (*99, 100*), suggesting that more intense stressors can lead to higher increases in energy expenditure.

The cognitive challenges in the mentioned studies lasted for 8-15 minutes; nonetheless, studies, where these same tasks were performed for about twice as long, reported an increase of ~40-70% in energy expenditure (*101-103*), suggesting that the prolonged stressors can lead to even further increases in energy expenditure. In line with this, an observational study involving individuals with anxiety, a trait that is strongly associated with perceived stress (*104*), reported that individuals with high anxiety presented ~14% higher energy expenditure than those with low anxiety (*105*). Consistently, individuals who regularly engage in relaxation practices that dampen arousal of the stress response like yoga, showed ~15% lower basal energy expenditure (*106*). Overall, these results suggest that the chronic activation of the stress response might indeed be associated with an increase in total basal energy expenditure. Aligned with this, basal circulating levels of both catecholamines (*107*) and cortisol (*108*, *109*) are positively associated with energy expenditure, and the experimental administration of both catecholamines (*110*) and cortisol (*111*) induces an increase in energy expenditure as well. Interestingly, the administration of synthetic corticosteroid prednisolone showed to increase energy expenditure during cold exposure (2h at 16–17 ºC), but do not exert any changes in warm conditions (2h at 23–24 ºC), suggesting that the effects of GC may be regulated by other physiological parameters as well (*112*).

The available studies in animals have reproduced what has been observed in humans. For instance, acute stress induced by 3 hours of restraint led to an increase in energy expenditure of ~20-25% in rats (*113*), while chronic unpredictable stress for three weeks induced an increase of ~12% (*114*). Studies in birds have reported similar results. Specifically, acute stress induced by 15 minutes of noise exposure led to an increased energy expenditure of ~15% (*115*). In this same study, the levels of corticosterone were positively associated with energy expenditure.

Consistently, other studies have shown that the dominant status in birds, associated with increased stress hormone levels, also shows a positive association with energy expenditure (*116-118*).

Whether the stress-induced elevations in energy expenditure arise from mental activity or peripheral physiological processes is not clear, and whether they have a toll on the body has not been explored. This is a particularly relevant question since hypermetabolism presents a strong association with both negative health outcomes and higher mortality risk. Studies have shown that among healthy individuals, those with hypermetabolism exhibit up to a 50% increased mortality rate over 20-40-year follow-up periods (*119, 120*), and among older individuals, hypermetabolism is associated with poorer health (*121*). Furthermore, among individuals with various illnesses (hepatitis B, amyotrophic lateral sclerosis, type 2 diabetes, cancers, and mitochondrial disease), hypermetabolism predicts a worse prognosis and mortality (*122-126*).

In Chapter 2, we show that chronic stress modeled as continuous GC stimulation in human primary fibroblasts induces cellular hypermetabolism and that this is accompanied by cellular damage (*127*). The detrimental nature of hypermetabolism is still poorly understood and represents another relevant question to be investigated. In Chapter 3, we propose that it may relate to general constraints on total energy flux that impose limits on molecular operations and lead to intracellular tradeoffs between competing energy-consuming processes. Specifically, we propose that in line with the whole-body optimization of energy utilization, there is a reduction of the energetic resources devoted to processes such as maintenance and repair, which then manifests as an increase in damage accumulation (*128*). Consistent with this notion there is data from human observational studies showing that high home-related stress and high work-related stress are associated with a lower antioxidant capacity in peripheral blood (*129*). In line with this, experimental studies in rodents have shown that chronic stress induced by sleep deprivation (*130, 131*) and social isolation

(*132*) induce a decrease in the activity of several antioxidant enzymes such as superoxide dismutase (SOD), catalase (CAT) and glutathione peroxidase (GPx) in the brain. In addition, other experimental studies in rodents have shown that chronic stress in the form of cage rotation (*133*) or repeated restraint (*134*) induces a decrease in DNA damage repair on the spleen and leukocytes, respectively. Similar results have been observed in *in vitro* studies, with NE and cortisol exposure inducing a decrease in DNA damage repair capacity in different cell lines (*135, 136*). Related to DNA damage repair is telomerase activity, critical for maintaining telomere length. Correspondingly, human observational studies have shown that chronic caregiving stress is associated with a decreased telomerase activity in leukocytes (*137*), and these same results were observed in *in vitro* studies with lymphocytes under cortisol exposure (*138*).

Whether stress-induced hypermetabolism induces intracellular energetic tradeoffs that may result in damage accumulation remains unclear and further work is required to test such hypothesis (*128, 139*). Notably, stress-induced hypermetabolism could also exert its deleterious effects through the increased demands on the cellular components responsible for energy production.

1.3. Mitochondria and ATP production

The energy required for carrying out most processes within the body, from complex cognitive and behavioral actions, all the way down to hormones and factors secretion, tissue remodeling, intracellular signaling, protein translation, and gene transcription, is provided by adenosine triphosphate (ATP). Thus, the ATP production capacity has a crucial role in the ability to cope with the sustained energetic demands induced by chronic stress.

In the cell, the two main pathways of ATP production are cytosolic glycolysis and mitochondrial oxidative phosphorylation (OxPhos). Glycolysis is a fast but fairly inefficient pathway for ATP production, rendering only 2 molecules of ATP per molecule of glucose.

Glycolysis-derived pyruvate enters the mitochondria via a voltage-dependent anion channel (VDAC) and the mitochondrial pyruvate carrier (MPC). Once in the mitochondrial matrix, pyruvate is converted by pyruvate dehydrogenase (PDH) into acetyl-coenzyme A (-CoA), which then is further metabolized in the tricarboxylic acid (TCA) and leads to the generation of the electrons carriers nicotinamide adenine dinucleotide (NADH) and flavin adenine dinucleotide ($FADH_2$). NADH and $FADH_2$ then transfer their electrons to the complex I (NADH: ubiquinone oxidoreductase) and complex II (succinate: ubiquinone oxidoreductase), respectively, of the electron transport chain (ETC) located in the inner mitochondrial membrane. From there the electrons are sequentially transferred to coenzyme Q (CoQ), then to complex III (ubiquinol: cytochrome c oxidoreductase), then to cytochrome c (Cyt-c), and then complex IV (cytochrome c oxidase), which finally transfers the electrons to molecular oxygen (O_2) reducing it to H_2O. In this process, complexes I, III, and IV pump protons (H^+) across the inner mitochondrial membrane towards the mitochondrial intermembrane space, creating an electrochemical gradient. This gradient is then utilized by Complex V (ATP synthase), which synthesizes ATP from adenosine diphosphate (ADP) and inorganic phosphate (Pi).

Overall, mitochondria produce approximately 36 molecules of ATP per molecule of glucose and are, therefore, almost 18 times more efficient than glycolysis. Additionally, since TCA can also be fueled by fatty acid metabolites and amino acids that are transported into the mitochondrial matrix, OxPhos is also more efficient when it comes to nutrient substrate utilization, and thus is the major source of ATP of most of the cells in the body. By harboring the major source of ATP production, mitochondria have a central role in the stress response and go through major recalibrations to cope with emerging energetic demands. These include increasing their number, by activating mitochondrial biogenesis, increasing their volume, by going through mitochondrial

fusion, and directly enhancing the ETC and OxPhos activity, by increasing mitochondrial cristae, upregulating the expression of OxPhos complex subunits, remodeling the ETC by the formation of supercomplexes, and also fine-tuning its ATP production coupling efficiency(*140, 141*). Nonetheless, the evidence suggests that while acute stress can lead to recalibrations that enhance mitochondrial activity, chronic stress can induce a maladaptive response that promotes mitochondrial dysfunction (*142-144*).

1.4. Stress and mitochondrial recalibrations

There is substantial evidence of the effects of stress on mitochondria, both from humans, but mostly from animal studies. Human observational studies have shown that individuals who suffered adverse childhood experiences present higher levels of mtDNA copy number (mtDNAcn), which can suggest an increased mitochondrial biogenesis and potentially an increase in mitochondrial content (*145, 146*). Nonetheless, one of these studies also showed that the increase in mtDNAcn was accompanied by a higher load of mtDNA mutations (i.e. mtDNA heteroplasmy) (*145*). This suggests that either there is a compensatory increase in mitochondrial biogenesis upon the accumulation of damaged mitochondria, or that the newly generated mitochondria might also be damaged themselves. Also related to mtDNA, it has been shown that suicidal attempers show significantly higher levels of cell-free mtDNA (cf-mtDNA) in peripheral blood (*147*). While the precedence and role of cf-mtDNA is still under study, evidence suggests that could be a signaling molecule and represent a marker of psychosocial stress (*148*).

Consistently with the notion of the presence of dysfunctional mitochondria, an observational study that evaluated mitochondrial health index (MHI), which is a proxy for mitochondrial OxPhos activity normalized by mitochondrial content, showed that individuals under caregiving stress have a significantly lower MHI in peripheral blood (*149*). In line with this,

two different studies showed that individuals with stress-related psychological disorders such as post-traumatic stress disorder (PTSD) present alterations in the transcription of genes associated with mitochondrial function (*150, 151*). Since these are all observational studies, their data cannot provide a causative link between stress and mitochondrial dysfunction; nonetheless, patients with long-term treatment with corticosteroids present mtDNA damage and a decreased activity of complex I (*152*), which suggests that such causality might indeed exist.

Experimental approaches in rodents also contribute to this notion. When it comes to mtDNA, there are disparate observations. One study showed that 40 days of unpredictable stress induced a *decrease* in mtDNAcn in the brain, which was accompanied by a decrease in mitochondrial content (*153*). This same study showed that 40 days of corticosterone administration led to the same effects (*153*), and consistently, another study showed that 12 days of corticosterone administration induced a decrease in mtDNAcn in muscle (*154*). On the other hand, other studies showed that 4 weeks of unpredictable chronic stress led to an *increase* in mtDNAcn in saliva, peripheral blood (*155*) and liver (*145*). Furthermore, chronic administration of both epinephrine (*156*) and dexamethasone (a synthetic glucocorticoid) (*157*) induced an increase in the expression of peroxisome proliferator-activated receptor-gamma coactivator 1-alpha (PCG-1α) in the liver, the main transcription coactivator involved in promoting mitochondrial biogenesis. These findings indicate a potential tissue-specific effect of the impact of chronic stress on mitochondrial biogenesis, but also a direct effect of both GC and catecholamine signaling on it.

In line with the results found in humans, one of the studies that found an increase in mtDNAcn also found an increase in mtDNA heteroplasmy (*145*), reinforcing the notion of a compensatory increase in mitochondrial biogenesis and the potential presence of damaged and dysfunctional mitochondria. Consistently, with this, another study showed that both acute (2 hours)

and repeated restraint (2 hours per day, for 2 or 10 days) led to an increase in mitochondrial content in the testis and that this was accompanied by mitochondrial swelling (*158*). Furthermore, another two studies also had found that acute stress induced by 1, 6, and 12 hours of noise exposure led to an increase in mitochondrial swelling in cardiomyocytes (*159, 160*).

Several studies have also evaluated different parameters of the ETC activity after both acute and chronic stress in different tissues. Most of them reported either a decrease or no changes in the activity of complex I-IV (*153, 161-167*), and only one reported an increase in the activity of complex I-III with no changes in the activity of complex IV (*168*). In line with a decrease in Complex I, III, and IV activities, all studies that evaluated mitochondrial membrane potential reported a significant decrease in it (*158, 169-171*). Consistently, of those studies that evaluated mitochondrial respiration, most reported a decrease (*155, 161, 170-172*) and only two reported no changes or an increase. The results on the activity of complex V were disparate, with a decrease, no change, and an increase being observed in three different studies (*160, 162, 173*). Finally, studies reported either no changes or a decrease in the coupling efficiency (*172, 173*). Relevant to changes in the ETC activity and coupling efficiency is the incomplete reduction of O_2 and the consequent production of reactive oxygen species (ROS), which represent both key mediators of intracellular signal transduction but also the major promoters of oxidative stress (*174, 175*).

1.5. Mitochondria and ROS production

Mitochondrial ETC complexes I, II, and III are the main intracellular sources of ROS production by transferring electrons directly to O_2 and generating superoxide ($O_2^{\bullet -}$) (*176-178*). Complex I is the major site of mitochondrial $O_2^{\bullet -}$ production, either under NAD^+-linked substrates that generate a high matrix NADH/ NAD^+ ratio, or under $FADH_2$-linked substrates that generate a high proton motive force and then drive the flow of electrons in reverse, a phenomenon known

as Reversal Electron Transfer (RET) (*179*). Complex II can generate $O_2^{\bullet-}$ under $FADH_2$-linked substrates but is usually not considered as an important contributor. This is partially because intracellular levels of succinate are usually low, and because the enzyme's structure does not allow O_2 to access the intrinsic FAD (*180*). Nonetheless, there are multiple studies showing that impaired electron transport in complex II leads to a substantial $O_2^{\bullet-}$ production (*181, 182*). Finally, complex III is also considered an important site of $O_2^{\bullet-}$ production (*183*).

Importantly, besides complex I and III, there are other dehydrogenases in the mitochondria that also contribute to the $O_2^{\bullet-}$ production. Among them are PDH, which converts glycolytic-derived pyruvate into Acetyl-CoA to its following entrance into the TCA cycle, and the TCA enzyme α-ketoglutarate dehydrogenase (α-KGDH), which converts α-ketoglutarate into succinyl CoA (*184*). Overall, the major sources of mitochondrial ROS production are associated with the production of ATP, and therefore changes in energetic demands are tightly associated with changes in ROS levels (*185*). Relevant to the stress response, other dehydrogenases that can contribute to ROS production are the monoamine oxidases such as MAO-A, responsible for the catabolism of catecholamines NE and E, and that generate H_2O_2 in the process (*185*).

The $O_2^{\bullet-}$ generated by complex I, complex II, PDH, and α-KGDH is released to the mitochondrial matrix and converted to H_2O_2 by the matrix-specific Mn-superoxide dismutase (SOD2), whereas the $O_2^{\bullet-}$ generated by complex III is released to the intermembrane space and converted to H_2O_2 by the intermembrane-space-specific Cu/Zn-superoxide dismutase (SOD1) (*186*). The generated H_2O_2 by the SODs and MAO-A can react with $O_2^{\bullet-}$ or with reduced transition metals and generate the hydroxyl radical ($OH^{\bullet}$), the most potent oxidizing agent among ROS. To avoid this, H_2O_2 is rapidly reduced to H_2O by the action of catalase (CAT), glutathione peroxidase (GPx), and thioredoxin peroxidase (TPx), at the expense of reduced glutathione (GSG) and

thioredoxin ($TrxS_2$) (*187*). While normally 0.4-4% of the oxygen consumed by mitochondria leads to ROS production (*177*), mitochondrial recalibrations involving changes in ETC activity can lead to an increase in ROS production and oxidative stress (*188*).

1.6. Stress and oxidative stress

There are only a couple of studies that have evaluated the effects of stress on ROS levels, and they show somehow disparate results. For instance, among the human studies, two of them showed that acute psychological stress involving observational and logical thinking induced a *decrease* in ROS levels in whole blood (*189, 190*). On the other hand, another study showed that acute stress induced by delivering a speech and performing mental math induced an *increase* in ROS levels in serum samples (*191*). The difference in these results could rely on the difference between whole blood and serum samples, which might be either due to physiological or purely technical reasons. Animal models also show some variation among their results, but more consistency. One study showed that both acute and repeated restraint cause an increase in ROS levels in gastrointestinal mucosa (*192*). On the other hand, acute restraint did not exert changes in ROS levels in the brain (*161*), while 40 days of chronic unpredictable stress did induce an increase in ROS levels in the brain (*153, 193*), suggesting a potential tissue-specific effect regarding the vulnerability upon the length of the exposure.

There have been other studies that evaluated the activity of antioxidant enzymes such as SOD, GPx, and CAT. As previously described, there is data from human observational studies showing that high home-related stress and high work-related stress are associated with a lower antioxidant capacity in peripheral blood (*129*), and from experimental studies in rodents showing that chronic stress induced by sleep deprivation (*130, 131*) and social isolation (*132*) induce a *decrease* in the activity of the antioxidant enzymes SOD, CAT and GPx in the brain. Nonetheless,

there are also studies showing that chronic sleep deprivation (*194*) and social isolation (*195*), as well as chronic unpredictable stress (*196*) and maternal deprivation (*197*), induce an *increase* in SOD, CAT, and GPx activity in the brain. It must be noted that the antioxidant activities are not a clear indicator of oxidative stress. For instance, a *decrease* in their activity could indeed lead to unbalanced ROS levels that result in oxidative damage. Nonetheless, an *increase* in their activity could also represent a compensatory response to an increase in ROS production or to a specific threshold of accumulated oxidative damage.

Most of the available data on oxidative stress is on its resulting oxidative damage. When ROS levels surpass the antioxidant capacity of the cell, oxidative stress is established, and oxidative damage occurs. ROS can induce nucleic acid oxidation and cause DNA breaks, mutations, and cross-linking with proteins. Due to its close contact with the source of production, mtDNA is particularly susceptible to oxidative damage (*198*), but nuclear DNA is also thoroughly affected and ROS are known to contribute to overall genomic instability (*199*). In addition, due to its rich content on guanine repeats, ROS are particularly damaging to telomeres and then can accelerate their shortening (*200*). Finally, by inducing DNA oxidation and histone oxidation, ROS can lead to epigenetic alterations that change methylation patterns, among others (*201*, *202*). ROS induces oxidation not only of histone proteins, but of virtually any protein in the cell, which in turn can result in either protein-protein cross-linkages and aggregation, or peptide fragmentation and proteolysis, contributing to the loss of proteostasis (*203*). Genome instability, telomere attrition, epigenetic alterations, and loss of proteostasis are considered to be the "*Primary Hallmarks of Aging*"; that is, the initiating triggers whose damaging effects underly the progressive decline in health as we age. Importantly, there is a vast amount of evidence linking stress to them.

1.7. Stress and Primary Aging Hallmarks

Genome instability

There is a vast literature that evidences the link between stress (*204*) or stress mediators (*205*) with genome instability, mostly in the form of 8-hydroxy-2-deoxyguanosine (8-OH-dG). Human observational studies have shown that basal levels of urinary cortisol are positively correlated with DNA damage (*206, 207*). In addition, chronic academic stress (*208*), work-related stress (*209*), caregiving stress (*210*), and bereavement (*211*) were positively correlated with DNA damage in peripheral blood. While these studies only provide correlational results, other human experimental studies showed that acute stress in the form of performing mental arithmetic (*212*) or defending themselves against a false accusation (*213*) induces an increase in DNA damage in peripheral blood, pointing to a causality role of stress in promoting DNA damage. Experimental studies in rodents have further contributed to this notion, also underscoring that a broad type of chronic stressors can induce DNA damage in a broad type of tissues. Specifically, studies have shown that chronic stressors including cage rotation, social isolation, noise, restraint, forced swimming, electric shock, and conditioned aversion lead to an increase in DNA damage in peripheral blood (*214, 215*), bone marrow (*134, 216*), spleen (*133*), gastrointestinal mucosa (*192*), kidney (*217*), liver (*218, 219*), breast (*136*), ear (*219*) and several brain regions such as amygdala, hippocampus, and prefrontal cortex (*219-221*). Furthermore, some studies have shown that the sole administration of a stress mediator such as isoproterenol (a NE mimetic) was enough to induce an increase in DNA damage both at the thymus and cerebellum (*222*). Consistent with this, *in vitro* studies have shown that isoproterenol, NE, E, and GC induced an increase in DNA damage in both primary (*135, 222, 223*) and immortalized normal cell lines (*222, 224, 225*), as well as tumoral cell lines (*136, 226, 227*).

Telomere attrition

Epel and collogues were the first to link psychosocial stress to telomere attrition, finding that maternal caregivers who reported higher perceived stress presented shorter telomere length and a lower telomerase activity in peripheral blood (*137*). Since then, numerous studies have linked a wide range of chronic stressors with an altered telomere biology (*228*). Human studies mostly use peripheral blood leukocytes, buccal cells, and saliva (which is composed predominantly of leukocytes) to estimate overall telomere length and have shown that perceived stress (*137, 229-231*) and severe life stress (*232-234*) are associated with shorter telomere length. Among the stressors evaluated, caregiving (*137, 235, 236*) and work-related stress (*237-239*) have been the most studied and consistently show an association with shorter telomere length. In recent years, four meta-analyses have further confirmed the association between chronic stress and shorter telomere length in humans (*230, 240-242*). In addition, experimental animal studies have contributed to exposing a causal role of stress in promoting telomere attrition. Specifically, experiments in rodents have shown that chronic crowding (*243*), infection (*244*), circadian disruption (*245*), and unpredictable stress (*155*) induce a decrease in telomere length. Finally, a comprehensive meta-analysis in non-human vertebrates showed that exposure to stressors is associated with shorter telomere length in numerous species including mammals, birds, reptiles, and fish (*246*).

Epigenetic alterations

There is also a vast body of literature showing the association of stress to altered epigenetic patterns such as histone acetylation, histone methylation, and DNA methylation (*247*). Observational human studies have shown that chronic stress in the form of low socioeconomic status is associated with more changes in both types of epigenetic modifications in peripheral blood

(*248-251*). While these studies only can show associations, there is one longitudinal study in which trauma exposure was associated with increased DNA methylation at multiple CpG loci, pointing out a causal role of stress over these changes (*252*). Studies in rodents have further confirmed this, showing that numerous chronic stressors including chronic unpredictable stress (*253-255*), social defeat (*256-258*), social isolation (*259*), restraint (*260, 261*), and conditional aversion learning (*262, 263*) induce changes in either histone acetylation, histone methylation, and DNA methylation. Interestingly, most of these studies have focused on brain regions like the hippocampus, amygdala, prefrontal cortex, and hypothalamus, central players in the activation of the stress response. There is strong evidence showing that stress and stress hormones induce epigenetic changes in genes associated with the stress response itself both in the brain (*264-266*) and the periphery (*264, 267, 268*) and that they can persist a long time and influence the response to future stressors (*269*). Relevant to aging biology are the DNA methylation-based epigenetic "clocks", built by multiple regression models from a set of DNA methylation markers that correlate with chronologic age and serve as molecular estimators of biological age in cells, tissues, and individuals (*270*). An increasing number of studies have evaluated the effects of chronic stress on epigenetic aging in humans (*271, 272*), and they have shown that lifelong trauma (*273, 274*), low socioeconomic status (*275-277*), racial discrimination (*278*), exposure to violence (*279*), and cumulative stress (*280*) are associated to increased epigenetic age or aging rate.

Loss of proteostasis

The link between stress and proteostasis is by far the least explored (*281, 282*). The data available in humans comes from studies of PTSD, major depressive disorder, bipolar disorder, and schizophrenia, which are not necessarily conditions of chronic stress but do maintain a strong association with it (*283-286*). Specifically, patients with PTSD (*287*) major depressive disorder

(*287, 288*), bipolar disorder (*289, 290*), and schizophrenia (*291*) show signs of endoplasmic reticulum (ER) stress, with altered expression of several components of the unfolded protein response (UPR) such as BiP, XB1, GRP78, GRP94, CHOP, ATF4, TCP1 and HSPA1A in peripheral blood (*287*), peripheral blood-derived lymphocytes (*289, 290*) and brain cortex (*291-293*), suggesting the occurrence of loss of proteostasis. Studies in rodents go in line with these findings, with chronic physical stress induced by prolonged exposure to cold (*294*) and chronic psychological stress induced by restraint (*295*) and social defeat (*296*) leading to increased levels of a set of the above-mentioned components in the adrenal gland, hippocampus, and amygdala. Furthermore, chronic corticosterone administration resulted in the upregulation of GRP78 and GRP94 in the hippocampus (*297*), underscoring the role of the chronic HPA axis activation in the potential loss of proteostasis.

1.8. The stress-aging-disease connection

Whether genome instability, telomere attrition, epigenetic alterations, and loss of proteostasis are produced due to an increase in ROS production (*298, 299*) or a decrease in the repair and maintenance process (*128*) is unclear, but the growing body of literature linking stress to them has prompted the hypothesis that the deleterious effects of chronic stress may occur due to an acceleration of biological aging (*299, 300*).

Biological aging is thought to originate from cumulative damage at the molecular level that disrupts normal cellular physiology, which in turn disrupts normal tissular and organ system physiology, resulting in the progressive decline in the individual's health (*301*). Specifically, it has been proposed that the *Primary Hallmarks* of aging lead to compensatory responses including i) an altered activity of the nutrient-sensing IGF-1 and insulin signaling (IIS), mTOR, AMPK, and sirtuin pathways to dampen metabolism and hence reduce cellular damage (*302*); ii) a decreased

efficiency on mitochondrial bioenergetics with the concomitant increase in ROS production that can act as survival signals (*303*); and iii) an increase in cellular senescence, that prevents the propagation of damaged cells and instead triggers their elimination by the immune system (*304*). These responses are aimed at mitigating the damage and thus are referred to as *"Antagonistic Hallmarks"* of aging. Nonetheless, when chronically activated they eventually become deleterious themselves. The exacerbated production of ROS leads to oxidative stress and further oxidative damage, exacerbating the primary hallmarks, and its release along the senescence-associated-secretory-phenotype (SASP) pro-inflammatory cytokines can act in an autocrine and paracrine way aggravating their own damage and inducing damage in their neighboring cells, which then become senescent too (*305, 306*). These altered intercellular communication and stem cell exhaustion are referred to as *"Integrative Hallmarks"* of aging, since they propagate across tissues and impair normal organ systems functioning, which ends up in the development of disease and an increased mortality risk of the organism (*301*).

It is important to note that aging is a self-perpetuating process and that once one of the hallmarks is established, it will conduce to further exacerbation of the rest of them. In the case of natural aging, this is thought to start with the unavoidable accumulation of molecular damage, normally accounted to the pure action of entropy and molecular imperfectness (*307*). Our hypothesis of hypermetabolism inducing energetic tradeoffs focuses the attention on the potential dampening of maintenance and repair processes that will increase damage accumulation, that is, inducing the primary hallmarks of aging, which then will trigger the antagonistic and integrative hallmarks, which further exacerbate the primary hallmarks, and keep the cycle going.

Nonetheless, we also recognize that the stress-induced hypermetabolism could exert recalibrations on the ETC that will lead to an increase in ROS and a concomitant increase in

oxidative damage. In this case, stress would induce an antagonistic hallmark that will then trigger the integrative hallmarks, which will exacerbate the primary hallmarks, and so on. Furthermore, the SAM and HPA-induced increases in circulating glucose and lipids levels could also lead to an altered nutrient sensing signaling, another of the antagonistic hallmarks, and follow that same path.

Finally, there is also the stress-induced dysregulation of the immune system, which can manifest in low-grade inflammation. Here, stress would be inducing an integrative hallmark that will exacerbate the primary hallmarks and start the cycle once more. Overall, it seems that the chronic activation of the stress response can exacerbate the aging process at any level, and it is not surprising its linked to the development or worsening of virtually any type of disease. Interestingly, dysregulation of the HPA axis and high levels of circulating CG is a characteristic of the aging process (*308-310*), suggesting a crucial role of GC signaling in feeding this vicious cycle.

1.9. Chronic stress and glucocorticoid signaling

It has been observed that under chronic stress conditions, there is an overall dysregulation of the HPA axis that results in an elevation of basal circulating glucocorticoid levels. Specifically, there is evidence of an altered AVP to CRH ratio production in the hypothalamic PVN, so that the hypothalamic activation of the pituitary gland changes from a predominantly CRH-dominant regulation to arginine AVP-dominant regulation (*311*). In addition, it has also been shown that chronic stress is associated with impaired glucocorticoid negative feedback on both CRH and ACTH (*312-314*). Chronic stress can also induce an increase in adrenal gland sensitivity to ACTH and a concomitant increase in cortisol synthesis (*315*), as well as a decrease in cortisol metabolism (*316*). Whereas there are cases in which chronic stress is associated with a blunted HPA response and lower cortisol levels, such as in PTSD patients (*317*), chronic stress is usually associated with high cortisol levels, individuals with high cortisol reactivity are more likely to exhibit adverse

health effects (*318-323*), and higher morning and nighttime cortisol was associated with mortality (*324*). Then, when investigating the link between stress and disease, understanding the molecular mechanisms of GC signaling results is particularly relevant.

Molecular mechanism of glucocorticoid signaling

Once secreted in the circulation, the majority of cortisol (75%) binds to transcortin and corticosteroid-binding globulin (CBG), but it is the unbound form the one that is responsible for the biological functions (*325*). The lipophilic nature of cortisol allows its diffusion through the cell membrane, and once inside the cell, it is the activity of the enzymes 11β-hydroxysteroid dehydrogenases HSD1 and HSD2 in the endoplasmic reticulum that regulates its intracellular concentration (*326*). The biological effects of cortisol are mediated by the nuclear receptors MR and GR. MR has a tenfold higher affinity for cortisol relative to GR, so while MR mediates most of the cortisol's effects when it is within basal levels, GR becomes engaged only when its levels are highest, at the zenith of the circadian cycle and in response to stressors (*327*). In the absence of ligand, GR remains in the cytoplasm as part of multiprotein complexes containing chaperones and immunophilins such as HSP90, HSP70, p59 immunophilin, FKBP52, and p23 phosphoprotein. Upon ligand binding, the receptor is hyperphosphorylated and changes conformation, which frees it from the inhibitory complex and allows its translocation into the nucleus (*328*). Once in the nucleus, the GR binds to DNA GC response elements (GRE) as a homodimer, and acts as a transcription factor, or as a monomer, and functions in composite with other transcription factors and co-regulators. Finally, it can also establish protein-protein interactions with other transcription factors and co-regulators and function as a coregulator itself (*329*). Importantly, there are also GRE in the mtDNA (*330*), and the action of GR in regulating mtDNA transcription has been confirmed in several cells and tissues (*331, 332*).

GR target genes can comprise up to 10-20% of the human genome, and while there is a strong representation of genes associated with cellular metabolism including nutrient sensing pathways and nucleic acid, carbohydrate, lipid, and protein metabolism, they are also those associated to major cellular process such as transcription regulation, vesicle transport, intracellular signaling, surface receptor-linked signal transduction, response to biotic stimuli, cell organization and biogenesis, cell proliferation, and programmed cell death (*333-335*) Nonetheless, the cellular response is extremely diverse, exhibiting great cellular and tissue specificity and sensitivity (*336*).

While the principal effects of glucocorticoids are mediated by transcriptional responses, that occur in minutes to hours, a growing body of evidence suggests that GR may also act via non-genomic mechanisms to elicit rapid cellular responses that occur within a few seconds to minutes (*337*). These actions seem to be elicited by membrane-bound GR (*338*) and involve a G-protein-coupled-receptor-like mechanism, where the ligand-binding-induced release of accessory proteins result in the cascade activation of various kinases, such as PI3K, AKT, and MAPKs (*339-343*) and the increase of second messengers, such as inositol-3-phosphate, cyclic adenosine monophosphate, and calcium ion (*344*). Importantly, GR non-genomic actions have been shown to influence several cellular functions including calcium influx, cytoskeleton dynamics, mitochondrial function, cell proliferation, cellular adhesion, and immune signaling (*339, 342, 343, 345-349*).

In the next chapter, we investigate the effects of chronic glucocorticoid stimulation in human primary fibroblasts. By deploying a longitudinal, high-frequency, repeated-measures strategy across their entire lifespan and measuring a broad spectrum of cellular features including cell volume and viability, cell division, cellular bioenergetics, DNA and cytokine secretion, as well as gene expression, gene methylation, and gene instability, we were aimed to establish an *in vitro* model of chronic psychosocial stress and define the cellular recalibrations in a multi-omic manner.

Chapter 2: Cellular Allostatic Load is Linked to Increased Energy Expenditure and Accelerated Biological Aging

This chapter is a reproduction of the paper *"Cellular Allostatic Load is Linked to Increased Energy Expenditure and Accelerated Biological Aging"* published in *Psychoneuroendocrinology* in June 2023. Here, we investigated the effects of chronic glucocorticoid stimulation in three independent human primary fibroblast lines, as an *in vitro* model of chronic psychosocial stress. By deploying a longitudinal, high-frequency, repeated-measures strategy across their entire lifespan, we were able to determine that chronically stressed cells present a significant increase in their total energy expenditure and that this stress-induced hypermetabolism is linked to an acceleration of their biological aging.

Cellular Allostatic Load is linked to Increased Energy Expenditure and Accelerated Biological Aging

Natalia Bobba-Alves[1], Gabriel Sturm[1,2], Jue Lin[2], Sarah A Ware[3], Kalpita R. Karan[1], Anna S. Monzel[1], Céline Bris[4,5], Vincent Procaccio[5], Guy Lenaers[4,5,6], Albert Higgins-Chen[7], Morgan Levine[7], Steve Horvath[7], Balaji S Santhanam[8], Brett A Kaufman[3], Michio Hirano[9], Elissa Epel[10], Martin Picard[1,9,11]

[1]Department of Psychiatry, Division of Behavioral Medicine, Columbia University Irving Medical Center, New York NY, United States

[2]Department of Biochemistry and Biophysics, University of California San Francisco, San Francisco CA, United States

[3]Department of Medicine, Vascular Medicine Institute and Center for Metabolic and Mitochondrial Medicine, University of Pittsburgh, Pittsburgh PA, United States

[4]Department of Genetics, Angers Hospital, Angers, France

[5]MitoLab, UMR CNRS 6015, INSERM U1083, Institut MitoVasc, Université d'Angers, Angers, France

[6]Department of Neurology, Angers Hospital, Angers, France

[7]Altos Lab, Los Altos CA, United States

[8]Departments of Biological Sciences, Systems Biology, and Biochemistry and Molecular Biophysics, Institute for Cancer Dynamics, Columbia University, New York NY, United States

[9]Department of Neurology, Merritt Center, Columbia Translational Neuroscience Initiative, Columbia University Irving Medical Center, New York NY, United States

[10]Department of Psychiatry and Behavioral Sciences, University of California San Francisco, San Francisco CA, United States

[11]New York State Psychiatric Institute, New York NY, United States

2.1. Abstract

Stress triggers anticipatory physiological responses that promote survival, a phenomenon termed allostasis. However, the chronic activation of energy-dependent allostatic responses results in allostatic load, a dysregulated state that predicts functional decline, accelerates aging and increases mortality in humans. The energetic cost and cellular basis for the damaging effects of allostatic load have not been defined. Here, by longitudinally profiling three unrelated primary human fibroblast lines across their lifespan, we find that chronic glucocorticoid exposure increases cellular energy expenditure by ~60%, along with a metabolic shift from glycolysis to mitochondrial oxidative phosphorylation (OxPhos). This state of stress-induced hypermetabolism is linked to mtDNA instability, non-linearly affects age-related cytokines secretion, and accelerates cellular aging based on DNA methylation clocks, telomere shortening rate, and reduced lifespan. Pharmacologically normalizing OxPhos activity while further increasing energy expenditure exacerbates the accelerated aging phenotype, pointing to total energy expenditure as a potential driver of aging dynamics. Together, our findings define bioenergetic and multi-omic recalibrations of stress adaptation, underscoring increased energy expenditure and accelerated cellular aging as interrelated features of cellular allostatic load.

2.2. Introduction

In response to environmental stressors, living organisms mount evolutionarily conserved responses that aim to increase resilience and promote survival, a phenomenon termed allostasis (*3, 350*). However, the chronic activation of these responses produces an allostatic load (*4, 351*). Allostatic load is a multisystem state that reflects the added load, or "cost", imposed by the activation of biological and physiological effects triggered by real or perceived stressors. Applied to humans, the allostatic load model predicts that when chronically sustained, allostatic load results in the maladaptive state of allostatic overload, which disrupts normal physiological functions and longevity (*8*). For example, while regular exercise improves glucose regulation and increases overall fitness (*352*), excessive exercise without appropriate recovery becomes damaging – disrupting glucose homeostasis and insulin secretion (*353*). Large-scale epidemiological studies also show that allostatic load, quantified by the abnormal levels of stress hormones, metabolites, and cardiovascular risk parameters, predicts physical and cognitive decline, as well as earlier mortality (*354-356*). These findings underscore the long-term, health-damaging effects arising from chronically activated stress pathways. However, the manifestations of allostatic load and overload at the cellular level, and whether they can accelerate cellular aging in a cell-autonomous manner, have not been fully defined.

Allostasis involves anticipatory processes that prepare the organism for potential threats – but it comes at a cost. Every cellular allostatic process – gene expression and protein synthesis, enzymatic reactions, hormone biosynthesis, and secretion, and many others – consumes energy in the form of ATP (*357*). In human cells, ATP is produced with moderate efficiency by glycolysis ($J_{ATP\text{-}Glyc}$) in the cytoplasm, and with highest efficiency by oxidative phosphorylation (OxPhos, $J_{ATP\text{-}OxPhos}$) within mitochondria. But building the molecular machinery for glycolysis and OxPhos

pathways also comes at a cost, which is substantially higher for OxPhos owing to the extensive proteome demands of mitochondrial biogenesis and maintenance (>1,000 proteins) relative to glycolysis (~10 proteins) (*358*). Thus, a precise balance of energy derived from both glycolytic and OxPhos pathways allows cells to maintain optimal energetic efficiency.

Beyond their role in energy transformation, mitochondria respond to stress mediators such as glucocorticoids(*142*) and also regulate multiple physiological processes that encompass allostasis (*359*). This dual role as energy producers that enable allostasis, and as targets of stress hormones, positions mitochondria as key mediators of cellular and whole-body stress responses (*141*). We previously outlined the theoretical functional and structural mitochondrial recalibrations, as well as the potential detrimental effects that may occur in response to chronic stress, known as mitochondrial allostatic load (MAL) (*360*). In brief, potential cellular recalibrations include changes in cell size, energy requirements sustained by differential reliance on energy production pathways, or in the number of mitochondrial DNA (mtDNA) copies required to sustain OxPhos activity, whereas mitochondrial recalibrations would include features such as the accumulation of mtDNA damage (mutations, deletions) and changes in gene expression for the OxPhos machinery (*360*). However, these hypothesized cellular recalibrations, in particular the total energetic cost of allostatic load and the potential downstream maladaptive consequences of allostatic overload, have not been defined in a human system.

A major evolutionary-conserved stress mediator in mammals is the hormone family of glucocorticoids (GC; cortisol in humans, corticosterone in rodents). GC signaling acts via the glucocorticoid receptor influencing the expression of both nuclear (*361*) and mitochondrial genomes (*331*). Physiologically, GC regulates energy metabolism by acting on the brain, liver, adipose tissue, and skeletal muscles, elevating circulating glucose and lipids to supply energetic

substrates and ensure readiness for potential threats. In human and animal studies, GC signaling is considered a major contributor to the allostatic load and stress pathophysiology (*362*). Chronically elevated circulating GC is linked to brain atrophy (*363*), cognitive decline, and increased risk of Alzheimer's disease (*56, 364*), as well as increased risk of cardiometabolic diseases (*56*). Therefore, based on previous short-term in vitro GC stimulation studies (*142, 365*), and the fact that any allostatic process requires active, ATP-dependent molecular events, we hypothesized that chronic GC signaling would trigger energy-dependent recalibrations among multiple domains of cellular behavior and bioenergetics. Moreover, in line with evidence in human studies (*280, 300, 366*) we further hypothesized that prolonged stress exposure in cells would trigger maladaptive outcomes, including multiple cellular aging markers and reduced cellular lifespan.

To quantify the bioenergetic and cellular manifestations of allostatic load across the lifespan, we apply chronic GC stimulation to primary fibroblasts from three healthy donors and deploy a longitudinal, high-frequency, repeated-measures strategy (*126, 367, 368*). We define the cellular features of allostatic load in four main parts. In Part 1, we quantify the bioenergetic and mitochondrial recalibrations and associated gene expression changes (Figures 1-4). In Part 2, we examine secreted cell-free DNA and cytokine signatures that mirror findings in human stress and aging studies (Figure 5-6). In Part 3, we profile well-established aging markers including mtDNA instability, DNA methylation-based epigenetic clocks, telomere length, and the Hayflick limit (Figure 7-8). In Part 4, we experimentally manipulate mitochondrial OxPhos to gain insight into the potential causal link between bioenergetics, aging, and cell death (Figure 9). Together, our findings define how cells recalibrate in response to chronic GC stress, highlighting increased energy expenditure (i.e., hypermetabolism) and accelerated cellular aging as interrelated, cell-autonomous features of allostatic load.

2.3. Results

Chronic GC stress decreases cell volume and increases cell death

In *Part 1* of this study, we examine the cellular and energetic effects of chronic glucocorticoid stimulation. We treated human fibroblasts isolated from three healthy donors (Donors 1, 2, and 3, *see Methods* **Table 1**) with the GC receptor agonist dexamethasone (Dex, 100 nM) at a concentration known to trigger GC receptor translocation from the cytoplasm to the nucleus (*368*). To quantify allostatic load across the cellular lifespan (up to 150-250 days, depending on the lifespan of each cell line), cytologic parameters were evaluated every 5-7 days, in parallel with cellular bioenergetics, secreted factors, DNA- and RNA-based measurements every 10-20 days until cells reached replicative senescence, marked by a near absence of cell division (**Fig. 1A**). This design presents the major advantage of reducing potential bias from single-time points and to resolve potential time-dependent effects of chronic GC stress. Moreover, compared to similar experiments performed in immortalized cell lines, primary human fibroblasts derived from unrelated female and male donors also provide a more stringent test of generalizability for our conclusions. Throughout, data from Dex-treated cells of each donor is presented relative to the respective untreated control condition from the same donor.

Qualitatively, chronic Dex altered cell morphology, marked by a flattened appearance with more membrane protrusions and fewer contacts with surrounding cells (**Fig. 1B**). Dex caused a 25-50% reduction in cell volume within the first 5 days of treatment, which persisted across most of the cellular lifespan in all three donors (**Fig. 1C**), resulting in an average 33% volume reduction across the study period ($p<0.0001$, **Fig. 1C-D**). Towards the end of the lifespan between 200-250 days, both Dex-treated cells and controls converged towards the same apparent minimal cell volume. Trypan blue-based measures of cell death showed no initial effect of Dex on cell death

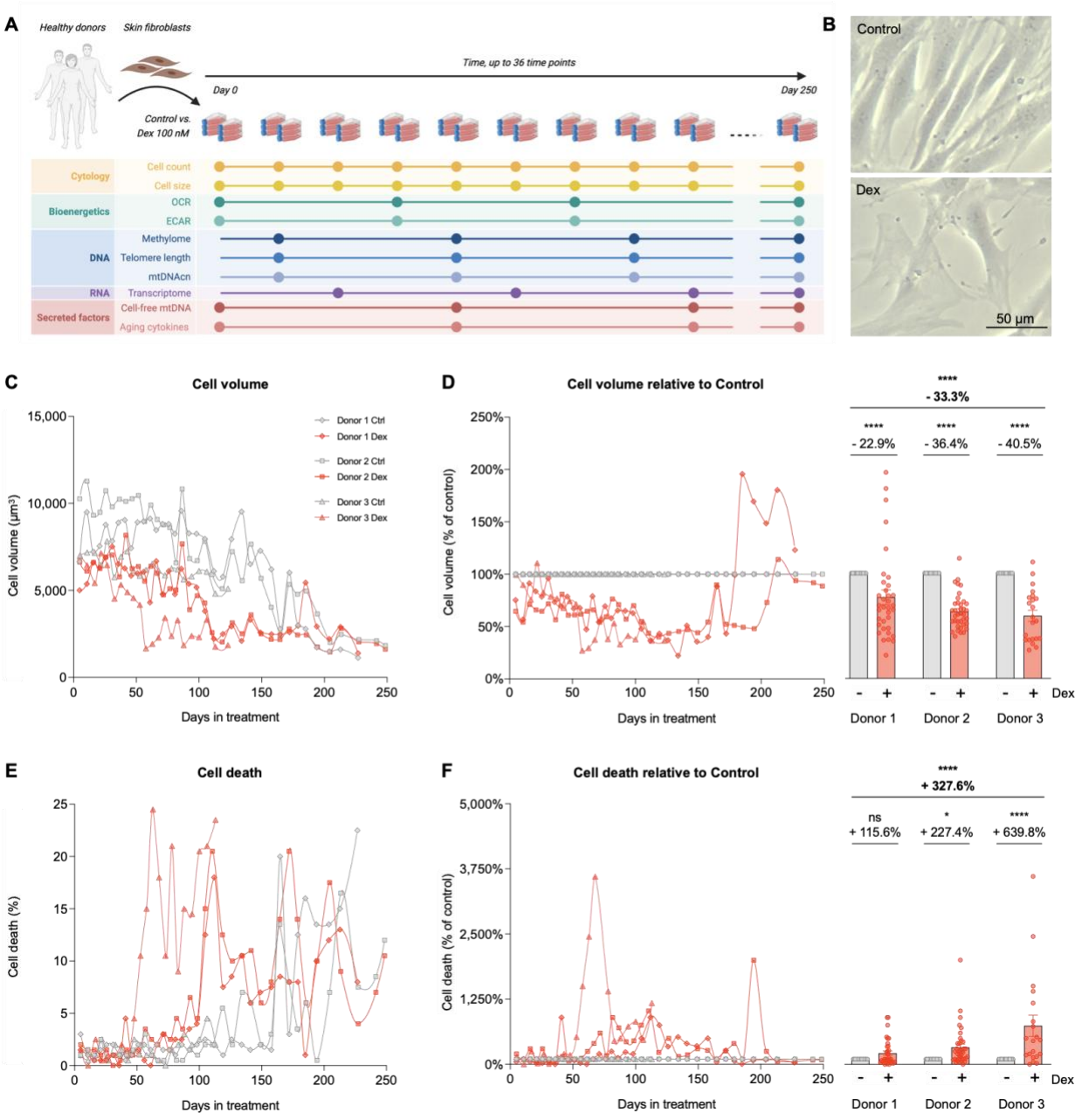

Figure 1. Longitudinal cytologic effects of chronic glucocorticoid signaling in primary human fibroblasts
(**A**) Study design: primary human fibroblasts derived from three healthy donors (Donors 1, 2, and 3) were cultured under standard conditions (control) or chronically treated with Dexamethasone (Dex, 100 nM) across their lifespan for up to 150-250 days, until replicative senescence. Cytologic parameters were evaluated every 5-7 days, while bioenergetics, DNA, RNA, and secreted factors parameters were evaluated every 10-20 days. (**B**) Representative images of untreated replicating control and Dex-treated cells from Donor 1 at 25 days of treatment. (**C**) Raw lifespan trajectories of cell volume. (**D**) To examine the effects of the chronic glucocorticoid signaling from the effects of aging, lifespan trajectories (left panel) and lifespan average effects (right panel) of Dex treatment on cell volume are expressed relative to the corresponding control time points for each donor. (**E-F**) Same as C-D but for the proportion of dead cells at each passage. n = 3 donors per group, n = 26-36 timepoints per donor. Lifespan average graphs are mean ± SEM, two-way ANOVA. * $p < 0.05$, **** $p < 0.0001$, ns: not significant.

for the first ~50 days (**Fig. 1E**). However, Dex subsequently caused a marked elevation in cell death, averaging a 3.3-fold increase across all three donors ($p<0.0001$, **Fig. 1E-F**). Thus, GC stress in this primary human cell system triggered robust time-dependent allostatic effects, including a reduction in cell volume and survival.

Chronic GC stress triggers hypermetabolism

Survival and growth can be limited by energy constraints, meaning that the finite amount of cellular energy available limits various aspects of normal cell behavior (*369-373*). Cellular energetic constraints could arise in two main ways: from an increase in energy expenditure (i.e., ATP consumption), or from a reduced capacity to produce ATP. To evaluate the effects of chronic Dex on total energy expenditure and ATP production capacity, we directly measured the extracellular flux of oxygen and pH (Seahorse extracellular flux analysis) longitudinally, every 10-28 days (***Supplementary Material* Fig. S1A**), using a validated mathematical approach to convert oxygen consumption rate (OCR) and extracellular acidification rates (ECAR) to ATP production rates (*374*). Under steady state, the ATP production rate is equal to the ATP consumption rate, such that ATP synthesis rates can be interpreted as cellular energy expenditure. Furthermore, to obtain energy consumption per unit of cell mass (similar to measuring whole-body energy consumption per kg of body weight in humans), we normalized bioenergetic measures to the closest available measurement in our model, cell volume. Using these strict parameters, we generated lifespan trajectories of three main parameters: i) resting (basal) ATP production rates derived from glycolysis ($J_{ATP\text{-}Glyc}$) and from OxPhos ($J_{ATP\text{-}OxPhos}$), which reflects how much energy cells *consume* to sustain life and divide; ii) the maximal $J_{ATP\text{-}Glyc}$ detected after pharmacologically inhibiting OxPhos, which reflects the glycolytic capacity to fulfill total basal cellular energetic demands; and iii) the maximal $J_{ATP\text{-}OxPhos}$, which reflects the built-in spare OxPhos capacity above

what is required to sustain cellular life (***Supplementary Material*** **Fig. S1B-C**). Around day 25, Dex caused an initial decrease in basal $J_{ATP\text{-}Glyc}$, which subsequently oscillated but remained on average 16% lower than control across the lifespan ($p<0.05$, **Fig 2A**). In contrast, Dex substantially increased basal mitochondrially-derived $J_{ATP\text{-}OxPhos}$, which remained markedly elevated, reaching up to 3 to 4-fold higher rates than control in mid-life ($p<0.0001$, **Fig 2B**). Absolute $J_{ATP\text{-}Glyc}$ and $J_{ATP\text{-}OxPhos}$ values showed similar longitudinal behaviors as $J_{ATP\text{-}Glyc}$ and $J_{ATP\text{-}OxPhos}$ normalized by cell volume, with lifespan averages significantly lower and higher than controls, respectively ($ps<0.0001$, ***Supplementary Material*** **Fig. S2A-B).** To quantify the total energetic costs of allostatic load in this system, we then calculated the combined basal ATP consumption rates derived from glycolysis and OxPhos. This total ATP consumption showed that Dex increased total resting energy expenditure across the lifespan ($J_{ATP\text{-}Total}$/cell volume) by a striking 61.9% ($p<0.001$, **Fig 2C**). Dex-treated cells consume more energy per unit of volume to sustain life, reflecting *hypermetabolism*. This chronic state of hypermetabolism suggested the existence of costly allostatic recalibrations that may also involve changes in the degree to which cells use glycolysis or OxPhos to satisfy their elevated energy demand, which we investigated next.

Chronic GC stress causes a metabolic shift towards OxPhos

To examine a potential shift in bioenergetics, we expressed $J_{ATP\text{-}Glyc}$ and $J_{ATP\text{-}OxPhos}$ as percentages of $J_{ATP\text{-}Total}$ and compared Dex to control. Dex induced a significant shift towards mitochondrial OxPhos as the major source of ATP. Across the lifespan, Dex-treated cells derived 75-80% of their ATP from OxPhos, compared to 55-60% in control cells ($p<0.0001$, **Fig 3A**). Accordingly, $J_{ATP\text{-}Total}$ in chronically stressed cells was strongly correlated to $J_{ATP\text{-}OxPhos}$ ($r_s=0.92$,

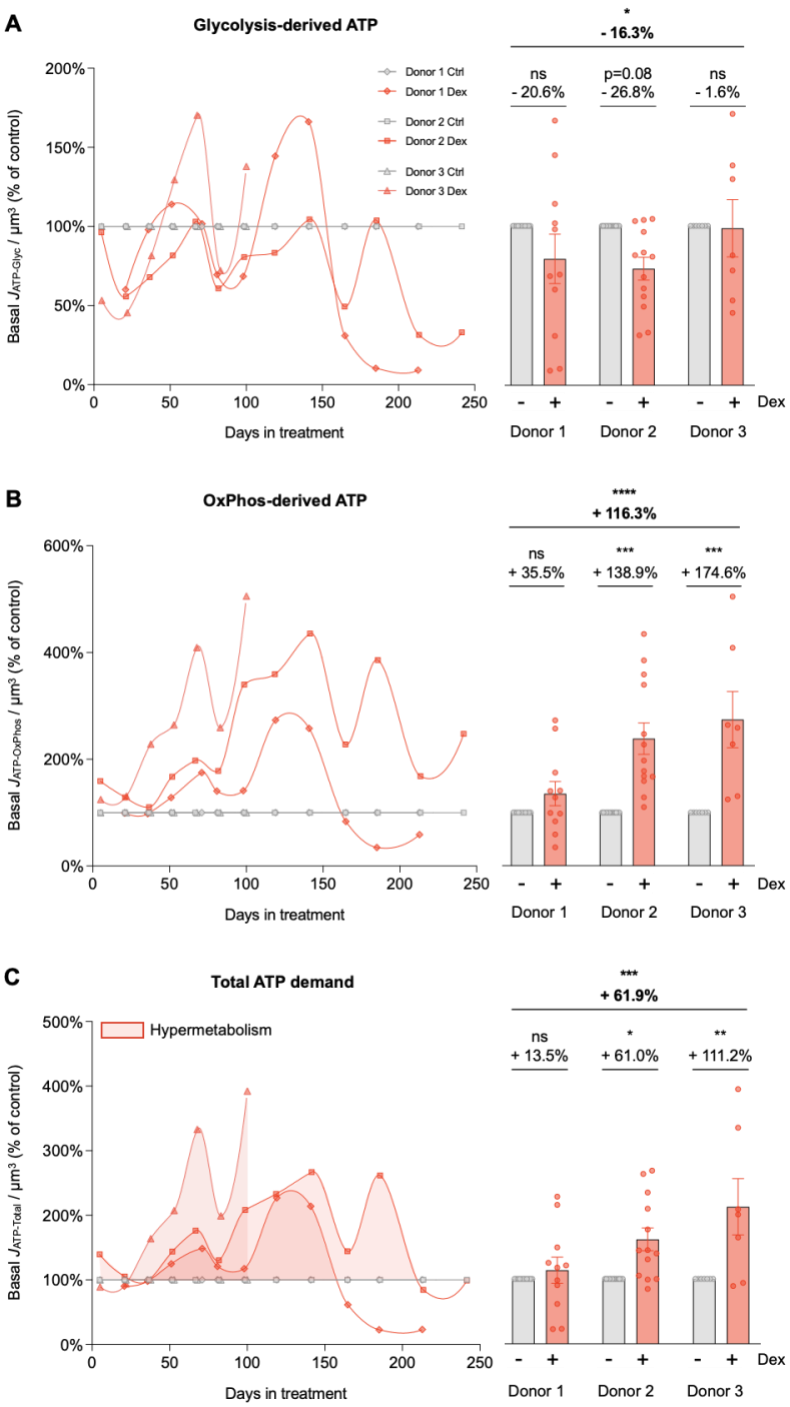

Figure 2. Cellular allostatic load is associated with hypermetabolism

(**A-C**) Energy expenditure trajectories across the cellular lifespan derived from Seahorse extracellular flux analyzer are described in detail in ***Supplementary Material*** **Fig. S1**. (**A**) Lifespan trajectories (left panel) and lifespan average effects (right panel) of Dex treatment expressed relative to the corresponding control time points for each donor on basal glycolysis-derived ATP ($J_{ATP-Glyc}$), (**B**) OxPhos-derived ATP ($J_{ATP-OxPhos}$), and (**C**) total ATP production ($J_{ATP-Total}$) corrected for cell volume. n = 3 donors per group, 8-13 time points per donor. Lifespan average graphs are mean ± SEM, two-way ANOVA * $p < 0.05$, ** $p < 0.01$, *** $p < 0.001$, **** $p < 0.0001$, ns: not significant. $J_{ATP-Total}$ is the algebraic sum of $J_{ATP-Glyc}$ and $J_{ATP-OxPhos}$.

$p<0.0001$, ***Supplementary Material*** **Fig. S2D**) and its variations along the lifespan were mostly explained by $J_{ATP\text{-}OxPhos}$ ($r^2=0.87$, $p<0.0001$, simple linear regression), highlighting the strong reliance of total energy expenditure on mitochondrial OxPhos**.** This result led us to examine whether chronic GC stress directly impaired or inhibited glycolysis. When OxPhos is acutely inhibited with the ATP synthase (i.e., complex V) inhibitor oligomycin, mammalian cells naturally increase glycolytic activity to compensate for the missing $J_{ATP\text{-}OxPhos}$ and fulfill the total cellular energetic demands (*375*). Here we found that after the addition of oligomycin, Dex-treated cells easily matched the basal $J_{ATP\text{-}Total}$ of their control counterparts by upregulating $J_{ATP\text{-}Glyc}$, and in fact sustain slightly higher than basal ATP consumption rates (ns, **Fig. 3B**). The intact glycolytic capacity of Dex-treated cells demonstrated that the metabolic shift towards OxPhos does not arise because of impaired glycolysis, but by upregulating OxPhos. Accordingly, Dex increased the spare OxPhos capacity over that of untreated control cells by an average of 83.9% ($p<0.0001$, **Fig. 3C**). This means that for a given amount of energy required to sustain basal cellular functions, Dex-treated fibroblasts maintained an even larger spare $J_{ATP\text{-}OxPhos}$ capacity than control cells – an effect that persisted across the lifespan ($p<0.0001$, **Fig. 3D**) and consistent with the anticipatory process of allostasis and allostatic load (*3, 4, 350, 351*). Such increases in OxPhos capacity could be explained by either increased mitochondrial respiratory efficiency or mitochondrial content. We first evaluated mitochondrial coupling efficiency, defined as the portion of oxygen consumption used towards ATP synthesis divided by the basal oxygen consumption rate. Dex did not change coupling efficiency, which oscillated by no more than 10% (within measurement error) from the control across the lifespan (n.s., **Fig. 3E**). Mitochondrial respiration efficiency then cannot explain the observed increase in the total energy expenditure nor the elevated OxPhos spare capacity.

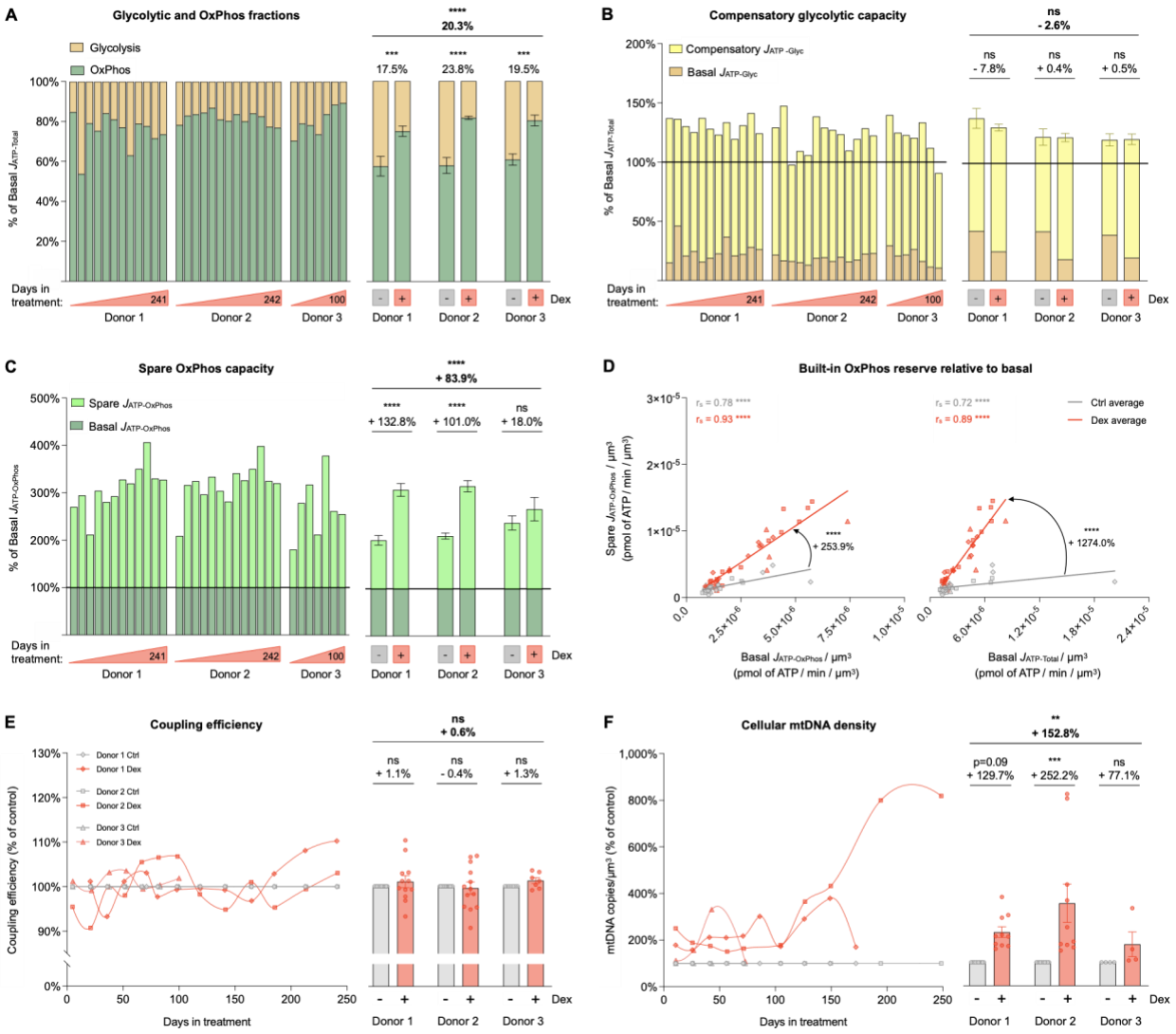

Figure 3. Cellular allostatic load involves a metabolic shift towards OxPhos

(**A**) Fraction of basal energy production from $J_{ATP\text{-}Glyc}$ (yellow) and basal $J_{ATP\text{-}OxPhos}$ (green) across the lifespan. (**B**) Compensatory glycolytic capacity, expressed as the percentage of basal $J_{ATP\text{-}Total}$, achieved when OxPhos ATP production is inhibited with oligomycin. Basal $J_{ATP\text{-}Glyc}$ levels are shown in dark yellow, and compensatory $J_{ATP\text{-}Glyc}$ is shown in bright yellow. (**C**) Same as B but for spare OxPhos capacity, expressed as the percentage of basal $J_{ATP\text{-}OxPhos}$ that can be achieved under uncoupled conditions with FCCP. Basal $J_{ATP\text{-}OxPhos}$ levels are shown in dark green, and spare $J_{ATP\text{-}OxPhos}$ are shown in bright green. (**D**) Correlation between spare $J_{ATP\text{-}OxPhos}$/cell volume and basal $J_{ATP\text{-}OxPhos}$/cell volume (left panel) and between spare $J_{ATP\text{-}OxPhos}$/cell volume and basal $J_{ATP\text{-}Total}$/cell volume (right panel). (**E**) Lifespan trajectories (left panel) and lifespan average effects (right panel) of Dex treatment on coupling efficiency expressed relative to the corresponding control time points for each donor. (**F**) Same as C but for mtDNA copy number/cell volume. n = 3 donors per group, 8-13 time points per donor. Lifespan average graphs are mean ± SEM, two-way ANOVA. Correlation graphs show Spearman r and thick lines represent simple linear regression for each group. ** p < 0.01, *** p < 0.001, **** p < 0.0001, ns: not significant. $J_{ATP\text{-}Glyc}$: ATP production rate derived from glycolysis. $J_{ATP\text{-}OxPhos}$: ATP production rate derived from OxPhos. $J_{ATP\text{-}Total}$: algebraic sum of $J_{ATP\text{-}Glyc}$ and $J_{ATP\text{-}OxPhos}$.

To indirectly monitor mitochondrial content, we next quantified total cellular mitochondrial DNA copy number (mtDNAcn) by qPCR, which showed that Dex induced approximately a doubling in mtDNAcn over the first 100 days of lifespan, followed by more substantial elevation at the end of life, particularly in one of the donors. On average across the lifespan, Dex-treated cells contained 936 mtDNA copies per cell, 97.8% higher than the control group ($p<0.05$, ***Supplementary Material* Fig. S3**). When accounting for the observed reduction in cell volume, cellular mtDNA density was 152.8% higher than in control ($p<0.01$, **Fig. 3F**), consistent with the increased reliance on OxPhos, the higher spare respiratory capacity, and the overall hypermetabolism in cells experiencing allostatic load.

Chronic GC stress upregulates OxPhos and mitochondrial biogenesis gene expression

To examine the transcriptional recalibrations associated with stress-induced cellular allostatic load and hypermetabolism, we performed RNA sequencing (RNAseq) at 9-10 time points across the lifespan of each donor and systematically queried the major glycolytic enzymes as well as OxPhos and mtDNA-related genes (**Fig. 4,** see ***Supplementary Material* Fig. S4** for individual gene labels). Consistent with the stable bioenergetic shift from glycolysis to OxPhos, chronic Dex downregulated most key glycolytic genes across the lifespan (**Fig. 4A**). This included the first enzyme in the sequence from glucose to pyruvate, hexokinase (HK2, -44.4%, $p<0.001$), as well as the rate-limiting enzyme phosphofructokinase (PFK, -28.5%, $p<0.001$). On the other hand, chronic Dex upregulated most individual core subunits of the five OxPhos complexes. The most highly upregulated genes were UQCRC1 (complex III, +69.7%, $p<0.001$) and COX7A1 (complex IV, +52.2%, $p<0.01$), indicating a coordinated upregulation of the genetic OxPhos program (**Fig. 4B**).

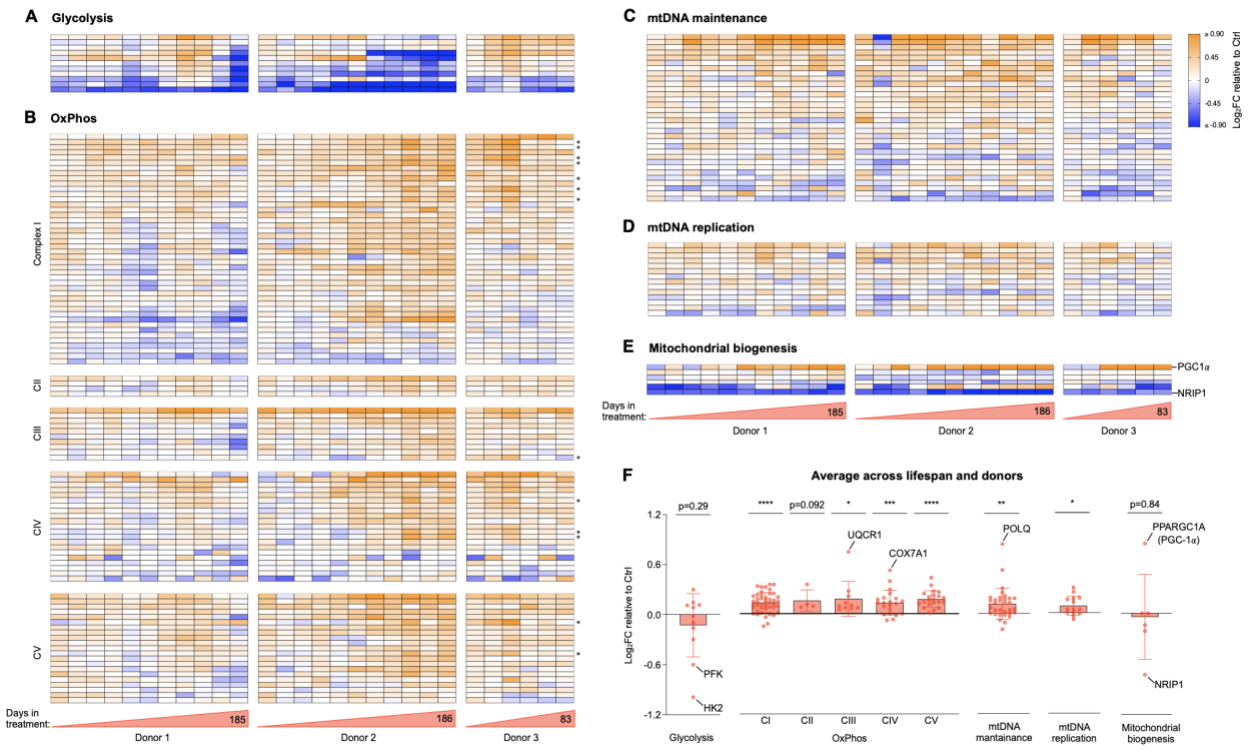

Figure 4. Cellular allostatic load involves transcriptional upregulation of OxPhos and mitochondrial biogenesis (**A**) Heatmaps showing the effect of Dex treatment on the expression of glycolytic genes, expressed as the Log_2 of fold change (Log_2FC) of normalized gene expression relative to the corresponding control time points for each donor. (**B**) Same as A but for genes encoding the subunits of complexes I, II, III, IV, and V of the OxPhos system, with mitochondrial-encoded genes marked with ❖ (**C-E**). Same as A and B but for genes encoding proteins associated with (**C**) mtDNA maintenance, (**D**) mtDNA replication, and (**E**) mitochondrial biogenesis. Two key regulators of mitochondrial biogenesis, one positive (PGC-1a) and one negative (NRIP1) are highlighted, showing expression signatures consistent with both activated and un-repressed mitochondrial biogenesis. (**F**) Average effect of Dex treatment shown in A-E. Each data point represents the gene average of the Log_2FC values throughout the entire lifespan of the three donors (n=28 timepoints). Average graphs are mean ± SEM, with each gene shown as a single data point. One-sample t-test different than 0, * $p < 0.05$, ** $p < 0.01$, *** $p < 0.001$, **** $p < 0.0001$, ns: not significant. n = 3 donors per group, 9-10 time points per donor. Heatmap row annotation with individual gene names is provided in ***Supplementary Material*** **Fig. S4**.

Moreover, consistent with the elevated mtDNAcn in Dex-treated cells, genes encoding mtDNA maintenance- and replication-related proteins were both upregulated (**Fig. 4C-D**). This included the DNA polymerase theta (POLQ), which plays a key role in repairing double-strand breaks by the theta-mediated end-joining mechanism (*376*) (+91.9%, p<0.001). This result also pointed to potential mtDNA instability as a feature of MAL (*360*) (see below, section "*Chronic GC stress causes mtDNA instability*"). Moreover, Dex upregulated the master regulator of

biogenesis PGC1α (peroxisome proliferator-activated receptor gamma coactivator 1-alpha, PPARGC1A (*377*)) by 106% across the lifespan, and simultaneously downregulated the inhibitor of biogenesis NRIP1 (nuclear receptor interacting protein 1, also RIP140 (*378, 379*)) by 61.5% (ps<0.001**, Fig. 4E**). Together, the transcriptomics data summarized in **Fig. 4F** reveal a sustained stress-induced upregulation of the genetic programs involved in building additional OxPhos capacity and mtDNA copy number, consistent with the bioenergetic recalibrations and the anticipatory processes of cellular allostatic load in Dex-treated cells.

Chronic GC stress increases cell-free mtDNA levels

In *Part 2* of this study, we turn our attention to the secretory profile of Dex-treated cells. In humans, two situations associated with allostatic load – acute psychological stress (*368, 380*) and aging (*381*) – are associated with increased circulating cell-free mtDNA. cf-mtDNA reflects the extracellular release of whole mitochondria or mitochondria-free mtDNA (*382, 383*) and is an emerging mitochondria-derived inter-cellular signaling pathway (*384*). Motivated by the changes in mitochondrial OxPhos and mtDNA density in our system, we longitudinally investigated extracellular cf-mtDNA levels.

On average, cf-mtDNA levels across the lifespan were 46.9% higher in Dex-treated cells than controls ($p<0.05$) (**Fig. 5A**). In two of the three donors, chronic Dex strongly increased cf-mtDNA levels in the media, which oscillated and eventually matched cf-mtDNA levels observed in control cells by the end of lifespan. Previous work showed that cf-mtDNA release can be a selective and regulated process not primarily driven by cell death (reviewed in (*148, 385*)). In our model, cf-mtDNA was significantly correlated with the proportion of cell death at each passage (Dex $r_s=0.69$, $P<0.001$, **Fig. 5B**), suggesting that a portion, although not all of the extracellular cf-mtDNA in fibroblasts under allostatic load is linked to increased cell death.

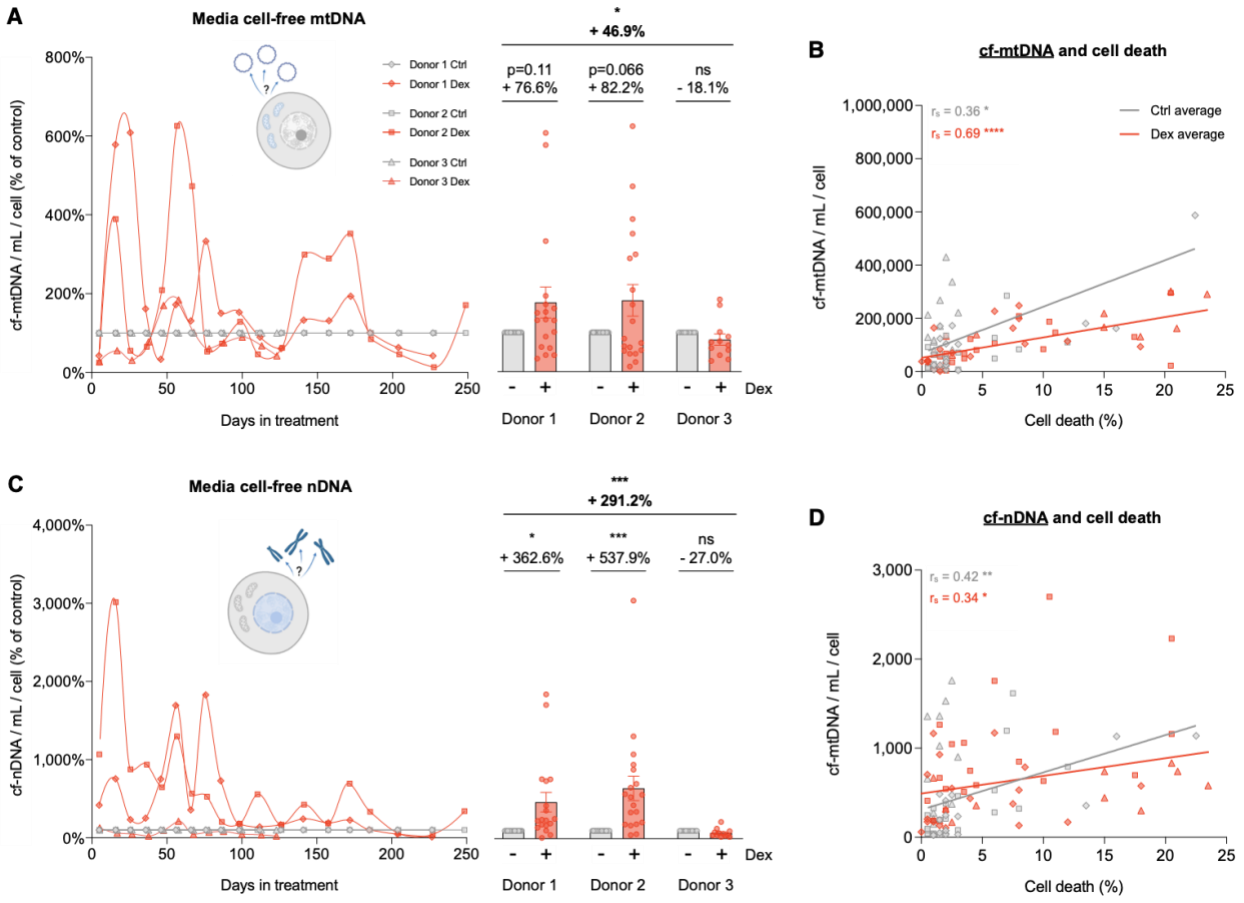

Figure 5. Cellular allostatic load increases cell-free DNA levels
(**A**) Lifespan trajectories (left panel) and lifespan average effects (right panel) of Dex treatment on cell-free mitochondrial DNA (cf-mtDNA) expressed relative to the corresponding control time points for each donor. (**B**) Correlation between cf-mtDNA and the proportion of dead cells at each passage. (**C**) Same as A but for cell-free nuclear DNA (cf-nDNA). (**D**) Same as B but for cf-nDNA. n = 3 donors per group, 6-10 time points per donor. Lifespan average graphs are mean ± SEM, two-way ANOVA. Correlation graphs show Spearman r and thick lines represent simple linear regression for each group, Pearson r correlation. * $p < 0.05$, ** $p < 0.01$, *** $p < 0.001$, **** $p < 0.0001$, ns: not significant.

Dex also robustly elevated cell-free nuclear DNA (cf-nDNA, measured in parallel with cf-mtDNA), and showed similar behavior to cf-mtDNA, with a strong increase along most of the lifespan for the same two donors followed by a gradual normalization. Dex-treated cells exhibited a lifespan average cf-nDNA 2-fold higher than controls ($p<0.001$, **Fig. 5C**). Similar to cf-mtDNA, cell death was significantly correlated with cf-nDNA but accounted for only a minor fraction (10-14%) of the variance in extracellular nuclear genome (Dex $r_s=0.34$, $p<0.05$, **Fig. 5D**), suggesting

that active processes other than cell death likely contributed to cell-free DNA release. Interestingly, whereas media cf-mtDNA and cf-nDNA were strongly correlated in control cells (r_s=0.90, $p<0.0001$), in response to chronic Dex, a large number of cf-mtDNA molecules were released at certain time points (up to 6-fold) without a corresponding elevation in cf-nDNA. This is reflected in a markedly lower correlation between cf-mtDNA and cf-nDNA in Dex-treated cells (r_s=0.36, $p<0.05$, ***Supplementary Material*** **Fig. S5**). This pattern makes it unlikely that both genomes are systematically co-released in this model. Overall, these data define the temporally sensitive release of extracellular mitochondrial and nuclear DNA as a feature of GC-induced cellular allostatic load. Because energy must be consumed to fuel DNA synthesis and its extracellular release, these results point to cf-DNA release as a potential contributor to hypermetabolism.

Chronic GC stress alters cytokine release

Considering that allostatic load in humans is characterized by elevated levels of neuroendocrine mediators (*386, 387*) as well as chronic inflammation (*388*), we next sought to investigate the effects of chronic Dex on the profiles of secreted cytokines. Using a custom-designed Luminex array of plasma cytokines associated with human aging (*389*), we detected a panel of 27 cytokines in the culture media of the three donors across the lifespan (**Fig. 6A**). While chronic Dex caused variable responses among different cytokines, it temporarily increased the secretion of multiple cytokines over the first 60 days, consistent with the classic inverted-U shaped stress responses (*142*) (**Fig 6B**). The peak cytokine response occurred around ∼30 days after the onset of GC stress, with a magnitude approximately double (i.e., ∼100% increase) for most cytokines relative to control cells. As for cf-DNA, because energy must be consumed to fuel cytokine/protein synthesis and their extracellular release, these results point to protein secretion as a potential contributor to hypermetabolism.

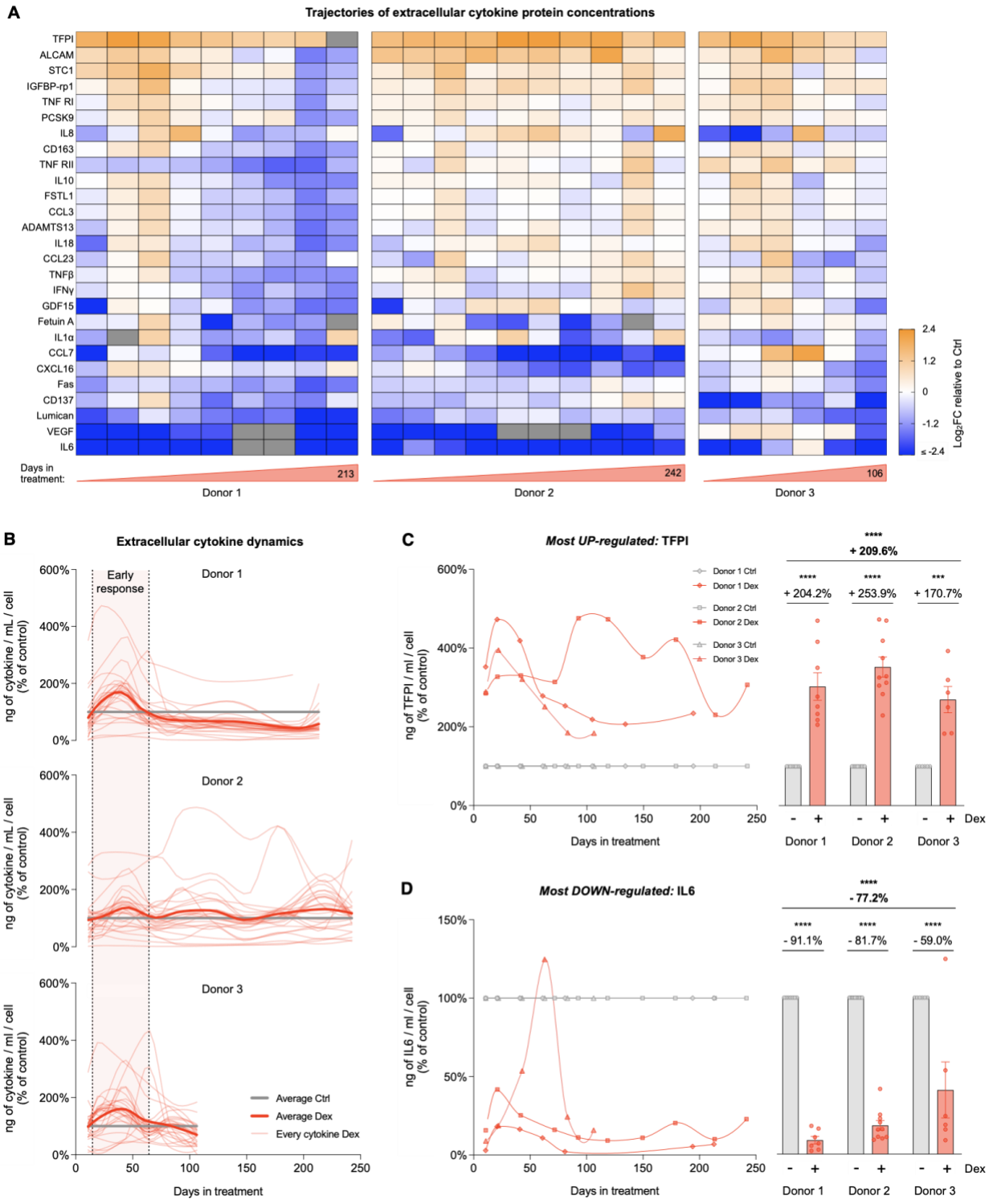

Figure 6. Cellular allostatic load alters cytokine release

(**A**) Heatmaps showing the effect of Dex treatment on the secretion of age-related cytokines, expressed as the Log_2 fold change (Log_2FC) of cytokine concentration (pg/mL of medium), relative to the corresponding control time points for each donor. (**B**) Lifespan trajectories of cytokine concentration in cells treated with Dex relative to the corresponding control time point for each donor. Thin curves in soft red represent individual cytokines; thick curves

in red represent the average of all cytokines evaluated; thick lines in gray represent the control level. (**C**) Lifespan trajectories (left panel) and average effects (right panel) of Dex treatment on TFPII (most upregulated cytokine) levels per mL of culture media expressed relative to the corresponding control time point for each donor. (**D**) Same as C but for IL6 (most downregulated cytokine). n = 3 donors per group, 6-10 time points per donor. Lifespan average graphs are mean ± SEM, two-way ANOVA. *** $p < 0.001$, **** $p < 0.0001$, ns: not significant. Lifespan trajectories and average effects of Dex treatment on levels of every cytokine detected are shown in ***Supplementary Material*** **Fig. S7**.

Further analysis revealed that Dex significantly altered the lifespan average secretion of 12 out of the 27 age-related cytokines. The strongest response was a stable elevation (average +210%) of Tissue Factor Pathway Inhibitor (TFPI, $p<0.001$, **Fig. 6C**), a cytokine related to the complement and coagulation cascades (*390*). The most strongly downregulated cytokine was Interleukin 6 (IL6, -77%, $p<0.001$, **Fig. 6D**), a pro-inflammatory cytokine well-known to be repressed by GC signaling (*391*).

Interestingly, when we queried the same cytokines at the transcript level, we observed a global downregulation in RNA levels among the three donors (***Supplementary Material*** **Fig. S6A-B**). In addition, the effect sizes across the lifespan were 2-3 times larger at the RNA level than at the extracellular protein level (***Supplementary Material*** **Fig. S6C-D**). Comparison of the secreted protein and transcriptomic data demonstrated that only half of the cytokines showed congruent (i.e., within 10% variation) responses (***Supplementary Material*** **Fig. S7**), highlighting a disconnect between quantitative measures of gene expression and cytokine release, and emphasizing the value of secreted protein quantification as an end phenotype. Thus, chronic GC signaling triggered a time-sensitive secretory phenotype, possibly involving non-transcriptional and/or non-genomic effects in the release of age-related cytokines.

Chronic GC stress causes mtDNA instability

Thus far, we have examined key bioenergetic features of cellular allostatic load and related extracellular signaling behavior. In *Part 3* of this study, we turn our attention to potential maladaptive consequences of sustained allostatic load, namely evidence of allostatic overload. *In vitro* and *in vivo* studies have shown that chronic metabolic stressors, primary energetic defects, and aging result in mtDNA instability, which manifests as the accumulation of mtDNA defects (*392-396*). In Dex-treated cells, long-range PCR (LR-PCR) provided initial evidence that chronic glucocorticoid signaling may trigger mtDNA instability, as illustrated in multiple subgenomic bands consistent with mtDNA deletions, detected at different time points across the lifespan in two (Donors 1 and 2) out of three donors (**Fig 7A** shows data for Donor 2). We confirmed the accumulation of mtDNA deletions in all donors through deep mtDNA sequencing and quantified their relative abundance (i.e. proportion of mutant and normal mtDNA genomes, or heteroplasmy) across the lifespan using the eKLIPse pipeline (*397*) (**Fig 7B, Fig S8A**). Dex induced a relatively large increase in total mtDNA deletion levels between days 20-50 of treatment among all three donors, suggesting that the effects of glucocorticoid stress on mtDNA instability may develop relatively rapidly. On average, Dex tended to increase the total mtDNA deletion burden by an average of 141.1% ($p=0.11$, **Fig 7C**). The absolute heteroplasmy levels remained low (0.02-0.33%) and therefore unlikely to have material effects on OxPhos capacity, as our data showed. This trend in mtDNA deletion load was not driven by an increase in the number of unique deletions, but rather by higher deletion heteroplasmy levels (**Fig S8B**). Furthermore, mtDNA deletions were i) moderately larger, and ii) tended to cover the D-loop (**Fig S8C-E**), a region that physically interacts with the mtDNA maintenance proteins whose gene expression was upregulated (*see* Fig 4F).

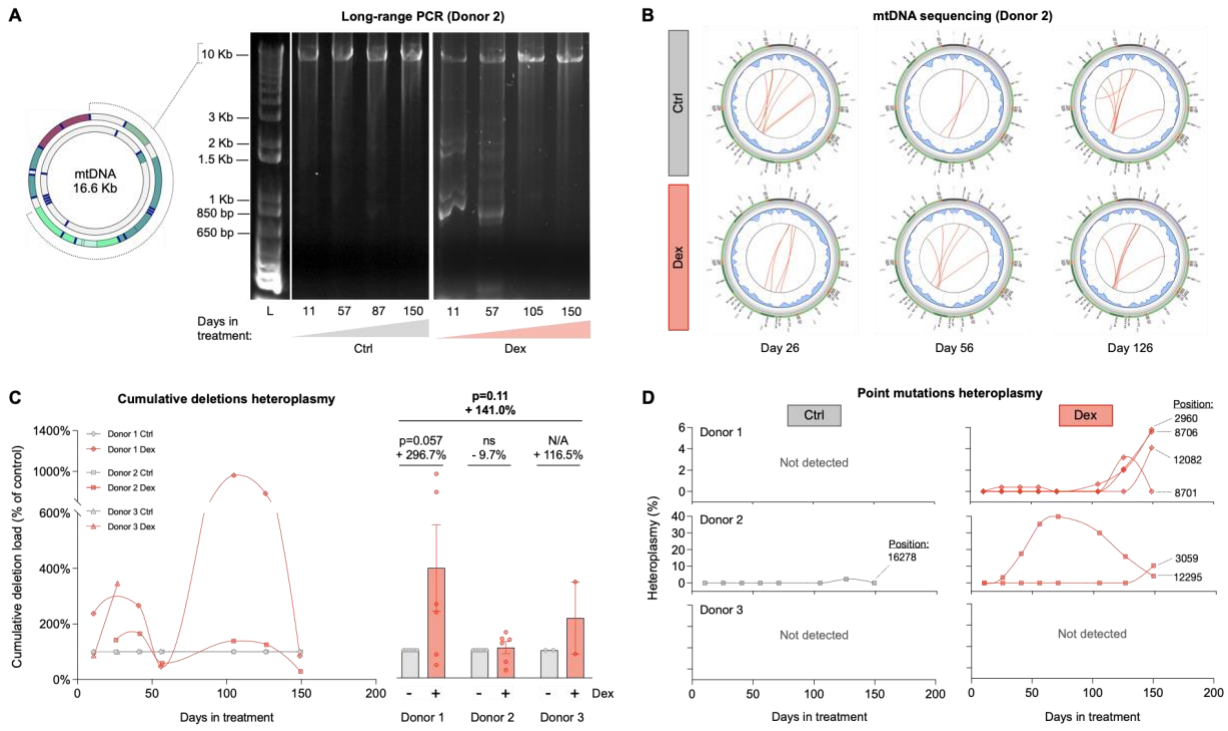

Figure 7. Cellular allostatic load causes mtDNA instability
(**A**) Long-range PCR (10 kb product) of mtDNA extracted from Donor 2 control and Dex-treated cells across lifespan, resolved by agarose gel electrophoresis. The presence of amplicons of sizes smaller than 10 kb reveals the presence of mtDNA molecules containing deletions. (**B**) Circos plots from mtDNA sequencing and eKLIPse analysis for mtDNA extracted from Donor 2 control and Dex-treated cells at days 26, 56, and 126. Each red line represents an individual deletion that spans the sequence contained between its two ends. The line thickness reflects the level of relative abundance or heteroplasmy for each deletion (see ***Supplementary Material*** **Fig. S8** for all donors). (**C**) Lifespan trajectories (*left* panel) and average effects (*right* panel) of Dex treatment on the cumulative heteroplasmy of all deletions present at a particular time point, expressed relative to the corresponding control time point for each donor. (**D**) Lifespan trajectories of individual point mutations heteroplasmy found in control (left panels) and Dex-treated cells (right panels) of the three donors. n = 3 donors per group, 2-8 time points per donor. Datapoints in lifespan trajectories are connected using the Akima spline curve, but the datapoints for Donor 3 in (C), for which due to insufficient time points the spline fit was not feasible and therefore data points were connected through a straight line. Lifespan average graphs are mean ± SEM, two-way ANOVA. ns: not significant, N/A: not applicable.

Another marker of mtDNA instability is the accumulation of single nucleotide variants (SNVs, also known as point mutations). Along the lifespan, except for one low SNVs heteroplasmy in Donor 2 detected on day 125, control cells largely did not accumulate novel SNVs. In comparison, during the same portion of lifespan, we identified 3 and 4 novel SNVs in Donors 1 and 2 (7 novel SNVs in total), one of which clonally expanded to reach 39.8% heteroplasmy (**Figure 7D**). Replicating cultured cells accumulate few novel mtDNA deletions and SNVs (*398*),

likely as a result of purifying selection (fibroblasts with deleterious mtDNA defects die and are eliminated from the cell population). Nevertheless, the apparent elevation in both spontaneous deletions and point mutations are consistent with the accumulation of damage as a feature of allostatic load and collectively point to mtDNA instability as a manifestation of cellular, specifically mitochondrial allostatic load (MAL).

Chronic GC stress accelerates cellular aging

Combined, the mtDNA instability, premature cell size reduction, elevated cell death, as well as the early induction of most human age-related cytokines suggested that cellular allostatic load could impact aging trajectories. We first examined the growth curves for each donor, which reveal the maximal number of population doublings (i.e., cell divisions) that can be accomplished by each donor before reaching replicative senescence. This feature, also known as the Hayflick limit (*399, 400*), is the most closely related outcome to human longevity in this simple cellular model and could reflect allostatic overload.

Consistent with the notion that chronic stress accelerates cellular aging in humans (reviewed in (*298, 401*), Dex caused a premature halting of population doubling, resulting in an average 19.8% reduction in the Hayflick limit across the three donors ($p<0.05$, **Fig. 8A-B**). This effect was associated with a decrease in cell division rate within the first 50 days of treatment (-21.5%, $p<0.001$, **Fig. 8C, *Supplementary Material* Fig. S9**). In the context of this substantial reduction in the division rate, and particularly given the reduced cell size in Dex-treated cells (-33% volume on average), the hypermetabolic phenotype of the allostatic load becomes particularly striking. Considering cellular doubling rate and cell size, chronically stressed fibroblasts expend 107.9% more energy than control cells over the course of *each cell division* ($p<0.001$, ***Supplementary Material* Fig. S9**).

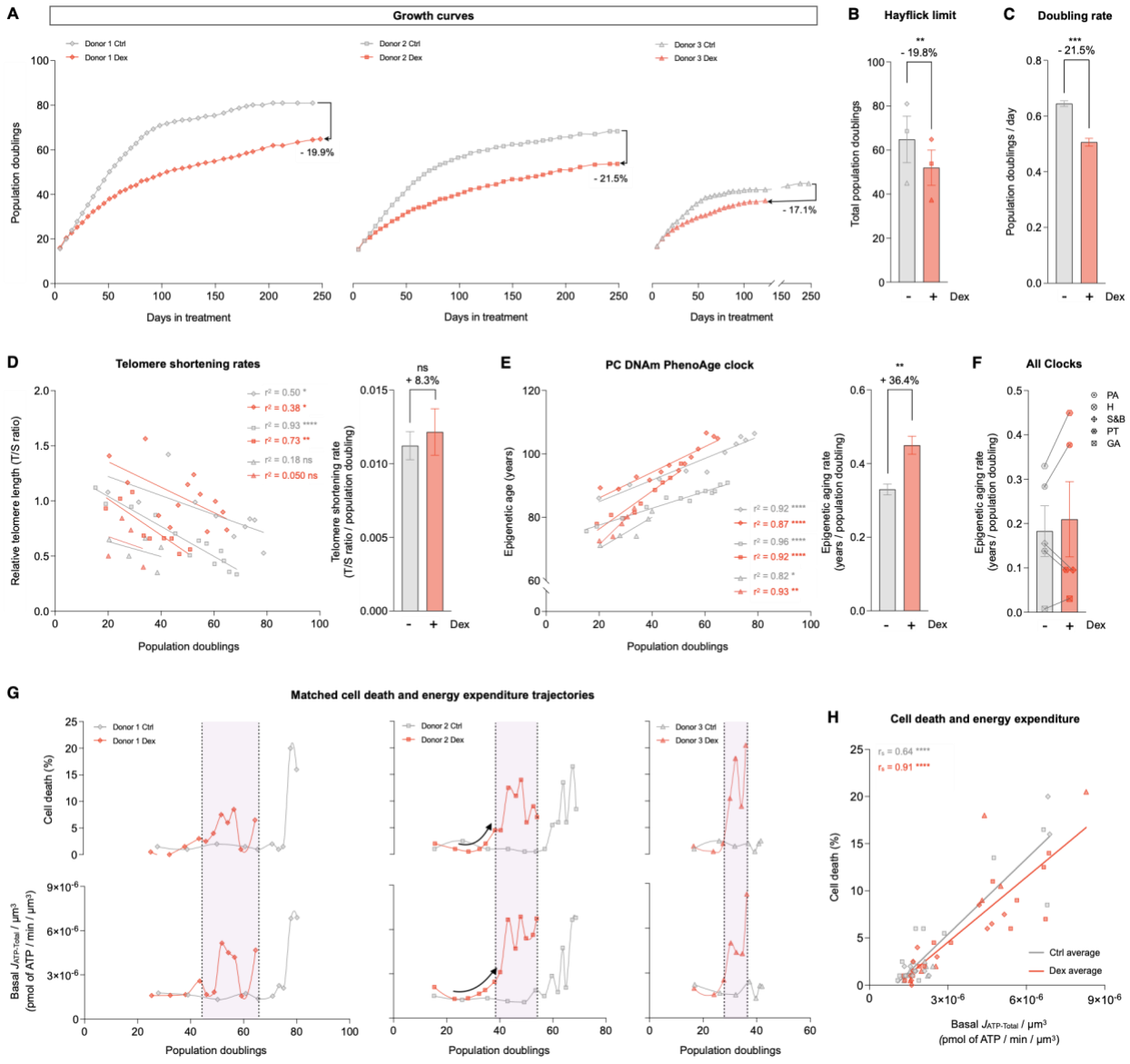

Figure 8. Cells under chronic allostatic load display accelerated cellular aging

(**A**) Lifespan trajectories of cumulative population doublings. (**B**) Hayflick limit for each donor of each group. (**C**) Group average early life doubling rate, inferred by a linear mixed model of the population doubling trajectories within the first 50 days of treatment. (**D**) Telomere length across population doublings, with simple linear regressions for each donor of each group (left panel), and group average telomere shortening rate inferred by linear mixed model along the whole lifespan (right panel). (**E**) Epigenetic age calculated by the principal components (PC) PhenoAge epigenetic clock, with linear regressions for each donor of each group (left panel), and group average epigenetic aging rate inferred by linear mixed model along the whole lifespan (right panel). (**F**) Epigenetic aging rate for all the PC epigenetic clocks evaluated: PA: PhenoAge, H: Hannum, S&B: Skin and Blood, PT: PanTissue, GA: GrimAge. Detailed analysis of these epigenetic clocks is in ***Supplementary Material*** **Fig. S11** (**G**) Percentage of dead cells (upper panels) and basal $J_{ATP\text{-}Total}$/cell volume (lower panels) across population doublings for Donor 1 (left panels), Donor 2 (middle panels) and Donor 3 (right panels). (**H**) Correlation between proportion of dead cells in every passage and Basal $J_{ATP\text{-}Total}$/cell volume. n = 3 donors per group; timepoints per donor: n = 26-36 in A, n = 4-14 in D-E, n = 8-13 in G-H. Bar graphs are mean ± SEM, Satterthwaite method. Correlation graphs show Spearman r and thick lines represent simple linear regression for each group. * $p < 0.05$, ** $p < 0.01$, **** $p < 0.0001$, ns: not significant.

To examine the potential basis for the reduced cellular lifespan, we next examined two orthogonal measures of replicative senescence and cellular aging: telomere length (*300*), and DNA methylation-based epigenetic clocks (*270, 402*). We first quantified relative telomere length by qPCR across the lifespan for each donor and computed the rate of telomere shortening per cell division. Using a mixed effects linear model to compare rates of change over time, Dex showed an 8.7% non-significant acceleration in the telomere shortening rate (**Fig. 8D**); directly comparing the linear slopes of each Dex-treated cell line to its corresponding control showed an average acceleration of 27.6% across the three donors ($p<0.05$, paired t-test). Telomere length was also estimated through a DNA methylation-based algorithm (*403*). This measure documented an effect of similar magnitude towards accelerated shortening rate per population doubling (+17.0%, $p<0.05$, ***Supplementary Material*** **Fig. S10A-B**). These data thus provided converging evidence that chronically stressed cells experience more rapid telomere attrition during each event of genome replication, consistent with increased genomic instability and accelerated aging.

At the gene expression level, accelerated telomere attrition was associated with alterations in the expression of genes encoding telomere capping proteins. In particular, the major component of the shelterin complex, TPP1(*404*) was significantly downregulated across the lifespan for the three donors (-26.7%, $p<0.0001$), indicating that the telomeres in Dex-treated cells could be more vulnerable to DNA damage (***Supplementary Material*** **Fig. S10C-D**). On the other hand, several genes encoding the core components of the telomerase holoenzyme (*404*) were upregulated, including TERC, which was the most highly upregulated telomerase gene (+68.6%, $p<0.0001$, ***Supplementary Material*** **Fig. S10C-D**). The upregulation of TERC in the context of accelerated telomere shortening in Dex-treated cells is in agreement with clinical associations of chronic life stress and upregulation of telomerase activity in leukocytes (*405, 406*), possibly reflecting a

(failed) attempt to reactivate telomerase to preserve or elongate telomeres, turning chronic allostatic load to overload.

Chronological age can also be predicted with high accuracy through DNA methylation-based algorithms, known as epigenetic clocks (*407-411*). Here, we generated a longitudinal DNA methylation dataset using the EPIC array (*367*) and deployed an approach that increases DNAmAge accuracy using a principal component adjustment of the classic epigenetic clocks (*412*). The difference between the initial epigenetic age of the donors and their chronological age at the time of the biopsy can be explained by the variable time and/or cell divisions undergone by each cell line before the beginning of the experiments, and because cells cultured *in vitro* experience an accelerated epigenetic aging rate compared to *in vivo* conditions (*413, 414*). Regardless of the estimated initial epigenetic age, by applying the clocks across the cellular lifespan, we can longitudinally quantify the rate of epigenetic aging relative to population doublings. The PC-PhenoAge clock (*411*) showed a significant 36.4% increase in the epigenetic aging rate ($p<0.01$, **Fig. 8E)**. A similar increase was found with the PC-Hannum clock (+33.1%, $p<0.05$**)**, whereas non-significant effects were obtained using other clocks (Horvath Skin and Blood, Horvath Pan Tissue, and GrimAge, ***Supplementary Material*** **Fig. S11)**. Results across these five different epigenetic clocks were heterogenous but indicated that chronic GC stress accelerated the rate of epigenetic aging in 3 out of 5 clocks (Fig. **8F**). Together, these telomere and DNA methylation data provided converging evidence in primary human cells experiencing allostatic overload that hypermetabolism is linked to the rate of cellular aging.

Age-related hypermetabolism and cell death occur near-synchronously

Given the premature age-related rise in cell death (*see* Fig. 1) and the profound mitochondrial and bioenergetic recalibrations associated with increased energy consumption in

Dex-treated cells (*see* Fig. 2 and Fig. 3), we leveraged the longitudinal nature of our dataset to examine whether cell death was temporally related to hypermetabolism. Plotting both mortality (% cell death) and total energy expenditure ($J_{ATPtotal}$/cell volume) relative to population doublings demonstrated that chronic Dex caused a left shift in the mortality curves, shifting the trajectory of each donor towards an earlier onset and progression along their lifespan (**Fig. 8G**, *upper* panels). Strikingly, Dex caused a similar and near synchronous left shift in energy expenditure trajectories, reflecting an early onset, hypermetabolic state that develops over weeks (**Fig. 8G**, *lower* panels). Comparing both mortality and energy expenditure at matched time points revealed a strong temporal correlation across the entire lifespan, among both control and Dex-treated cells (r_s=0.64 and r_s=91, respectively, ps<0.001, **Fig. 8H**), where 75-84% of the variance in cell death can be explained by the basal energy expenditure (i.e., how much energy cells must consume to sustain allostatic load), and vice-versa. In line with results linking the rate of telomere shortening and lifespan across species (*415*), these results underscore the close temporal association between the energetic cost of allostatic load (i.e., hypermetabolism) and possibly the ultimate consequence of allostatic overload, cell death or mortality.

Hypermetabolism, not the metabolic shift towards OxPhos, predicts cell death

Previous work suggested that the shift from glycolysis towards OxPhos (e.g., during the differentiation of stem cells to "mortal" cell lineages) drives the susceptibility to detrimental age-related molecular alterations (*416*). Furthermore, mitochondria appear required for key cellular senescence features to manifest (*417*). Therefore, in *Part 4* of this study, we investigated whether in our model of cellular allostatic load the association of hypermetabolism with cell death and lifespan was specifically related to increased mitochondrial OxPhos activity ($J_{ATP\text{-}OxPhos}$), or the total energy expenditure ($J_{ATP\text{-}Total}$).

To disentangle these factors, we repeated the chronic Dex lifespan experiments while simultaneously downregulating OxPhos activity using a combination of inhibitors to block the mitochondrial import of the major carbon sources: pyruvate (UK5099 (*418*)), fatty acids (Etomoxir (*419*)), and glutamine (BPTES (*420*)) (**Fig 9A**, ***Supplementary Material*** **Fig. S12A**). As expected, the mitochondrial nutrient uptake inhibitors (mitoNUITs) decreased OxPhos-derived ATP production in Dex-treated cells by an average of 21.2% ($p<0.0001$, ***Supplementary Material*** **Fig. S12B)**. This partial inhibition of OxPhos was associated with a supra-compensatory increase in glycolytic ATP production rates (+443.2%, $p<0.0001$, ***Supplementary Material*** **Fig. S12C**). Consequently, the Dex+mitoNUITs treatment induced an average increase in $J_{ATP\text{-}Total}$ of 78.9% above the energy demand in Dex-treated cells ($p<0.0001$, **Fig. 9B**). Thus, compared to chronic Dex alone, Dex+mitoNUITs successfully suppressed OxPhos but triggered an even more severe state of hypermetabolism (sustained predominantly by glycolysis). Therefore, we reasoned that if the observed allostatic overload phenotype – accelerated aging and premature cell death – was driven by the enhanced energy flux through OxPhos, the addition of mitoNUITs should at least partially rescue it. On the other hand, if cellular allostatic overload was directly driven by the total energy expenditure and hypermetabolism, then Dex+mitoNUITs would aggravate the pro-aging effects of allostatic overload.

Consistent with the latter alternative, the Dex+mitoNUITs combination either exacerbated or did not alter the pro-aging effects of Dex. Compared to Dex alone, Dex+mitoNUITs reduced the Hayflick limit by a further 18.5% ($n=3$ donors, $p<0.05$, **Fig. 9D-E)**, which was associated with a decrease in comparable cell division rate within the first 50 days of treatment (-14.7%, $p<0.01$, **Fig. 9F**). Dex+mitoNUITs tended to increase telomere attrition rate per population doubling (+50.6%, $p=0.11$, linear mixed model; +19.2%, $p=0.45$, paired t-test between slopes, **Fig. 9G**).

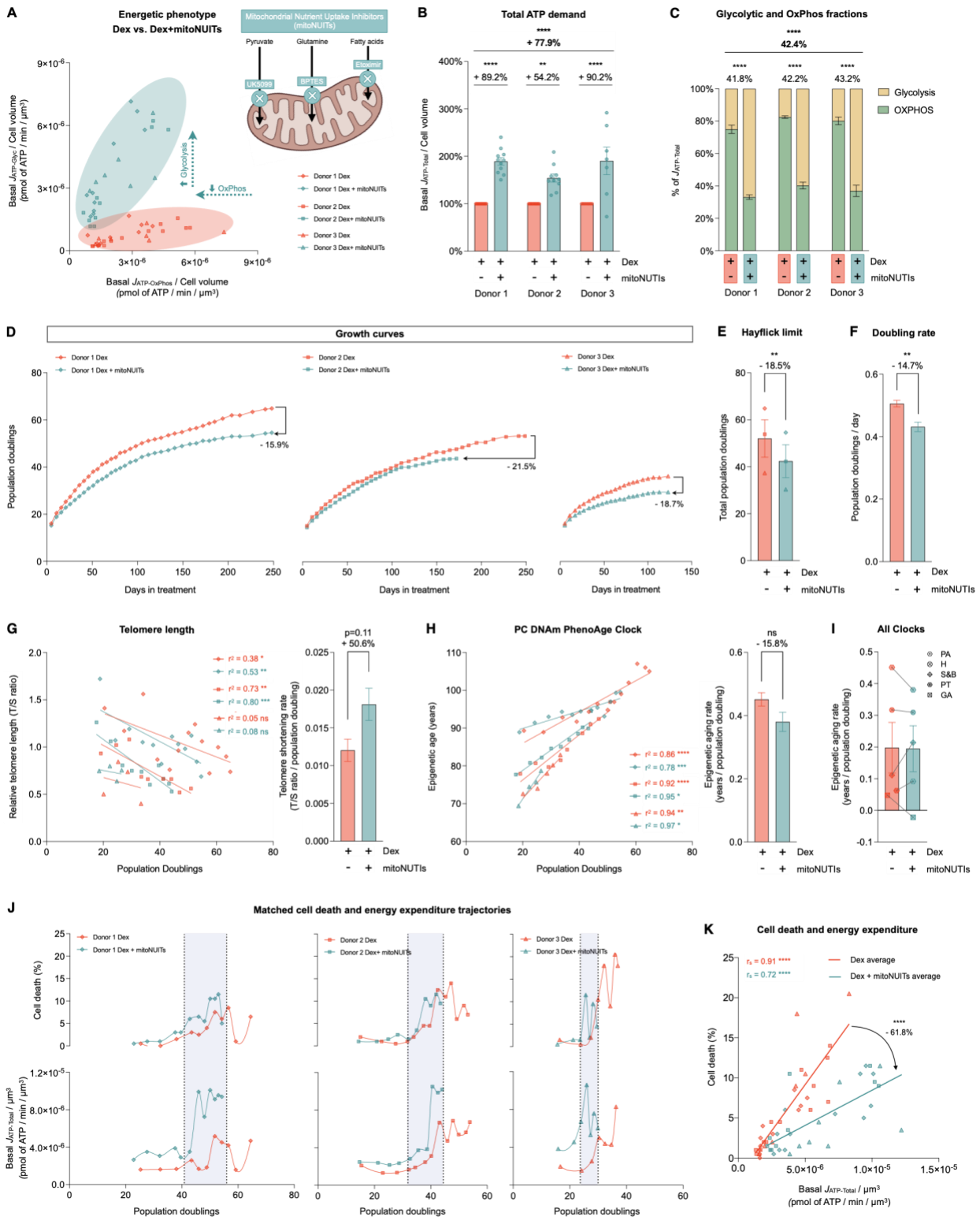

Figure 9. Hypermetabolism, not the metabolic shift towards OxPhos, predicts cell death

(**A**) Energetic phenotype of cells treated with Dex and Dex+mitoNUITs defined by Basal $J_{ATP\text{-}OxPhos}$/cell volume and Basal $J_{ATP\text{-}Glyc}$/cell volume across lifespan. (**B**) Lifespan average effects of Dex+mitoNUITs treatment on $J_{ATP\text{-}Total}$/cell

volume. (**C**) Values across lifespan (left panel) and average effects (right panel) of basal $J_{ATP\text{-}Glyc}$ (yellow) and basal $J_{ATP\text{-}OxPhos}$ (green) expressed as percentage of basal $J_{ATP\text{-}Total}$. (**D**) Lifespan trajectories of cumulative population doublings. (**E**) Hayflick limit for each donor of each group. (**F**) Group averages of early life doubling rate, inferred by a linear mixed model of the population doubling trajectories within the first 50 days of treatment. (**G**) Telomere length across population doublings, with simple linear regressions for each donor of each group (left panel), and group average telomere shortening rate inferred by linear mixed model along the whole lifespan (right panel). (**H**) Epigenetic age calculated by the principal components (PC)-adjusted PhenoAge epigenetic clock, with simple linear regressions for each donor of each group (left panel), and group average epigenetic aging rate inferred by linear mixed model along the whole lifespan (right panel). (**J**) Epigenetic aging rate for all the PC-adjusted epigenetic clocks evaluated: PA: Pheno Age, H: Hannum, S&B: Skin and Blood, PT: Pan Tissue, GA: Grimm Age. (**K**) Percentage of dead cells (upper panels) and basal $J_{ATP\text{-}Total}$/cell volume (lower panels) across population doublings for Donor 1 (left panels), Donor 2 (middle panels), and Donor 3 (right panels). (**H**) Correlation between proportion of dead cells in every passage and Basal $J_{ATP\text{-}Total}$/cell volume. n = 3 donors per group; timepoints per donor: n=7-11 in B-C, n = 26-36 in D, n = 4-14 in G-H, n = 8-13 in J-K. Lifespan average graphs are mean ± SEM, two-way ANOVA in B, Satterthwaite method in E, F, H, and I. Correlation graphs show Spearman r and thick lines represent simple linear regression for each group. * $p < 0.05$, ** $p < 0.01$, *** $p < 0.001$, **** $p < 0.0001$, ns: not significant. mitoNUITs: Mitochondrial nutrient uptake inhibitors. $J_{ATP\text{-}Glyc}$: ATP production rate derived from glycolysis. $J_{ATP\text{-}OxPhos}$: ATP production rate derived from OxPhos. $J_{ATP\text{-}Total}$: algebraic sum of $J_{ATP\text{-}Glyc}$ and $J_{ATP\text{-}OxPhos}$.

However, the DNAm clocks-based rates of aging were not different between Dex and Dex+mitoNUITS (**Fig. 9H and 9I**), pointing either to potential mechanistic divergences or to a ceiling effect already achieved with Dex for epigenetic clocks.

In relation to cell death, the Dex+mitoNUITs treatment combination further left-shifted both the mortality and energy expenditure trajectories towards an earlier onset along the lifespan (**Fig 9J**), indicating a trend towards increased cell death compared to Dex alone (+28.6%, p=0.09). Again, the temporal correlation between energy expenditure and death across the lifespan remained strong and significant in Dex+mitoNUITs-treated cells (r_s=0.72-0.91, p<0.001, **Fig. 9K**). Thus, diverting energy flux from OxPhos and elevating hypermetabolism with Dex+mitoNUITs treatment further exacerbated allostatic overload and age-related outcomes, implicating hypermetabolism, rather than flux through OxPhos, as the main driver of chronic stress-induced cellular allostatic overload. In summary, our findings define the effects of chronic GC stress on cellular, bioenergetic, and molecular recalibrations in primary human fibroblasts, highlighting increased energy expenditure (i.e., hypermetabolism) and accelerated cellular aging as interrelated, cell-autonomous features of allostatic load (**Fig. 10**).

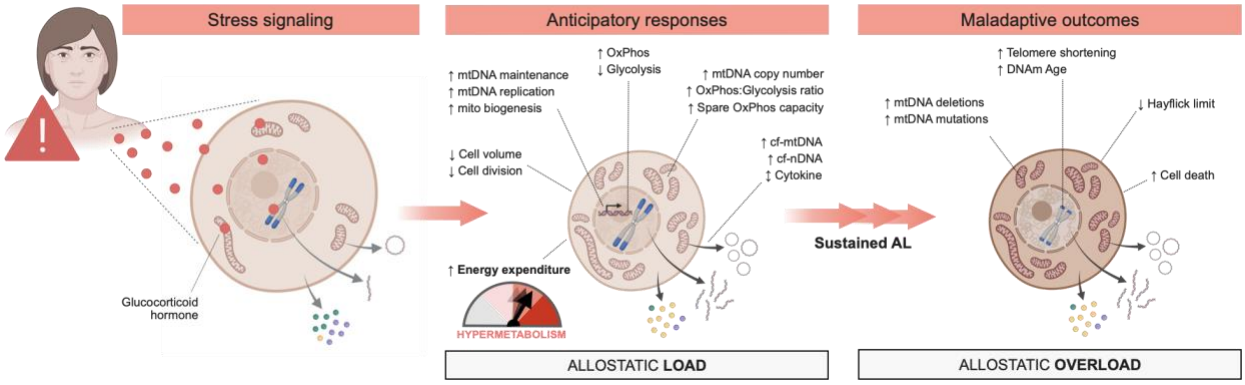

Figure 10. Summary diagram
Proposed model for the transduction of glucocorticoid signaling into cellular allostatic load and its interrelated cellular features, and the chronic downstream consequences of allostatic overload on cellular aging.

2.4. Discussion

Although in humans the long-term effects of chronic stress on clinical outcomes such as cognitive and functional decline are well documented (*354*, *355*), our understanding of how allostatic load manifests at the cellular level has remained incomplete. Our *in vitro* findings highlight hypermetabolism as a core manifestation of allostatic load, providing to our knowledge the first quantitative estimate of the energetic cost of allostatic load, increasing energy expenditure by >60% in this cellular model. Furthermore, our longitudinal data using well-established biological age indicators validated in humans such as mtDNA instability, telomere length, and epigenetic clocks, also link hypermetabolism to accelerated aging biology as features of cellular allostatic overload. Lastly, stress-induced hypermetabolism was tightly linked to the time of cell death, similar to the associations with mortality observed in humans. Thus, our results demonstrate that glucocorticoid signaling triggers energy-dependent allostatic recalibrations, which translates into age-related signs of allostatic overload. These results align with recent evidence of chronic stress pathophysiology in humans (*280*) and fill an important knowledge gap by defining the

cellular and sub-cellular features of the original allostatic load model of chronic stress from McEwen and Stellar (*4*).

In healthy individuals, acute psychological stress associated with elevated cortisol increases whole-body energy expenditure by 9-67% (*128*). Previous *in vitro* work in cultured rat neurons indicated that GC signaling could influence mitochondrial membrane potential over 72 hours (*142*), providing a basis for our first hypothesis that chronic GC stress could have long-term cellular bioenergetic consequences. Our cellular lifespan data allowed us to quantify the long-term, persistent cost of the anticipatory allostatic load. Our main finding is that it costs fibroblasts chronically exposed to Dex more energy (+62%) to sustain life, and remarkably more (+108%) to undergo each cell division. Plotting total energy consumption together with cell death also revealed a striking shift – potentially reflecting the transition from allostatic load to allostatic overload, where hypermetabolism and cell death were closely associated. Further work will be required to establish whether there is a causal link between hypermetabolism and fibroblast mortality. We note that relative to Dex, although the partial re-routing of metabolic flux to glycolysis with mitoNUITs did not rescue and in fact exacerbated the premature mortality phenotype (+28.6% mortality compared to Dex alone), it reduced the slope of the association between hypermetabolism and cell death (61.8%, $p<0.001$, *see* Fig. 9K). This relatively substantial shift may point to adaptive processes whereby cells are able to tolerate higher levels of hypermetabolism when deriving a portion of their energetic needs through both major pathways (OxPhos and glycolysis) (*358*), rather than through a single pathway. Nevertheless, our findings highlight the primary importance of total energy expenditure rather than of either pathway as a potential driver of allostatic overload. Because our *in vitro* system consists of isolated cells, the observed effects must be cell-autonomous – meaning that they occur independent of inter-organ crosstalk, of the

brain, and of other stress mediators encountered *in vivo*. This supports the idea that allostatic load is not a unique phenomenon of brain-bearing, complex multi-organ organisms. Instead, our findings point to allostatic load and allostatic overload as conserved processes able to manifest at the single-cell level. Thus, the evolution of allostasis and allostatic load likely predated the evolution of the brain (*421*).

These results also begin to address potential mechanisms for how chronic GC stress causes hypermetabolism. Our data directly rules out three major potential confounders, namely cell volume, division rate, and mitochondrial OxPhos uncoupling. Larger and faster-dividing cells would require greater ATP demand. However, we found that chronically stressed cells under allostatic load were significantly smaller and divided significantly more slowly (possibly as an attempt to curtail the rising energetic cost arising from the demands of allostatic load). Within mitochondria, increased proton leak across the inner mitochondrial membrane, which uncouples respiration from ATP synthesis, can also drive cellular energy expenditure (*422*). However, our data show that Dex-treated cells exhibit equal coupling efficiency than controls, ruling out this process as a cause of hypermetabolism in this system. Thus, our results implicate other active cellular processes as potential contributors to the increased "load" or energetic cost of living.

This state of hypermetabolism is likely driven not by a single process or signaling pathway, but by a multitude of interrelated processes. The major energetic costs within cells arise from gene transcription and translation (*423, 424*), from the maintenance of the plasma membrane potential, and additional costs arising from protein (i.e., cytokine) secretion (*425*). The biogenesis of organelles is also expected to consume large amounts of ATP (*426*). This is particularly true for mitochondria, which contain large proteomes whose synthesis entails substantial energy expenditure and requires genome replication (*426*). Furthermore, the heteroplasmic mixture of

mutant and normal mtDNA molecules caused by mtDNA instability is predicted to directly increase the energetic cost of organelle maintenance (*427*). This cost may be particularly substantial in cells that upregulate mitochondrial biogenesis to build and sustain spare OxPhos capacity, well in excess of basal needs, as in our fibroblasts under allostatic load. Adding to these maintenance costs, our results revealed elevated extracellular secretion of cytokines and cf-mtDNA. Thus, the increases in mtDNAcn, the modest levels of mtDNA heteroplasmy, and secretion-related costs observed across the lifespan may all contribute to the increased energetic cost of living in Dex-treated fibroblasts. Additional work is required to determine the specific sequence of events whereby a neuroendocrine signal such as GC signaling leads to hypermetabolism and the degree to which more complex stressors, such as chronic psychosocial stress, trigger hypermetabolism in whole animals, including in humans (*128*).

Another open question concerns the link between hypermetabolism and the reduced cellular lifespan that reflects allostatic overload. Our data cannot definitively establish directionality: does hypermetabolism cause the premature aging phenotype, or do accelerated biological aging processes drive increased energy expenditure? Nevertheless, to begin addressing this question we can consider two relevant bodies of literature: allometric scaling of metabolic rates and lifespan, and prospective studies of energy expenditure and mortality in humans.

First, there are well-defined relationships among body size, energy expenditure, and aging between animal species. These relationships show that animals of smaller sizes (e.g., mice, shrews) have correspondingly higher metabolic rates, age faster, and predictably live shorter lives than larger mammals (e.g., elephants) (*428-430*). Body weight and lifespan between animal species also scale linearly with the rate of telomere shortening, meaning that smaller animals with higher metabolic rates (i.e., relative hypermetabolism) exhibit correspondingly faster telomere shortening

rates (*415*). These inter-species regularities, to which there are notable exceptions (*431, 432*), are at least superficially analogous to our human fibroblast data. Dex-induced allostatic load shifted cells towards a smaller cell size, correspondingly accelerated their mass-specific metabolic rates, and accelerated the rate of telomere shortening and epigenetic aging, thus predictably resulting in a shortened lifespan.

The second relevant body of literature prospectively links hypermetabolism, measured as elevated basal metabolic rate (BMR), with health outcomes and mortality in humans. Among healthy individuals, independent of well-recognized risk factors (e.g., age, body mass index, smoking, white blood cell count, and diabetes), hypermetabolism is associated with poor health in older individuals (*121*). In two other cohorts, elevated BMR also predicted earlier mortality over the subsequent 20-25 years (*119, 120*). Similarly, in patients with various illnesses (hepatitis B, amyotrophic lateral sclerosis, type 2 diabetes, and cancers), hypermetabolism predicts worse prognosis and mortality (*122-125*). Thus, we propose a model where hypermetabolism reflects the magnitude of allostatic load – i.e., how much energy cells and organisms are expending to maintain stable physiology. For reasons that still lack a molecular basis, hypermetabolism subsequently drives the accumulation of molecular damage and sub-cellular manifestations of allostatic overload, which accelerate biological aging and drive early mortality. This is recapitulated in cells and in patients with primary OxPhos defects, where genetically- or pharmacologically-induced hypermetabolism is associated with accelerated aging and shortened lifespan (*126*). The damaging nature of hypermetabolism may relate to general constraints on total energy flux imposing limits on molecular operations (i.e., Gibbs free energy dissipation rate (*433*)), or to intracellular tradeoffs between competing energy-consuming processes (*128*), although more work is required to understand how such constraints operate in human cells. One potential mechanism linking

hypermetabolism and accelerated aging may involve oxidative stress, which is associated with psychosocial stress in humans (*137, 434, 435*), is induced by stress paradigms in animal models (*436-440*) and may play a role as one of the hallmarks of aging (*301*). Further studies are required to establish the directionality, modifiability, and mechanistic basis of this stress-hypermetabolism-aging cascade.

In relation to aging biology, our study makes two noteworthy observations. First, it confirms the usefulness of replicative cellular lifespan models (*441-443*) with high temporal resolution sampling as an experimental approach to quantify the chronic effects of allostasis on a number of cellular, bioenergetic, and molecular outcomes, with normal human cells. Moreover, deploying aging biomarkers validated in human populations to this *in vitro* system directly contributes to the interpretability of our findings and their potential physiological significance. Second, our relative telomere length data revealed that the loss of telomeric repeats is not a fixed quantity per genome duplication event (i.e., cell division), but that these can be decoupled by chronic stress exposure. The accelerated erosion of telomeric repeats per cell division caused by Dex implicates an effect of GC-mediated allostatic load on genomic stability, or on other aspects of telomere maintenance. Another study of Dex-treated human fibroblasts (one fibroblast line, aged for up to 51 days) reported no effect of cortisol or Dex on the rate of telomere shortening *per day in culture* (*444*). Our study (three donors, aged for up to 250 days) agrees with this observation when telomere shortening is expressed per day in culture. However, taking into account the reduced cell division rate revealed a markedly accelerated rate of shortening per event of genome replication, which we regard as the most relevant independent variable to understand telomere maintenance. Thus, future studies monitoring cell divisions over sufficiently long periods have the

potential to uncover connections between neuroendocrine stress exposure, hypermetabolism, and cellular aging.

Finally, some limitations of our study should be noted. While the epigenetic clocks can act as accurate molecular biomarkers of epigenetic age in several cell types and models, they still face challenges that make them less accurate in some models (*270*). Here, we used the PC clocks approach which predicts age and age-related phenotypes utilizing principal components rather than individual CpGs (*412*). This approach stabilizes test-retest reliability and improves the mortality prediction of classic DNAm clocks (*412*). In relation to our cellular model, compared to convenient immortalized cell lines, or to an experimental design that would include a single arbitrarily chosen donor, we noted substantial inter-individual variation among several measures between our three donors; Donor 1 was least affected, whereas Donor 3 was most affected on several variables. Unlike Donors 1 and 2 cells, which were obtained from the breast of healthy 18-year-old individuals, Donor 3 cells were obtained from the foreskin of a newborn who died prematurely shortly after birth (see *Methods* for details). This could have affected some of the basal cellular phenotype and responses to Dex, including the shorter lifespan of Donor 3. This variability likely reflects true inter-individual differences. Thus, although this multi-donor design increases experimental variability, it importantly guards against the overfitting of results to a single donor/cell line, and therefore likely yields more robust and generalizable findings. In relation to the stressor, whereas chronic psychosocial stressors in humans involve the action of multiple hormones and metabolic factors, Dex is admittedly a simplistic model of stress. Therefore, although this targeted glucocorticoid stressor provides a strong proof-of-concept of the cell-autonomous energetic and molecular consequences of allostatic load, additional studies with other (combinations of) stress mediators are warranted. Finally, our analyses of the RNA sequencing

and DNA methylation omics datasets are only partial, and more complete analyses of these data beyond the scope of the present manuscript could yield new insights into the global, longitudinal recalibrations and mechanisms underlying glucocorticoid-driven cellular allostatic load and the resulting allostatic overload. To examine these and related questions, the multi-omics dataset of chronic Dex is made available as a community resource (as well as other exposures, see *Data Availability Statement*) (*367*).

Finally, it is uncertain how the data in replicating cells reported here relates to cellular allostatic load in non-dividing, post-mitotic tissues. Our results documenting hypermetabolic, hypersecretory, and accelerated aging phenotypes are derived from actively replicating cells, which is similar to lymphoid and myeloid immune cells in the human body, but unlike the post-mitotic cells that populate several adult human tissues including the brain. We note that animal and human studies have demonstrated increases in whole-body energy expenditure in response to both acute (*98, 115*) and chronic stress (*105, 113*), collectively suggesting that stress-induced allostasis (cellular and systemic) are linked to hypermetabolism at the organism level (where most cells are post-mitotic). Moreover, the reported associations between perceived stress levels and the hallmarks of aging, including telomere shortening, DNA damage, mitochondrial impairments, cellular senescence, and inflammatory markers, appear to occur in both mitotic cells such as bone marrow leukocytes and thymocytes, as well as in post-mitotic brain tissue from different cortical and subcortical areas, including pre-frontal complex, amygdala and hippocampus (reviewed in (*299*)). Comparing metabolic and aging indicators longitudinally in both replicative and non-replicative cells could provide additional insights into the generalizable manifestations and mechanisms of cellular allostatic load.

In summary, we have defined multiple cell-autonomous features of GC-induced allostatic load and mapped the long-term consequences associated with cellular allostatic overload in primary human fibroblasts. *First*, our work quantifies the added energetic costs of chronic anticipatory responses at the cellular level, thereby defining hypermetabolism as a feature of allostatic load. *Second*, we describe a hypersecretory phenotype that may contribute to hypermetabolism and mirrors findings from clinical studies. *Third*, we document manifestations of mitochondrial and cellular allostatic load including elevated mtDNA copy number and mtDNA density per cell, mtDNA instability, accelerated telomere shortening, and epigenetic aging per cell division. In particular, we report a robust and specific temporal association between hypermetabolism and premature cell death, aligning with prospective observations in the human literature where hypermetabolism increases mortality risk. Finally, our experimental modulation of OxPhos and total J_{ATP} suggests that total energy expenditure, rather than flux through mitochondrial OxPhos, may have a particularly influential effect on cellular aging. Elucidating the mechanisms linking stress exposure, hypermetabolism, and shortened cellular lifespan will require further experimental work, as well as subsequent extension to well-controlled human studies. Resolving the cellular and bioenergetic basis of allostatic load and chronic stress biology should reveal bioenergetic principles that can be leveraged to increase human resilience and health across the lifespan.

2.5. Methods

Human fibroblasts

Primary human fibroblasts of 3 healthy donors were obtained from certified distributors and described in detail in (*367*). A portion of lifespan data for the control (untreated) group was reported in (*126*). The characteristics of the three cell lines are summarized in Table 1. The ‘age’

column indicates the age of the donor at the time of the tissue biopsy. During the course of the experiments, it came to our attention that Donor 3 was likely unhealthy since he had died prematurely of unknown cause 4 days after birth, which could have contributed to the variability in glucocorticoid responses and aging trajectories observed between the donors.

Table 1. Primary human fibroblast information

	Distributor	Catalog #	Genetic	Sex	Ethnicity	Age	Biopsy	Passage
Donor 1	Lifeline Cell Technology	FC-0024 Lot: 03099	Normal	Female	Caucasian	18 years	Dermal Breast	1
Donor 2	Lifeline Cell Technology	FC-0024 Lot: 00967	Normal	Male	Caucasian	18 years	Dermal Breast	1
Donor 3	Coriell Institute	AG01439	Normal	Male	Black	Newborn	Foreskin	4

Tissue culture

Cells were cultured under standard conditions of atmospheric O2, 5% CO2 and 37°C in DMEM (Thermo Fisher Scientific #10567022) supplemented with 10% Fetal Bovine Serum (FBS, Thermo Fisher Scientific), 50 μg/mL uridine (Sigma-Aldrich), 1% MEM non-essential amino acids (Thermo Fisher Scientific), and 10 μM-1.7 μM palmitate-BSA conjugate (Sigma-Aldrich). Treatment with dexamethasone (Dex, Sigma-Aldrich #D4902, 100 nM) and Dex plus the Mitochondrial Nutrients Uptake InhibiTors cocktail (Dex+mitoNUITs) began after 15-days of culturing post-thaw to allow the cells to adjust to the in vitro environment and were dosed every passage. The mitoNUITs cocktail included i) UK5099 (Sigma-Aldrich #PZ0160, 2 μM), an inhibitor of the mitochondrial pyruvate carrier (MPC) that interferes with the pyruvate import into the mitochondrial matrix ii) Etomoxir (Sigma-Aldrich #E1905, 4 μM), an inhibitor of carnitine palmitoyltransferase-1 (CPT-1) that interferes with the fatty-acid-derived Acyl-CoA import into the mitochondrial matrix; and iii) BPTES (Sigma-Aldrich #SML0601, 3 μM), an inhibitor of

glutaminase 1 (GLS1) that prevents the conversion of glutamine to glutamate into the mitochondrial matrix. The combined action of these three compounds ultimately abates the availability of the tricarboxylic acid cycle (TCA) to produce Acetyl-CoA.

Cells were passaged every 5 ± 1 days through standard procedure using Trypsin-EDTA 0.25% (Sigma-Aldrich #T4049). Cell counts and cell volume assessment were performed using 0.4% Trypan Blue Stain and the Countess II Automated Cell Counter (Thermo Fisher Scientific #AMQAF1000). Total cell counts were used to calculate the doubling rate at each passage, and to determine the number of cells needed to reach ~90% cell confluency by the time of the following passage. Cells not used for seeding or bioenergetic measurements were harvested and stored at -80°C for molecular analyses. Individual cell lines were terminated after exhibiting less than one population doubling over a 30-day period. The Hayflick limit was calculated as the cumulative number of population doublings of a cell line after termination. Brightfield microscopy images were obtained right before passaging using an inverted phase-contrast microscope (10X and 20X magnification, Thermo Fisher Scientific). The chronic Dex exposure experiments were performed once in each cell line. The reproducibility of the lifespan growth trajectories for each donor, and the reliability of specific outcome measures were established as described in (*367*).

Mycoplasma testing was performed according to the manufacturer's instructions (R&D Systems) on media samples at the end of lifespan for each treatment and cell line used. All tests were negative.

Bioenergetic parameters

The Seahorse XF Cell Mito Stress Test was performed in a XFe96 Seahorse extracellular flux analyzer (Agilent). ATP production rates derived from glycolysis ($J_{ATP\text{-}Glyc}$) and oxidative phosphorylation (OxPhos, $J_{ATP\text{-}OxPhos}$) were calculated from simultaneous measurements of

cellular oxygen consumption rate (OCR) and extracellular acidification rate (ECAR) on a monolayer of 20,000 cells, with 10-12 replicates per group. The experimental conditions were, in sequence, as follows: i) 1 μM oligomycin-A, ii) 4 μM FCCP, and iii) 1 μM rotenone and 1 μM antimycin-A (Sigma-Aldrich). Raw OCR and ECAR measurements were normalized by a Hoechst-based cell count for each well (Cytation1 Cell Imager, BioTek), which provided more robust (i.e., less well-to-well variation) and stable results than results normalized to protein content. As illustrated in Supplementary Material Fig. S1, Basal OCR, basal ATP-linked OCR, proton leak OCR, maximal OCR, maximal ATP-linked OCR, compensatory OCR, coupling efficiency, basal ECAR, maximal ECAR, and compensatory ECAR were then utilized to derive ATP production rates from glycolysis and OxPhos as described previously by Mookerjee et. al. (*374*). OCR and ECAR measurements in the absence of glucose (0mM) or with 2-deoxyglucose (2-DG) were performed to confirm the specificity of the ECAR signal in control primary human fibroblasts under these culture conditions (*126*).

mtDNA copy number

Cellular DNA was extracted using DNeasy Blood and Tissue Kit (Qiagen #69504). Duplex qPCR reactions with Taqman chemistry were used to quantify mitochondrial (mtDNA, ND1) and nuclear (nDNA, B2M) amplicons, as described previously (*445*). Primers and probes utilized were the following: ND1-Fwd: [5'-GAGCGATGGTGAGAGCTAAGGT-3'], ND1-Rev: [5'-CCCTAAAACCCGCCACATCT-3'], ND1-Probe: [5'-/5HEX/CCATCACCC/ZEN/TCTACATCACCGCCC/2IABkGQ/-3']; B2M-Fwd: [5'-TCTCTCTCCATTCTTCAGTAAGTCAACT-3'], B2M-Rev: [5'-CCAGCAGAGAATGGAAAGTCAA-3', B2M-Probe: 5'-/56-FAM/ATGTGTCTG/ZEN/GGTTTCATCCATCCGACCA/3IABkFQ/-3']. Each sample was

evaluated in triplicates. Triplicates with average Ct >33 were discarded. Triplicates with C.V. > 10% were also discarded. mtDNA copy number (mtDNAcn) was calculated as $2^{\Delta Ct}$ x 2, where ΔCt = average nDNA Ct - average mtDNA Ct.

mtDNA deletions and point mutations

Long-range PCR (LR-PCR) was performed with mtDNA extracted as described in the mtDNA copy number section. Isolated DNA was amplified by PCR using Hot Start TaKaRa LA Taq kit to yield a 10-Kb product (Takara Biotechnology, #RR042A). Primers utilized were the following: Fwd: [5'-AGATTTACAGTCCAATGCTTC-3'], Rev: [5'-AGATACTGCGACATAGGGTG-3']. PCR products were separated on 1% agarose gel electrophoresis in 1X TBE buffer, stained with GelGreen (Biotium #41005), and imaged using a GelDoc Go Imager (Biorad).

mtDNA next-generation sequencing was used to identify and quantify deletions and point mutations. The entire mtDNA was obtained through the amplification of two overlapping fragments by LR-PCR, using Kapa Long Range DNA polymerase according to the manufacturer's recommendations (Kapa Biosystems). The primer pairs utilized were tested first on Rho zero cells, devoided of mtDNA, to remove nuclear-encoded mitochondrial pseudogene (NUMTS) amplification. Primers utilized were the following: PCR1: Fwd: [5'-AACCAAACCCCAAAGACACC-3'], Rev: [5'-GCCAATAATGACGTGAAGTCC-3']; PCR2: Fwd: [5'-TCCCACTCCTAAACACATCC-3'], Rev: [5'-TTTATGGGGTGATGTGAGCC-3']. PCR products were separated on a 1% agarose gel electrophoresis and NGS Libraries were generated using an enzymatic DNA fragmentation approach with Ion Xpress Plus Fragment Library Kit (Thermo Fisher Scientific). Sequencing was performed using an Ion Torrent S5XL platform with an Ion 540 chip, and signal processing and base calling were performed through the

pre-processing embedded in house pipeline as described elsewhere (*446*). Demultiplexed reads were mapped according to the mtDNA reference sequence (NC_012920.1), and further analysis was performed through the eKLIPse pipeline (*397*) (https://github.com/dooguypapua/eKLIPse).

RNA sequencing and transcriptomic analysis

Cells were lysed and stored at -80°C in TRIzol (Thermo Fisher Scientific). RNA isolation of all samples was performed as a single batch using a RNeasy Kit (Qiagen). All samples had an RNA integrity number (RIN) score >8.0, a A260/A280 ratio between 1.8-2.2, and no detectable levels of DNA. cDNA library was prepared from 1,500 ng of RNA using QIAseq FastSelect – rRNA HMR Kit (Qiagen) and NEBNext® Ultra™ II RNA Library Prep Kit for Illumina (New England Biolabs). cDNA was sequenced using paired-end 150 bp chemistry on a HiSeq 4000 System (Illumina) and yielded an average sequencing depth of 40 million reads per sample. Sequenced reads were aligned using the pseudoalignment tool kallisto (*447*) (v0.44.0) and imported using the 'tximport' package (*448*) (v1.18.0). Variance stabilizing transformation (VST) was performed using the 'DEseq2' package (*449*) (v1.30.1). Heatmaps and time courses show transcript levels as the Log2 of fold change (Log2FC) of normalized expression relative to the corresponding control time point for each donor. Categorized genes were selected using MitoCarta 3.0 (*450*) and related literature on mitochondrial biogenesis (*376-379*).

Cell-free DNA

At each passage, culture media was collected, centrifuged at 500g for 5 min, and the supernatant stored at -80°C until analyses until samples were processed as a single batch. To avoid cellular contamination, thawed media was further centrifuged at 1000g for 5 min, and the supernatant transferred to 96-well plates. Total cell-free DNA (cf-DNA) was isolated from 75 µL

of cell culture media using an automated, high-throughput methodology based on the MagMAX Cell-Free DNA Isolation Kit (Thermo Fisher Scientific) that has been previously described (*451*). Duplex qPCR reactions with Taqman chemistry were used to simultaneously quantify mitochondrial (cf-mtDNA, ND1) and nuclear (cf-nDNA, B2M) amplicons, using the same primers and probes as described in the mtDNA copy number section. Serial dilutions of pooled human placenta DNA were used as a standard curve. mtDNA and nDNA copy number (copies/µL) of the standard curve samples were measured using singleplex, chip-based digital PCR (dPCR) on a Quant-studio 3D system (Thermo Fisher Scientific) according to the manufacturer's protocol. The obtained values were then used to calculate the copy number of the experimental samples from the standard curve.

Cytokines

Cytokine levels were quantified on the same culture media samples used for cf-DNA measurements. Two multiplex fluorescence-based arrays (R&D) were custom-designed with selected cytokines and chemokines whose levels in human plasma had been reported to be correlated with chronological age (*389*). Media samples were run along with negative controls (fresh untreated media), positive controls (healthy fibroblast aged for >200 days), and a standard curve following manufacturer's instructions (Luminex). Cytokine concentrations were then normalized to the number of cells counted at the time of media collection to generate estimates of cytokine production on a per-cell basis.

Relative telomere length

Relative telomere length was evaluated on the same genomic material used for other DNA-based measurements. Measurements were performed by single-plex qPCR reactions with SYBR

Green chemistry and expressed as the ratio of telomere to single-copy gene abundance (T/S ratio), as previously described (*452*, *453*). Primers utilized for the telomere (T) PCR were: tel1b: [5'-CGGTTT (GTTTGG)5GTT-3'], and tel2b: [5'-GGCTTG (CCTTAC)5CCT-3']. Primers utilized for the single-copy gene (human beta globin) PCR were: Fwd: [5' GCTTCTGACACAACTGTGTTCACTAGC-3'] and Rev: [5'-CACCAACTTCATCCACGTTCACC-3']. Each sample was evaluated in triplicates. Triplicates were subjected to Dixon's Q test for outlier removal, and averaged values of T and S were used to calculate the T/S ratios. T/S ratio for each sample was measured twice. When duplicates showed C.V. > 7%, the sample was run a third time and the two closest values were used.

DNA methylation and DNAmAge

Global DNA methylation was evaluated on the same genomic material used for other DNA-based measurements. DNA samples were submitted to the UCLA Neuroscience Genomic Core (UNGC) for bisulfite conversion and hybridization using the Infinium Methylation EPIC BeadChip kit (Illumina). DNA methylation data was processed in R (v4.0.2), using the 'minfi' package (*454*) (v1.36.0). Data was normalized using functional normalization (Fun Norm), and RCP and ComBat adjustments were applied using the 'sva' package (*455*) (v3.12.0) to correct for probe-type and plate bias, respectively.

Original DNAmAge was calculated using the online calculator (https://dnamage.genetics.ucla.edu/new) with normalization, using the age of the donor as the input age. This outputted the Horvath1 (i.e., PanTissue clock), Horvarth2 (i.e., Skin&Blood clock), PhenoAge, Hannum, and GrimAge estimated DNAmAges. More recent versions of the epigenetic clocks based on shared extracted variances among CpGs from principal components were also computed, yielding the PC-based DNAmAges for each clock (*412*). Stable estimates of the rate of

epigenetic aging were obtained from the linear regression for each cell line between 27 to 210 days of growth, yielding three values per treatment condition.

Statistical analyses

All statistical analyses were performed using GraphPad Prism (v9.0) and R (v4.0.2) using RStudio (v1.3.1056). All analyses were restricted to matching timepoints between control and the Dex or Dex+mitoNUITs treatments from the CellularLifespan dataset (*367*). In graphs of lifespan trajectories, datapoints are connected using the Akima spline curve. Lifespan average graphs show each passage as a single datapoint, and bars represents mean ± standard error of the mean (SEM). The percent differences between groups (i.e., Control vs Dex; or Dex vs mitoNUITs) was computed separately for each cell line (i.e., Donors 1, 2, 3), and groups were compared by two-way ANOVA treating each timepoint as a unique observation. Analyses of gene expression (i.e., HK2, PFK, UQCRC1, COX7A1, POLQ, PPARGC1A, and NRIP1, TPP1, TERC) were similarly performed by two-way ANOVA across all donors, without adjustment for multiple comparisons. To analyze temporal associations between variables, we performed non-parametric Spearman correlation, and report the correlation coefficient rs. To obtain proportions of shared variance between variable pairs, the squared coefficient of correlation from simple linear regression was calculated. To estimate the average expression of transcriptional pathways, the average Log2 fold change values of each gene were averaged across all timepoints of the lifespan of three donors, and p values obtained using a one-sample t-test against the reference value = 0 (i.e., no change in expression relative to control). For analyses of the Hayflick limit, a single value was obtained per donor (total n=3), and group averages were compared using ratio paired t-test (two-tailed). Because of the small sample sizes for these outcomes the p values are less reliable than the estimated differences (%) across multiple aging biomarkers. For analysis of the early-life doubling rate (i.e.,

first 50 days in treatment), doubling rate was modeled with linear mixed models using the lme4 package v1.1-26 (*456*) with fixed effects for population doublings, treatment condition (Dexamethasone vs. control), and their interaction. We used random intercepts at the cell line level:

$$DR_{ij} = (\beta_0 + b_{0i}) + \beta_1 * DIT_{ij} + \beta_2 * T_i + \beta_3 * DIT_{ij} * T_i + e_{ij}$$

Where DR is doubling rate, i, j are cell line and measurement respectively, β and b denote fixed and random effects, DIT is days in treatment, T is treatment condition (0 = Control, 1 = Dexamethasone), and e is error. We assessed statistical significance using the Satterthwaite method implemented in the lmerTest package v3.1-3 (*457*). Analyses of telomere shortening rate and epigenetic aging rate were performed using linear mixed models in the same way described above, but across population doublings instead of days in treatment. The significance threshold for all analyses was arbitrarily set at 0.05, and effect sizes are provided throughout.

2.6. Additional information

Author contributions

G.S. and M.P. designed experiments. G.S. performed cellular lifespan studies. A.S.M. performed quality control experiments. B.S.S. performed alignment and quality control of transcriptomic data. G.S. measured mtDNAcn. S.A.D. and B.K. measured cf-mtDNA. K.R.K. performed cytokine arrays and LR-PCR. C.B., V.P., G.L. performed mtDNA sequencing. J.L. and E.S.E. measured telomere length. S.H., A.H.C., and M.L. contributed the original and PC-DNAm clocks. G.S and N.B.A curated the database. N.B.A. performed the data processing and prepared the figures. N.B.A. analyzed and interpreted the data with G.S. and M.P. N.B.A. drafted the manuscript with G.S. and M.P. All authors reviewed the final version of the manuscript.

Funding

This work was supported by NIH grants R35GM119793 and R01AG066828, the Wharton Fund, and the Baszucki Brain Research Fund to M.P., the Medical Informatics Fellowship Program at the West Haven, CT Veterans Healthcare Administration to A.H.C., and an Aviesan INSERM genomic variability project grant to VP.

Data availability statement

All data presented in this manuscript are available for download at our Cellular Lifespan Study shiny app: https://columbia-picard.shinyapps.io/shinyapp-Lifespan_Study. Additional information on source data and R code utilized for data processing are described in (*367*). Further information is available upon request from the corresponding author.

2.7. Supplementary Material

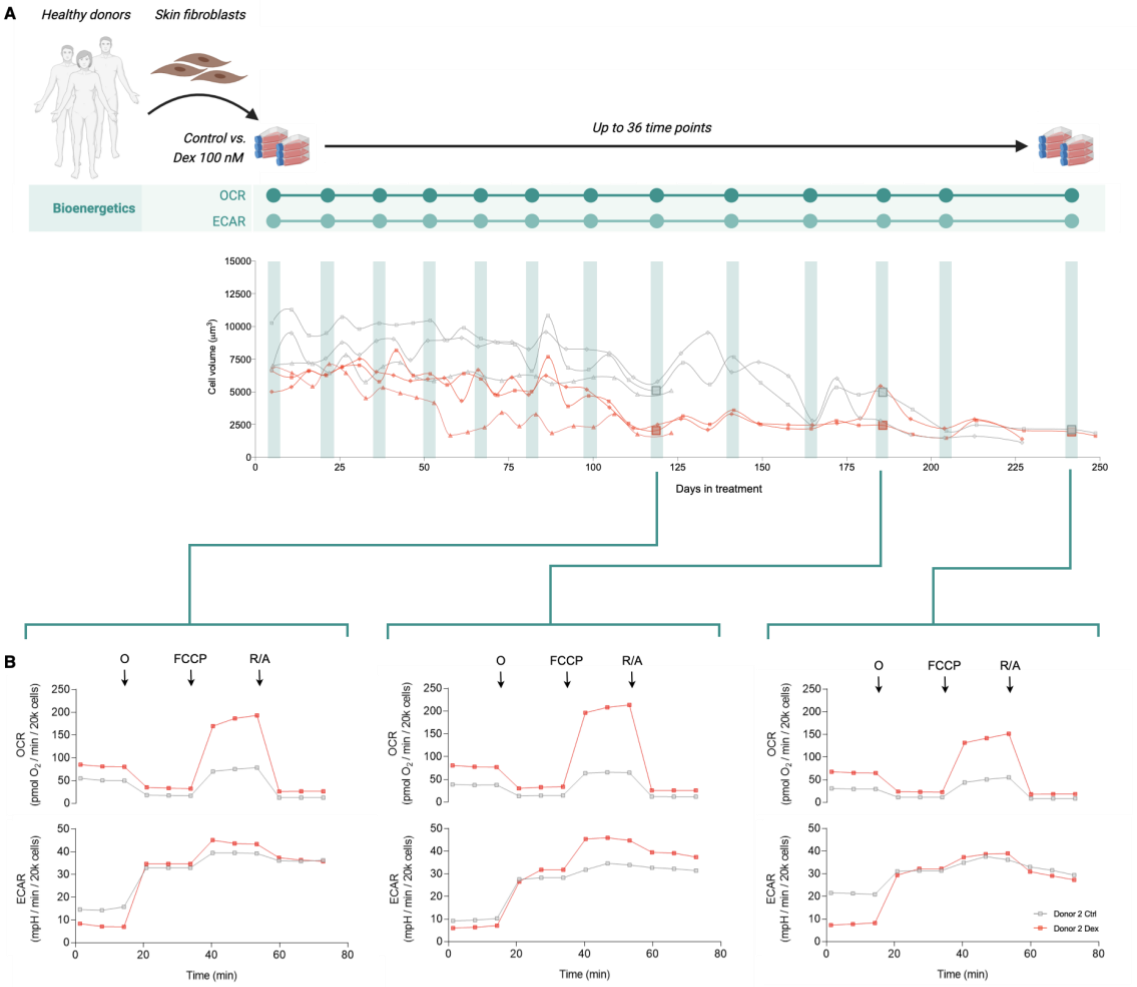

C

Basal $J_{ATP\text{-}Glyc}$	ATP production rate derived from glycolysis under basal conditions
Basal $J_{ATP\text{-}OxPhos}$	ATP production rate derived from OxPhos under basal conditions
Basal $J_{ATP\text{-}Total}$	ATP production rate derived from both glycolysis and OxPhos under basal conditions
Compensatory $J_{ATP\text{-}Glyc}$	ATP production rate derived from glycolysis under inhibition of OxPhos ATP production
Compensatory glycolytic capacity	Compensatory $J_{ATP\text{-}Glyc}$ expressed as a percentage of basal $J_{ATP\text{-}Total}$
Maximal $J_{ATP\text{-}OxPhos}$	ATP production rate derived from OxPhos under maximal respiratory activity
Spare $J_{ATP\text{-}OxPhos}$	ATP production rate derived from OxPhos under maximal respiratory activity without accounting for the basal $J_{ATP\text{-}OxPhos}$
Spare OxPhos capacity	ATP production rate derived from OxPhos expressed as a percentage of basal $J_{ATP\text{-}OxPhos}$

Figure S1. Evaluation of bioenergetic parameters

(**A**) Study design: primary human fibroblasts derived from three healthy donors (Donors 1, 2, 3) were cultured under standard conditions or chronically treated with Dexamethasone (Dex, 100 nM) across its lifespan for up to 150-250 days. Bioenergetics parameters were evaluated every 15-10 days by performing the Seahorse Mito Stress Test (Agilent). Green bars highlight the cell volume values the day prior to the test, which were then utilized to normalize the bioenergetic parameters. (**B**) Representative curves of cellular oxygen consumption rate (OCR) and extracellular acidification rate (ECAR) were obtained throughout the Seahorse Mito Stress Test (**C**)**.** Bioenergetic parameters that can be derived from ECAR and OCR curves in B. $J_{ATP\text{-}Glyc}$: ATP production rate derived from glycolysis. $J_{ATP\text{-}OxPhos}$: ATP production rate derived from OxPhos. O: Oligomycin. FCCP: Carbonyl cyanide-p-trifluoromethoxyphenyl-hydrazone. R/A: Rotenone/Antimycin A.

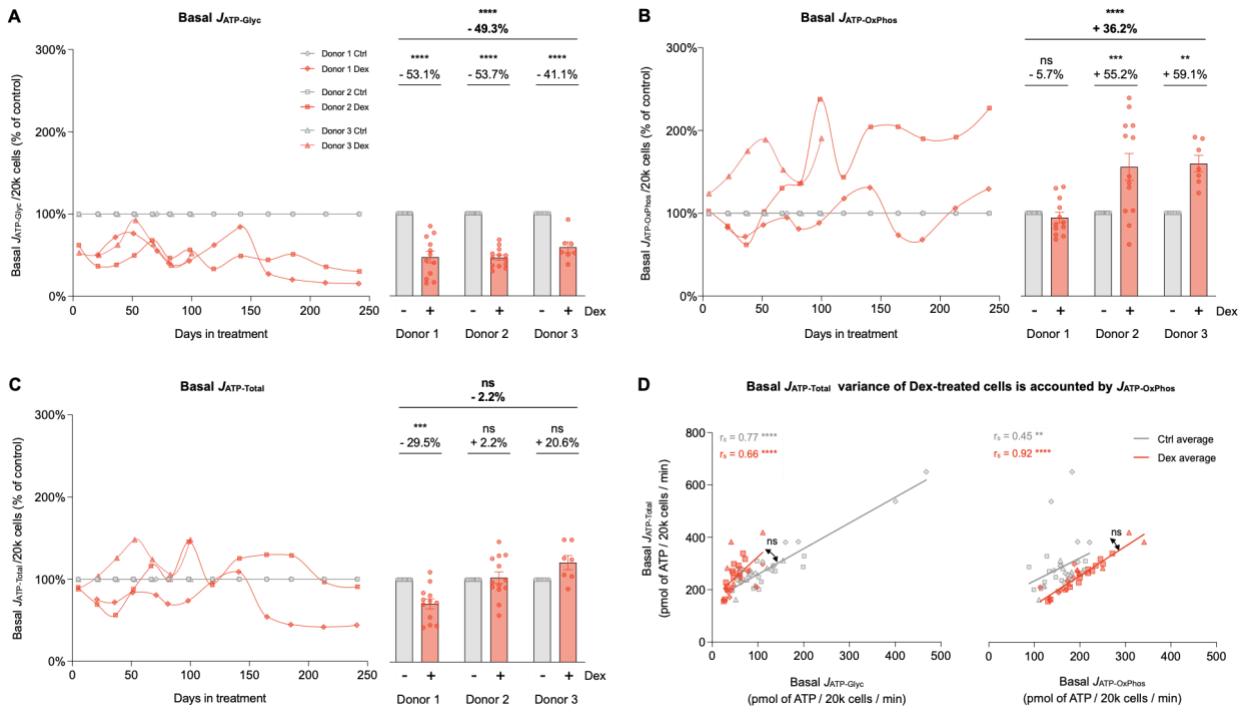

Figure S2. Effects of chronic glucocorticoid signaling on basal bioenergetic parameters

(A) Lifespan trajectories (*left* panel) and lifespan average effects (*right* panel) of Dex treatment on basal $J_{ATP-Glyc}$ /20k cells expressed relative to the corresponding control time points for each donor. (**B**) Same as A but for $J_{ATP-OxPhos}$/20k cells. (**C**) Same as A but for $J_{ATP-Total}$/20k cells. (**D**) Correlation between basal $J_{ATP-Total}$ and basal $J_{ATP-Glyc}$ (*left* panel) and between basal $J_{ATP-Total}$ and basal $J_{ATP-OxPhos}$ (*right* panel). n = 3 donors per group, 8-13 timepoints per donor. Lifespan average graphs are mean ± SEM, two-way ANOVA. Correlation graphs show Spearman r and thick lines represent simple linear regression for each group. ** p < 0.01, *** p < 0.001, **** p < 0.0001, ns: not significant. $J_{ATP-Glyc}$: ATP production rate derived from glycolysis. $J_{ATP-OxPhos}$: ATP production rate derived from OxPhos. $J_{ATP-Total}$: algebraic sum of $J_{ATP-Glyc}$ and $J_{ATP-OxPhos}$.

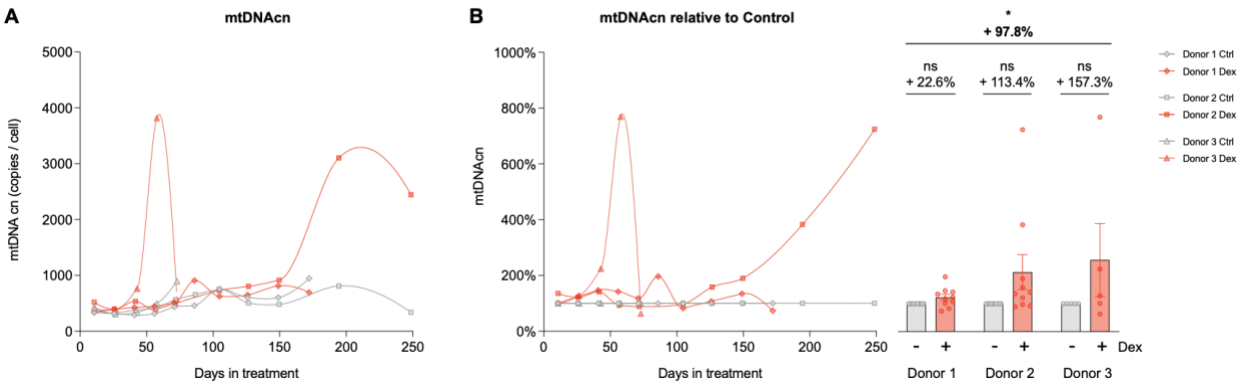

Figure S3. Effects of chronic glucocorticoid signaling on mtDNAcn

(**A**) Lifespan trajectories of Dex treatment on mtDNA copy number (mtDNAcn). (**B**) Lifespan trajectories (*left* panel) and lifespan average effects (*right* panel) of Dex treatment on mtDNAcn expressed relative to the corresponding control time points for each donor. n = 3 donors per group, 5-8 timepoints per donor. Lifespan average graphs are mean ± SEM, two-way ANOVA. * $p < 0.05$, ns: not significant.

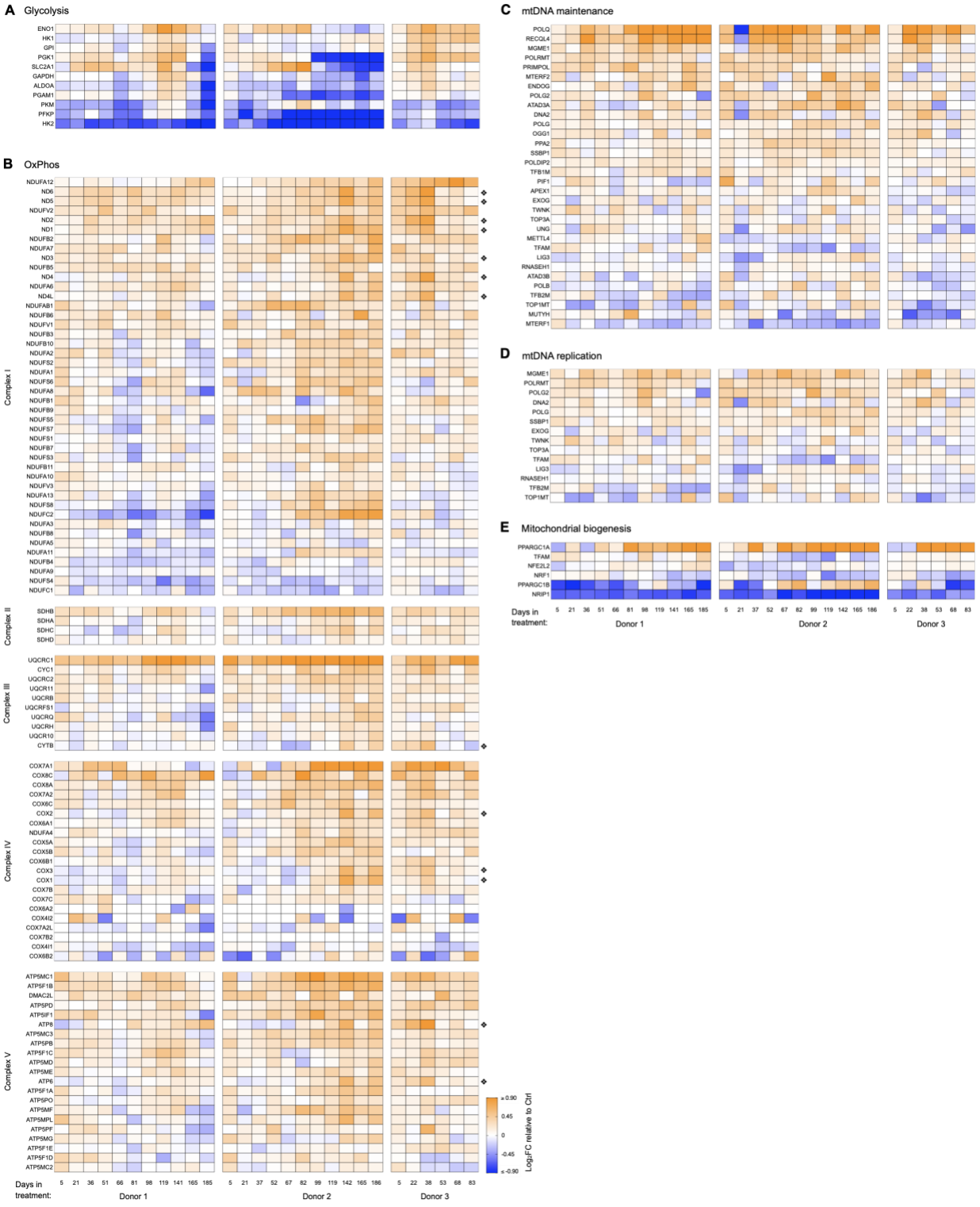
A Glycolysis
ENO1
HK1
GPI
PGK1
SLC2A1
GAPDH
ALDOA
PGAM1
PKM
PFKP
HK2
B OxPhos
NDUFA12
ND6
ND5
NDUFV2
ND2
ND1
NDUFB2
NDUFA7
ND3
NDUFB5
ND4
NDUFA6
ND4L
NDUFAB1
NDUFB6
NDUFV1
NDUFB3
NDUFB10
NDUFA2
NDUFS2
NDUFA1
NDUFS6
NDUFA8
NDUFB1
NDUFB9
NDUFS5
NDUFS7
NDUFS1
NDUFB7
NDUFS3
NDUFB11
NDUFA10
NDUFV3
NDUFA13
NDUFS8
NDUFC2
NDUFA3
NDUFB8
NDUFA5
NDUFA11
NDUFB4
NDUFA9
NDUFS4
NDUFC1
Complex I
SDHB
SDHA
SDHC
SDHD
Complex II
UQCRC1
CYC1
UQCRC2
UQCR11
UQCRB
UQCRFS1
UQCRQ
UQCRH
UQCR10
CYTB
Complex III
COX7A1
COX8C
COX8A
COX7A2
COX6C
COX2
COX6A1
NDUFA4
COX5A
COX5B
COX6B1
COX3
COX1
COX7B
COX7C
COX6A2
COX4I2
COX7A2L
COX7B2
COX4I1
COX6B2
Complex IV
ATP5MC1
ATP5F1B
DMAC2L
ATP5PD
ATP5IF1
ATP8
ATP5MC3
ATP5PB
ATP5F1C
ATP5MD
ATP5ME
ATP6
ATP5F1A
ATP5PO
ATP5MF
ATP5MPL
ATP5PF
ATP5MG
ATP5F1E
ATP5F1D
ATP5MC2
Complex V
Days in treatment:
5 21 36 51 66 81 98 119 141 165 185
Donor 1
5 21 37 52 67 82 99 119 142 165 186
Donor 2
5 22 38 53 68 83
Donor 3
≥ 0.90
0.45
0
-0.45
≤ -0.90
LogFC relative to Ctrl
C mtDNA maintenance
POLQ
RECQL4
MGME1
POLRMT
PRIMPOL
MTERF2
ENDOG
POLG2
ATAD3A
DNA2
POLG
OGG1
PPA2
SSBP1
POLDIP2
TFB1M
PIF1
APEX1
EXOG
TWNK
TOP3A
UNG
METTL4
TFAM
LIG3
RNASEH1
ATAD3B
POLB
TFB2M
TOP1MT
MUTYH
MTERF1
D mtDNA replication
MGME1
POLRMT
POLG2
DNA2
POLG
SSBP1
EXOG
TWNK
TOP3A
TFAM
LIG3
RNASEH1
TFB2M
TOP1MT
E Mitochondrial biogenesis
PPARGC1A
TFAM
NFE2L2
NRF1
PPARGC1B
NRIP1
Days in treatment:
5 21 36 51 66 81 98 119 141 165 185
Donor 1
5 21 37 52 67 82 99 119 142 165 186
Donor 2
5 22 38 53 68 83
Donor 3

Figure S4. Effects of chronic glucocorticoid signaling on gene expression

(**A-E**) Heatmaps from Figure 4 are shown with complete labeling for gene-specific resolution. (**A**) Heatmaps showing the effect of Dex treatment on the expression of glycolytic genes, expressed as the Log_2 of fold change (Log_2FC) of normalized gene expression relative to the corresponding control time point for each donor. (**B**) Same as A but for genes that encode for the subunits of Complex I, II, III, IV, and V (CI, CII, CIII, CIV, and CV) of OxPhos, with mitochondrial-encoded genes marked with ❖. (**C-E**) Same as A, but for genes associated with (**C**) mtDNA replication, (**D**) mtDNA maintenance, and (**E**) mitochondrial biogenesis. n = 3 donors per group, 9-10 time points per donor.

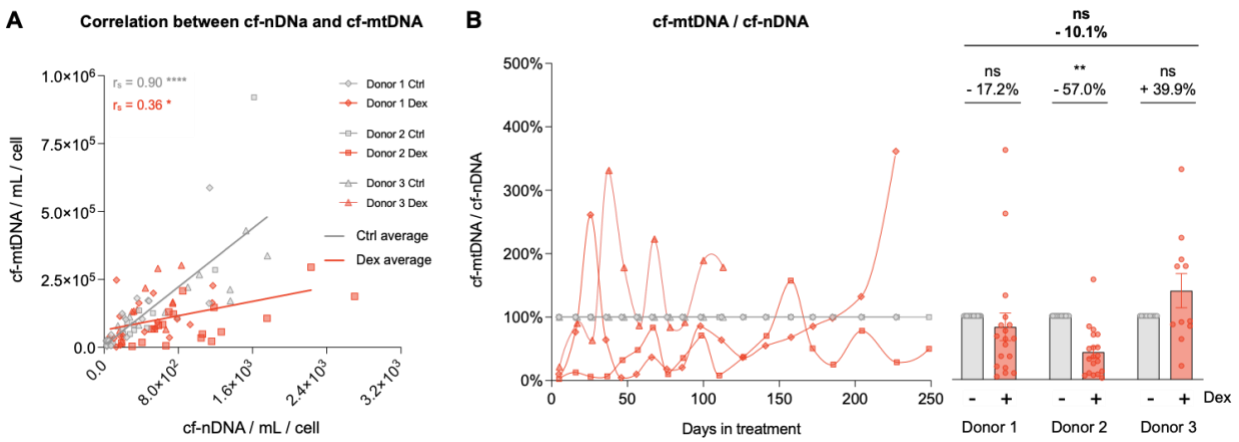

Figure S5. Effects of chronic glucocorticoid signaling on mtDNAcn

(**A**) Correlation between cell-free mitochondrial DNA (cf-mtDNA) and cell-free nuclear DNA (cf-nDNA). (**B**) Lifespan trajectories (*left* panel) and lifespan average effects (*right* panel) of Dex treatment on cf-mtDNA/cf-nDNA ratio expressed relative to the corresponding control time points for each donor. n = 3 donors per group, 6-10 timepoints per donor. Lifespan average graphs are mean ± SEM, two-way ANOVA. Correlation graphs show Spearman r and thick lines represent simple linear regression for each group. * $p < 0.05$, ** $p < 0.01$, **** $p < 0.0001$, ns: not significant.

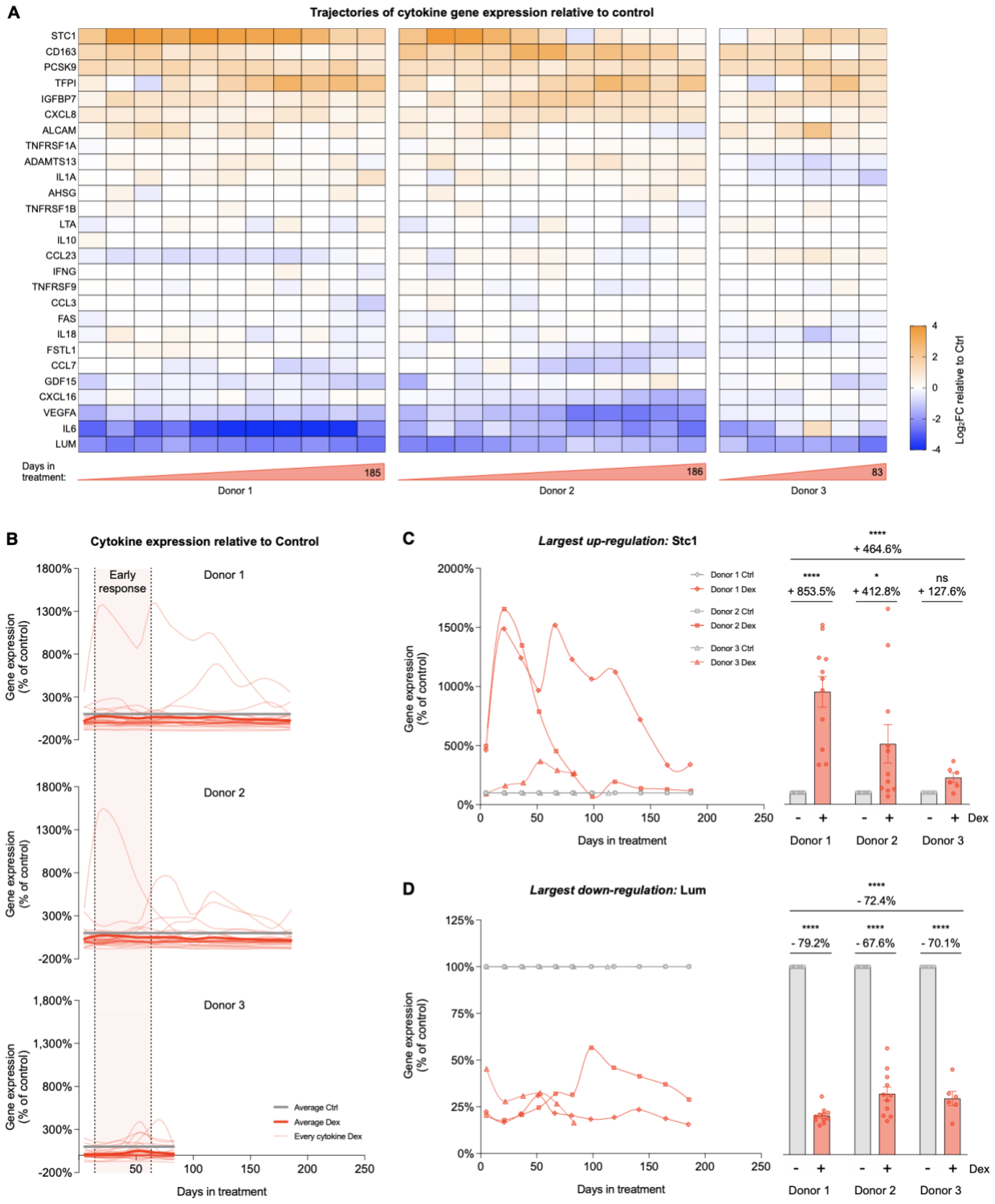

Figure S6. Effects of chronic glucocorticoid signaling on gene expression of age-related cytokines

(**A**) Heatmaps showing the effect of Dex treatment on the expression of age-related cytokines, expressed as the Log_2 of fold change (Log_2FC) normalized gene expression relative to the corresponding control time points for each donor. (**B**) Lifespan trajectories of gene expression in cells treated with Dex relative to the corresponding control time points for each donor. Thin curves in soft red represents individual cytokines; thick curves in red represent the average of all

cytokines evaluated; thick lines in gray represent the control level. (**C**) Lifespan trajectories (*left* panel) and average effects (*right* panel) of Dex treatment on *Stc1* gene (most upregulated gene) expression expressed relative to the corresponding control time point for each donor. (**D**) Same as C but for *Lum* gene (most downregulated gene). n = 3 donors per group, 9-10 timepoints per donor. Lifespan average graphs are mean ± SEM, two-way ANOVA. * $p < 0.05$, **** $p < 0.0001$, ns: not significant.

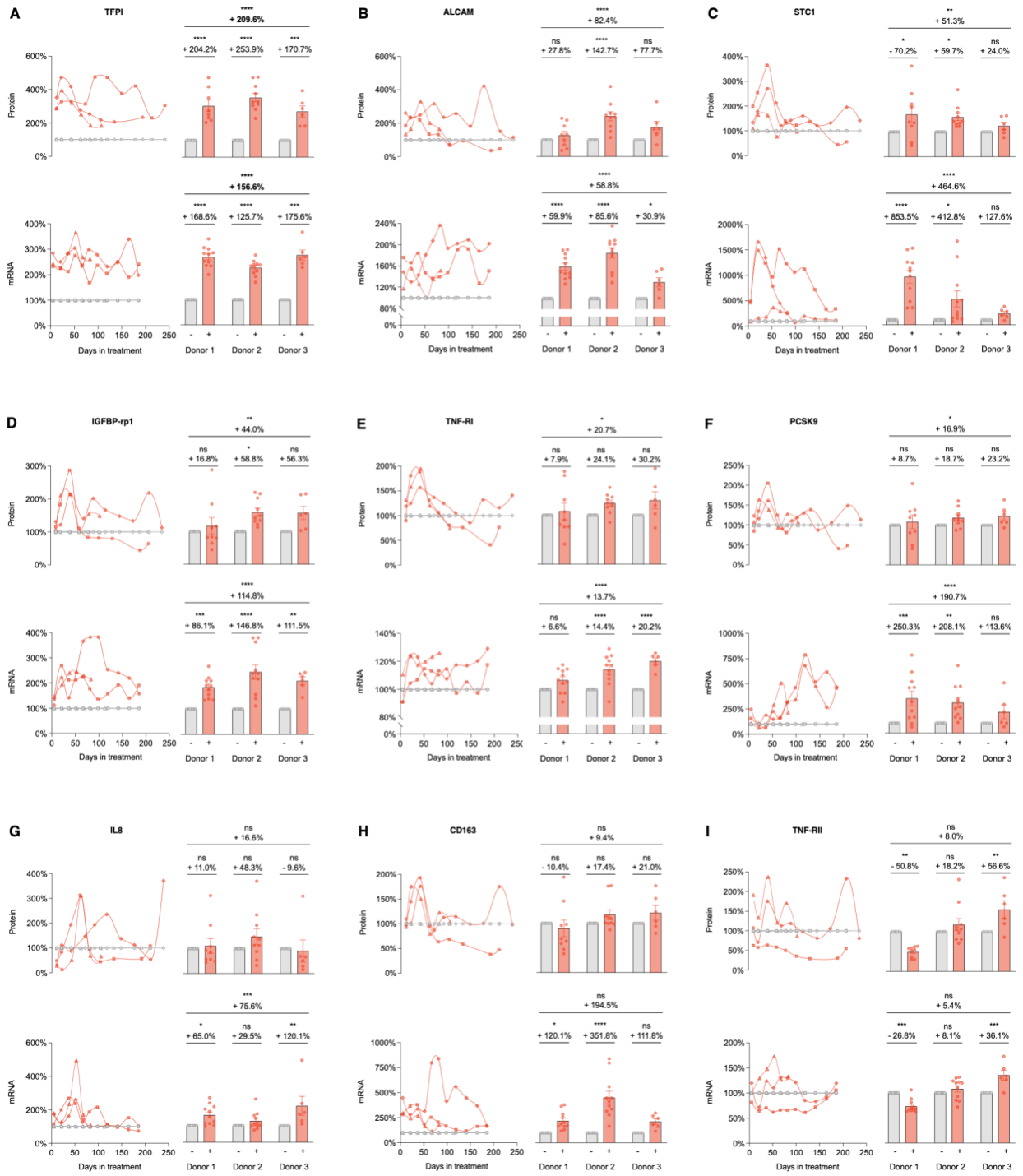

Figure S7. Effects of chronic glucocorticoid signaling on secretion and gene expression of age-related cytokines

(Continues on next page)

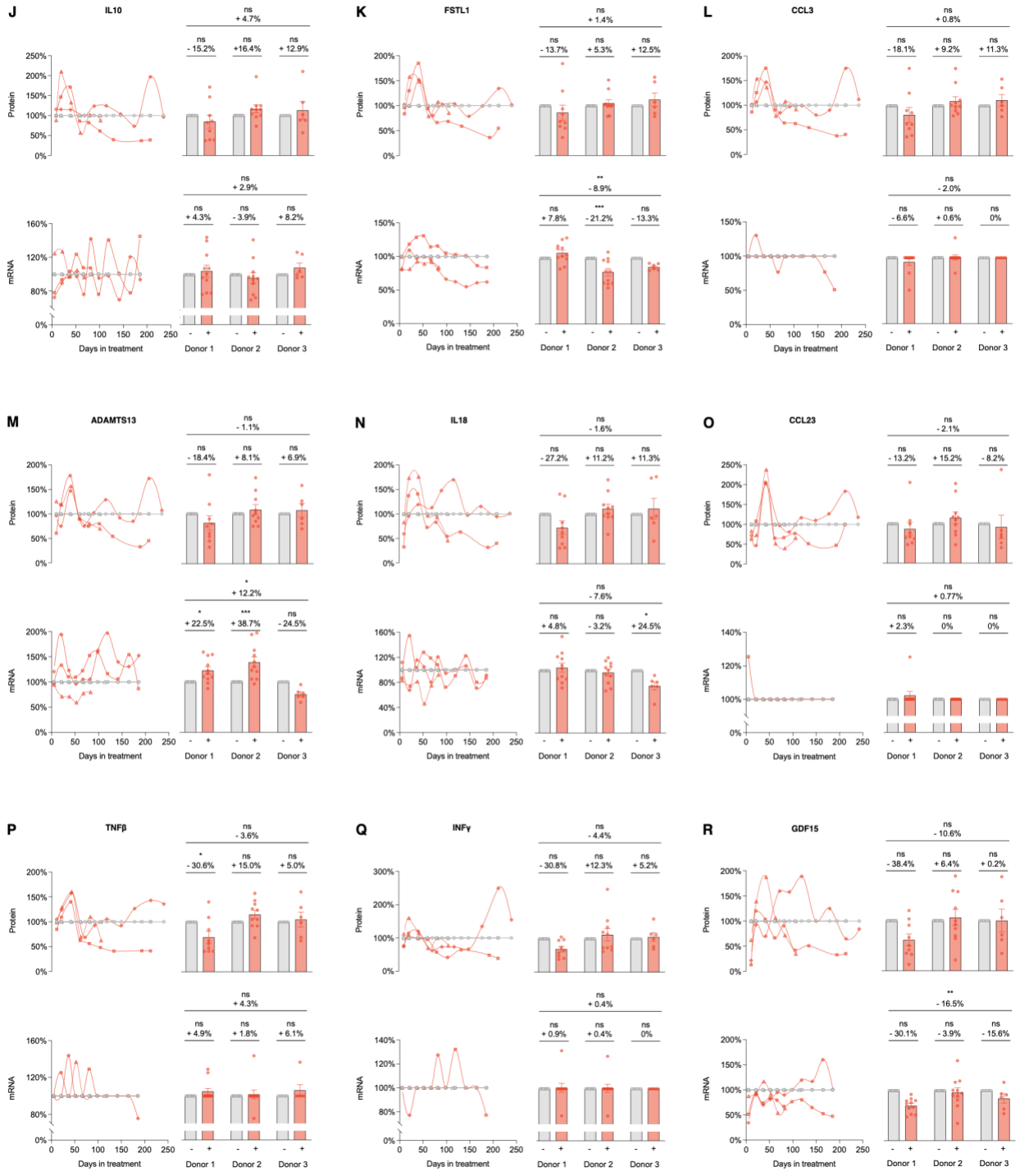

Figure S7. Effects of chronic glucocorticoid signaling on secretion and gene expression of age-related cytokines
(Continues on next page)

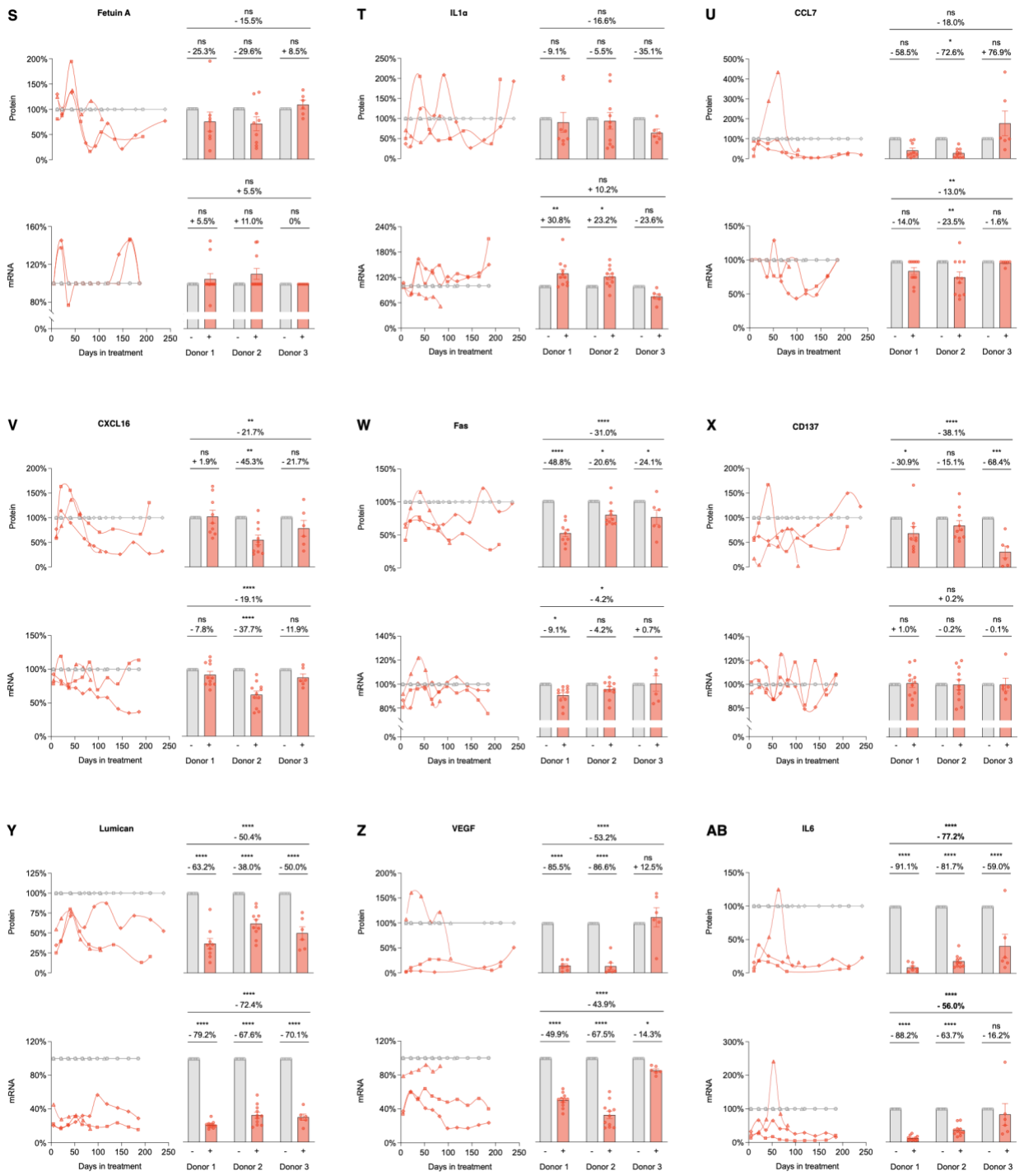

Figure S7. Effects of chronic glucocorticoid signaling on secretion and gene expression of age-related cytokines
(**A-AB**) Lifespan trajectories (*left* panel) and average effects (*right* panel) of Dex treatment on age-related cytokines levels per mL of culture media (u*pper* panel) and normalized gene expression (*lower* panel), expressed relative to the corresponding control time point for each donor. n = 3 donors per group, 6-10 timepoints per donor. Lifespan average graphs are mean ± SEM, two-way ANOVA. * $p < 0.05$, ** $p < 0.01$, *** $p < 0.001$, **** $p < 0.0001$, ns: not significant.

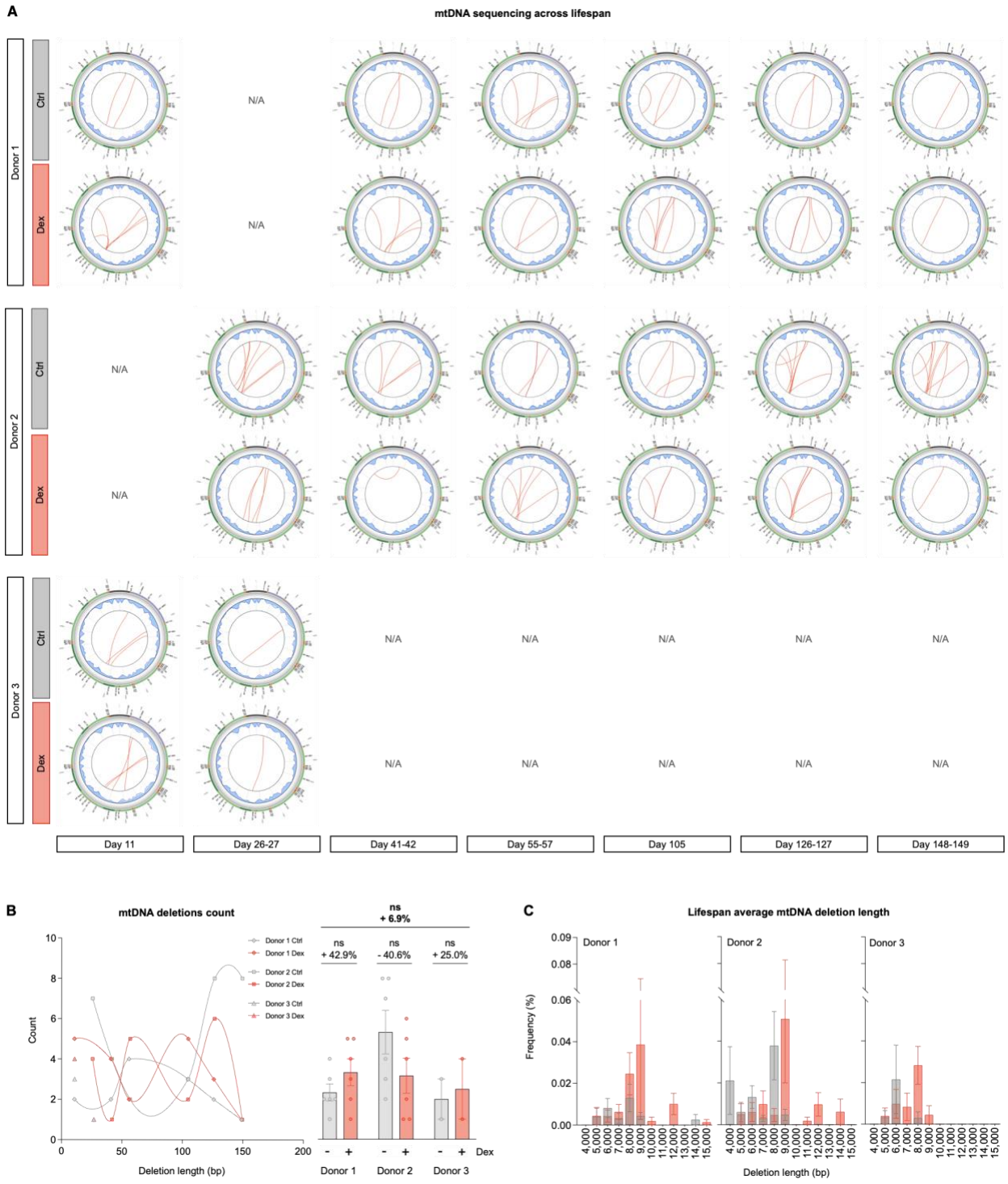

Figure S8. Effects of chronic glucocorticoid signaling on mtDNA instability

(Continues on next page)

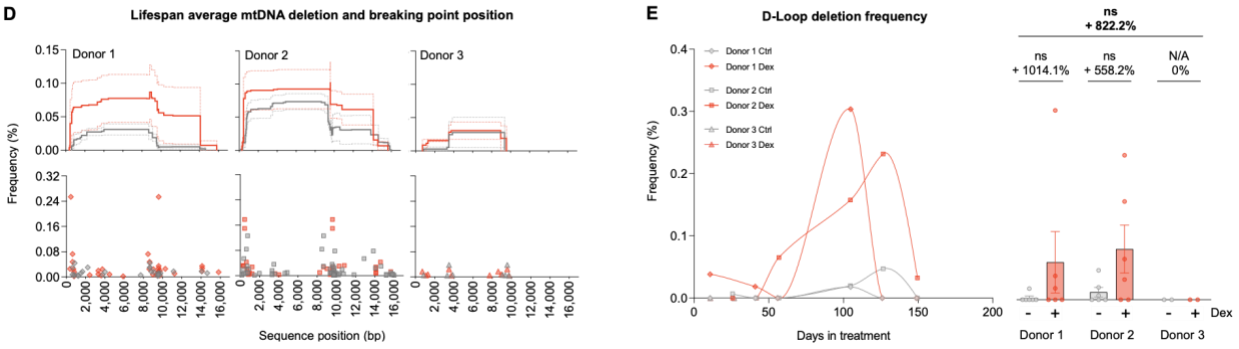

Figure S8. Effects of chronic glucocorticoid signaling on mtDNA instability

(**A**) Circos plots from mtDNA sequencing and eKLIPse analysis for mtDNA. Red lines represent individual deletion break points that span the sequence contained between its two ends, and line darkness reflects the level of heteroplasmy for each deletion. The blue histograms represent coverage depth along the mtDNA sequence. (**B**) Lifespan trajectories (left panel) and lifespan average effects (right panel) of Dex treatment on the individual deletions count. (**C**) Frequency distribution of deletion lengths for all timepoints across lifespan. (**D**) Frequency of deletions (upper panels) and frequency of deletion break points (lower panels) along the mtDNA sequence. (**E**) Lifespan trajectories (left panel) and lifespan average effects (right panel) of Dex treatment on the deletions that span the D-loop region of the mtDNA. n = 3 donors per group, 2-6 timepoints per donor. Lifespan average graphs are mean ± SEM, two-way ANOVA. ns: not significant; N/A: not applicable.

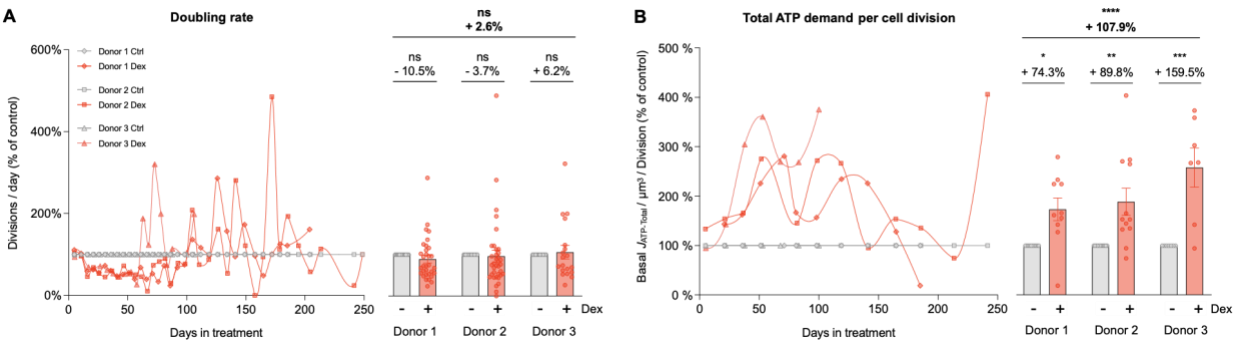

Figure S9. Effects of chronic glucocorticoid signaling on cell division

(**A**) Lifespan trajectories (*left* panel) and average effects (*right* panel) of Dex treatment on doubling rate (divisions/day) expressed relative to the corresponding control time points for each donor. (**B**) Same as A but for $J_{ATP\text{-}Total}$/cell volume/division. n = 3 donors per group, timepoints per donor: n = 26-36 in A, 8-13 in B. Lifespan average graphs are mean ± SEM, two-way ANOVA. **** $p < 0.0001$. ns: not significant. $J_{ATP\text{-}Total}$: algebraic sum of $J_{ATP\text{-}Glyc}$ and $J_{ATP\text{-}OxPhos}$. $J_{ATP\text{-}Glyc}$: ATP production rate derived from glycolysis. $J_{ATP\text{-}OxPhos}$: ATP production rate derived from OxPhos.

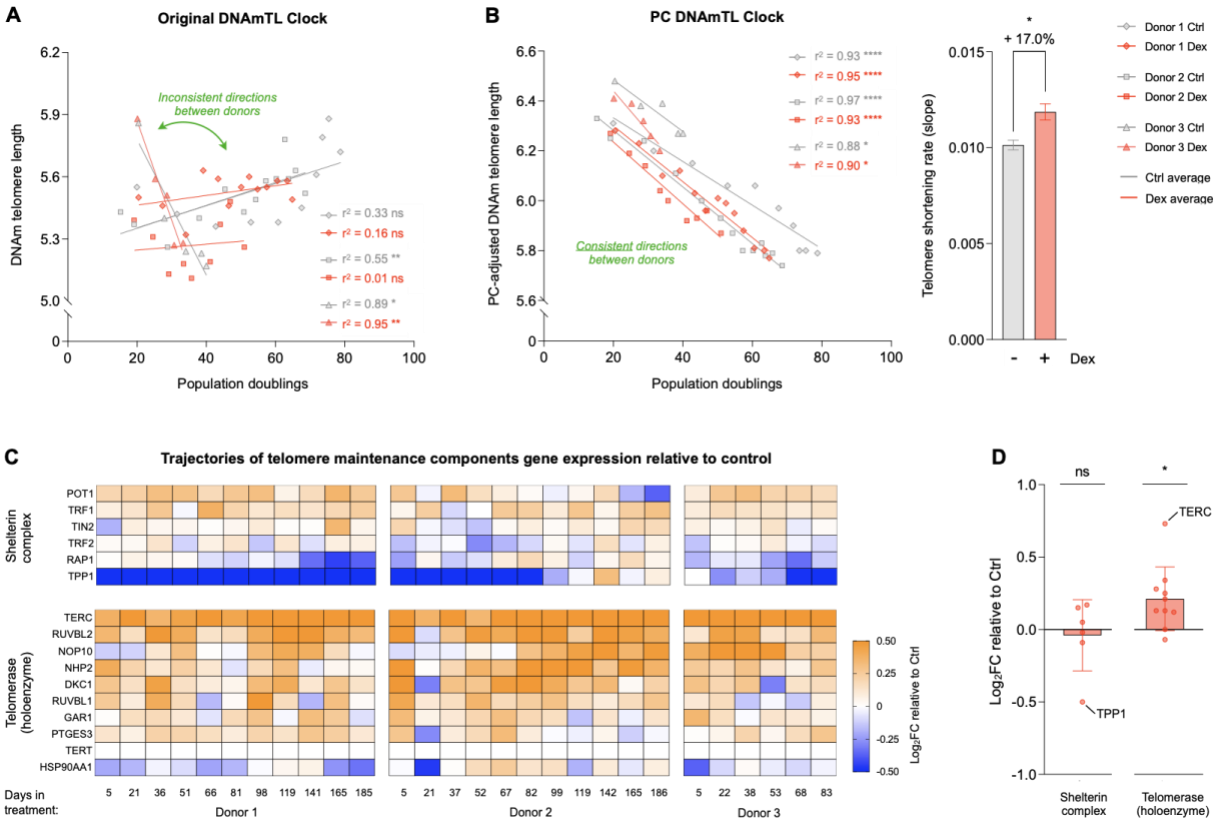

Figure S10. Effects of chronic glucocorticoid signaling on telomeres

(**A**) Telomere length across population doublings calculated by the DNAmTL epigenetic clock with linear regressions for each donor of each group (**B**) Telomere length across population doublings calculated by the principal components (PC)DNAmTL epigenetic clock with linear regressions for each donor of each group (*left* panel), and telomere shortening rate inferred by linear mixed model along the whole lifespan (*right* panel). (**C**) Heatmaps showing the effect of Dex treatment on the expression of telomere maintenance-associated genes, expressed as the Log_2 fold change (Log_2FC) relative to the corresponding control time point for each donor. (**D**) Average effect of Dex treatment shown in C. Each datapoint represents the gene average of the Log_2FC values throughout the entire lifespan of the three donors. n = 3 donors per group, timepoints per donor: n = 4-13 in A-B, n = 9-10 in C. Thin lines in correlation graphs show linear regression for each donor, Pearson r correlation. Bar graphs are mean ± SEM, Satterthwaite method in B, and one-sample t-test different than 0 in D. * $p < 0.05$, ns: not significant.

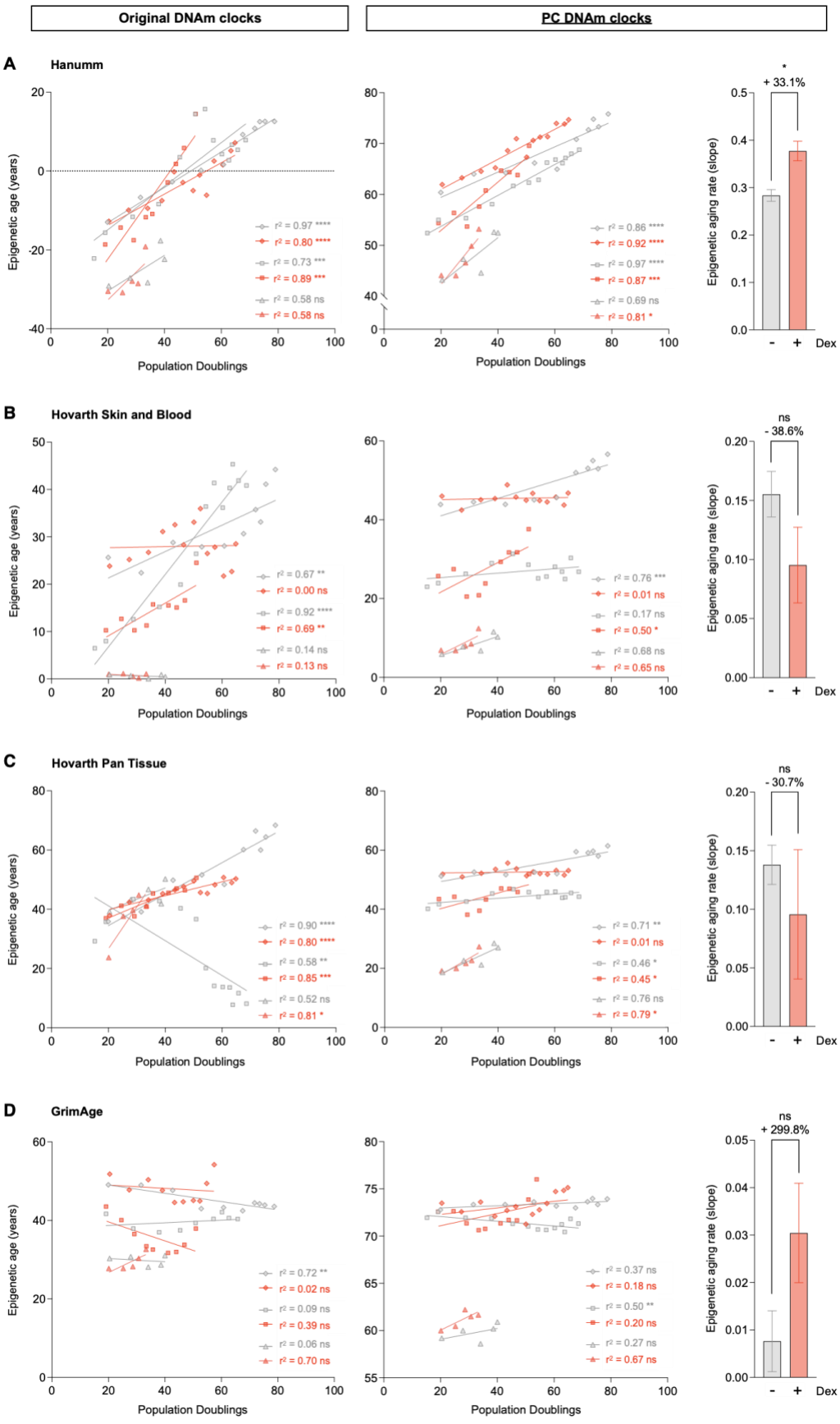
Original DNAm clocks
PC DNAm clocks
A
Hanumm
Epigenetic age (years)
Population Doublings
r² = 0.97 ****
r² = 0.80 ****
r² = 0.73 ***
r² = 0.89 ***
r² = 0.58 ns
r² = 0.58 ns
r² = 0.86 ****
r² = 0.92 ****
r² = 0.97 ****
r² = 0.87 ***
r² = 0.69 ns
r² = 0.81 *
Epigenetic aging rate (slope)
*
+ 33.1%
- + Dex
B
Hovarth Skin and Blood
r² = 0.67 **
r² = 0.00 ns
r² = 0.92 ****
r² = 0.69 **
r² = 0.14 ns
r² = 0.13 ns
r² = 0.76 ***
r² = 0.01 ns
r² = 0.17 ns
r² = 0.50 *
r² = 0.68 ns
r² = 0.65 ns
ns
- 38.6%
C
Hovarth Pan Tissue
r² = 0.90 ****
r² = 0.80 ****
r² = 0.58 **
r² = 0.85 ***
r² = 0.52 ns
r² = 0.81 *
r² = 0.71 **
r² = 0.01 ns
r² = 0.46 *
r² = 0.45 *
r² = 0.76 ns
r² = 0.79 *
ns
- 30.7%
D
GrimAge
r² = 0.72 **
r² = 0.02 ns
r² = 0.09 ns
r² = 0.39 ns
r² = 0.06 ns
r² = 0.70 ns
r² = 0.37 ns
r² = 0.18 ns
r² = 0.50 **
r² = 0.20 ns
r² = 0.27 ns
r² = 0.67 ns
ns
+ 299.8%

Figure S11. Effects of chronic glucocorticoid signaling on aging epigenetic clocks

(**A**) Epigenetic age across population doublings calculated by the DNAm Hannum epigenetic clock (*left* panel) and the principal components (PC) version of it (*middle* panel), with linear regressions for each donor of each group, and the epigenetic aging rate inferred by linear mixed model along the whole lifespan (*right* panel). (**B-D**) Same as A but for Skin and Blood, Pan Tissue and GrimAge epigenetic clocks, respectively. n = 3 donors per group, 4-13 timepoints per donor. Thin lines in correlation graphs show linear regression for each donor, Pearson r correlation. Bar graphs are mean ± SEM, Satterthwaite method. * $p < 0.05$, ns: not significant.

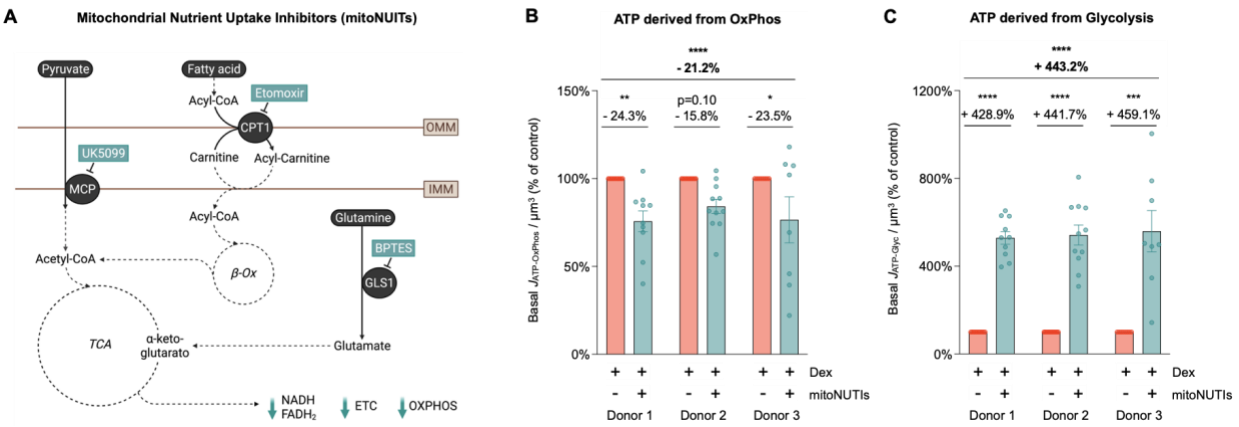

Figure S12. Effects of chronic glucocorticoid signaling and mitochondrial nutrient uptake inhibitors on basal bioenergetic parameters

(**A**) Schematic of mitoNUITs mechanism of action, three pharmacological inhibitors of nutrient uptake in the mitochondria. (**B**) Lifespan average effects of Dex+mitoNUITs treatment on $J_{ATP\text{-}OxPhos}$/cell volume. (**C**) Same as (B) but for $J_{ATP\text{-}Glyc}$/cell volume. N = 3 donors per group, n=7-11 timepoints per donor. Lifespan average graphs are mean ± SEM, two-way ANOVA. * $p < 0.05$, ** $p < 0.01$, *** $p < 0.001$, **** $p < 0.0001$. mitoNUITs: Mitochondrial nutrient uptake inhibitors. $J_{ATP\text{-}Glyc}$: ATP production rate derived from glycolysis. $J_{ATP\text{-}OxPhos}$: ATP production rate derived from OxPhos

Chapter 3: The Energetic Cost of Allostasis and Allostatic Load

This chapter is a reproduction of the paper *"The Energetic Cost of Allostasis and Allostatic Load"* published in *Psychoneuroendocrinology* in October 2022. Here, we reviewed the literature relative to the energetic costs associated with the activation of the stress response and emphasized the potential negative effects associated with chronic hypermetabolism. We proposed the "Energetic Model of Allostatic Load", by which chronic stress induces the redirection of energetic resources toward allostatic responses and away from growth, maintenance, and repair processes. This would in turn lead to the accumulation of damage, which will further contribute to the development of disease and increased risk of mortality. Finally, we highlighted new avenues to quantify allostatic load and its link to health via the integration of systemic and cellular energy expenditure measurements together with classic biomarkers, that could contribute to further advances in the stress field.

The Energetic Cost of Allostasis and Allostatic Load

Natalia Bobba-Alves[1], Robert-Paul Juster[2,3], Martin Picard[1,4,5]

[1] Division of Behavioral Medicine, Department of Psychiatry, Columbia University Irving Medical Center, New York, NY, USA.

[2] Center on Sex/Gender, Allostasis, and Resilience, Research Center of the Montreal Mental Health University Institute, Montreal, QC, Canada.

[3] Department of Psychiatry and Addiction, University of Montreal, Montreal, QC, Canada.

[4] Department of Neurology, H. Houston Merritt Center and Columbia Translational Neuroscience Initiative, Columbia University Irving Medical Center, New York, NY, USA.

[5] New York State Psychiatric Institute, New York, NY, USA.

3.1. Abstract

Chronic psychosocial stress increases disease risk and mortality, but the underlying mechanism remain largely unclear. Here we outline an energy-based model for the transduction of chronic stress into disease over time. The energetic model of allostatic load (EMAL) emphasizes the energetic cost of allostasis and allostatic load, where the "load" is the additional energetic burden required to support allostasis and stress-induced energy needs. Living organisms have a limited capacity to consume energy. Overconsumption of energy by allostatic brain-body processes leads to *hypermetabolism*, defined as excess energy expenditure above the organism's optimum. In turn, hypermetabolism accelerates physiological decline in cells, laboratory animals, and humans, and may drive biological aging. Therefore, we propose that the transition from adaptive allostasis to maladaptive allostatic states, allostatic load, and allostatic overload arises when the added energetic cost of stress competes with longevity-promoting growth, maintenance, and repair. Mechanistically, the energetic restriction of growth, maintenance and repair processes leads to the progressive wear-and-tear of molecular and organ systems. The proposed model makes testable predictions around the physiological, cellular, and sub-cellular energetic mechanisms that transduce chronic stress into disease risk and mortality. We also highlight new avenues to quantify allostatic load and its link to health across the lifespan, via the integration of systemic and cellular energy expenditure measurements together with classic allostatic load biomarkers.

3.2. Introduction

The fundamental distinguishing feature between life and death is the flow of energy. Compared to the living human body, the dead body harbors the same DNA sequence and molecular composition, the same number of cells, and the identical anatomical arrangement of organs. The dead body, however, lacks energy flow. Energy fuels our ability to sense and feel, our behaviors, the thinking process, and the consciousness through which we perceive and respond to the world around us (*458*). As a result, the living human experience, including stress responses (*357*), consumes a considerable amount of measurable energy (*459*). Yet, we know remarkably little about the mechanisms that sustain and guide energy consumption and, specifically, how bioenergetic disturbances contribute to disease risk and mortality (*460*).

A topic of paramount importance to biomedical sciences concerns the mechanisms by which psychological factors promote states of health and disease (*461*). Living organisms evolved the ability to anticipate internal and environmental perturbations, and in turn mobilize adaptive physiological recalibrations to minimize deviations, a phenomenon termed *allostasis* (*3*). Building on this concept, McEwen and Stellar proposed that the chronic activation of allostatic systems leads to maladaptive recalibrations that end up "wearing out" the organism's organ systems. This phenomenon was termed *allostatic load* (*4*).

Over the last few decades, the allostatic load model (*351*) has evolved and guided research on the stress-disease cascade. This model provides an integrative theoretical framework to conceptualize and measure chronic stress, including the central role of the brain in transducing subjective experiences into biological changes (*462*) and the availability of environmental energetic resources that support allostasis (*8*). The internal, biological basis for the "wear-and-tear" of allostasis over time as it becomes allostatic load, however, still remains as a major

knowledge gap in the stress-disease cascade. Understanding the manifestations of allostatic load and overload at multiple levels of biological complexity (organismal, cellular, sub-cellular) has the potential to help clarify *why* allostatic load is damaging. What is it about the allostatic load primary mediators (e.g., stress hormones, cytokines, metabolites) that disrupt health-sustaining biological and physiological functions? *When does adaptive allostasis become allostatic load and overload?* We argue that a more complete allostatic load model is achieved by understanding the interplay of allostasis and allostatic load with the fundamental biological constraints related to energy transformation and allocation within the brain-body unit.

Limits to energy transformation impact health

At any given time, cells can transform only a finite amount of energy (*463*). The biophysical limit to sustainable energy transformation constrains both *cellular behavior*, such as how rapidly cells can divide (*464*), and *human physiology*, such as how long one can run or how well one can reproduce (*465*). Stress-related physiology under the control of the nervous system is also naturally energy-dependent (*466*). As a result, among living organisms, including humans, energy flow drives function and sets the boundaries of adaptive capacity. The constant requirement for energy to power life-sustaining cellular and physiological activities explain why deficits in available energy can impair health and contribute to various disease states (*467*).

The requirement for energy to sustain human health is illustrated perhaps most clearly in individuals with rare mitochondrial disorders. *Mitochondria* are small intracellular organelles that transform energy using oxygen and food substrates (*468*). People with mitochondria that cannot efficiently transform energy suffer from multisystem disease and die prematurely (*469, 470*), highlighting the central role of mitochondria, and energy more generally, in human health (*471*). If we want to better understand health, resilience, and disease risk, we must therefore understand

how the body's limited energetic resources are allocated and distributed between competing processes.

In this narrative review and perspective paper, we discuss the energetic basis of allostasis, allostatic states, allostatic load, and allostatic overload. We describe how limits to energy consumption or expenditure may establish a threshold wherein adaptive allostasis turns into damaging allostatic states, allostatic load, and allostatic overload. We draw from three bodies of complimentary literature – cell biology, human physiology, and psychology – to illustrate how the increased energy expenditure known as *hypermetabolism* may represent the linchpin of the stress-disease cascade. In turn, this energetic view of stress and health illuminates potential mechanisms of stress resilience and vulnerability, advancing the science of allostatic load.

3.3. The allostatic model of the stress-disease cascade

The **Glossary** defines key historical terms developed to pinpoint specific stages of the allostatic load model of the stress-disease cascade. Here we summarize the progression across these stages.

When living organisms experience real or imagined stressors, a set of anticipatory *allostatic responses* are triggered to cope and promote survival. As these stressors persist, the resulting allostatic responses are sustained over time, becoming under- or over-activated. The normal regulatory set-points and/or dynamic range are consequently altered, transitioning transitory allostatic responses to *allostatic states* (*472*). Allostatic states, as originally outlined by McEwen, can take different forms including repeated activation, lack of habituation, prolonged response, and inadequate response (*351*). Persistent activation of allostatic states incurs additional energetic costs and triggers more lasting cellular and physiological recalibrations – such as hyperglycemia, elevated blood lipids, and elevated circulating stress mediators (cortisol,

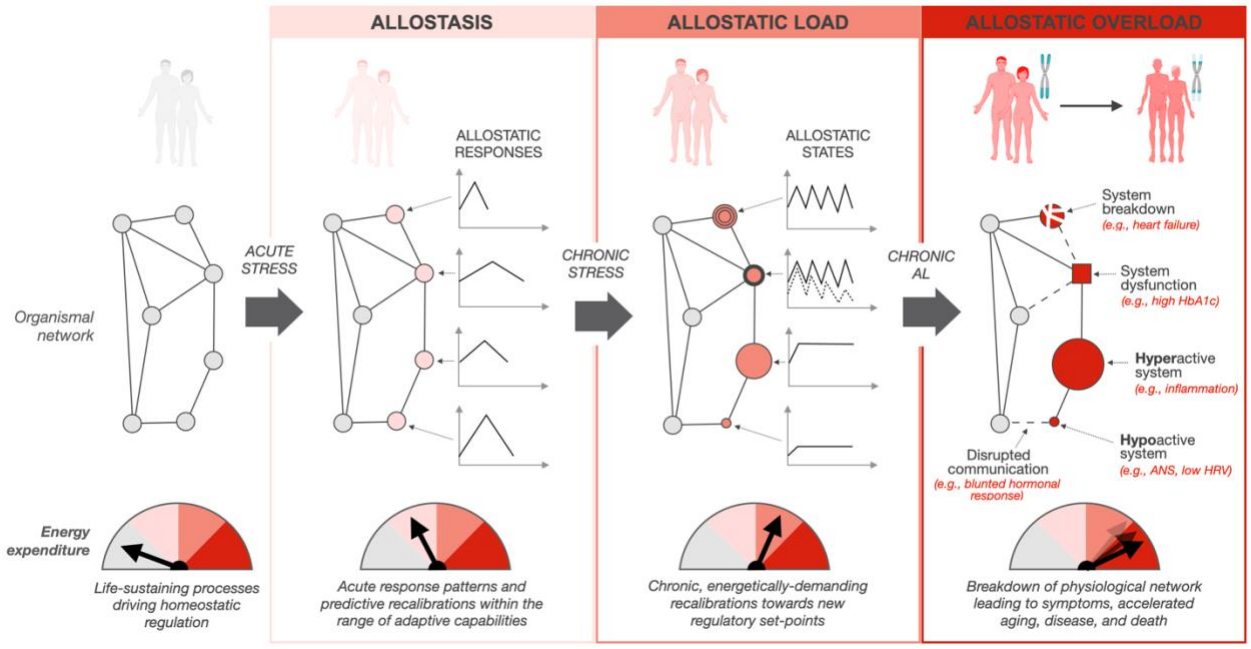

Figure 1. The energetic underpinnings of the allostatic load model of the stress-disease cascade
Real or imagined stressors trigger an energy dependent cascade progressing from adaptive allostasis to allostatic states and allostatic load, to allostatic overload, ultimately manifesting as an increased disease risk and accelerated rate of aging. The physiological network, illustrated as nodes and edges, depicts the constant communication (edges) between cells, tissues, organs, and systems (nodes) within the human body under the influence of biopsychosocial and environmental forces. The change in appearance of nodes illustrates the dysfunction, breakdown, and hypo- and hyper-activation of organ systems in response to allostatic load and overload. Dashed lines illustrate impaired communication between organ systems. These changes manifest as measurable circulating biomarkers that eventually become clinical signs and symptoms. The allostatic states are adapted from McEwen's proposed allostatic load time-course (McEwen 1998). *Abbreviations*: *PSNS*, parasympathetic nervous system; *AL*, allostatic load; *HRV*, heart rate variability; *HbA1c*, glycated hemoglobin.

catecholamines, etc.) – that constitute *allostatic load*. When sustained over time, allostatic load triggers compensatory functional and structural recalibrations causing progressive dysregulation among the organism's physiological network. Well known physiological examples include the stiffening of the arteries to sustain high blood pressure, the downregulation of hormone receptors on target tissues to counteract overstimulation, and the remodeling of the brain circuitry and anatomy in response to neurochemical factors. Over time, these end stage recalibrations lead to the breakdown of communication and of regulatory systems, termed *allostatic overload* (*8*). At the cellular level, allostatic overload manifests in molecular changes, like the accumulation of damage

and accelerated aging, culminating in the onset and progression of disease, and ultimately premature death. Importantly, this stress-disease cascade progressing from adaptive allostasis, to maladaptive allostatic states and allostatic load, and finally to allostatic overload activates a large spectrum of *energy-consuming* processes (**Fig. 1**).

3.4. What is the purpose of allostasis?

Energy is the driving force of life, but also is a limited resource. As mentioned above, living organisms operate under energetic constraints imposed by their ability to transform energy (*464*). The behaviors of their cells, tissues, and organs, like the brain and immune system, are bound and limited in scope by how much energy they can transform at any given moment. This constraint has forced the evolutionary selection of organisms optimized for energy efficiency that can sustain life at the lowest amount of energy expenditure possible (*473*). By maximizing energetic efficiency, organisms can allocate energy to fuel adaptative processes and other health- and longevity-promoting functions, including reproduction and cognition.

From this energetic perspective, the evolution of likes and dislikes, feelings and emotions, and approach/withdrawal behaviors arose to minimize the energetic cost of life (*474*). We tend to like things that give or save us energy (e.g., palatable food and warm clothes, respectively), and dislike things that cost us energy (e.g., cold rain). These and other dimensions of physiological regulation allow organisms to anticipate and avoid energetically costly exposures, in favor of more "comfortable" (i.e., energy saving) conditions that minimize physiological perturbations (*421*). Below we discuss allostasis and its relation to the human mind.

Anticipation, allostasis, and adaptation

On a daily basis, the imperative to maximize energetic efficiency exists in a direct tradeoff with our natural instincts to anticipate, prepare, and adapt to stressors. Through anticipation, allostasis prepares the organism for upcoming challenges, thereby increasing the future probability of survival (*475*). Consider a person facing a potential predator. Upon the *perceived* threat of an attack, an evolutionary selected allostatic defense response immediately kicks into action. The release of catecholamines and cortisol is triggered, increasing breathing and heart rates, activating sweating, and liberating glucose and lipids in the bloodstream.

The adaptive value of this *integrated* allostatic or stress response is clear: i) the elevated breathing and heart rates increase blood pressure and oxygen delivery to all vital organs that would require rapid energy delivery should 'fight-or-flight' (or 'tend-and-befriend' (*476*)) responses be necessary; ii) the sweat response preemptively cools down the body to prevent overheating expected from the heat released during muscle contraction and brain activity; and iii) the mounting hyperglycemia/hyperlipidemia ensures that energy substrates are readily available in our blood for energy transformation within the brain's mitochondria, to power the planning and execution of the fight-or-flight response. A beautifully coordinated, whole-body response to a potential threat and anticipation of endpoints.

Allostasis is often anticipatory, which means that the above-described cascade can occur whether or not the threat ultimately materializes. Indeed, the human mind is among the most potent triggers of wasteful allostasis. Self-preservation (*477*) and the self-sustained adverse psychological states, in the form of preservative cognitions like worry and rumination (*478*), directly drive energy-dependent allostatic responses. From an evolutionary point of view, the existence of anticipatory and future-oriented behaviors suggests that allostatic mechanisms are more

advantageous than the alternative that consists of reacting and producing emergency responses only after the stressor has happened (*479*). Emergency responses, such as healing wounds and fighting infection (because one was unable to run fast enough), have a higher energetic cost and are potentially harmful. By anticipating the future, allostasis therefore puts the organism in the best possible state to face current and upcoming challenges.

The brain is central to anticipatory allostatic responses (*462*). As a threat-detecting master, the brain is an organ specialized in reacting, anticipating, and ruminating. These processes optimize behavior by minimizing uncertainty (*480*). Uncertainty is fundamentally costly because it leads to larger deviations from the optimum. Not knowing what the future holds precludes the ability to anticipate change, producing larger, more energetically costly deviations to correct. Adequately predicting future exposures lowers uncertainty, allowing an organism to (theoretically) perfectly prepare and adapt optimally to upcoming challenges.

Optimal adaptation means the lowest degree of perturbation, which requires the least amount of energy expenditure to correct deviations (*481*). As a result, the brain integrates inputs from multiple senses and compares them against memories of past experiences to predict future exposures. By doing so, it minimizes the deviation between the state of the organism and reality. This idea is captured by the free-energy principle (*480*), which provides a framework to understand the existence and function of future-oriented energy-saving strategies used by allostasis. Allostasis minimizes the energetic costs associated with uncertainty, possibly explaining why allostasis is adaptive and why it evolved in the first place (*421*). Allostasis likely exists because, in the long-term, it conserves energy.

3.5. Allostasis costs energy

Although allostasis sustains health in the long-term by ensuring preparedness and minimizing the energetic cost of adaptation, *it itself costs energy* in the short-term (*466*). Allostasis imposes an *energetic load* on the system. As this cost persists and rises, it contributes to allostatic states and allostatic load. Here we propose that the *load* in allostatic load is the additional energetic burden that the organism must bear to adapt and survive. Excess energy consumption above one's optimum is defined as *hypermetabolism*. In this section we review the limited quantitative evidence that stress-induced allostasis and acute responses to mental stress consume excess energy and trigger hypermetabolism.

Experimental studies in laboratory animals and humans

The idea that psychological or mental stress, and the resulting allostatic processes, influence energy expenditure goes back almost a century (*94*, *95*). The hypermetabolic effects of acute and chronic stress, and some potential mechanisms, have been examined in both laboratory animals and humans.

Most studies have addressed the link between stress and energy expenditure by a technique called indirect calorimetry, where oxygen consumption (ideally in parallel with carbon dioxide production to increase precision) is measured from the expired breath (*96*). In birds, one study found that acute stress from noise exposure (15 minutes) increased energy expenditure by ~15%, the magnitude of which correlated with the elevation in blood corticosterone (*115*). Similarly, restraint stress (3 hours) in rats increased energy expenditure by ~20-25% (*113*), whereas milder chronic unpredictable stress (3 weeks) increased energy expenditure by a more modest ~12% (*114*). Overall, these and other animal studies show that non-injurious experimental mental stressors reliably activate allostatic processes that increase the energetic cost of living in animals.

Allostasis from acute psychological stress also increases energy expenditure in humans. For example, healthy men solving Ravens matrixes (combination of detailed observation and abstract reasoning) exhibited up to a ~9% increase in total body energy expenditure, whereas performing mental arithmetic under time pressure (12 minutes) increased energy expenditure by ~13% (*97*). In another study, mental arithmetic under time pressure (15 minutes) caused a ~28% increase in energy expenditure (*98*). Similarly, mental arithmetic (8 minutes) with rising time pressure and involving elements of competition (an observer taking scores, a leader board, and performance incentive) and punishment (losing points, brief loud aversive sound with failure), increased energy expenditure by ~37-42% (*99, 100*), suggesting the potential escalating effect of psychological stress/threat on the energetic cost of allostasis. In line with this idea, one study found that a longer version (30 minutes) of the stressful combination of mental arithmetic and Stroop's color-world conflict test increased energy expenditure by ~67% (*103*). While most studies only evaluated men, two studies showed similar effects in women. Healthy women performing a combination of mental arithmetic and Stroop's color-world conflict test (15 or 30 minutes) exhibited a 39-45% increase in energy expenditure (*101, 102*). Just as in rodents and birds, mental stress consistently increases whole-body resting energy expenditure in humans by ~9%-67%, depending on stressor intensity and duration.

Non-experimental studies

Non-experimental studies of human psychological traits and stress hormones also provide converging evidence for the hypermetabolic effects of allostasis and allostatic load. For example, young men with high trait anxiety were found to have ~14% higher energy expenditure than those with low anxiety (*105*). On the other hand, individuals who regularly engage in relaxation practices like yoga, which dampen arousal and allostatic processes, may consume up to ~15% less energy

at rest (*106*). Thus, both default arousal-generating (i.e., threat) and calming (i.e., safety) psychological states (*482*) can influence energy metabolism.

Hormones also directly influence energy expenditure. Basal circulating levels of both catecholamines (*107*) and cortisol (*108, 109*), which reflect the activation of two major stress axes contributing to allostasis and allostatic load, positively correlate with how much energy the body-brain unit consumes to sustain life over a 24-hour period. Moreover, experimental administration of catecholamines and glucocorticoids is sufficient to trigger hypermetabolism (*110, 111*). In the context of clinical hypermetabolism, such as in burn patients, blocking adrenergic signaling can mitigate hypermetabolism (*483*), providing direct evidence that primary stress mediators can contribute to physiological hypermetabolism. Based on laboratory stress studies, at least a third of the hypermetabolic effects of acute psychological stress may be attributable to sympathetic nervous system activation and to the elevation in heart rate (*98*), providing initial clues about the origins of hypermetabolism during stress. In fact, *whole-body energy expenditure can be understood as the integrated cost of the major stress systems*, including glucocorticoid signaling by the hypothalamic pituitary-adrenal (HPA) axis, adrenergic signaling by the sympathetic-adrenal-medullary (SAM) axis, and other stress response pathways. Psychological stress alone, therefore, is sufficient to increase energy expenditure in humans, possibly through well-known allostatic mediators.

Sources of hypermetabolism and mental activity

Whether stress-related elevations in energy expenditure arises from mental activity or peripheral physiological processes is not entirely resolved. The long history of interest in the cost of mental activity (*484*) has largely concluded that the energetic cost of mental operations is less than our intuition would suggest. Brain energy consumption increases only marginally during

deliberate mental activity (*485, 486*). This increase likely arises from the fact that the brain, despite its relatively small size representing <2% of body weight, consumes ~20-24% of the body's total energy expenditure at rest (*487, 488*). One explanation for the cheap, nearly free, cost of mental activity is that the brain appears to compensate for task-evoked energy expenditures. Imaging studies have shown that local task-evoked increases in brain activity in specific areas – which are typically less than 5% in magnitude (*489*) – are offset by decreases in activity in other brain areas. As a result, specific mental operations yield only a modest global increase in brain activity and energy consumption (*490*). The fact that stress-induced hypermetabolism cannot be explained by increased brain energy consumption implicates other multi-system, brain-body processes. Next, we return to energy expenditure at the organism level and discuss the partitioning of energy costs across transitions from allostasis to allostatic load.

3.6. Allostasis & stress-induced energy expenditure (ASEE)

From an accounting perspective, the energetic costs of allostasis are added on top of other costs that sustain the organism. The human energy expenditure literature generally distinguishes between three main sources of energetic costs (*491*). First, the *basal metabolic rate* (BMR) includes the cost of all vital operations that regulate and maintain physiological functions: breathing to sustain blood flow and ensure the availability of nutrients systemically, neural activity that allows cognition and anticipation, plus physiological functions including hematopoiesis (i.e., the production of blood cells in the bone marrow) and many others. Second, the *thermic effect of food (TEF)* that refers to the energy required for digestion. Third, the *activity-related energy expenditure (AEE)* that sustains the demands of waking life, including movement, talking, listening, climbing stairs, typing on the computer and other daily activities. Finally, *thermoregulation* – the energy required to maintain body temperature – is generally grouped

together with BMR or AEE. Together, these costs add up to an individual's *total energy expenditure (TEE) (492)*, reflecting how much energy it costs an organism to stay alive.

On top of the life- and behavior-sustaining energy costs are the energy costs of stress-induced allostatic states, allostatic load, and allostatic overload. We term this component *allostasis & stress-induced energy expenditure* (*ASEE*). To position the additional energy costs associated with allostatic load within this energy landscape, we divide energy expenditure into different categories and consider the concept of the energy reserve.

The *energy reserve* component does not relate to physical energy storage forms such as adipose tissue or material access to food. It reflects the portion of the energy *transformation* capacity or budget that isn't normally utilized to sustain life, but that is available as a buffer when needed (*360, 421, 493*). For example, engaging in multi-day athletic performances or pregnancy increases energy expenditure integrated over periods of sustained effort above baseline TEE (*494*). This indicates that additional energetic resources are available above TEE, although there certainly is a constraint or limit to the organism's total energy budget (*494*). Similarly, cells isolated *in vitro* and within the organism operate at sub-maximal metabolic rates, maintaining a "spare" or reserve bioenergetic capacity (*495*). Here also, there is a limit to the capacity of different cell types to dynamically transform and consume energy, as in the human organism. We posit that the portion of the organism's finite energy budget consumed by ASEE can tap into the limited reserve capacity.

Together, these energetic components add up to the *total energy budget*, reflecting the total amount of energy available to the organism over time (**Fig. 2**). Note that for most humans living in urbanized civilizations, the total energy budget is not limited by environmental supply as originally described by McEwen and Wingfield from an evolutionary or animal ecology

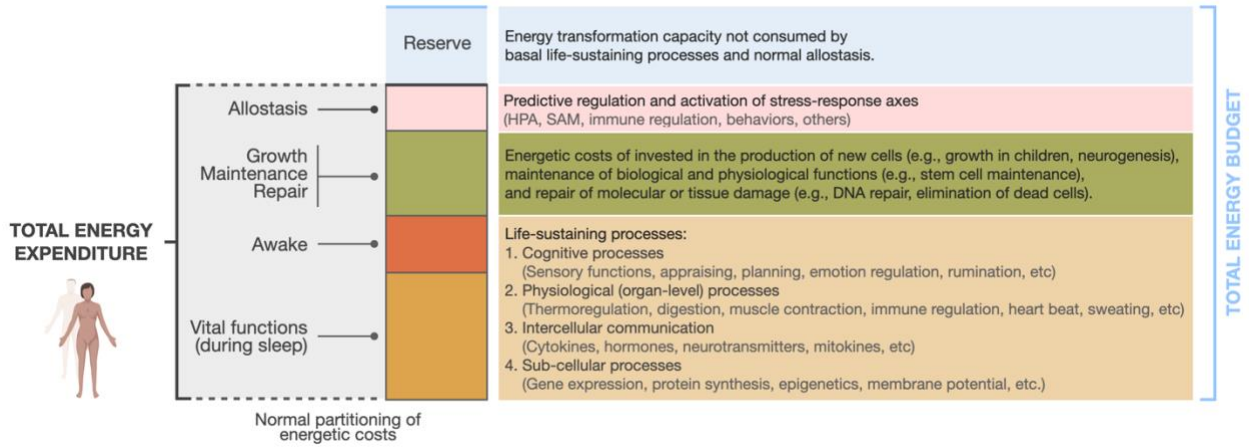

Figure 2. Theoretical partitioning of total energetic resources in the organism
Integrated over long periods of time, the human body can transform a finite amount of energy per unit of time, derived from the oxygen we breathe and the food we consume. Based on limited available evidence, we reason that vital regulatory and predictive allostatic processes consume a non-negligeable portion of the total energy budget. Growth, maintenance, and repair (GMR) processes are essential to replace damaged molecules and cells, and to offset the natural decay of matter over time (i.e., to overcome the inevitable second law of thermodynamics that states that everything is bound to increase in entropy). The leftover portion of the energy budget is the reserve capacity, which is hypothesized to exist as a buffer for allostasis, and the increasing energetic demands of allostatic load in the organism.

perspective (2003), although digestive capacity may be limiting in extreme contexts (*494*). Rather, the total energy budget appears set by internal energy transformation systems, including glycolysis and mitochondrial oxidative phosphorylation (*374*), and physical limits to energy dissipation rates (*463*, *464*).

Spending down the total energy budget

An organism's total energy budget can be spent at different rates. A useful analogy for this concept is the modern smartphone. A smartphone has a given battery charge that can be consumed more or less rapidly depending on the amount of ongoing internal processing. Keeping a phone "on" costs energy, such that the battery goes down, albeit slowly. The energy required to keep a phone "on" is the cost of vital functions. On "airplane mode", the phone consumes less energy, and the battery lasts longer. In normal mode, powering the antenna and searching for signal,

keeping apps running, and the readiness to receive incoming messages are classically allostatic processes in nature. Now add texting, talking, and streaming. Like stressors, these demands activate internal energy-consuming processes, draining the battery's energy more rapidly. These additional activities are analogous to allostatic states and allostatic load, representing the added energetic cost of chronic (over)activation of allostatic processes (i.e., ASEE), consuming energy at a higher rate than would be required just to keep the device on.

In keeping with the smartphone analogy, allostatic overload represents the material degradation over time whereby the device begins to wear out, run out of memory storage, slow down processing speed, and malfunction. The mechanical analogy does not fully encompass the complexity of living processes within the human organism, where endogenous repair processes and recalibrations always take place. Nevertheless, the *escalating load of activities draining a finite amount of available energy* appropriately captures the energetic cost of activities during allostatic load.

The cost of adaptation wasted

As described above, by preparing the organism for future exposures, allostasis effectively reduces the total energetic costs associated with novelty, surprise, and damage repair that stressors engender. But when anticipated threats do not materialize, the organism pays the cost of allostasis *without* reaping the potential long-term benefits. The cost allostasis is then wasted as futile hypermetabolism.

Futile stress responses may be particularly (or uniquely) prevalent in humans. Humans have highly developed cognitive abilities, enabling us to autonomously initiate allostatic cascades by imagining or sustaining potential threats (i.e., anxiety, ruminating, worrying) for periods of time longer than necessary (*477, 478, 482*). As an interesting link between futile mental activity

and energy, rumination appears to be the strongest psychological predictor of *fatigue* (*496*), the subjective experience of energy deficiency. Allostatic responses mobilized unnecessarily lead to the waste of limited energy resources; the regulatory systems shift unnecessarily, wasting precious energy. This waste in turn drives the overconsumption or redirection of energy above one's optimum, promoting damaging hypermetabolism.

3.7. Why is hypermetabolism damaging?

Having established that the constellation of allostatic processes costs energy, the next logical question is why expending more energy is damaging to health. *How does elevated energy expenditure, or hypermetabolism, during allostasis contribute to allostatic load and allostatic overload over time?* To address this question, we consider three related bodies of literature.

Energy expenditure scales with the rate of aging and lifespan in animals

First, there exists evolutionary-conserved, cross-species relations whereby animals with higher metabolic rate age faster and die younger (*497*). For every minute of life, smaller animals such as flies, shrews, and mice spend significantly more energy per unit of body weight to sustain life than their larger counterparts like baboons, elephants, and whales (*429, 430*). In parallel, smaller animals also have much shorter lifespans: flies live days, shrews live less than a year, mice live 2-3 years, whereas elephants and whales can live around and over a century (*428*). Faster breathing animals who exhibit comparatively higher energy expenditure – or *relative hypermetabolism* – also erode their telomeres faster (*415*) and tend to have predictably shorter lifespans.

Hypermetabolism predicts mortality in humans

Second, among otherwise healthy individuals, those with higher energy expenditure exhibit a 25-53% increased mortality rate over 20-40-year follow up periods (*119, 120*). Higher resting heart rate – which generally scales linearly with metabolic rate (*498*) – also was associated with a 80-90% increased risk of death over a 12-year follow up (*499*). In clinical populations with equivalent diagnoses (e.g., cancer, diabetes, and renal disease) patients with hypermetabolism also are more likely to die than those with normal resting metabolic rate (*123-125*). Thus, physiological states that chronically elevate energy expenditure – which we propose is a consequence of allostatic load and overload – induces a more "mouse-like" state that predicts earlier mortality.

Stress signaling triggers hypermetabolism and accelerates cellular aging in vitro

All tissues and cell types express receptors for canonical stress hormones allowing them to respond to hormonal stimulation within minutes to hours. Consequently, glucocorticoids can be used *in vitro* to model HPA axis signaling and chronic "psychosocial" or neuroendocrine stress. In neurons and other cell types, glucocorticoid signaling induces robust bioenergetic and mitochondrial recalibrations (*127, 142, 428*), and sustained exposure drives mitochondrial biogenesis (i.e., the production of new mitochondria) and the number of mtDNA copies per cell (*127*), which are hallmarks of increased energy expenditure. In a long-term model of chronic glucocorticoid stress, energy expenditure was increased by ~60% (*127*), reflecting ASEE and robust hypermetabolism.

Over time, hypermetabolic cells under allostatic load also show signs of allostatic overload. This includes an accelerated rate of telomere shortening, epigenetic aging, and decreased cellular lifespan (*127*). Thus, cells age faster and are more likely to die when their ASEE is elevated by stress exposure. This observation is consistent with the cross-species allometric scaling of

metabolic rates and aging biology (i.e., animals with higher energy expenditure age faster), and with the prospective human studies linking hypermetabolism to increased mortality (people with higher energy expenditure die earlier) reviewed above. These *in vitro* results complement physiological results in whole organisms and mechanistically link glucocorticoid signaling, hypermetabolism, and the molecular wear-and-tear that underlie biological aging independent of complex physiological processes.

3.8. The Energetic Model of Allostatic Load (EMAL)

Above we have described the energetic cost of allostasis and how the organism's total energy budget is allocated. We also have discussed how imagined threats drive cognitive, physiological, and cellular allostatic responses, increasing allostasis and stress-related energy expenditure (ASEE). When sustained, this leads to allostatic load, which burns an increasing fraction of the energy budget above baseline TEE – like an overactive phone rapidly draining its battery. Additionally, we have presented three lines of evolutionary, population-based, and *in vitro* evidence that hypermetabolism is health damaging and accelerates aging. The EMAL integrates these notions, predicting that allostatic load and allostatic overload develop and become health-damaging when the total energy budget becomes overspent, or "bankrupt", and forced to steal from other cellular and physiological process processes (**Fig. 3**).

Overall, if energy expenditure was a direct driver of allostatic overload and aging, the sequence leading from allostasis to allostatic states, allostatic load, and eventually overload (e.g., accelerated telomere shortening) could be understood as follows: stress-induced allostasis and allostatic load processes makes the human body more "mouse-like", triggering hypermetabolism and thereby accelerating the rate of energy expenditure to make it more akin to that of a shorter-lived, rapidly aging organism.

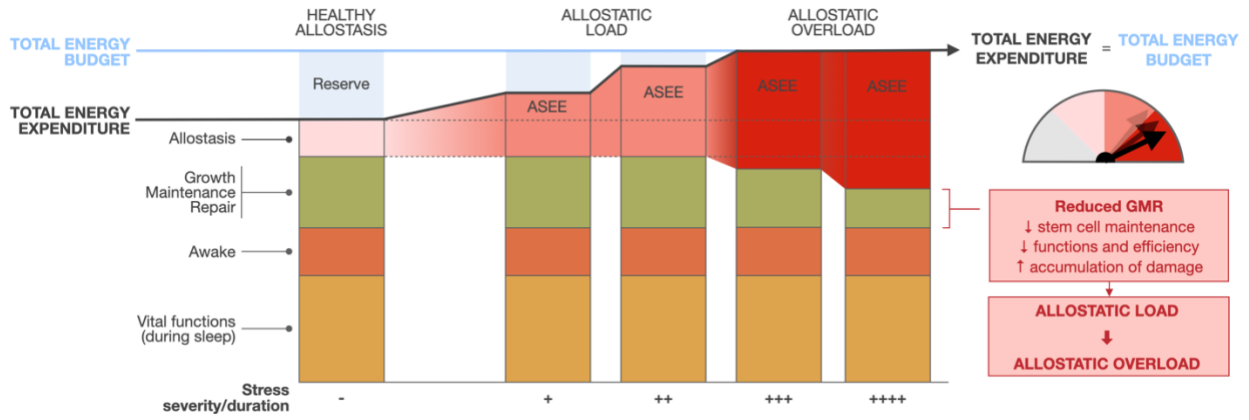

Figure 3. The Energetic Model of Allostatic Load (EMAL)
This figure illustrates the effects of stress-induced allostasis on the partitioning of energy costs within the organism, and the transition from allostasis to allostatic load and overload. Real or imagined stressors increase allostasis and stress-induced energy expenditure (ASEE), which consumes the reserve portion of the organism's total energy budget. When this excess energetic cost exceeds the reserve capacity, it impinges on growth, maintenance, and repair (GMR) processes that are required to sustain health and prevent the entropic decay of cells and systems. As a result, the compression of available resources constrains GMR processes, accelerating the decay of structures leading to allostatic overload marked by the 'wear-and-tear' of cellular and physiological systems. Taken together, allostatic load and allostatic overload arise when the energetic costs of stress-induced allostasis supersede or the organism's available energetic reserve, or when they are prioritized over GMR owing to some other evolutionary mechanism.

Some assumptions central to this model require validation and rigorous empirical testing. The first is that there is a fixed total energy budget (*465*). But individuals can sustain abnormally high total energy expenditure (e.g., endurance athletes) for days to weeks (*494*) and some disease states trigger hypermetabolism (*500*), bringing into question the absoluteness or fixity of total energy expenditure. The concept of an energetic reserve addresses this point. The second assumption is that the relative energetic costs of each component are stable over time and that energy tradeoffs only occur over absolute thresholds. Functional tradeoffs at the cellular (*463, 464*) and organismal levels (*501*) could arise not just at a fixed arbitrary value in energy expenditure, but from a combination of energetic, hormonal, and behavioral factors that triggers a biological reprioritization of certain processes over others (see next section). The entire reserve capacity, therefore, may not need to be fully spent before ASEE costs impinge upon and "steal" energetic resources from GMR processes. Finally, stress disrupts sleep, which may occur early in the

sequence of events leading to allostatic load and overload (*77*). Sleep disruption could thus increase the cost of vital functions, manifesting in elevated energy expenditure during sleep, or elevated basal metabolic rate during wakefulness (*502*). Thus, the components shown in Figure 3 are not independent from one another but likely interact in complex bi-directional ways.

Energy tradeoffs: When allostasis becomes allostatic load and allostatic overload

When the whole budget becomes spent, additional energy costs from mounting allostatic processes can only be met by redirecting energy from other processes. In these tradeoffs, the most urgent processes divert or steal energy from less urgent ones. Pro-survival allostatic and stress-related processes come with some level of evolutionary-endowed biological urgency (*475*). Therefore, we posit that they force tradeoffs and steal energy from less immediately required processes. This process of energy reallocation is similar to how excessive exercise can cause tradeoffs with reproductive or immune functions (*465*), how excessive immune activation can curtail growth in children (*503*), and how glucocorticoid stress responses or mitochondrial defects slows down division in cells (*127, 504*). One must first survive immediate threats to later grow, think, and behave. Therefore, the evolutionary-shaped urgency to mobilize stress pathways position ASEE costs as physiological priority.

The prioritization of stress responses may explain why survival and adaptation driven ASEE can divert energy resources from non-immediately essential processes. Non-immediately essential growth, maintenance, and repair processes include those contributing to lifespan and longevity. Examples of *GMR* processes include the formation of immune cells in the bone marrow and the maintenance of memory lymphocytes (*505*), the elimination of defective cells of cancerous potential or the removal of waste products from the brain (*506*), the formation of new neurons and other cell types from stem cells (*507*), and the maintenance of DNA integrity via telomere

maintenance and DNA repair (*508*). Unlike the acutely life-sustaining processes such as the beating heart, breathing, and neuroendocrine regulation of glycemia, one can survive variable periods of time (days to weeks) without hematopoiesis, autophagy, neurogenesis, nor DNA repair.

In relation to aging, GMR processes include all molecular events that combat thermodynamic decay and maintain the integrity of life, such as cell division, DNA and other molecular repair pathways, antioxidant defenses, etc. These processes prevent the accumulation of damage and errors in DNA and other cellular components over time, which are hallmarks of aging (*301*, *509*).

GMR processes are energetically costly because they rely on energy-dependent enzymes and molecular operations. Within the cytoplasm, mitochondria, the nucleus, and other organelles, the enzymes of GMR such as telomerase and antioxidant enzymes consume high-energy intermediates (e.g., ATP) to preserve the integrity of molecules, generate new proteins and DNA, and to build new cellular components (e.g., mitochondrial biogenesis). Growth, maintenance, and repair delay or prevent the accumulation of age-related damage. The suppression of GMR processes by ASEE-driven energy tradeoffs could therefore account for the health-damaging "wear-and-tear" effects of chronic stress.

The chronic tradeoff between ASEE and GMR could manifest in two main quantifiable ways. An organism could develop observable hypermetabolism, measurable directly over periods of minutes, hours, and/or days as an elevated resting or total energy expenditure. Alternatively, and more insidiously, the organism could divert energetic resources away from GMR, potentially *without elevating total energy expenditure*. In this second scenario, our model predicts that subcellular energy tradeoffs would only be measurable by the molecular sequelae of halting or slowing of GMR, including DNA damage, telomere shortening, oxidative stress, epigenetic drift,

and reduced hematopoiesis (*510*). The energetic model of allostatic load reframes these traditional age-related markers as indicators of impaired GMR processes and therefore, as potential indicators of ongoing deleterious energetic tradeoffs.

Evidence of energy tradeoffs hampering GMR

Previous observations are consistent with the proposed EMAL. As reviewed above, increased energy expenditure and secondary markers of halted GMR in humans have been linked to accelerated biological aging, increased mortality, and shortened lifespan. At the cellular level, the breakdown of regulatory systems and damage accumulation manifests as telomere instability and accelerated shortening rate (*138, 504*). Moreover, in humans chronic psychosocial stress and other toxic environmental exposures that lead to allostatic load also accelerate telomere shortening (*137, 228, 511*). Thus, energetic tradeoffs may explain the cellular manifestations of allostatic load and allostatic overload.

Direct mechanistic evidence that allostatic processes are prioritized over GMR mainly comes from *in vitro* studies where cellular-level energetic tradeoff accelerates biological aging. For example, impaired mitochondrial energy production capacity leading to energetic stress triggers the costly secretion of extracellular signaling molecules, forcing a tradeoff with cell growth pathways, and culminates in a reduction of cell size and division rate (thus reducing growth-related costs) (*504, 512, 513*). Similarly, glucocorticoid-exposed cells that engage in costly molecular operations involving the production and release of cytokines divide less rapidly, show evidence of molecular damage to the mitochondrial genome, and exhibit higher mortality, potentially reflecting energetic tradeoffs hypermetabolism (*127*).

Physiologically, energy is acutely redirected to fuel neuroendocrine cascades, including, but not limited to, the HPA-axis and sympathetic nervous system, which suppress immune

functions and cytokine production in the long-term. Allostasis and stress-induced energy costs appear to be prioritized over other processes that usually protect us from infections (*65, 514*) and promote wound healing (*515, 516*). Based on our model, this would occur because mobilizing acute stress responses is more acutely vital than accelerating epithelialization, surveilling pathogens, or preserving telomeres. The EMAL model proposes that the suppression of immune surveillance and wound healing, as well as anti-aging cellular strategies, for examples, take a backseat under the pressure of mounting ASEE consume a growing portion of the energetic budget.

The EMAL model also makes two predictions. The first states that the physiological systems that most require constant renewal and repair to sustain their functions, such as immune cells with high turnover rate, or portions of the brain with high levels of neurogenesis (e.g., the hippocampus), exhibit preferential vulnerability to the forced tradeoff of the limited energy resources for ASEE. The second prediction is that vulnerability is exacerbated during developmental and lifespan stages where growth energy costs are higher-than-average, such as during childhood (*492*). When applied to developmental trajectories, this model may help to understand the embedding of stressful experiences, particularly around sensitive periods of development (when energy costs are the highest), and the preferential vulnerability of specific organ systems, like the immune and nervous systems.

3.9. Allostatic load across levels of biological complexity

Allostatic load has traditionally been conceptualized as a whole-body process, but it is important to recognize that it transcends levels of biological complexity. At the scale of the organism, multi-organ physiological allostatic processes occur in parallel with cellular allostatic load processes, coordinated by the brain. The human brain plays a central role in the integration of interoceptive and sensory perceptions (*517*), in addition to the anticipation, initiation, and

maintenance of allostasis (*462*). Costly brain-body physiological endocrine and immune processes, among others, are coordinated by stress hormones that transmit the perception of a potential danger to all cells in the organism. These responses entail multi-organ physiological processes, but the cellular and intracellular details of these events remain poorly understood.

Two main situations can be envisioned to explain the evolutionary development of allostatic load. If allostatic load existed only among brain-body organism and was absent from isolated cells, it would likely indicate that, on the evolutionary scale, allostasis was an innovation of multicellular, thinking and feeling creatures. However, if allostatic load naturally took place at the cellular level – in the Petri dish without a brain – it would be consistent with the notion that allostatic mechanisms are ancient, evolutionary conserved mechanisms, and that their origin likely predated the evolution of the brain (*421*).

The cellular glucocorticoid experiments described above unambiguously demonstrate and isolate the anticipatory nature of energy-dependent cellular allostatic recalibrations. In these experiments, where there is only a single cell type without a brain nor real injurious threat, cellular responses can be isolated from systemic psychophysiological, brain-body processes, reflecting *cellular allostatic load* (CAL). Given our goal to better understand the forces underlying human health, the existence of cellular allostatic load broadens our perspective by illustrating how every cell can sense and respond to stress mediators and develop micro-allostatic responses. In response to endocrine and metabolic stressors, sub-cellular organelles, like mitochondria, also can exhibit structural and functional recalibrations reflecting allostatic load, a phenomenon known as *mitochondrial allostatic load* (MAL) (*360*). Thus, systemic (AL), cellular (CAL), and mitochondrial (MAL) allostatic load reflect the same set of evolutionary-conserved, energy-consuming, adaptive strategies to optimize health across levels of biological complexity (**Fig. 4)**.

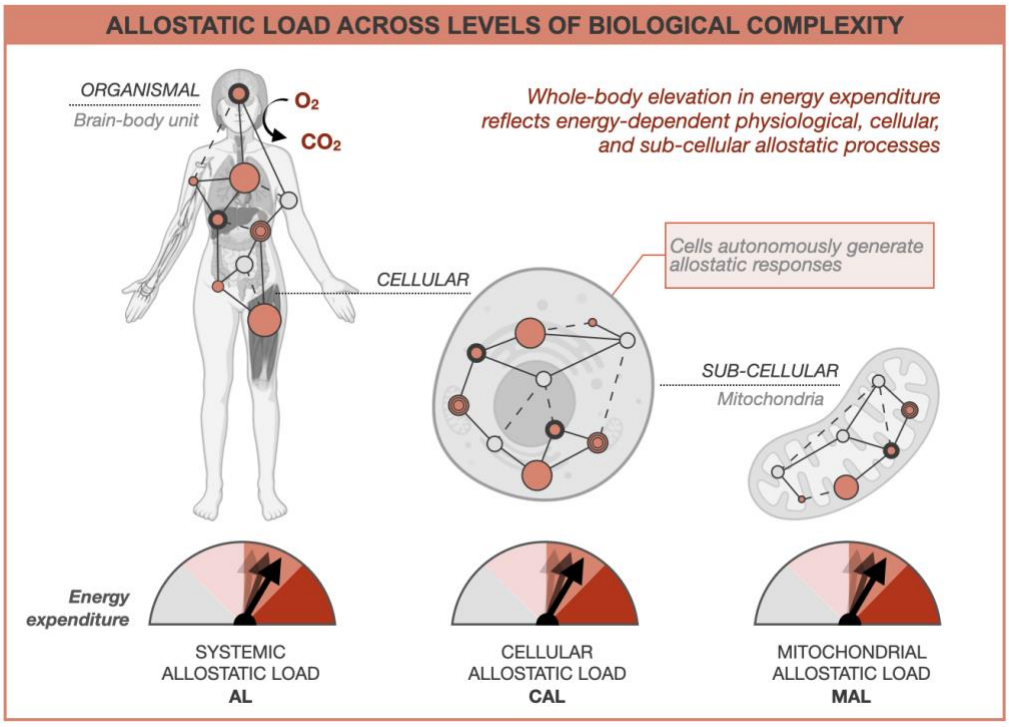

Figure 4. Allostatic load across levels of biological complexity
The added energetic cost and biological 'wear-and-tear' that brain-body allostatic states impose on the organism during chronic stress is a more complex expression of the same process that also take place in cells, and in sub-cellular organelles, such as the energy-transforming mitochondria. See *Glossary* for definitions.

Cellular bioenergetic recalibrations to life stress in humans

If chronic life stress and the resulting systemic allostatic load produced a sustained elevation in energy expenditure, the adaptive response in the healthy organism would consist in increasing the cellular energy producing capacity. Accordingly, a series of studies on mixed white blood cells has reported that cellular oxygen consumption (a good estimate of energy expenditure) was elevated in women with a history of early life trauma (*518, 519*). Cellular energy consumption was correlated with trauma severity and circulating cortisol levels (*519, 520*), consistent with the notion that more severe trauma and activation of the HPA axis mediate these effects. When examining immune cells of 3-6-year-old children, higher maternal allostatic load during pregnancy also predicted higher mitochondrial content – and, therefore, greater energy production capacity –

pointing to the potential transfer of the energetic load of stress across generations (*521*). Other studies, although not all (*149, 522*), have reported elevated numbers of mitochondrial DNA copies per cell (mtDNAcn, (*523*)) in the blood of individuals with early adversity and psychopathology (*146, 155*). Together, these results point to immune bioenergetic recalibrations and mitochondrial allostatic load in response to chronic life stress (*360*), calling for precise, longitudinal studies in specific cell types (*524, 525*).

Implications for allostatic load from organelle to organism

The conservation of allostatic load across several levels of biological complexity, from organelle to organism, is enlightening in three main ways. First, it gives insights into the nature and origin of allostatic load – not as a modern invention of brain-bearing bodies, but as an evolutionary-conserved natural phenomenon across living creatures. Second, it highlights the many potential mechanisms for hypermetabolism – physiological, behavioral, cellular, and subcellular. These highlighted mechanisms can then help us build more accurate causal interdisciplinary models for the transduction of chronic stress into disease risk, aging, and mortality. Third, an understanding of allostatic load across levels of complexity may eventually illuminate ways in which we can intervene to enhance resilience and promote health. In theory, interventions to mitigate the adverse effects of systemic allostatic load on human health could be targeted to any of these levels to offset the damaging effects of hypermetabolism and energy tradeoffs.

3.10. An energetic view of resilience-promoting factors

The EMAL provides a mechanistic lens through we can view allostasis and underscores a few important insights of interest to brain-body scientists. First, this model provides a hypothesis

to understand why some behavioral and psychosocial factors promote resilience to chronic stress. For example, *exercise* is among the best described factors that buffers against the deleterious effects of psychological stress on cellular aging (*231, 526*). Besides increasing the pool of well-functioning mitochondria (*352*), thereby enhancing reserve capacity and the total energy budget, exercise increases physiological efficiency (*491*). In other words, the trained organism can perform life-sustaining activities in its daily life more efficiently (i.e., at a lower energetic cost). Although exercise costs energy acutely, the trained organism presumably undergoes adaptive responses that subsequently allow it to sustain life with lower basal energetic costs. This phenomenon is termed *metabolic compensation*, which might arise from reduced costs in other domains such as reproduction, stress physiology, and inflammation (*465*). Thus, the effective energy "saving" afforded by physical activity and exercise may act by either expanding the organism's energy reserve or by improving efficiency, thereby freeing a portion of the total energy budget for GMR (**Fig. 5**). Similarly, the health-promoting intervention (and lifespan extending, in animals) of calorie restriction also may reduce energy expenditure (*527*).

In the context of the energetic model of allostatic load, other factors known to modulate allostatic load deserve further research, most notably, the social regulation of allostasis (*528, 529*). Social support and social dynamics (*530, 531*) impact health and lifespan and can buffer against the deleterious effects of chronic stress exposure (*532*). In animal studies, sociality affords energetic cost savings in response to physical challenges (*533, 534*) and social threats (*535*). Sociality and social support, therefore, could confer health protective effects because they improve metabolic efficiency, or because they reduce another component of the energy budget in a way that protects GMR. Further research is needed to test these possibilities.

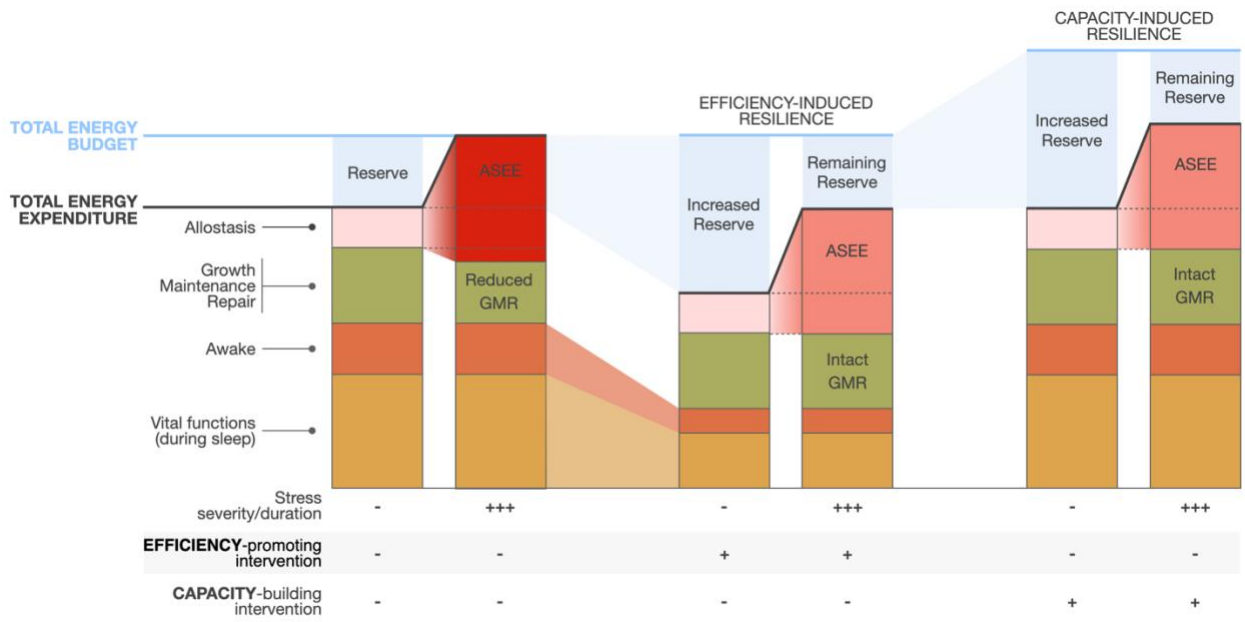

Figure 5. Potential influence of resilience-promoting interventions on the total energy budget and partitioning of energy costs within the organism
Illustrated are two types of hypothetical scenarios for resilience-promoting interventions. Compared to the situation (*left*) where allostasis and stress-induced energy expenditure (ASEE) bankrupts the total energy budget and steals energy from growth, maintenance and repair (GMR), resilience to the same stressor can arise from either a reduction in basal metabolic costs (metabolic compensation, *middle*) or increase the total energy budget (*right*). The shifting of the threshold for allostatic overload can increase the ability of the organism to tolerate chronic stress with less of the damaging effects of allostatic overload.

In humans, little is known about the effects of social allostatic load on energy expenditure. Given the tight embedding of our physiology and social contexts (*528*, *532*), future studies should quantify the influence of socioeconomic status, discrimination, social isolation and social support, and other prosocial forces on energy expenditure. Both energy-saving and energy-draining effects of positive and negative social interactions, respectively, should be considered (*536*). We anticipate that precise measures of basal metabolic rate and total energy expenditure (*96*, *537*), ideally also with experimental stress studies, will help to precisely quantify the psychobiological energetic tradeoffs among key components of the total energy budget.

3.11. Applying the energetic model of allostatic load (EMAL)

If the EMAL is (partially) correct, it should be possible to demonstrate that chronic stress is damaging *because* it increases the cost of living or steals energy from GMR processes. A translational combination of cellular, animal, and human studies will be required to fully examine and refine portions of the model. If validated in humans, there would be direct implications for the design of health-promoting and resilience-building interventions.

For example, a new class of interventions could be designed with the explicit goal to reduce the adverse effects of stress by *directly targeting energy expenditure*. The therapeutic goal would be to prevent hypermetabolism or promote "normometabolism". A successful outcome would consist of optimizing metabolic efficiency during daily life and upon stress exposure. For example, in the intensive care unit setting – a naturally stressful environment where hypermetabolism predicts mortality – using energy expenditure to design individualized care improved patient outcomes (*538*). Energy expenditure, we argue, represents a more integrative, and possibly more accurate, measure of optimal physiological functions than individual molecular markers can reflect. The EMAL suggests that incorporating measures of energy expenditure and metabolic efficiency could increase the sensitivity and specificity afforded by approaches focused on traditional organ-specific allostatic biomarkers. This could in turn help to evaluate the effectiveness of existing interventions in reducing allostatic load, or the magnitude of physiological dysregulation more generally.

For example, the beneficial or adverse effects of new drugs could be evaluated globally on their overall energetic cost of life, not just a specific molecular marker or organ system (see **Fig. 4**). Based on the EMAL, if a new medication increased basal or total energy expenditure, this would indicate that while the target pharmacological effects may be achieved (e.g., symptom

suppression), the drug has induced a broader set of off-target, or secondary, energetically costly deviations from the organism's optimal state. If the drug lowered energy expenditure *without adverse side effects*, this would indicate a favorable organismal response to the treatment.

The proposed model also predicts that reducing ASEE frees up energy for longevity promoting GMR. Therefore, reducing ASEE should allow organisms to thrive – i.e., to adapt and age optimally. Living creatures almost universally have a beginning and an end. It therefore seems unlikely, and possibly unwise, that decay and aging should be eliminated. Striving to ensure that all necessary energetic resources are available for GMR (as we do at a gross level with nutrition), however, should optimize one's development, growth, healthspan and lifespan. Equipped with a conceptual model and tools to examine the energetic underpinnings and molecular manifestations of GMR processes, investigators can design quantifiable and testable cross-sectional and longitudinal hypotheses.

Besides exercise and social factors that may promote energy efficiency, other approaches could contribute to minimize ASEE and hypermetabolism. For instance, mindfulness and meditation practice may represent effective means of improving metabolic efficiency and promoting restoration. Early studies directly measuring energy expenditure through oxygen consumption during meditation reported up to ∼40% reductions in metabolic rate (*539*, *540*). Relative to controls, advanced yoga practitioners also exhibited a stable 15% lower basal resting energy expenditure (see (*541*) for a systematic review). In the most extreme cases, the surprising level of metabolic efficiency achieved during meditation appears to exceed that naturally achieved during sleep states, when allostasis and ASEE costs dramatically subside and GMR processes are expected to be active. This body of literature calls for well-controlled studies to quantify modifiable psychosocial states influence energy expenditure, both acutely and chronically.

Overall, interventions that improve the organism's energetic efficiency, such as exercise, calorie restriction, and meditation are currently among the most promising interventions to reduce the wear-and-tear of stress, and to promote health across the lifespan. Based on energetic principles, the beneficial effects of these interventions could lie in either: i) their ability to expand energetic reserves, thereby increasing the total energy budget of a person; or ii) by increasing the efficiency of vital and activity-related energy costs, such that life can be sustained at a lower basic energy cost. Both possibilities converge upon an expanded reserve capacity that protects GMR processes from the forced, punctual energetic tradeoffs with stress-induced allostasis. This expanded reserve capacity, in turn, should optimize the organism's resilience and ability to live a long, healthy life.

The parallel between energetic and psychological coping resources

The discussion above has centered mostly on the biological and physiological underpinnings of the EMAL, without directly addressing its link with human psychology. In this final section, we attempt to establish some preliminary theoretical connections between the limits to energy expenditure, energetic tradeoffs with health-promoting processes, and psychological stress theory.

The cost-benefits of energetic expenditure discussed above are similar in spirit to psychosocial models of approach-withdrawal behaviors that are part of transactional models of stress. In situations of acute stress, organisms must decide whether the specific situation threatens their personal well-being and survival. Consequentially, in this transactional model (*542*), the decision to mount a stress response and subsequent allostatic load is determined by the demands of the encounter relative to the person's judgement of whether the threat supersedes their coping resources. This appraisal can be conceptualized from our energetic framework since the body and

brain must recalibrate biological and physiological activities according to their evaluation of the adaptative value of stress responses. Just as cognitive contextualization is an energetically expensive endeavor, so too is the transactional decision to activate allostatic processes or not given the energy and effort required.

In human stress reactivity studies, stress-induction paradigms that use *social-evaluative threats* to trigger psychophysiological stress responses are routinely used to assess allostatic stress responses (*477*). Stress reactivity occurs specifically in situations that diminish one's control and where the prospect of being negatively evaluated, rejected, and/or shamed are contextually manipulated (*543*). In addition to this allostatic process, humans are motivated by strong needs to preserve their social selves and will expend considerable energy to do so. The motivation towards preserving one's *social self*-vis-à-vis others' evaluations involves complex interactions among cognitive appraisals, affective processes, and physiological responses (*543-545*). Our energetic model, together with work around social allostasis (*528, 532*), illustrates how social forces push energetic levers within the organism.

Much of the stress literature centers on uncontrollability as a central determinant of over-reactivity that contributes to allostatic load. Here, we propose a reframe that focuses on the energetic level that contributes to the cost-benefit transactional analyses that shapes stress and coping responses. For example, changes in mitochondrial energy production capacity in specific brain regions may modulate social behaviors (e.g., dominant vs subordinate (*546*)), and brain signatures of energy metabolism may account for situational stress and state anxiety related to self-efficacy in humans (*547*). This concept that *behavior and psychological states are regulated by energy* (*548, 549*) compliments work on 'homeostats' and 'allostats' that use thermostats as an analogy for thresholds that regulate allostasis and allostatic states (*550*).

Some outstanding challenges include: i) determining to what extent mitochondrial and organismal energetics play an instructive role on psychological experiences in humans; and ii) how psychological states influence energetics across levels of biological complexity. We propose that the psychosocial and behavioral factors that can increase energy reserves (e.g., physical activity, social support, caloric restriction, sleep quality, sense of purpose) or promote efficiency (e.g., exercise training, meditation – see below) will need to be investigated in relation to individual differences in coping and stress reactivity.

3.12. Conclusion

We have outlined an energetic model of allostatic load (EMAL) to account for the stress-disease cascade in humans. Every biological process cost energy. Consequently, the anticipatory allostatic processes induced by real and imagined threats consume the organism's limited energetic resources. Because of evolutionary-acquired cellular and physiological energy constraints, allostasis and stress-induced energy expenditure can divert energy away from GMR processes. Thus, we propose that *the physiological transition between adaptive allostasis and maladaptive allostatic load is the point at which stress-induced energy costs compete with health-sustaining and longevity-promoting growth, maintenance, and repair*.

The proposed model opens several testable questions regarding the energetic basis of resilience or susceptibility to stress. Studies specifically designed to test these hypotheses should examine, beyond current models based exclusively on molecular biomarkers, how much added value sensitive and specific measures of energy expenditure contribute to predict meaningful health outcomes. Empirically, these measures could be applied at both the (sub)cellular and whole-body levels, leveraging approaches from both mitochondrial science and human energetics. Importantly, an energetic understanding of the allostatic load theory and of the stress-disease

cascade emphasizes the interplay of mind and body processes, and how their interactions rely on energy to survive and thrive across the lifespan.

3.13. Glossary

Allostasis

Energy-dependent, anticipatory recalibrations (i.e. allostatic responses) triggered by potential stressors or actual environmental demands, to maintain stability of vital functional parameters (*3*). Allostasis is epitomized as "stability through change".

Allostatic responses

Molecular, organellar, cellular, inter-cellular, physiological, behavioral, and cognitive processes that consume energy, and which are mobilized in anticipation of future threats and perturbations.

Allostatic states

Energy-dependent patterns of allostatic responses mobilized in response to acute and chronic stressors, leading to sustained activity and recalibration of inter-connected physiological systems (*472*).

Allostatic load

The added energetic cost and biological 'wear-and-tear' that neural, endocrine, metabolic, cardiovascular, immune, and other allostatic states impose on the organism during chronic stress, which in synergy with unhealthy behaviors, contribute to stress-related diseases (*4*).

Allostatic load index

Numerical value calculated from the number of neuroendocrine (e.g., cortisol), immune/inflammatory (e.g., cytokines), metabolic (e.g., glyco-lipid profiles), and cardiovascular systems (e.g., blood pressure, heart rate variability) (*551*) biomarkers that show either sub-clinical (e.g., high-risk percentiles) or clinical deviations (*355, 552, 553*).

Allostatic overload

Long-term energy-dependent functional and/or structural dysregulation and breakdown that arise as consequences of chronic allostatic load, leading to accelerated aging, disease onset and progression, and increased mortality risk (*8*).

Energy expenditure

The amount of energy expended or consumed to perform molecular, cellular, physiological, and mental operations required to sustain life and support allostasis in living animals (*429*). This is also known as "metabolic rate", fueled in animals by the aerobic (i.e., oxygen-consuming) transformation of food substrates in mitochondria.

Cellular allostatic load

The added energetic cost and biological 'wear-and-tear' that allostatic mechanisms impose on the *cell* during chronic stress, including the bioenergetic, transcriptional, inflammatory, morphological, signaling, and other cellular behaviors induced by the signaling action of even single stress mediators (*127*).

Mitochondrial allostatic load

The added energetic cost and biological 'wear-and-tear' that allostatic mechanisms impose on mitochondria during chronic stress, including the molecular, structural, and functional recalibrations that mitochondria undergo in response to metabolic, endocrine, biochemical, and other stressors (*360*).

Energetic model of allostatic load (EMAL)

Theoretical model highlighting the measurable energetic costs allostasis and stress-induced energy expenditure (ASEE), which force energetic tradeoffs with health- and longevity-promoting growth, maintenance, and repair (GMR) processes, culminating in the accelerated wear-and-tear of the organism.

3.14. Additional Information

Acknowledgments

The authors are grateful to Bruce S. McEwen for the generous inspiration and support he provided to R.P.J. and M.P. during his lifetime, and to Alan Cohen for comments on the model.

Funding

Work of the authors is supported by NIH grants R01MH122706, R01AG066828, R01MH119336, R21MH123927, the Wharton Fund, and the Baszucki Brain Research Fund to M.P. R.P.J. receives salary support from the Fonds de recherche santé Québec and holds a Canadian Institutes of Health Research Sex and Gender Science Chair.

Chapter 4: Perspectives and Future Directions

In the previous chapters, we reviewed the physiology of the stress response and the evidence that links its chronic activation to increased risk of morbidity and mortality. We went over the effects of stress on energetic demands and mitochondrial function, and how these can lead to an increase in damage and result in accelerated aging and thus contribute to the development of disease. We then examined novel experimental data suggesting that these effects are reproducible *in vitro*, in which we showed that human primary fibroblasts chronically stimulated with GC present a significant increase in their total energy expenditure and that this stress-induced hypermetabolism is linked to an acceleration of their biological aging. Finally, we reviewed the "Energetic Model of Allostatic Load", where we propose that chronic stress causes a redirection of the energetic resources toward allostatic responses and away from growth, maintenance, and repair processes, which in turn leads to the accumulation of damage that will contribute to the development of disease and increased risk of mortality. In this chapter, we will further review the perspectives that arise from our work and the future directions that could broaden our understanding of the stress-disease connection.

4.1. Expanding the Allostatic Load Model

As framed by McEwen & Stellar, the chronic activation of the stress response imposes an allostatic load on the system that contributes to the increased risk for disease development and mortality (*4, 6-8, 362*). The allostatic load model provided an integrative theoretical framework to conceptualize and measure chronic stress and therefore has been fundamental in guiding the research on the disease-stress connection. Nonetheless, the model was conceptualized at the organismal level, and its manifestation at other levels of biological complexity hasn't been

determined yet. Furthermore, whereas it was proposed that allostatic load leads to the progressive wear and tear of the system, the underlying basis of this phenomenon has remained elusive. Finally, the negative outcomes of allostatic load have only been gauged based on the available environmental energetic resources, without considering the internal energetic constraints that the systems might bear. Our work touches upon these three aspects and therefore expands the scope of the allostatic model, contributing to a deeper understanding of the stress-disease connection.

4.2. Cellular Allostatic Load

To investigate the manifestations of allostatic load at the cellular level, we cultured primary human skin fibroblasts under standard conditions and chronically treated them with the GR agonist, Dexamethasone. In other words, our design consisted of a clonal monolayer of human cells that do not have a main role in the stress response, living without any actual perturbation but the chronic exposure to a stress mediator. Even in such a simple design, we observed features that resemble the ones observed during chronic stress at the organism level: an increase in energy expenditure (i.e. increased $J_{ATP\text{-}Total}$/cell volume) and metabolic recalibrations aimed to cope with it (i.e. metabolic shift towards OxPhos), with concomitant negative outcomes that increase the risk of mortality (i.e. accelerated cellular aging) and compromised lifespan (i.e. increased cell death and decreased Hayflick limit). Our results come with several key implications. First, it corroborates that allostatic load transcends the organismal level of biological complexity and can be traced all the way down to the cellular level. This supports the notion that allostasis and allostatic load is not unique to complex-multiorgan organisms but that instead is an evolutionarily conserved phenomena that might have arisen in unicellular organisms (*421*). Second, it shows that virtually all cell types in the body will be affected by chronic stress, regardless of how central their role is in the stress response. This goes in line with the fact that chronic stress has a negative impact

on both mental and physical health and it has been linked to the causation and/or exacerbation of diseases in most organ systems of the body (*37, 38*). Finally, it validates the exposure of cultured cells to a stress mediator as an *in vitro* model of chronic stress to investigate the cellular and molecular basis of the damaging nature of allostatic load, and therefore contributes to further understanding of the stress-disease connection and insights about potential interventions to enhance resilience and promote health.

4.3. Hypermetabolism as an indicator of Allostatic Load

As we reviewed in Chapter 1, the activation of the stress response involves major metabolic recalibrations that maintain an effective blood supply to the organ systems in the body, maintain continuous availability of the circulating oxygen and nutrient substrates, and optimize their utilization by vital tissues (*93*). These recalibrations are critical because the mental and/or behavioral actions required to overcome the stressor impose a significant increase in the total body energy expenditure, as demonstrated both in animal (*113-115*) and human (*97-103, 105*) studies. In line with this, we found that chronic GC stimulation induced a significant increase in energy expenditure of human skin fibroblasts. Until now, whether stress-induced hypermetabolism arises from mental activity or peripheral physiological processes, and if the latter, whether they arise from specific organ systems or the entire body, was never evaluated. Our work suggests that the presence of stress mediators can initiate energy-consuming responses in virtually every cell of the body, which will then contribute to the overall organismal hypermetabolism. Thus, we propose that hypermetabolism reflects the magnitude of allostatic load at any level of biological complexity – i.e., how much energy cells, tissues, organ systems or organisms are expending to maintain stable physiology.

4.4. Does hypermetabolism cause damage?

Even though stress-induced hypermetabolism is well established, whether it has a toll on the body and contributes to the increase in risk of morbidity and mortality has not been determined. As we mentioned in Chapter 1, human studies have shown that both among healthy individuals (*119-121*) and individuals with illnesses (*122-126*), hypermetabolism is associated with poorer health, worse prognosis, and higher risk of mortality. In line with this, our *in vitro* study showed that Dex-induced hypermetabolism was linked to an accelerated cellular aging phenotype, an increase in cell death, and a decreased cellular Hayflick limit. Furthermore, the Dex+mitoNUITs treated cells that showed an exacerbated hypermetabolism also showed an exacerbated cellular aging phenotype, with even higher levels of cell death and even lower Hayflick limit. Nonetheless, while both human studies and our *in vitro* work show a strong association between hypermetabolism and poorer health (either organismal or cellular), neither of them can definitely establish the causal directionality.

Further *in vitro* studies pharmacologically inducing hypermetabolism could help to elucidate this phenomenon. The increase in energy demand could be achieved by leveraging the critical role of plasma membrane potential in normal cellular physiology and the ATP-dependent nature of the ion pumps responsible for maintaining it. Specifically, we could use the ionophore Monensin to induce the exchange of extracellular Na^+ for intracellular K^+, stimulating the influx of extracellular Na^+ and concomitant rise of the cytosolic Na^+ concentration. This in turn would cause the Na^+/K^+-ATPase to pump Na^+ out to restore cytosolic Na^+ at the expense of ATP, inducing an increase in the total ATP demand (*375*). By using a carefully titrated concentration of Monensin, we could impose chronic hypermetabolism along the entire lifespan of a cell line while

deploying a longitudinal, high-frequency, repeated-measures strategy to evaluate the effects on macromolecular damage, as well as cellular aging and cell death.

Among macromolecular damage, there is DNA damage in the form of mutations and deletions, which can be evaluated by whole-genome sequencing (WGS) (*554*). There can also be DNA breaks, usually assessed by Comet Assay (*555*), as well as telomere shortening, easily evaluated through qPCR (*556*). DNA damage can also result in its cross-linking with proteins, which can be evaluated by performing either DNA or protein-targeted isolation methods followed by mass spectrometry (*557*). Similarly, protein damage can result in protein-protein cross-linkages and aggregation, as well as general peptide fragmentation and proteolysis, all of which can be evaluated by mass spectrometry (*557, 558*). Finally, lipid damage results in loss of membrane fluidity and elasticity, as well as membrane deformation. These can be evaluated by optical methods including Fluorescence Recovery After Photobleaching (FRAP) and Atomic Force Microscopy (AFM), as well as spectroscopic methods such as Electron Spin Resonance (ESR) and Nuclear Magnetic Resonance (NMR) spectroscopy, among others (*559*). The damage to nucleic acids, proteins, and lipids leads to general dysregulation of gene expression, altered signaling pathways, abnormal metabolite transport, and deformation of intracellular structures, which in turn induces overall cellular dysfunction with accelerated cellular aging and higher susceptibility to cell death (*560*). If hypermetabolism does cause damage, then by imposing chronic Monensin-induced hypermetabolism along the entire lifespan, and deploying the above-mentioned methodology, we should be able to detect higher levels of macromolecule damage accompanied by accelerated cellular aging and increased cell death.

4.5. How can hypermetabolism cause damage?

The detrimental nature of hypermetabolism is still poorly understood and represents another relevant question to be investigated. As we mentioned in Chapter 2, some authors have proposed that stress-induced hypermetabolism could exert its deleterious effects through the increased demands on the cellular components responsible for energy production such as the mitochondrial ETC. In Chapter 3, we propose that it may also relate to general constraints on total energy flux that impose limits on molecular operations and lead to intracellular tradeoffs between competing energy-consuming processes. These two mechanisms could coexist and further work is required to test their validity and physiological relevance.

Effects on mitochondrial ETC and ROS production

It has been proposed that the stress-induced hypermetabolism would lead to a compensatory increase in mitochondrial ETC activity and OxPhos ATP production, which in turn would increase ROS production, causing oxidative stress and the concomitant oxidative damage (*298*, *299*). In line with this, our work showed that Dex caused hypermetabolism and was accompanied by an increase in ETC activity and OxPhos ATP production, as well as accelerated cellular and cell death. It is important to note that even if the hypermetabolism led to a compensatory increase in glycolytic ATP production instead, it could also increase ROS production. Specifically, in conditions of decreased ETC activity, electrons tend to accumulate in the initial steps such as complex I and coenzyme Q, and then transferred directly to molecular oxygen to give $O_2^{\bullet -}$ (*561*). Furthermore, a decrease in ETC activity can result in a decrease of the mitochondrial electrochemical gradient sufficient for inducing the reversal action of complex V, which will transport protons from the mitochondrial matrix into the intermembrane space while hydrolyzing ATP, and therefore contributing to the increase in energy demand (*562*). Importantly,

the reverse action of complex V can induce Reverse Electron Transport (RET), which in turn induces a high production of ROS (*563*). In line with this, when we treated our cells with Dex and the mitochondrial nutrient uptake inhibitors (mitoNUITs) to block the entrance of the major carbon sources to the TCA and thus cause a decreased ETC activity, there was greater hypermetabolism and an exacerbated aging phenotype compared to when we treated our cells only with Dex. Therefore, hypermetabolism could induce either an increase or a decrease in the mitochondrial ETC activity and both situations could increase ROS production, causing oxidative stress and the concomitant oxidative damage.

To investigate whether hypermetabolism causes an increase in ROS production and whether differential mitochondrial ETC activity could affect it we could impose chronic Monensin-induced hypermetabolism while simultaneously modulating i) the glycolytic activity with inhibitors such as 2-Deoxy-d-Glucose (2DG), ii) the entrance of the major carbon source into the mitochondria with mitoNUITs, and iii) the flow of electrons through the ETC either by mitochondrial membrane uncouplers such as FCCP, or complex-specific inhibitors such as Rotenone (complex I), 3-nitropropionic acid (Complex II), Antimycin A (Complex III), ADDA5 (complex IV) and oligomycin (Complex V), to then carry out direct measurements of ROS levels.

The measurement of ROS can be done through quantitative methods that provide absolute ROS concentrations, or semi-quantitative methods that provide indirect and/or relative readouts of changes in ROS concentrations (*564*). The main quantitative method is electron paramagnetic resonance spectroscopy (*565*), and among the semi-quantitative methods, some quantify the fluorescence signal of a chemical or proteinaceous reporter molecule, such as hydroethidine/lucigenin and HyPer, respectively (*566*). It should be emphasized that due to their short lifespan rapid reactivity and diffusivity, and the general lack of truly ROS-specific reporter

molecules, performing accurate and precise measurements of ROS levels with the available methods is challenging, and ongoing reporter optimization could provide better results (*567, 568*).

The next step to verify if hypermetabolism causes damage through the increase in ROS production would be evaluating macromolecule oxidation. The most common marker of nucleic acid oxidation is 8-oxo-7,8-dihydro-2′-deoxyguanosine (8OHdG), and there is only limited data on modification of other bases (*564, 569*). Whereas this modification can be assessed by ELISA, better results are achieved by Liquid Chromatography with tandem mass spectrometry (LC–M/MS) (*570*). Protein oxidation is usually evaluated in the form of protein carbonyls. These can be assessed by ELISA, fluorescein-5-thiosemicarbazide (FTC), and immunoblotting methods, although LC–M/MS is preferred both due to its specificity and because its ability to identify other modifications such as hydroxylation, nitration, and chlorination (*571*). Finally, lipid oxidation is evaluated in the form of 4-hydroxynonenal (4HNE), malondialdehyde (MDA) (*572*) and the F_2-IsoP isomer, 8-iso-$PGF_2\alpha$ (*573*), and similar to nucleic acid and protein oxidation, these can be evaluated by ELISA, but LC–M/MS is preferred.

As extensively reviewed in the literature, macromolecule oxidation results in its damage or altered structure which in turn induces accelerated cellular aging and higher susceptibility to cell death (*198-200, 203, 574, 575*). If the damaging nature of hypermetabolism indeed stems from the increase in ROS production, then by imposing chronic Monensin-induced hypermetabolism along the entire lifespan of a cell line we should be able to detect higher ROS levels, as well as higher macromolecule oxidation levels. Furthermore, we should be able to observe some kind of correlation between these parameters and macromolecule damage, cellular aging, and cell death levels. To further test this hypothesis, we could also induce hypermetabolism while simultaneously enhancing the antioxidant cellular defenses and evaluating the same parameters. This could be

achieved through pharmacological interventions such as chronic treatment with antioxidant molecules like vitamin C, vitamin E, vitamin A, and N-acetylcysteine (NAC), or genetic interventions involving the stable or inducible overexpression of antioxidant enzymes such as SOD, CAT, GPx, and TPx, and by doing so we should be able to mitigate, at least partially, the detrimental effects of hypermetabolism.

Effects on energetic tradeoffs and GMR processes

In Chapter 3 we introduced the Energetic Model of Allostatic Load, based on the notion that living systems present inherent energetic constraints that force intracellular tradeoffs between competing energy-consuming processes. Specifically, we proposed that stress-induced hypermetabolism causes a redirection of the energetic resources toward allostatic responses and away from expendable processes such as growth, maintenance, and repair processes, which in turn leads to the accumulation of damage. In line with this notion, our results showed that Dex induced hypermetabolism, and it was accompanied by a significant decrease in cell volume and cell division, the latter resulting in a significant decrease in Hayflick limit, as well as accelerated cellular aging and increased cell death.

To investigate whether this model is accurate, we should first evaluate whether hypermetabolism induces energetic tradeoffs and then confirm that these cause a decrease in the growth, maintenance, and repair process activity. The occurrence of energetic tradeoffs could be evaluated by profiling the cellular energetic partition, i.e. what percentage of the produced ATP is being consumed by the different cellular processes. This can be achieved through extracellular flux assays, by determining the decrease in OCR and/or ECAR when individual cellular processes are inhibited pharmacologically (*374*, *576*). By using specific inhibitors either individually or in combination, we can then estimate energetic share for DNA/RNA synthesis (inhibited by

Actinomycin D), protein synthesis (Cycloheximide, Chloramphenicol), protein maintenance (MG-132), cytoskeleton dynamics (Nocodazole, Latrunculin A), plasma membrane potential maintenance (Ouabain, Thapsigargin, $LaCl_3$), antioxidant defenses (LCS-1, 3-aminotriazole, PX-12), and G-Protein Coupled Receptor (GPCR) signaling (SCH-202676, Pertussis, YM-254890), among other major cellular processes. Nonetheless, it is important to emphasize that this approach has several limitations that need to be considered when interpreting the results. First, given that virtually all cellular processes consume ATP, even if successfully inhibiting all major cellular processes we will be unable to completely profile the total cellular ATP consumption. Second, the ATP consumption of certain cellular processes might only represent a small share of the total ATP consumption, so the decrease in the OCR and ECAR might stay below the detection range. Third, the inhibition achieved might be incomplete, which would result in an underestimation of the ATP consumed by the targeted cellular process. Fourth, the inhibitor might show unspecific effects and also inhibit other -unknown- cellular processes, which would result in an overestimation of the ATP consumed by the targeted cellular process. Finally, the inhibition of each cellular process will likely induce compensatory processes that can in turn affect the ATP consumption, which could result in either an underestimation or overestimation of the ATP consumed by the targeted cellular process. Despite these limitations, this approach is currently the only one available for profiling the cellular energetic partition (*464*), and it has been proven useful to demonstrate changes in ATP consumption shares in different cellular physiological states (*374*).

The next step to verify if hypermetabolism causes damage through energetic tradeoffs would be evaluating cellular growth, as well as maintenance, and repair capacity. To evaluate cellular growth, we could follow our strategy, carrying out passaging at regular time intervals and performing cell counts and cell volume assessments using Trypan Blue Stain or live/death

fluorescent dyes and the Countess II Automated Cell Counter. Instead of image-based methods, we could also use Electronic Current Exclusion (ECE) and Pulse Field Analysis-based equipment such as CASY cell counters, which do not require any kind of sample treatment and provide more accurate results both in terms of cell volume and live/death percentages.

Regarding maintenance and repair capacity, we could assess antioxidant defenses, as well as well as those mechanisms responsible for DNA, protein, and lipid membrane homeostasis. The cellular antioxidant capacity can be evaluated through several methods including measuring total antioxidant capacity (*577*), as well as measuring the levels of specific antioxidant molecules, such as reduced glutathione (GSH), vitamin C, vitamin E, vitamin A, or measuring specific antioxidant enzymes activity, including SOD, CAT, GPx, and TPx (*578, 579*). On the other hand, DNA repair capacity can be assessed by an adapted version of the Comet Assay, where cells are exposed to a genotoxic agent and the extent of DNA repair is assessed by measuring the comet tail lengths over time (*580*), as well as through fluorescence-based assays, where fluorescently labeled DNA substrates containing specific lesions are incorporated and the extent of DNA repair is determined by measuring the decrease in fluorescence as repair enzymes remove the lesion (*581*). Protein repair capacity can be assessed by classic pulse-chase assays (*582*), as well as other methods that evaluate chaperone (*583*) and ubiquitin-proteasome activity (*584, 585*). Finally, lipid membrane repair is the least explored of these mechanisms but can be evaluated by electron microscopy or by evaluating the recruitment of repair protein complexes along the membrane by fluorescent-based methods (*586*).

The decrease in maintenance and repair capacity can occur both by a decrease in enzymatic activity, mostly through post-translational modifications, or by a decrease in protein levels, mostly through a decrease in gene expression. Importantly, the latter could represent a strong sign for the

cell redirecting energetic resources away from these processes. Then, we could use classic techniques such as Western Blot and qPCR to analyze protein and transcript levels of specific enzymes. Alternatively, we could carry out proteomic and transcriptomic analysis, by which we could have a broader picture of how the expression maintenance and repair processes are expressed compared to others through enrichment analysis.

If the damaging nature of hypermetabolism stems from energetic tradeoffs that result in the decrease of cellular maintenance and repair activity, then by imposing chronic Monensin-induced hypermetabolism along the entire lifespan of a cell line we should be able to detect a reduction in the energetic share consumed and the activity of these, and maybe also a decrease in their protein content and gene expression, especially compared to others. Furthermore, we should be able to observe some kind of correlation between these parameters and macromolecule damage, cellular aging, and cell death levels. To further test this hypothesis, we could carry out a combinatorial approach and induce hypermetabolism while simultaneously enhancing the maintaining and maintenance, and repair capacity of genetic interventions involving the stable or inducible overexpression of specific enzymes, and by doing so we should be able to mitigate, at least partially, the detrimental effects of hypermetabolism.

4.6. Expanding the Energetic Model of Allostatic Load

Whether we believe that the Energetic Model of Allostatic Load could represent a mechanism through which stress and stress-induced hypermetabolism cause damage, further work needs to be done to test this. First, our model involved only the chronic exposure of a synthetic agonist of the glucocorticoid receptor in a fairly high concentration. Future studies could involve more physiological conditions, including using cortisol at the concentrations that are observed under chronic stress, and ideally perform the treatment in a way that could incorporate its natural

circadian oscillations (*587*). Furthermore, we could also incorporate the other major stress mediators, catecholamines, in the form of chronic treatment with norepinephrine and epinephrine at concentrations that are observed under chronic stress. Finally, incorporating the changes that occur in other hormones such as thyroid hormones, growth hormones, and insulin (*588*) and especially in metabolic parameters such as circulating glucose and fatty acid levels (*30, 34, 35*) could also help us gain a better understanding of the cellular recalibration that occurs under chronic stress and how this could increase the risk of morbidity and mortality.

Another important aspect to assess is whether this model applies to other cell types. As we mentioned before, our model involves human skin fibroblast. Future studies should involve cell types derived from different organs, both from those with a crucial role in the stress response such as brain, cardiac and skeletal muscle, liver, and adipose tissue, as well as from those organs whose activity is decreased during the stress response, such as digestive, kidney and reproductive systems (*31*). Of particular interest are the cells of the immune system, which is known to suffer strong dysregulation under chronic stress (*62, 63*). Does stress induce hypermetabolism in all these cell types? Does this induce changes in the ETC activity that increase ROS production? Does this induce energetic tradeoffs as well? Does the initial energetic partition of the cell influence how damaging these tradeoffs can be?

In conclusion, our work had made significant insights by revealing hypermetabolism and accelerated biological aging as interlinked features of cellular allostatic load. Whereas further studies are required to establish the causal role of hypermetabolism and elucidate the molecular basis of its damaging nature, we believe that our research will serve as a steppingstone to expand our comprehension of the stress-disease connection.

References

1. C. Bernard, *Lectures on the phenomena of life common to animals and plants*. (Thomas, 1974).
2. W. B. Cannon, *The wisdom of the body*. (W.W. Norton & Co., 1932).
3. P. Sterling, J. Eyer, Allostasis: A new paradigm to explain arousal pathology. (1988).
4. B. S. McEwen, E. Stellar, Stress and the individual: mechanisms leading to disease. *Arch Intern Med* **153**, 2093-2101 (1993).
5. B. S. McEwen, The neurobiology of stress: from serendipity to clinical relevance. *Brain Res* **886**, 172-189 (2000).
6. B. S. Mcewen, Stress, Adaptation, and Disease: Allostasis and Allostatic Load. *Annals of the New York Academy of Sciences* **840**, 33-44 (1998).
7. B. S. McEwen, Stressed or stressed out: what is the difference? *J Psychiatry Neurosci* **30**, 315-318 (2005).
8. B. S. McEwen, J. C. Wingfield, The concept of allostasis in biology and biomedicine. *Horm Behav* **43**, 2-15 (2003).
9. J. S. Shahoud, T. Sanvictores, N. R. Aeddula, *Physiology, Arterial Pressure Regulation*. StatPearls (2023).
10. C. J. Morris *et al.*, Day/Night Variability in Blood Pressure: Influence of Posture and Physical Activity. *American Journal of Hypertension* **26**, 822-828 (2013).
11. T. M. Spruill, Chronic Psychosocial Stress and Hypertension. *Current Hypertension Reports* **12**, 10-16 (2010).
12. G. C. Oh, H.-J. Cho, Blood pressure and heart failure. *Clinical Hypertension* **26**, (2020).

13. W. B. Cannon, Organization for physiological homeostasis. *Physiological Reviews* **9**, 399-431 (1929).

14. W. B. Cannon, *Bodily changes in pain, hunger, fear and rage; an account of recent researches into the function of emotional excitement*. (D. Appleton and Co., ed. 2d, 1929).

15. H. Selye, *The stress of life*. (McGraw-Hill, 1956).

16. H. Selye, *Stress without distress*. (Penguin Group Inc., 1975).

17. H. Selye, A syndrome produced by diverse nocuous agents. 1936. *J Neuropsychiatry Clin Neurosci* **10**, 230-231 (1998).

18. D. A. Girdano, D. E. Dusek, G. S. Everly, *Controlling Stress and Tension*. (Pearson, 2013).

19. G. P. Chrousos, P. W. Gold, The concepts of stress and stress system disorders. Overview of physical and behavioral homeostasis. *JAMA* **267**, 1244-1252 (1992).

20. G. Fink, *McEwen BS. Definitions and concepts of stress. In: Stress: Concepts, Cognition, Emotion, and Behavior: Handbook of Stress Series, Volume 1*. (Elsevier Science, 2016).

21. K. L. Harkness, S. M. Monroe, The assessment and measurement of adult life stress: Basic premises, operational principles, and design requirements. *J Abnorm Psychol* **125**, 727-745 (2016).

22. R. S. Lazarus, *Stress and Emotion: A New Synthesis*. (Springer Publishing Company, 2006).

23. A. Ellis, *Reason and Emotion in Psychotherapy*. (Carol Publishing Group, 1962).

24. Y. M. Ulrich-Lai, J. P. Herman, Neural regulation of endocrine and autonomic stress responses. *Nat Rev Neurosci* **10**, 397-409 (2009).

25. G. Fink, *Encyclopedia of Stress 4 Vol Set*. (Academic Press Inc., 2007).

26. M. Gunnar, K. Quevedo, The neurobiology of stress and development. *Annu Rev Psychol* **58**, 145-173 (2007).

27. C.-J. Huang, H. E. Webb, M. C. Zourdos, E. O. Acevedo, Cardiovascular reactivity, stress, and physical activity. *Frontiers in Physiology* **4**, (2013).

28. P. G. Guyenet, The sympathetic control of blood pressure. *Nat Rev Neurosci* **7**, 335-346 (2006).

29. R. G. Goldie, J. W. Paterson, K. M. Lulich, Adrenoceptors in airway smooth muscle. *Pharmacol Ther* **48**, 295-322 (1990).

30. K. Nonogaki, New insights into sympathetic regulation of glucose and fat metabolism. *Diabetologia* **43**, 533-549 (2000).

31. E. Caraffa-Braga, L. Granata, O. Pinotti, Changes in blood-flow distribution during acute emotional stress in dogs. *Pflügers Archiv* **339**, 203-216 (1973).

32. S. Kuckuck *et al.*, Glucocorticoids, stress and eating: The mediating role of appetite-regulating hormones. *Obes Rev* **24**, e13539 (2023).

33. R. M. de Guia, Stress, glucocorticoid signaling pathway, and metabolic disorders. *Diabetes Metab Syndr* **14**, 1273-1280 (2020).

34. T. Kuo, A. McQueen, T. C. Chen, J. C. Wang, Regulation of Glucose Homeostasis by Glucocorticoids. *Adv Exp Med Biol* **872**, 99-126 (2015).

35. A. J. Peckett, D. C. Wright, M. C. Riddell, The effects of glucocorticoids on adipose tissue lipid metabolism. *Metabolism* **60**, 1500-1510 (2011).

36. U. S. O. o. t. A. S. f. Health, S. General, U. S. O. o. t. A. S. f. Health, *Healthy People: The Surgeon General's Report on Health Promotion and Disease Prevention*. (U.S.

Department of Health, Education, and Welfare, Public Health Service, Office of the Assistant Secretary for Health and Surgeon General, 1979).

37. S. Cohen, D. Janicki-Deverts, G. E. Miller, Psychological stress and disease. *JAMA* **298**, 1685-1687 (2007).

38. B. S. McEwen, Central effects of stress hormones in health and disease: Understanding the protective and damaging effects of stress and stress mediators. *Eur J Pharmacol* **583**, 174-185 (2008).

39. J. P. Herman, J. Flak, R. Jankord, Chronic stress plasticity in the hypothalamic paraventricular nucleus. *Prog Brain Res* **170**, 353-364 (2008).

40. E. Woo, L. H. Sansing, A. F. T. Arnsten, D. Datta, Chronic Stress Weakens Connectivity in the Prefrontal Cortex: Architectural and Molecular Changes. *Chronic Stress (Thousand Oaks)* **5**, 24705470211029254 (2021).

41. X. Zhang *et al.*, Stress-Induced Functional Alterations in Amygdala: Implications for Neuropsychiatric Diseases. *Front Neurosci* **12**, 367 (2018).

42. E. J. Kim, B. Pellman, J. J. Kim, Stress effects on the hippocampus: a critical review. *Learn Mem* **22**, 411-416 (2015).

43. J. J. Kim, D. M. Diamond, The stressed hippocampus, synaptic plasticity and lost memories. *Nat Rev Neurosci* **3**, 453-462 (2002).

44. O. V. Burenkova, O. Y. Naumova, E. L. Grigorenko, Stress in the onset and aggravation of learning disabilities. *Dev Rev* **61**, (2021).

45. B. S. McEwen, L. Eiland, R. G. Hunter, M. M. Miller, Stress and anxiety: structural plasticity and epigenetic regulation as a consequence of stress. *Neuropharmacology* **62**, 3-12 (2012).

46. B. S. McEwen, Glucocorticoids, depression, and mood disorders: structural remodeling in the brain. *Metabolism* **54**, 20-23 (2005).

47. B. S. McEwen, Protection and damage from acute and chronic stress: allostasis and allostatic overload and relevance to the pathophysiology of psychiatric disorders. *Ann N Y Acad Sci* **1032**, 1-7 (2004).

48. M. Kivimaki, A. Bartolomucci, I. Kawachi, The multiple roles of life stress in metabolic disorders. *Nat Rev Endocrinol* **19**, 10-27 (2023).

49. H. Yaribeygi, M. Maleki, A. E. Butler, T. Jamialahmadi, A. Sahebkar, Molecular mechanisms linking stress and insulin resistance. *EXCLI J* **21**, 317-334 (2022).

50. D. Vedantam *et al.*, Stress-Induced Hyperglycemia: Consequences and Management. *Cureus* **14**, e26714 (2022).

51. C. Catalina-Romero *et al.*, The relationship between job stress and dyslipidemia. *Scand J Public Health* **41**, 142-149 (2013).

52. M. Kivimaki *et al.*, Neighbourhood socioeconomic disadvantage, risk factors, and diabetes from childhood to middle age in the Young Finns Study: a cohort study. *Lancet Public Health* **3**, e365-e373 (2018).

53. M. Razzoli, C. Pearson, S. Crow, A. Bartolomucci, Stress, overeating, and obesity: Insights from human studies and preclinical models. *Neurosci Biobehav Rev* **76**, 154-162 (2017).

54. S. E. Jackson, C. Kirschbaum, A. Steptoe, Hair cortisol and adiposity in a population-based sample of 2,527 men and women aged 54 to 87 years. *Obesity (Silver Spring)* **25**, 539-544 (2017).

55. A. Santosa *et al.*, Psychosocial Risk Factors and Cardiovascular Disease and Death in a Population-Based Cohort From 21 Low-, Middle-, and High-Income Countries. *JAMA Network Open* **4**, e2138920 (2021).

56. R. A. Hackett, A. Steptoe, Type 2 diabetes mellitus and psychological stress — a modifiable risk factor. *Nature Reviews Endocrinology* **13**, 547-560 (2017).

57. S. J. Kelly, M. Ismail, Stress and type 2 diabetes: a review of how stress contributes to the development of type 2 diabetes. *Annu Rev Public Health* **36**, 441-462 (2015).

58. S. Shea *et al.*, Non-Alcoholic Fatty Liver Disease (NAFLD) and Potential Links to Depression, Anxiety, and Chronic Stress. *Biomedicines* **9**, (2021).

59. T. T. Laitinen *et al.*, Childhood Socioeconomic Disadvantage and Risk of Fatty Liver in Adulthood: The Cardiovascular Risk in Young Finns Study. *Hepatology* **71**, 67-75 (2020).

60. J. E. Dimsdale, Psychological stress and cardiovascular disease. *J Am Coll Cardiol* **51**, 1237-1246 (2008).

61. A. Steptoe, M. Kivimaki, Stress and cardiovascular disease. *Nat Rev Cardiol* **9**, 360-370 (2012).

62. J. I. Webster Marketon, R. Glaser, Stress hormones and immune function. *Cell Immunol* **252**, 16-26 (2008).

63. F. S. Dhabhar, Effects of stress on immune function: the good, the bad, and the beautiful. *Immunol Res* **58**, 193-210 (2014).

64. J. K. Kiecolt-Glaser, J. R. Dura, C. E. Speicher, O. J. Trask, R. Glaser, Spousal caregivers of dementia victims: longitudinal changes in immunity and health. *Psychosom Med* **53**, 345-362 (1991).

65. S. Cohen, D. A. Tyrrell, A. P. Smith, Psychological stress and susceptibility to the common cold. *N Engl J Med* **325**, 606-612 (1991).

66. M. Jafferany, Psychodermatology. *The Primary Care Companion to The Journal of Clinical Psychiatry* **09**, 203-213 (2007).

67. E. Chen, G. E. Miller, Stress and inflammation in exacerbations of asthma. *Brain, Behavior, and Immunity* **21**, 993-999 (2007).

68. N. D. Dave, L. Xiang, K. E. Rehm, G. D. Marshall, Stress and Allergic Diseases. *Immunology and Allergy Clinics of North America* **31**, 55-68 (2011).

69. L. Ge *et al.*, Psychological stress in inflammatory bowel disease: Psychoneuroimmunological insights into bidirectional gut–brain communications. *Frontiers in Immunology* **13**, (2022).

70. D. Ahn, H. Kim, B. Lee, D.-H. Hahm, Psychological Stress-Induced Pathogenesis of Alopecia Areata: Autoimmune and Apoptotic Pathways. *International Journal of Molecular Sciences* **24**, 11711 (2023).

71. A. W. Evers *et al.*, Does stress affect the joints? Daily stressors, stress vulnerability, immune and HPA axis activity, and short-term disease and symptom fluctuations in rheumatoid arthritis. *Ann Rheum Dis* **73**, 1683-1688 (2014).

72. L. Rousset, B. Halioua, Stress and psoriasis. *Int J Dermatol* **57**, 1165-1172 (2018).

73. L. Stojanovich, D. Marisavljevich, Stress as a trigger of autoimmune disease. *Autoimmun Rev* **7**, 209-213 (2008).

74. S. Dai *et al.*, Chronic Stress Promotes Cancer Development. *Frontiers in Oncology* **10**, (2020).

75. E. J. Rodriquez, S. E. Gregorich, J. Livaudais-Toman, E. J. Pérez-Stable, Coping With Chronic Stress by Unhealthy Behaviors: A Re-Evaluation Among Older Adults by Race/Ethnicity. *Journal of Aging and Health* **29**, 805-825 (2017).

76. D. A. Kalmbach, J. R. Anderson, C. L. Drake, The impact of stress on sleep: Pathogenic sleep reactivity as a vulnerability to insomnia and circadian disorders. *J Sleep Res* **27**, e12710 (2018).

77. E. J. Kim, J. E. Dimsdale, The effect of psychosocial stress on sleep: a review of polysomnographic evidence. *Behav Sleep Med* **5**, 256-278 (2007).

78. A. J. Tomiyama, M. F. Dallman, E. S. Epel, Comfort food is comforting to those most stressed: Evidence of the chronic stress response network in high stress women. *Psychoneuroendocrinology* **36**, 1513-1519 (2011).

79. G. Oliver, J. Wardle, Perceived effects of stress on food choice. *Physiol Behav* **66**, 511-515 (1999).

80. M. A. Stults-Kolehmainen, R. Sinha, The Effects of Stress on Physical Activity and Exercise. *Sports Medicine* **44**, 81-121 (2014).

81. E. I. Fransson *et al.*, Job Strain as a Risk Factor for Leisure-Time Physical Inactivity: An Individual-Participant Meta-Analysis of Up to 170,000 Men and Women: The IPD-Work Consortium. *American Journal of Epidemiology* **176**, 1078-1089 (2012).

82. R. Sinha, Chronic Stress, Drug Use, and Vulnerability to Addiction. *Annals of the New York Academy of Sciences* **1141**, 105-130 (2008).

83. M. Virtanen *et al.*, Long working hours and alcohol use: systematic review and meta-analysis of published studies and unpublished individual participant data. *BMJ* **350**, g7772-g7772 (2015).

84. A. Prior *et al.*, The Association Between Perceived Stress and Mortality Among People With Multimorbidity: A Prospective Population-Based Cohort Study. *American Journal of Epidemiology* **184**, 199-210 (2016).

85. G. D. Batty, M. Hamer, C. R. Gale, Life-course Psychological Distress and Total Mortality by Middle Age: The 1970 Birth Cohort Study. *Epidemiology* **32**, 740-743 (2021).

86. M. A. Bellis *et al.*, Measuring mortality and the burden of adult disease associated with adverse childhood experiences in England: a national survey. *Journal of Public Health* **37**, 445-454 (2015).

87. A. Prior *et al.*, Bereavement, multimorbidity and mortality: a population-based study using bereavement as an indicator of mental stress. *Psychological Medicine* **48**, 1437-1443 (2018).

88. C. L. Crowe *et al.*, Associations of Loneliness and Social Isolation With Health Span and Life Span in the U.S. Health and Retirement Study. *The Journals of Gerontology: Series A* **76**, 1997-2006 (2021).

89. S. Stringhini *et al.*, Socioeconomic status and the 25 × 25 risk factors as determinants of premature mortality: a multicohort study and meta-analysis of 1·7 million men and women. *The Lancet* **389**, 1229-1237 (2017).

90. J. R. Falvey, A. M. Hajduk, C. R. Keys, S. I. Chaudhry, Association of Financial Strain With Mortality Among Older US Adults Recovering From an Acute Myocardial Infarction. *JAMA Intern Med* **182**, 445-448 (2022).

91. M. Kivimäki *et al.*, Work stress and risk of death in men and women with and without cardiometabolic disease: a multicohort study. *The Lancet Diabetes & Endocrinology* **6**, 705-713 (2018).

92. J. Ervasti *et al.*, Long working hours and risk of 50 health conditions and mortality outcomes: a multicohort study in four European countries. *Lancet Reg Health Eur* **11**, 100212 (2021).

93. E. Charmandari, C. Tsigos, G. Chrousos, Endocrinology of the Stress Response. *Annual Review of Physiology* **67**, 259-284 (2005).

94. R. Christie, Some types of respiration in neuroses. *QJM: An International Journal of Medicine* **4**, 427-428 (1935).

95. J. Whitehorn, H. Lundholm, G. Gardner, The metabolic rate in emotional moods induced by suggestion in hypnosis. *American Journal of Insanity* **86**, 661-666 (1930).

96. N. M. Mehta *et al.*, Accuracy of a simplified equation for energy expenditure based on bedside volumetric carbon dioxide elimination measurement--a two-center study. *Clin Nutr* **34**, 151-155 (2015).

97. D. Carroll, J. R. Turner, J. C. Hellawell, Heart rate and oxygen consumption during active psychological challenge: the effects of level of difficulty. *Psychophysiology* **23**, 174-181 (1986).

98. A. Sawai, K. Ohshige, K. Yamasue, T. Hayashi, O. Tochikubo, Influence of mental stress on cardiovascular function as evaluated by changes in energy expenditure. *Hypertens Res* **30**, 1019-1027 (2007).

99. D. Carroll, A. C. Phillips, G. M. Balanos, Metabolically exaggerated cardiac reactions to acute psychological stress revisited. *Psychophysiology* **46**, 270-275 (2009).

100. G. M. Balanos *et al.*, Metabolically exaggerated cardiac reactions to acute psychological stress: the effects of resting blood pressure status and possible underlying mechanisms. *Biol Psychol* **85**, 104-111 (2010).

101. G. Seematter, M. Dirlewanger, V. Rey, P. Schneiter, L. Tappy, Metabolic effects of mental stress during over- and underfeeding in healthy women. *Obes Res* **10**, 49-55 (2002).

102. G. Seematter *et al.*, Effects of mental stress on insulin-mediated glucose metabolism and energy expenditure in lean and obese women. *Am J Physiol Endocrinol Metab* **279**, E799-805 (2000).

103. J. Delarue *et al.*, Fish oil prevents the adrenal activation elicited by mental stress in healthy men. *Diabetes Metab* **29**, 289-295 (2003).

104. M. Racic *et al.*, Self- perceived stress in relation to anxiety, depression and health-related quality of life among health professions students: A cross-sectional study from Bosnia and Herzegovina. *Slovenian Journal of Public Health* **56**, 251-259 (2017).

105. W. D. Schmidt, P. J. O'Connor, J. B. Cochrane, M. Cantwell, Resting metabolic rate is influenced by anxiety in college men. *J Appl Physiol (1985)* **80**, 638-642 (1996).

106. A. Tyagi, M. Cohen, J. Reece, S. Telles, An explorative study of metabolic responses to mental stress and yoga practices in yoga practitioners, non-yoga practitioners and individuals with metabolic syndrome. *BMC Complement Altern Med* **14**, 445 (2014).

107. T. Hollstein *et al.*, Urinary Norepinephrine Is a Metabolic Determinant of 24-Hour Energy Expenditure and Sleeping Metabolic Rate in Adult Humans. *J Clin Endocrinol Metab* **105**, (2020).

108. C. G. Haase, A. K. Long, J. F. Gillooly, Energetics of stress: linking plasma cortisol levels to metabolic rate in mammals. *Biol Lett* **12**, 20150867 (2016).

109. S. S. Damjanovic *et al.*, Relationship between basal metabolic rate and cortisol secretion throughout pregnancy. *Endocrine* **35**, 262-268 (2009).

110. K. M. Ratheiser, D. J. Brillon, R. G. Campbell, D. E. Matthews, Epinephrine produces a prolonged elevation in metabolic rate in humans. *Am J Clin Nutr* **68**, 1046-1052 (1998).

111. P. A. Tataranni *et al.*, Effects of glucocorticoids on energy metabolism and food intake in humans. *Am J Physiol* **271**, E317-325 (1996).

112. L. E. Ramage *et al.*, Glucocorticoids Acutely Increase Brown Adipose Tissue Activity in Humans, Revealing Species-Specific Differences in UCP-1 Regulation. *Cell Metab* **24**, 130-141 (2016).

113. R. B. Harris, J. Palmondon, S. Leshin, W. P. Flatt, D. Richard, Chronic disruption of body weight but not of stress peptides or receptors in rats exposed to repeated restraint stress. *Horm Behav* **49**, 615-625 (2006).

114. D. F. Garcia-Diaz *et al.*, Chronic mild stress induces variations in locomotive behavior and metabolic rates in high fat fed rats. *J Physiol Biochem* **63**, 337-346 (2007).

115. B. Jimeno, M. Hau, S. Verhulst, Corticosterone levels reflect variation in metabolic rate, independent of 'stress'. *Sci Rep* **8**, 13020 (2018).

116. D. M. Bryant, A. V. Newton, Metabolic costs of dominance in dippers, Cinclus cinclus. *Animal Behaviour* **48**, 447-455 (1994).

117. O. Hogstad, It Is Expensive to Be Dominant. *The Auk* **104**, 333-336 (1987).

118. E. Røskaft, T. Järvi, M. Bakken, C. Bech, R. E. Reinertsen, The relationship between social status and resting metabolic rate in great tits (Parus major) and pied flycatchers (Ficedula hypoleuca). *Animal Behaviour* **34**, 838-842 (1986).

119. C. Ruggiero *et al.*, High basal metabolic rate is a risk factor for mortality: the Baltimore Longitudinal Study of Aging. *J Gerontol A Biol Sci Med Sci* **63**, 698-706 (2008).

120. R. Jumpertz *et al.*, Higher energy expenditure in humans predicts natural mortality. *J Clin Endocrinol Metab* **96**, E972-976 (2011).

121. J. A. Schrack, N. D. Knuth, E. M. Simonsick, L. Ferrucci, "IDEAL" aging is associated with lower resting metabolic rate: the Baltimore Longitudinal Study of Aging. *J Am Geriatr Soc* **62**, 667-672 (2014).

122. A. Sampath Kumar *et al.*, Correlation between basal metabolic rate, visceral fat and insulin resistance among type 2 diabetes mellitus with peripheral neuropathy. *Diabetes Metab Syndr* **13**, 344-348 (2019).

123. C. Vazeille *et al.*, Relation between hypermetabolism, cachexia, and survival in cancer patients: a prospective study in 390 cancer patients before initiation of anticancer therapy. *Am J Clin Nutr* **105**, 1139-1147 (2017).

124. F. J. Steyn *et al.*, Hypermetabolism in ALS is associated with greater functional decline and shorter survival. *J Neurol Neurosurg Psychiatry* **89**, 1016-1023 (2018).

125. J. Yao *et al.*, Persistently Increased Resting Energy Expenditure Predicts Short-Term Mortality in Patients with Acute-on-Chronic Liver Failure. *Ann Nutr Metab* **73**, 2-9 (2018).

126. G. Sturm *et al.*, OxPhos defects cause hypermetabolism and reduce lifespan in cells and in patients with mitochondrial diseases. *Commun Biol* **6**, 22 (2023).

127. N. Bobba-Alves *et al.*, Cellular allostatic load is linked to increased energy expenditure and accelerated biological aging. *Psychoneuroendocrinology* **155**, 106322 (2023).

128. N. Bobba-Alves, R. P. Juster, M. Picard, The energetic cost of allostasis and allostatic load. *Psychoneuroendocrinology* **146**, 105951 (2022).

129. J. F. Lesgards *et al.*, Assessment of lifestyle effects on the overall antioxidant capacity of healthy subjects. *Environ Health Perspect* **110**, 479-486 (2002).

130. K. H. Alzoubi, O. F. Khabour, B. A. Rashid, I. M. Damaj, H. A. Salah, The neuroprotective effect of vitamin E on chronic sleep deprivation-induced memory impairment: the role of oxidative stress. *Behav Brain Res* **226**, 205-210 (2012).

131. L. Ramanathan, S. Gulyani, R. Nienhuis, J. M. Siegel, Sleep deprivation decreases superoxide dismutase activity in rat hippocampus and brainstem. *Neuroreport* **13**, 1387-1390 (2002).

132. J. Djordjevic, A. Djordjevic, M. Adzic, M. B. Radojcic, Chronic Social Isolation Compromises the Activity of Both Glutathione Peroxidase and Catalase in Hippocampus of Male Wistar Rats. *Cellular and Molecular Neurobiology* **30**, 693-700 (2010).

133. R. Glaser, B. E. Thorn, K. L. Tarr, J. K. Kiecolt-Glaser, S. M. D'Ambrosio, Effects of stress on methyltransferase synthesis: an important DNA repair enzyme. *Health Psychol* **4**, 403-412 (1985).

134. K. E. Rentscher, J. E. Carroll, L. R. Polsky, D. M. Lamkin, Chronic stress increases transcriptomic indicators of biological aging in mouse bone marrow leukocytes. *Brain Behav Immun Health* **22**, 100461 (2022).

135. S. N. O'Brien, L. L. Larcom, E. G. Baxley, Correlates of plasma cortisol and DNA repair in human peripheral lymphocytes: suppression of repair in women taking estrogen. *Horm Res* **39**, 241-246 (1993).

136. R. L. Flaherty *et al.*, Glucocorticoids induce production of reactive oxygen species/reactive nitrogen species and DNA damage through an iNOS mediated pathway in breast cancer. *Breast Cancer Research* **19**, (2017).

137. E. S. Epel *et al.*, Accelerated telomere shortening in response to life stress. *Proceedings of the National Academy of Sciences* **101**, 17312-17315 (2004).

138. J. Choi, S. R. Fauce, R. B. Effros, Reduced telomerase activity in human T lymphocytes exposed to cortisol. *Brain, Behavior, and Immunity* **22**, 600-605 (2008).

139. E. Bolund, The challenge of measuring trade-offs in human life history research. *Evolution and Human Behavior* **41**, 502-512 (2020).

140. S. R. Lee *et al.*, Glucocorticoids and their receptors: insights into specific roles in mitochondria. *Prog Biophys Mol Biol* **112**, 44-54 (2013).

141. I. Manoli *et al.*, Mitochondria as key components of the stress response. *Trends in Endocrinology & Metabolism* **18**, 190-198 (2007).

142. J. Du *et al.*, Dynamic regulation of mitochondrial function by glucocorticoids. *Proc Natl Acad Sci U S A* **106**, 3543-3548 (2009).

143. M. Picard, B. S. Mcewen, Psychological Stress and Mitochondria: A Systematic Review. *Psychosomatic Medicine* **80**, 141-153 (2018).

144. V. M. Tang, A. H. Young, H. Tan, C. Beasley, J. F. Wang, Glucocorticoids increase protein carbonylation and mitochondrial dysfunction. *Horm Metab Res* **45**, 709-715 (2013).

145. N. Cai *et al.*, Genetic Control over mtDNA and Its Relationship to Major Depressive Disorder. *Current Biology* **25**, 3170-3177 (2015).

146. A. R. Tyrka *et al.*, Alterations of Mitochondrial DNA Copy Number and Telomere Length With Early Adversity and Psychopathology. *Biological Psychiatry* **79**, 78-86 (2016).

147. D. Lindqvist *et al.*, Increased plasma levels of circulating cell-free mitochondrial DNA in suicide attempters: associations with HPA-axis hyperactivity. *Translational Psychiatry* **6**, e971-e971 (2016).

148. C. Trumpff *et al.*, Stress and circulating cell-free mitochondrial DNA: A systematic review of human studies, physiological considerations, and technical recommendations. *Mitochondrion* **59**, 225-245 (2021).

149. M. Picard *et al.*, A Mitochondrial Health Index Sensitive to Mood and Caregiving Stress. *Biological Psychiatry* **84**, 9-17 (2018).

150. Y. A. Su *et al.*, Dysregulated Mitochondrial Genes and Networks with Drug Targets in Postmortem Brain of Patients with Posttraumatic Stress Disorder (PTSD) Revealed by Human Mitochondria-Focused cDNA Microarrays. *International Journal of Biological Sciences*, 223-235 (2008).

151. L. Zhang *et al.*, Mitochondria-focused gene expression profile reveals common pathways and CPT1B dysregulation in both rodent stress model and human subjects with PTSD. *Transl Psychiatry* **5**, e580 (2015).

152. T. Mitsui *et al.*, Mitochondrial damage in patients with long-term corticosteroid therapy: development of oculoskeletal symptoms similar to mitochondrial disease. *Acta Neuropathologica* **104**, 260-266 (2002).

153. W. Liu, C. Zhou, Corticosterone reduces brain mitochondrial function and expression of mitofusin, BDNF in depression-like rodents regardless of exercise preconditioning. *Psychoneuroendocrinology* **37**, 1057-1070 (2012).

154. M. Duclos *et al.*, Effects of corticosterone on muscle mitochondria identifying different sensitivity to glucocorticoids in Lewis and Fischer rats. *Am J Physiol Endocrinol Metab* **286**, E159-167 (2004).

155. N. Cai *et al.*, Molecular Signatures of Major Depression. *Current Biology* **25**, 1146-1156 (2015).

156. G. Napolitano, D. Barone, S. Di Meo, P. Venditti, Adrenaline induces mitochondrial biogenesis in rat liver. *Journal of Bioenergetics and Biomembranes* **50**, 11-19 (2018).

157. J. C. Yoon *et al.*, Control of hepatic gluconeogenesis through the transcriptional coactivator PGC-1. *Nature* **413**, 131-138 (2001).

158. I. A. Gak *et al.*, Stress triggers mitochondrial biogenesis to preserve steroidogenesis in Leydig cells. *Biochim Biophys Acta* **1853**, 2217-2227 (2015).

159. M. Gesi *et al.*, Morphological alterations induced by loud noise in the myocardium: The role of benzodiazepine receptors. *Microscopy Research and Technique* **59**, 136-146 (2002).

160. P. Soldani *et al.*, SEM/TEM investigation of rat cardiac subcellular alterations induced by changing duration of noise stress. *Anat Rec* **248**, 521-532 (1997).

161. C. Batandier *et al.*, Acute stress delays brain mitochondrial permeability transition pore opening. *Journal of Neurochemistry* **131**, 314-322 (2014).

162. J. L. Madrigal *et al.*, Glutathione Depletion, Lipid Peroxidation and Mitochondrial Dysfunction Are Induced by Chronic Stress in Rat Brain. *Neuropsychopharmacology* **24**, 420-429 (2001).

163. S. Martín-Aragón, Á. Villar, J. Benedí, Age-dependent effects of esculetin on mood-related behavior and cognition from stressed mice are associated with restoring brain antioxidant status. *Prog Neuropsychopharmacol Biol Psychiatry* **65**, 1-16 (2016).

164. G. T. Rezin *et al.*, Inhibition of mitochondrial respiratory chain in brain of rats subjected to an experimental model of depression. *Neurochem Int* **53**, 395-400 (2008).

165. P. Rinwa, A. Kumar, Piperine potentiates the protective effects of curcumin against chronic unpredictable stress-induced cognitive impairment and oxidative damage in mice. *Brain Res* **1488**, 38-50 (2012).

166. P. Rinwa, A. Kumar, Modulation of nitrergic signalling pathway by American ginseng attenuates chronic unpredictable stress-induced cognitive impairment, neuroinflammation, and biochemical alterations. *Naunyn-Schmiedeberg's Archives of Pharmacology* **387**, 129-141 (2014).

167. J. S. Seo *et al.*, Behavioral stress causes mitochondrial dysfunction via ABAD up-regulation and aggravates plaque pathology in the brain of a mouse model of Alzheimer disease. *Free Radic Biol Med* **50**, 1526-1535 (2011).

168. C. F. Ortmann *et al.*, Enriched Flavonoid Fraction from Cecropia pachystachya Trécul Leaves Exerts Antidepressant-like Behavior and Protects Brain Against Oxidative Stress in Rats Subjected to Chronic Mild Stress. *Neurotoxicity Research* **29**, 469-483 (2016).

169. Y.-F. Li *et al.*, Anti-Stress Effects of Carnosine on Restraint-Evoked Immunocompromise in Mice through Spleen Lymphocyte Number Maintenance. *PLoS ONE* **7**, e33190 (2012).

170. Y. Gong, Y. Chai, J. H. Ding, X. L. Sun, G. Hu, Chronic mild stress damages mitochondrial ultrastructure and function in mouse brain. *Neurosci Lett* **488**, 76-80 (2011).

171. S. A. Andric *et al.*, The opposite roles of glucocorticoid and α1-adrenergic receptors in stress triggered apoptosis of rat Leydig cells. *Am J Physiol Endocrinol Metab* **304**, E51-59 (2013).

172. Y. Kambe, A. Miyata, Potential involvement of the mitochondrial unfolded protein response in depressive-like symptoms in mice. *Neurosci Lett* **588**, 166-171 (2015).

173. X. H. Liu *et al.*, Proteomic analysis of mitochondrial proteins in cardiomyocytes from chronic stressed rat. *PROTEOMICS* **4**, 3167-3176 (2004).

174. B. D'Autréaux, M. B. Toledano, ROS as signalling molecules: mechanisms that generate specificity in ROS homeostasis. *Nature Reviews Molecular Cell Biology* **8**, 813-824 (2007).

175. M. D. Brand, Mitochondrial generation of superoxide and hydrogen peroxide as the source of mitochondrial redox signaling. *Free Radic Biol Med* **100**, 14-31 (2016).

176. R. J. Mailloux, An Update on Mitochondrial Reactive Oxygen Species Production. *Antioxidants* **9**, 472 (2020).

177. P. Murphy, Michael, How mitochondria produce reactive oxygen species. *Biochemical Journal* **417**, 1-13 (2009).

178. C. L. Quinlan, I. V. Perevoshchikova, M. Hey-Mogensen, A. L. Orr, M. D. Brand, Sites of reactive oxygen species generation by mitochondria oxidizing different substrates. *Redox Biol* **1**, 304-312 (2013).

179. J. Hirst, S. King, Martin, R. Pryde, Kenneth, The production of reactive oxygen species by complex I. *Biochemical Society Transactions* **36**, 976-980 (2008).

180. V. Yankovskaya *et al.*, Architecture of succinate dehydrogenase and reactive oxygen species generation. *Science* **299**, 700-704 (2003).

181. L. Zhang, L. Yu, C.-A. Yu, Generation of Superoxide Anion by Succinate-Cytochromec Reductase from Bovine Heart Mitochondria. *Journal of Biological Chemistry* **273**, 33972-33976 (1998).

182. T. Ishii *et al.*, A mutation in the SDHC gene of complex II increases oxidative stress, resulting in apoptosis and tumorigenesis. *Cancer Res* **65**, 203-209 (2005).

183. L. Bleier, S. Dröse, Superoxide generation by complex III: from mechanistic rationales to functional consequences. *Biochim Biophys Acta* **1827**, 1320-1331 (2013).

184. V. Adam-Vizi, L. Tretter, The role of mitochondrial dehydrogenases in the generation of oxidative stress. *Neurochem Int* **62**, 757-763 (2013).

185. G. Loschen, A. Azzi, L. Flohé, Mitochondrial H₂O₂ formation: Relationship with energy conservation. *FEBS Letters* **33**, 84-88 (1973).

186. Y. Wang, R. Branicky, A. Noë, S. Hekimi, Superoxide dismutases: Dual roles in controlling ROS damage and regulating ROS signaling. *Journal of Cell Biology* **217**, 1915-1928 (2018).

187. A. V. Snezhkina *et al.*, ROS Generation and Antioxidant Defense Systems in Normal and Malignant Cells. *Oxidative Medicine and Cellular Longevity* **2019**, 1-17 (2019).

188. D. Trachootham, W. Lu, M. A. Ogasawara, N. R.-D. Valle, P. Huang, Redox Regulation of Cell Survival. *Antioxidants & Redox Signaling* **10**, 1343-1374 (2008).

189. D. Atanackovic, M. C. Brunner-Weinzierl, H. Kröger, S. Serke, H. C. Deter, Acute psychological stress simultaneously alters hormone levels, recruitment of lymphocyte subsets, and production of reactive oxygen species. *Immunol Invest* **31**, 73-91 (2002).

190. D. Atanackovic, J. Schulze, H. Kröger, M. C. Brunner-Weinzierl, H. C. Deter, Acute psychological stress induces a prolonged suppression of the production of reactive oxygen species by phagocytes. *J Neuroimmunol* **142**, 159-165 (2003).

191. E. Kim *et al.*, Association of acute psychosocial stress with oxidative stress: Evidence from serum analysis. *Redox Biol* **47**, 102138 (2021).

192. D. Bagchi *et al.*, Acute and chronic stress-induced oxidative gastrointestinal mucosal injury in rats and protection by bismuth subsalicylate. *Mol Cell Biochem* **196**, 109-116 (1999).

193. G. Lucca *et al.*, Increased oxidative stress in submitochondrial particles into the brain of rats submitted to the chronic mild stress paradigm. *J Psychiatr Res* **43**, 864-869 (2009).

194. V. D'Almeida *et al.*, Sleep deprivation induces brain region-specific decreases in glutathione levels. *Neuroreport* **9**, 2853-2856 (1998).

195. M. Möller, J. L. Du Preez, R. Emsley, B. H. Harvey, Isolation rearing-induced deficits in sensorimotor gating and social interaction in rats are related to cortico-striatal oxidative stress, and reversed by sub-chronic clozapine administration. *Eur Neuropsychopharmacol* **21**, 471-483 (2011).

196. L. Wen *et al.*, Exercise prevents raphe nucleus mitochondrial overactivity in a rat depression model. *Physiol Behav* **132**, 57-65 (2014).

197. N. Uysal *et al.*, Age-dependent effects of maternal deprivation on oxidative stress in infant rat brain. *Neurosci Lett* **384**, 98-101 (2005).

198. F. M. Yakes, B. Van Houten, Mitochondrial DNA damage is more extensive and persists longer than nuclear DNA damage in human cells following oxidative stress. *Proceedings of the National Academy of Sciences* **94**, 514-519 (1997).

199. M. S. Cooke, M. D. Evans, M. Dizdaroglu, J. Lunec, Oxidative DNA damage: mechanisms, mutation, and disease. *The FASEB Journal* **17**, 1195-1214 (2003).

200. T. von Zglinicki, Oxidative stress shortens telomeres. *Trends Biochem Sci* **27**, 339-344 (2002).

201. M. R. Branco, G. Ficz, W. Reik, Uncovering the role of 5-hydroxymethylcytosine in the epigenome. *Nature Reviews Genetics* **13**, 7-13 (2012).

202. J. J. Galligan *et al.*, Stable histone adduction by 4-oxo-2-nonenal: a potential link between oxidative stress and epigenetics. *J Am Chem Soc* **136**, 11864-11866 (2014).

203. R. Kehm, T. Baldensperger, J. Raupbach, A. Höhn, Protein oxidation - Formation mechanisms, detection and relevance as biomarkers in human diseases. *Redox Biol* **42**, 101901 (2021).

204. Y. Gidron, K. Russ, H. Tissarchondou, J. Warner, The relation between psychological factors and DNA-damage: a critical review. *Biol Psychol* **72**, 291-304 (2006).

205. D. Costantini, V. Marasco, A. P. Møller, A meta-analysis of glucocorticoids as modulators of oxidative stress in vertebrates. *Journal of Comparative Physiology B*, (2011).

206. I. Bortolotto *et al.*, DNA damage, salivary cortisol levels, and cognitive parameters in a nursing team. *Mutat Res Genet Toxicol Environ Mutagen* **861-862**, 503300 (2021).

207. A. Joergensen *et al.*, Association between urinary excretion of cortisol and markers of oxidatively damaged DNA and RNA in humans. *PLoS One* **6**, e20795 (2011).

208. M. Sivonová *et al.*, Oxidative stress in university students during examinations. *Stress* **7**, 183-188 (2004).

209. M. Irie, S. Asami, S. Nagata, M. Miyata, H. Kasai, Relationships between perceived workload, stress and oxidative DNA damage. *Int Arch Occup Environ Health* **74**, 153-157 (2001).

210. E. Dimitroglou *et al.*, DNA damage in a human population affected by chronic psychogenic stress. *Int J Hyg Environ Health* **206**, 39-44 (2003).

211. M. Irie *et al.*, Psychosocial factors as a potential trigger of oxidative DNA damage in human leukocytes. *Jpn J Cancer Res* **92**, 367-376 (2001).

212. K. Aschbacher *et al.*, Good stress, bad stress and oxidative stress: insights from anticipatory cortisol reactivity. *Psychoneuroendocrinology* **38**, 1698-1708 (2013).

213. K. Z. Knickelbein, M. Flint, F. Jenkins, A. Baum, Psychological Stress and Oxidative Damage in Lymphocytes of Aerobically Fit and Unfit Individuals¹. *Journal of Applied Biobehavioral Research* **13**, 1-19 (2008).

214. Y. Nishio *et al.*, Social Stress Induces Oxidative DNA Damage in Mouse Peripheral Blood Cells. *Genes and Environment* **29**, 17-22 (2007).

215. H. K. Fischman, R. W. Pero, D. D. Kelly, Psychogenic stress induces chromosomal and DNA damage. *Int J Neurosci* **84**, 219-227 (1996).

216. H. K. Fischman, D. D. Kelly, Chromosomes and stress. *Int J Neurosci* **99**, 201-219 (1999).

217. M. Irie, S. Asami, S. Nagata, M. Miyata, H. Kasai, Classical conditioning of oxidative DNA damage in rats. *Neurosci Lett* **288**, 13-16 (2000).

218. S. Adachi, K. Kawamura, K. Takemoto, Oxidative damage of nuclear DNA in liver of rats exposed to psychological stress. *Cancer Res* **53**, 4153-4155 (1993).

219. L. E. Van Campen, W. J. Murphy, J. R. Franks, P. I. Mathias, M. A. Toraason, Oxidative DNA damage is associated with intense noise exposure in the rat. *Hear Res* **164**, 29-38 (2002).

220. M. R. Hara, B. D. Sachs, M. G. Caron, R. J. Lefkowitz, Pharmacological blockade of a β₂AR-β-arrestin-1 signaling cascade prevents the accumulation of DNA damage in a behavioral stress model. *Cell Cycle* **12**, 219-224 (2013).

221. A. R. Consiglio, A. L. Ramos, J. A. Henriques, J. N. Picada, DNA brain damage after stress in rats. *Prog Neuropsychopharmacol Biol Psychiatry* **34**, 652-656 (2010).

222. M. R. Hara *et al.*, A stress response pathway regulates DNA damage through β2-adrenoreceptors and β-arrestin-1. *Nature* **477**, 349-353 (2011).

223. V. B. Valente *et al.*, Stress hormones promote DNA damage in human oral keratinocytes. *Scientific Reports* **11**, (2021).

224. M. S. Flint *et al.*, Chronic exposure to stress hormones promotes transformation and tumorigenicity of 3T3 mouse fibroblasts. *Stress* **16**, 114-121 (2013).

225. M. S. Flint, A. Baum, W. H. Chambers, F. J. Jenkins, Induction of DNA damage, alteration of DNA repair and transcriptional activation by stress hormones. *Psychoneuroendocrinology* **32**, 470-479 (2007).

226. R. Lamboy-Caraballo *et al.*, Norepinephrine-Induced DNA Damage in Ovarian Cancer Cells. *International Journal of Molecular Sciences* **21**, 2250 (2020).

227. A. Acevedo, R. Caraballo-Lamboy, G. Armaiz-Peña, Catecholamine-Induced DNA Damage in Ovarian Cancer Cells. *The FASEB Journal* **34**, 1-1 (2020).

228. K. E. Rentscher, J. E. Carroll, C. Mitchell, Psychosocial Stressors and Telomere Length: A Current Review of the Science. *Annual Review of Public Health* **41**, 223-245 (2020).

229. S. Georgin-Lavialle *et al.*, Leukocyte telomere length in mastocytosis: correlations with depression and perceived stress. *Brain Behav Immun* **35**, 51-57 (2014).

230. M. B. Mathur *et al.*, Perceived stress and telomere length: A systematic review, meta-analysis, and methodologic considerations for advancing the field. *Brain Behav Immun* **54**, 158-169 (2016).

231. E. Puterman *et al.*, The Power of Exercise: Buffering the Effect of Chronic Stress on Telomere Length. *PLoS ONE* **5**, e10837 (2010).

232. N. Lopizzo *et al.*, Transcriptomic analyses and leukocyte telomere length measurement in subjects exposed to severe recent stressful life events. *Translational Psychiatry* **7**, e1042-e1042 (2017).

233. S. L. Van Ockenburg *et al.*, Stressful life events and leukocyte telomere attrition in adulthood: a prospective population-based cohort study. *Psychological Medicine* **45**, 2975-2984 (2015).

234. E. Puterman, J. Lin, J. Krauss, E. H. Blackburn, E. S. Epel, Determinants of telomere attrition over 1 year in healthy older women: stress and health behaviors matter. *Molecular Psychiatry* **20**, 529-535 (2015).

235. G. H. Brody, T. Yu, S. R. H. Beach, R. A. Philibert, Prevention Effects Ameliorate the Prospective Association Between Nonsupportive Parenting and Diminished Telomere Length. *Prevention Science* **16**, 171-180 (2015).

236. K. Litzelman *et al.*, Association Between Informal Caregiving and Cellular Aging in the Survey of the Health of Wisconsin: The Role of Caregiving Characteristics, Stress, and Strain. *American Journal of Epidemiology* **179**, 1340-1352 (2014).

237. K. Ahola *et al.*, Work-Related Exhaustion and Telomere Length: A Population-Based Study. *PLoS ONE* **7**, e40186 (2012).

238. C. G. Parks *et al.*, Employment and work schedule are related to telomere length in women. *Occupational and Environmental Medicine* **68**, 582-589 (2011).

239. K. K. Ridout *et al.*, Physician-Training Stress and Accelerated Cellular Aging. *Biol Psychiatry* **86**, 725-730 (2019).

240. G. V. Pepper, M. Bateson, D. Nettle, Telomeres as integrative markers of exposure to stress and adversity: a systematic review and meta-analysis. *Royal Society Open Science* **5**, 180744 (2018).

241. N. S. Schutte, J. M. Malouff, The Relationship Between Perceived Stress and Telomere Length: A Meta-analysis. *Stress and Health* **32**, 313-319 (2016).

242. B. S. Oliveira *et al.*, Systematic review of the association between chronic social stress and telomere length: A life course perspective. *Ageing Res Rev* **26**, 37-52 (2016).

243. A. Kotrschal, P. Ilmonen, D. J. Penn, Stress impacts telomere dynamics. *Biology Letters* **3**, 128-130 (2007).

244. P. Ilmonen, A. Kotrschal, D. J. Penn, Telomere Attrition Due to Infection. *PLoS ONE* **3**, e2143 (2008).

245. E. Grosbellet *et al.*, Circadian desynchronization triggers premature cellular aging in a diurnal rodent. *The FASEB Journal* **29**, 4794-4803 (2015).

246. M. Chatelain, S. M. Drobniak, M. Szulkin, The association between stressors and telomeres in non-human vertebrates: a meta-analysis. *Ecology Letters* **23**, 381-398 (2020).

247. B. C. J. Dirven, J. R. Homberg, T. Kozicz, M. J. A. G. Henckens, Epigenetic programming of the neuroendocrine stress response by adult life stress. *Journal of Molecular Endocrinology* **59**, R11-R31 (2017).

248. B. L. Needham *et al.*, Life course socioeconomic status and DNA methylation in genes related to stress reactivity and inflammation: The multi-ethnic study of atherosclerosis. *Epigenetics* **10**, 958-969 (2015).

249. M. Suderman *et al.*, Lymphoblastoid cell lines reveal associations of adult DNA methylation with childhood and current adversity that are distinct from whole blood associations. *International Journal of Epidemiology* **44**, 1331-1340 (2015).

250. D. Mcguinness *et al.*, Socio-economic status is associated with epigenetic differences in the pSoBid cohort. *International Journal of Epidemiology* **41**, 151-160 (2012).

251. L. L. Lam *et al.*, Factors underlying variable DNA methylation in a human community cohort. *Proceedings of the National Academy of Sciences* **109**, 17253-17260 (2012).

252. L. Sipahi *et al.*, Longitudinal epigenetic variation of DNA methyltransferase genes is associated with vulnerability to post-traumatic stress disorder. *Psychological Medicine* **44**, 3165-3179 (2014).

253. C. L. Ferland, L. A. Schrader, Regulation of histone acetylation in the hippocampus of chronically stressed rats: a potential role of sirtuins. *Neuroscience* **174**, 104-114 (2011).

254. D. Liu *et al.*, Histone acetylation and expression of mono-aminergic transmitters synthetases involved in CUS-induced depressive rats. *Exp Biol Med (Maywood)* **239**, 330-336 (2014).

255. Q. Wan *et al.*, Histone modifications of the Crhr1 gene in a rat model of depression following chronic stress. *Behav Brain Res* **271**, 1-6 (2014).

256. H. E. Covington *et al.*, Antidepressant Actions of Histone Deacetylase Inhibitors. *The Journal of Neuroscience* **29**, 11451-11460 (2009).

257. E. Elliott *et al.*, Dnmt3a in the Medial Prefrontal Cortex Regulates Anxiety-Like Behavior in Adult Mice. *The Journal of Neuroscience* **36**, 730-740 (2016).

258. N. M. Tsankova *et al.*, Sustained hippocampal chromatin regulation in a mouse model of depression and antidepressant action. *Nature Neuroscience* **9**, 519-525 (2006).

259. M. B. Wilkinson *et al.*, Imipramine Treatment and Resiliency Exhibit Similar Chromatin Regulation in the Mouse Nucleus Accumbens in Depression Models. *Journal of Neuroscience* **29**, 7820-7832 (2009).

260. T. L. Roth, P. R. Zoladz, J. D. Sweatt, D. M. Diamond, Epigenetic modification of hippocampal Bdnf DNA in adult rats in an animal model of post-traumatic stress disorder. *Journal of Psychiatric Research* **45**, 919-926 (2011).

261. R. G. Hunter, K. J. Mccarthy, T. A. Milne, D. W. Pfaff, B. S. Mcewen, Regulation of hippocampal H3 histone methylation by acute and chronic stress. *Proceedings of the National Academy of Sciences* **106**, 20912-20917 (2009).

262. F. D. Lubin, T. L. Roth, J. D. Sweatt, Epigenetic Regulation ofbdnfGene Transcription in the Consolidation of Fear Memory. *The Journal of Neuroscience* **28**, 10576-10586 (2008).

263. C. A. Miller, J. D. Sweatt, Covalent Modification of DNA Regulates Memory Formation. *Neuron* **53**, 857-869 (2007).

264. T. Klengel *et al.*, Allele-specific FKBP5 DNA demethylation mediates gene–childhood trauma interactions. *Nature Neuroscience* **16**, 33-41 (2013).

265. I. C. G. Weaver *et al.*, Epigenetic programming by maternal behavior. *Nature Neuroscience* **7**, 847-854 (2004).

266. X. Yang *et al.*, Glucocorticoid-induced loss of DNA methylation in non-neuronal cells and potential involvement of DNMT1 in epigenetic regulation of Fkbp5. *Biochemical and Biophysical Research Communications* **420**, 570-575 (2012).

267. R. S. Lee *et al.*, Chronic Corticosterone Exposure Increases Expression and Decreases Deoxyribonucleic Acid Methylation of Fkbp5 in Mice. *Endocrinology* **151**, 4332-4343 (2010).

268. R. S. Lee *et al.*, A measure of glucocorticoid load provided by DNA methylation of Fkbp5 in mice. *Psychopharmacology* **218**, 303-312 (2011).

269. D. Mehta, E. B. Binder, Gene × environment vulnerability factors for PTSD: the HPA-axis. *Neuropharmacology* **62**, 654-662 (2012).

270. C. G. Bell *et al.*, DNA methylation aging clocks: challenges and recommendations. *Genome Biology* **20**, (2019).

271. H. Palma-Gudiel, L. Fañanás, S. Horvath, A. S. Zannas, *Psychosocial stress and epigenetic aging*. International Review of Neurobiology (Elsevier, 2020).

272. E. J. Wolf *et al.*, Traumatic stress and accelerated DNA methylation age: A meta-analysis. *Psychoneuroendocrinology* **92**, 123-134 (2018).

273. M. P. Boks *et al.*, Longitudinal changes of telomere length and epigenetic age related to traumatic stress and post-traumatic stress disorder. *Psychoneuroendocrinology* **51**, 506-512 (2015).

274. A. S. Zannas *et al.*, Lifetime stress accelerates epigenetic aging in an urban, African American cohort: relevance of glucocorticoid signaling. *Genome Biology* **16**, (2015).

275. G. Fiorito *et al.*, Social adversity and epigenetic aging: a multi-cohort study on socioeconomic differences in peripheral blood DNA methylation. *Scientific Reports* **7**, (2017).

276. R. L. Simons *et al.*, Economic hardship and biological weathering: The epigenetics of aging in a U.S. sample of black women. *Social Science & Medicine* **150**, 192-200 (2016).

277. E. Chen, G. E. Miller, T. Yu, G. H. Brody, The Great Recession and health risks in African American youth. *Brain, Behavior, and Immunity* **53**, 234-241 (2016).

278. G. H. Brody, G. E. Miller, T. Yu, S. R. Beach, E. Chen, Supportive Family Environments Ameliorate the Link Between Racial Discrimination and Epigenetic Aging: A Replication Across Two Longitudinal Cohorts. *Psychol Sci* **27**, 530-541 (2016).

279. T. Jovanovic *et al.*, Exposure to Violence Accelerates Epigenetic Aging in Children. *Scientific Reports* **7**, (2017).

280. Z. M. Harvanek, N. Fogelman, K. Xu, R. Sinha, Psychological and biological resilience modulates the effects of stress on epigenetic aging. *Translational Psychiatry* **11**, (2021).

281. M. L. Díaz-Hung, C. Hetz, Proteostasis and resilience: on the interphase between individual's and intracellular stress. *Trends Endocrinol Metab* **33**, 305-317 (2022).

282. T. Hayashi, Conversion of psychological stress into cellular stress response: Roles of the sigma-1 receptor in the process. *Psychiatry and Clinical Neurosciences* **69**, 179-191 (2015).

283. L. Yang *et al.*, The Effects of Psychological Stress on Depression. *Current Neuropharmacology* **13**, 494-504 (2015).

284. K. L. Nugent, J. Chiappelli, L. M. Rowland, L. E. Hong, Cumulative stress pathophysiology in schizophrenia as indexed by allostatic load. *Psychoneuroendocrinology* **60**, 120-129 (2015).

285. L. Y. Maeng, M. R. Milad, Post-Traumatic Stress Disorder: The Relationship Between the Fear Response and Chronic Stress. *Chronic Stress* **1**, 247054701771329 (2017).

286. M. Zhang *et al.*, Chronic Stress in Bipolar Disorders Across the Different Clinical States: Roles of HPA Axis and Personality. *Neuropsychiatric Disease and Treatment* **Volume 18**, 1715-1725 (2022).

287. L. Nevell *et al.*, Elevated systemic expression of ER stress related genes is associated with stress-related mental disorders in the Detroit Neighborhood Health Study. *Psychoneuroendocrinology* **43**, 62-70 (2014).

288. P. W. Gold, J. Licinio, M. G. Pavlatou, Pathological parainflammation and endoplasmic reticulum stress in depression: potential translational targets through the CNS insulin, klotho and PPAR-γ systems. *Molecular Psychiatry* **18**, 154-165 (2013).

289. A. Hayashi *et al.*, Aberrant endoplasmic reticulum stress response in lymphoblastoid cells from patients with bipolar disorder. *The International Journal of Neuropsychopharmacology* **12**, 33 (2009).

290. J. So, J. J. Warsh, P. P. Li, Impaired endoplasmic reticulum stress response in B-lymphoblasts from patients with bipolar-I disorder. *Biol Psychiatry* **62**, 141-147 (2007).

291. D. Arion, T. Unger, D. A. Lewis, P. Levitt, K. Mirnics, Molecular Evidence for Increased Expression of Genes Related to Immune and Chaperone Function in the Prefrontal Cortex in Schizophrenia. *Biological Psychiatry* **62**, 711-721 (2007).

292. Y. Yoshino, Y. Dwivedi, Elevated expression of unfolded protein response genes in the prefrontal cortex of depressed subjects: Effect of suicide. *Journal of Affective Disorders* **262**, 229-236 (2020).

293. C. Bown, Increased Temporal Cortex ER Stress Proteins in Depressed Subjects Who Died by Suicide. *Neuropsychopharmacology* **22**, 327-332 (2000).

294. M. Prasad *et al.*, Endoplasmic Reticulum Stress Enhances Mitochondrial Metabolic Activity in Mammalian Adrenals and Gonads. *Molecular and Cellular Biology* **36**, 3058-3074 (2016).

295. M. Timberlake, K. Prall, B. Roy, Y. Dwivedi, Unfolded protein response and associated alterations in toll-like receptor expression and interaction in the hippocampus of restraint rats. *Psychoneuroendocrinology* **89**, 185-193 (2018).

296. G.-B. Huang *et al.*, Effects of chronic social defeat stress on behaviour, endoplasmic reticulum proteins and choline acetyltransferase in adolescent mice. *International Journal of Neuropsychopharmacology* **16**, 1635-1647 (2013).

297. M. Ishisaka *et al.*, Luteolin Shows an Antidepressant-Like Effect via Suppressing Endoplasmic Reticulum Stress. *Biological and Pharmaceutical Bulletin* **34**, 1481-1486 (2011).

298. J. Lin, E. Epel, Stress and telomere shortening: Insights from cellular mechanisms. *Ageing Res Rev* **73**, 101507 (2021).

299. L. R. Polsky, K. E. Rentscher, J. E. Carroll, Stress-induced biological aging: A review and guide for research priorities. *Brain Behav Immun* **104**, 97-109 (2022).

300. E. S. Epel, The geroscience agenda: Toxic stress, hormetic stress, and the rate of aging. *Ageing Res Rev* **63**, 101167 (2020).

301. C. López-Otín, M. A. Blasco, L. Partridge, M. Serrano, G. Kroemer, The Hallmarks of Aging. *Cell* **153**, 1194-1217 (2013).

302. G. A. Garinis, G. T. J. Van Der Horst, J. Vijg, J. H.J. Hoeijmakers, DNA damage and ageing: new-age ideas for an age-old problem. *Nature Cell Biology* **10**, 1241-1247 (2008).

303. S. Hekimi, J. Lapointe, Y. Wen, Taking a "good" look at free radicals in the aging process. *Trends in Cell Biology* **21**, 569-576 (2011).

304. D. J. Baker *et al.*, Clearance of p16Ink4a-positive senescent cells delays ageing-associated disorders. *Nature* **479**, 232-236 (2011).

305. J.-P. Coppé, P.-Y. Desprez, A. Krtolica, J. Campisi, The Senescence-Associated Secretory Phenotype: The Dark Side of Tumor Suppression. *Annual Review of Pathology: Mechanisms of Disease* **5**, 99-118 (2010).

306. I. Liguori *et al.*, Oxidative stress, aging, and diseases. *Clinical Interventions in Aging* **Volume 13**, 757-772 (2018).

307. V. N. Gladyshev, The origin of aging: imperfectness-driven non-random damage defines the aging process and control of lifespan. *Trends in Genetics* **29**, 506-512 (2013).

308. J. R. Piazza, D. M. Almeida, N. O. Dmitrieva, L. C. Klein, Frontiers in the use of biomarkers of health in research on stress and aging. *J Gerontol B Psychol Sci Soc Sci* **65**, 513-525 (2010).

309. M. Kumari *et al.*, Identifying patterns in cortisol secretion in an older population. Findings from the Whitehall II study. *Psychoneuroendocrinology* **35**, 1091-1099 (2010).

310. M. P. Gardner *et al.*, Dysregulation of the hypothalamic pituitary adrenal (HPA) axis and physical performance at older ages: an individual participant meta-analysis. *Psychoneuroendocrinology* **38**, 40-49 (2013).

311. X.-M. Ma, A. Levy, S. L. Lightman, Emergence of an Isolated Arginine Vasopressin (AVP) Response to Stress after Repeated Restraint: A Study of Both AVP and Corticotropin-Releasing Hormone Messenger Ribonucleic Acid (RNA) and Heteronuclear RNA¹. *Endocrinology* **138**, 4351-4357 (1997).

312. M. Serra, M. G. Pisu, I. Floris, G. Biggio, Social isolation-induced changes in the hypothalamic–pituitary–adrenal axis in the rat. *Stress* **8**, 259-264 (2005).

313. K. Mizoguchi, A. Ishige, M. Aburada, T. Tabira, Chronic stress attenuates glucocorticoid negative feedback: involvement of the prefrontal cortex and hippocampus. *Neuroscience* **119**, 887-897 (2003).

314. G. Boero *et al.*, Impaired glucocorticoid-mediated HPA axis negative feedback induced by juvenile social isolation in male rats. *Neuropharmacology* **133**, 242-253 (2018).

315. B. Gibbison *et al.*, Dynamic Pituitary-Adrenal Interactions in Response to Cardiac Surgery*. *Critical Care Medicine* **43**, 791-800 (2015).

316. B. Peeters *et al.*, Adrenocortical function during prolonged critical illness and beyond: a prospective observational study. *Intensive Care Medicine* **44**, 1720-1729 (2018).

317. R. Yehuda *et al.*, Low urinary cortisol excretion in patients with posttraumatic stress disorder. *J Nerv Ment Dis* **178**, 366-369 (1990).

318. H. Lindholm *et al.*, Morning Cortisol Levels and Perceived Stress in Irregular Shift Workers Compared with Regular Daytime Workers. *Sleep Disorders* **2012**, 1-5 (2012).

319. E. J. Lenze *et al.*, Elevated Cortisol in Older Adults With Generalized Anxiety Disorder Is Reduced by Treatment: A Placebo-Controlled Evaluation of Escitalopram. *The American Journal of Geriatric Psychiatry* **19**, 482-490 (2011).

320. D.-D. Qin *et al.*, Prolonged secretion of cortisol as a possible mechanism underlying stress and depressive behaviour. *Scientific Reports* **6**, 30187 (2016).

321. M. Uhart, L. Oswald, M. E. Mccaul, R. Chong, G. S. Wand, Hormonal Responses to Psychological Stress and Family History of Alcoholism. *Neuropsychopharmacology* **31**, 2255-2263 (2006).

322. R. R. Teixeira *et al.*, Chronic Stress Induces a Hyporeactivity of the Autonomic Nervous System in Response to Acute Mental Stressor and Impairs Cognitive Performance in Business Executives. *PLOS ONE* **10**, e0119025 (2015).

323. M. Cay *et al.*, Effect of increase in cortisol level due to stress in healthy young individuals on dynamic and static balance scores. *North Clin Istanb* **5**, 295-301 (2018).

324. R. M. M. Schoorlemmer, G. M. E. E. Peeters, N. M. Van Schoor, P. Lips, Relationships between cortisol level, mortality and chronic diseases in older persons. *Clinical Endocrinology* **71**, 779-786 (2009).

325. I. Perogamvros, L. Aarons, A. G. Miller, P. J. Trainer, D. W. Ray, Corticosteroid-binding globulin regulates cortisol pharmacokinetics. *Clinical Endocrinology* **74**, 30-36 (2011).

326. N. Draper, P. M. Stewart, 11β-Hydroxysteroid dehydrogenase and the pre-receptor regulation of corticosteroid hormone action. *Journal of Endocrinology* **186**, 251-271 (2005).

327. E. Gomez-Sanchez, C. E. Gomez-Sanchez, The Multifaceted Mineralocorticoid Receptor. *Comprehensive Physiology*, 965-994 (2014).

328. S. Vandevyver, L. Dejager, C. Libert, On the Trail of the Glucocorticoid Receptor: Into the Nucleus and Back. *Traffic* **13**, 364-374 (2012).

329. O. J. Schoneveld, I. C. Gaemers, W. H. Lamers, Mechanisms of glucocorticoid signalling. *Biochim Biophys Acta* **1680**, 114-128 (2004).

330. C. E. Sekeris, The mitochondrial genome: a possible primary site of action of steroid hormones. *In Vivo* **4**, 317-320 (1990).

331. A.-M. G. Psarra, C. E. Sekeris, Glucocorticoids induce mitochondrial gene transcription in HepG2 cells. *Biochimica et Biophysica Acta (BBA) - Molecular Cell Research* **1813**, 1814-1821 (2011).

332. K. Scheller *et al.*, Localization of glucocorticoid hormone receptors in mitochondria of human cells. *Eur J Cell Biol* **79**, 299-307 (2000).

333. T. E. Reddy *et al.*, Genomic determination of the glucocorticoid response reveals unexpected mechanisms of gene regulation. *Genome Research* **19**, 2163-2171 (2009).

334. J.-C. Wang *et al.*, Chromatin immunoprecipitation (ChIP) scanning identifies primary glucocorticoid receptor target genes. *Proceedings of the National Academy of Sciences* **101**, 15603-15608 (2004).

335. P. Phuc Le *et al.*, Glucocorticoid Receptor-Dependent Gene Regulatory Networks. *PLoS Genetics* **1**, e16 (2005).

336. S. C. Biddie, B. L. Conway-Campbell, S. L. Lightman, Dynamic regulation of glucocorticoid signalling in health and disease. *Rheumatology* **51**, 403-412 (2012).

337. R. A. Samarasinghe, S. F. Witchell, D. B. Defranco, Cooperativity and complementarity: Synergies in non-classical and classical glucocorticoid signaling. *Cell Cycle* **11**, 2819-2827 (2012).

338. B. Gametchu, C. S. Watson, S. Wu, Use of receptor antibodies to demonstrate membrane glucocorticoid receptor in cells from human leukemic patients. *Faseb j* **7**, 1283-1292 (1993).

339. E. Solito *et al.*, Dexamethasone Induces Rapid Serine-Phosphorylation and Membrane Translocation of Annexin 1 in a Human Folliculostellate Cell Line via a Novel Nongenomic Mechanism Involving the Glucocorticoid Receptor, Protein Kinase C, Phosphatidylinositol 3-Kinase, and. *Endocrinology* **144**, 1164-1174 (2003).

340. J. D. Croxtall, Q. Choudhury, R. J. Flower, Glucocorticoids act within minutes to inhibit recruitment of signalling factors to activated EGF receptors through a receptor-dependent, transcription-independent mechanism. *British Journal of Pharmacology* **130**, 289-298 (2000).

341. C. Strehl, F. Buttgereit, Unraveling the functions of the membrane-bound glucocorticoid receptors: first clues on origin and functional activity. *Annals of the New York Academy of Sciences* **1318**, 1-6 (2014).

342. S. B. Koukouritaki, A. Gravanis, C. Stournaras, Tyrosine phosphorylation of focal adhesion kinase and paxillin regulates the signaling mechanism of the rapid nongenomic action of dexamethasone on actin cytoskeleton. *Mol Med* **5**, 731-742 (1999).

343. J. Qiu, C. G. Wang, X. Y. Huang, Y. Z. Chen, Nongenomic mechanism of glucocorticoid inhibition of bradykinin-induced calcium influx in PC12 cells: possible involvement of protein kinase C. *Life Sci* **72**, 2533-2542 (2003).

344. A. W. Norman, M. T. Mizwicki, D. P. G. Norman, Steroid-hormone rapid actions, membrane receptors and a conformational ensemble model. *Nature Reviews Drug Discovery* **3**, 27-41 (2004).

345. D. J. Morgan *et al.*, Glucocorticoid receptor isoforms direct distinct mitochondrial programs to regulate ATP production. *Scientific Reports* **6**, 26419 (2016).

346. R. A. Samarasinghe *et al.*, Nongenomic glucocorticoid receptor action regulates gap junction intercellular communication and neural progenitor cell proliferation. *Proceedings of the National Academy of Sciences* **108**, 16657-16662 (2011).

347. L. Liu *et al.*, Rapid non-genomic inhibitory effects of glucocorticoids on human neutrophil degranulation. *Inflammation Research* **54**, 37-41 (2005).

348. C. Stellato, Post-transcriptional and Nongenomic Effects of Glucocorticoids. *Proceedings of the American Thoracic Society* **1**, 255-263 (2004).

349. F. Long *et al.*, Rapid nongenomic inhibitory effects of glucocorticoids on phagocytosis and superoxide anion production by macrophages. *Steroids* **70**, 55-61 (2005).

350. H. Weiner, E. Mayer, The organism in health and disease. On the path to an integrated biomedical model: sequelae of the theory of psychosomatic medicine. *Psychother Psychosom Med Psychol* **40**, 81-101 (1990).

351. B. S. McEwen, Protective and damaging effects of stress mediators. *N Engl J Med* **338**, 171-179 (1998).

352. P. D. Neufer *et al.*, Understanding the Cellular and Molecular Mechanisms of Physical Activity-Induced Health Benefits. *Cell Metab* **22**, 4-11 (2015).

353. M. Flockhart *et al.*, Excessive exercise training causes mitochondrial functional impairment and decreases glucose tolerance in healthy volunteers. *Cell Metab* **33**, 957-970 e956 (2021).

354. T. L. Gruenewald, T. E. Seeman, C. D. Ryff, A. S. Karlamangla, B. H. Singer, Combinations of biomarkers predictive of later life mortality. *Proc Natl Acad Sci U S A* **103**, 14158-14163 (2006).

355. R. P. Juster, B. S. McEwen, S. J. Lupien, Allostatic load biomarkers of chronic stress and impact on health and cognition. *Neurosci Biobehav Rev* **35**, 2-16 (2010).

356. T. E. Seeman, B. S. McEwen, J. W. Rowe, B. H. Singer, Allostatic load as a marker of cumulative biological risk: MacArthur studies of successful aging. *Proc Natl Acad Sci U S A* **98**, 4770-4775 (2001).

357. M. Picard, B. S. McEwen, E. S. Epel, C. Sandi, An energetic view of stress: Focus on mitochondria. *Front Neuroendocrinol* **49**, 72-85 (2018).

358. M. Basan *et al.*, Overflow metabolism in Escherichia coli results from efficient proteome allocation. *Nature* **528**, 99-104 (2015).

359. M. Picard *et al.*, Mitochondrial functions modulate neuroendocrine, metabolic, inflammatory, and transcriptional responses to acute psychological stress. *Proceedings of the National Academy of Sciences* **112**, E6614-E6623 (2015).

360. M. Picard, R.-P. Juster, B. S. Mcewen, Mitochondrial allostatic load puts the 'gluc' back in glucocorticoids. *Nature Reviews Endocrinology* **10**, 303-310 (2014).

361. S. John *et al.*, Chromatin accessibility pre-determines glucocorticoid receptor binding patterns. *Nature Genetics* **43**, 264-268 (2011).

362. B. S. McEwen, Allostasis and allostatic load: implications for neuropsychopharmacology. *Neuropsychopharmacology* **22**, 108-124 (2000).

363. S. J. Lupien *et al.*, Cortisol levels during human aging predict hippocampal atrophy and memory deficits. *Nature Neuroscience* **1**, 69-73 (1998).

364. S. Ouanes, J. Popp, High Cortisol and the Risk of Dementia and Alzheimer's Disease: A Review of the Literature. *Front Aging Neurosci* **11**, 43 (2019).

365. C. S. Leung *et al.*, Chronic stress-driven glucocorticoid receptor activation programs key cell phenotypes and functional epigenomic patterns in human fibroblasts. *iScience* **25**, 104960 (2022).

366. S. M. Gold *et al.*, Comorbid depression in medical diseases. *Nature Reviews Disease Primers* **6**, (2020).

367. G. Sturm *et al.*, A multi-omics longitudinal aging dataset in primary human fibroblasts with mitochondrial perturbations. *Sci Data* **9**, 751 (2022).

368. C. Trumpff *et al.*, Acute psychological stress increases serum circulating cell-free mitochondrial DNA. *Psychoneuroendocrinology* **106**, 268-276 (2019).

369. C. N. Passow, R. Greenway, L. Arias-Rodriguez, P. D. Jeyasingh, M. Tobler, Reduction of Energetic Demands through Modification of Body Size and Routine Metabolic Rates in Extremophile Fish. *Physiological and Biochemical Zoology* **88**, 371-383 (2015).

370. W. U. Blanckenhorn, The Evolution of Body Size: What Keeps Organisms Small? *The Quarterly Review of Biology* **75**, 385-407 (2000).

371. J. Dark, I. Zucker, Seasonal Cycles in Energy Balance: Regulation by Lighta. *Annals of the New York Academy of Sciences* **453**, 170-181 (1985).

372. P. Vuarin, M. Dammhahn, P. Y. Henry, Individual flexibility in energy saving: body size and condition constrain torpor use. *Functional Ecology* **27**, 793-799 (2013).

373. R. L. Boal *et al.*, Height as a Clinical Biomarker of Disease Burden in Adult Mitochondrial Disease. *The Journal of Clinical Endocrinology & Metabolism* **104**, 2057-2066 (2019).

374. S. A. Mookerjee, A. A. Gerencser, D. G. Nicholls, M. D. Brand, Quantifying intracellular rates of glycolytic and oxidative ATP production and consumption using extracellular flux measurements. *Journal of Biological Chemistry* **292**, 7189-7207 (2017).

375. S. A. Mookerjee, D. G. Nicholls, M. D. Brand, Determining Maximum Glycolytic Capacity Using Extracellular Flux Measurements. *PLoS One* **11**, e0152016 (2016).

376. J. Schimmel, R. Van Schendel, J. T. Den Dunnen, M. Tijsterman, Templated Insertions: A Smoking Gun for Polymerase Theta-Mediated End Joining. *Trends in Genetics* **35**, 632-644 (2019).

377. Z. Wu *et al.*, Mechanisms Controlling Mitochondrial Biogenesis and Respiration through the Thermogenic Coactivator PGC-1. *Cell* **98**, 115-124 (1999).

378. A. Seth *et al.*, The Transcriptional Corepressor RIP140 Regulates Oxidative Metabolism in Skeletal Muscle. *Cell Metabolism* **6**, 236-245 (2007).

379. A. M. Powelka, Suppression of oxidative metabolism and mitochondrial biogenesis by the transcriptional corepressor RIP140 in mouse adipocytes. *Journal of Clinical Investigation* **116**, 125-136 (2005).

380. E. M. Hummel *et al.*, Cell-free DNA release under psychosocial and physical stress conditions. *Transl Psychiatry* **8**, 236 (2018).

381. M. Pinti *et al.*, Circulating mitochondrial DNA increases with age and is a familiar trait: Implications for "inflamm-aging". *European Journal of Immunology* **44**, 1552-1562 (2014).

382. O. R. Stephens *et al.*, Characterization and origins of cell-free mitochondria in healthy murine and human blood. *Mitochondrion* **54**, 102-112 (2020).

383. P. Sansone *et al.*, Packaging and transfer of mitochondrial DNA via exosomes regulate escape from dormancy in hormonal therapy-resistant breast cancer. *Proc Natl Acad Sci U S A* **114**, E9066-E9075 (2017).

384. L. V. Collins, S. Hajizadeh, E. Holme, I. M. Jonsson, A. Tarkowski, Endogenously oxidized mitochondrial DNA induces in vivo and in vitro inflammatory responses. *J Leukoc Biol* **75**, 995-1000 (2004).

385. S. Miliotis, B. Nicolalde, M. Ortega, J. Yepez, A. Caicedo, Forms of extracellular mitochondria and their impact in health. *Mitochondrion* **48**, 16-30 (2019).

386. B. S. Mcewen, Interacting mediators of allostasis and allostatic load: towards an understanding of resilience in aging. *Metabolism* **52**, 10-16 (2003).

387. J. M. Mccaffery, A. L. Marsland, K. Strohacker, M. F. Muldoon, S. B. Manuck, Factor Structure Underlying Components of Allostatic Load. *PLoS ONE* **7**, e47246 (2012).

388. D. Furman *et al.*, Chronic inflammation in the etiology of disease across the life span. *Nature Medicine* **25**, 1822-1832 (2019).

389. T. Tanaka *et al.*, Plasma proteomic signature of age in healthy humans. *Aging Cell* **17**, e12799 (2018).

390. J. P. Wood, P. E. Ellery, S. A. Maroney, A. E. Mast, Biology of tissue factor pathway inhibitor. *Blood* **123**, 2934-2943 (2014).

391. A. Waage, G. Slupphaug, R. Shalaby, Glucocorticoids inhibit the production of IL 6 from monocytes, endothelial cells and fibroblasts. *European Journal of Immunology* **20**, 2439-2443 (1990).

392. M. Picard, D. M. Turnbull, Linking the metabolic state and mitochondrial DNA in chronic disease, health, and aging. *Diabetes* **62**, 672-678 (2013).

393. Y. Wang, X. Guo, K. Ye, M. Orth, Z. Gu, Accelerated expansion of pathogenic mitochondrial DNA heteroplasmies in Huntington's disease. *Proc Natl Acad Sci U S A* **118**, (2021).

394. H. U. Klein *et al.*, Characterization of mitochondrial DNA quantity and quality in the human aged and Alzheimer's disease brain. *Mol Neurodegener* **16**, 75 (2021).

395. M. Picard *et al.*, Mitochondrial dysfunction and lipid accumulation in the human diaphragm during mechanical ventilation. *Am J Respir Crit Care Med* **186**, 1140-1149 (2012).

396. C. Meissner, P. Bruse, M. Oehmichen, Tissue-specific deletion patterns of the mitochondrial genome with advancing age. *Exp Gerontol* **41**, 518-524 (2006).

397. D. Goudenege *et al.*, eKLIPse: a sensitive tool for the detection and quantification of mitochondrial DNA deletions from next-generation sequencing data. *Genet Med* **21**, 1407-1416 (2019).

398. S. Spendiff *et al.*, Mitochondrial DNA deletions in muscle satellite cells: implications for therapies. *Hum Mol Genet* **22**, 4739-4747 (2013).

399. L. Hayflick, The Limited in Vitro Lifetime of Human Diploid Cell Strains. *Exp Cell Res* **37**, 614-636 (1965).

400. L. Hayflick, P. S. Moorhead, The serial cultivation of human diploid cell strains. *Exp Cell Res* **25**, 585-621 (1961).

401. Y. E. Yegorov, A. V. Poznyak, N. G. Nikiforov, I. A. Sobenin, A. N. Orekhov, The Link between Chronic Stress and Accelerated Aging. *Biomedicines* **8**, 198 (2020).

402. S. Horvath, K. Raj, DNA methylation-based biomarkers and the epigenetic clock theory of ageing. *Nature Reviews Genetics* **19**, 371-384 (2018).

403. A. T. Lu *et al.*, DNA methylation-based estimator of telomere length. *Aging* **11**, 5895-5923 (2019).

404. R. Diotti, D. Loayza, Shelterin complex and associated factors at human telomeres. *Nucleus* **2**, 119-135 (2011).

405. E. G. Jacobs, E. S. Epel, J. Lin, E. H. Blackburn, N. L. Rasgon, Relationship between leukocyte telomere length, telomerase activity, and hippocampal volume in early aging. *JAMA Neurol* **71**, 921-923 (2014).

406. A. Zalli *et al.*, Shorter telomeres with high telomerase activity are associated with raised allostatic load and impoverished psychosocial resources. *Proc Natl Acad Sci U S A* **111**, 4519-4524 (2014).

407. A. T. Lu *et al.*, DNA methylation GrimAge strongly predicts lifespan and healthspan. *Aging* **11**, 303-327 (2019).

408. S. Horvath, DNA methylation age of human tissues and cell types. *Genome Biology* **14**, R115 (2013).

409. S. Horvath *et al.*, Epigenetic clock for skin and blood cells applied to Hutchinson Gilford Progeria Syndrome and ex vivo studies. *Aging* **10**, 1758-1775 (2018).

410. G. Hannum *et al.*, Genome-wide Methylation Profiles Reveal Quantitative Views of Human Aging Rates. *Molecular Cell* **49**, 359-367 (2013).

411. M. E. Levine *et al.*, An epigenetic biomarker of aging for lifespan and healthspan. *Aging* **10**, 573-591 (2018).

412. A. T. Higgins-Chen *et al.*, A computational solution for bolstering reliability of epigenetic clocks: Implications for clinical trials and longitudinal tracking. *Nat Aging* **2**, 644-661 (2022).

413. G. Sturm *et al.*, Human aging DNA methylation signatures are conserved but accelerated in cultured fibroblasts. *Epigenetics* **14**, 961-976 (2019).

414. G. Sturm *et al.*, Accelerating the clock: Interconnected speedup of energetic and molecular dynamics during aging in cultured human cells. *bioRxiv*, (2023).

415. K. Whittemore, E. Vera, E. Martinez-Nevado, C. Sanpera, M. A. Blasco, Telomere shortening rate predicts species life span. *Proc Natl Acad Sci U S A* **116**, 15122-15127 (2019).

416. Y. Kim *et al.*, Mitochondrial Aging Defects Emerge in Directly Reprogrammed Human Neurons due to Their Metabolic Profile. *Cell Reports* **23**, 2550-2558 (2018).

417. C. Correia-Melo *et al.*, Mitochondria are required for pro-ageing features of the senescent phenotype. *EMBO J* **35**, 724-742 (2016).

418. J. C. Hildyard, C. Ammala, I. D. Dukes, S. A. Thomson, A. P. Halestrap, Identification and characterisation of a new class of highly specific and potent inhibitors of the mitochondrial pyruvate carrier. *Biochim Biophys Acta* **1707**, 221-230 (2005).

419. Y. T. Kruszynska, H. S. Sherratt, Glucose kinetics during acute and chronic treatment of rats with 2[6(4-chloro-phenoxy)hexyl]oxirane-2-carboxylate, etomoxir. *Biochem Pharmacol* **36**, 3917-3921 (1987).

420. M. M. Robinson *et al.*, Novel mechanism of inhibition of rat kidney-type glutaminase by bis-2-(5-phenylacetamido-1,2,4-thiadiazol-2-yl)ethyl sulfide (BPTES). *Biochem J* **406**, 407-414 (2007).

421. P. Sterling, *What is health? Allostasis and the evolution of human design.*, (The MIT Press, Cambridge, MA, 2020).

422. A. Rovini *et al.*, Quantitative analysis of mitochondrial membrane potential heterogeneity in unsynchronized and synchronized cancer cells. *FASEB J* **35**, e21148 (2021).

423. M. Kafri, E. Metzl-Raz, G. Jona, N. Barkai, The Cost of Protein Production. *Cell Reports* **14**, 22-31 (2016).

424. F. Buttgereit, M. D. Brand, A hierarchy of ATP-consuming processes in mammalian cells. *Biochemical Journal* **312**, 163-167 (1995).

425. J. M. Gutierrez *et al.*, Genome-scale reconstructions of the mammalian secretory pathway predict metabolic costs and limitations of protein secretion. *Nature Communications* **11**, (2020).

426. D. Molenaar, R. Van Berlo, D. De Ridder, B. Teusink, Shifts in growth strategies reflect tradeoffs in cellular economics. *Molecular Systems Biology* **5**, 323 (2009).

427. H. Hoitzing *et al.*, Energetic costs of cellular and therapeutic control of stochastic mitochondrial DNA populations. *PLoS Comput Biol* **15**, e1007023 (2019).

428. K. Healy *et al.*, Ecology and mode-of-life explain lifespan variation in birds and mammals. *Proceedings of the Royal Society B: Biological Sciences* **281**, 20140298 (2014).

429. D. F. Rolfe, G. C. Brown, Cellular energy utilization and molecular origin of standard metabolic rate in mammals. *Physiol Rev* **77**, 731-758 (1997).

430. G. B. West, W. H. Woodruff, J. H. Brown, Allometric scaling of metabolic rate from molecules and mitochondria to cells and mammals. *Proc Natl Acad Sci U S A* **99 Suppl 1**, 2473-2478 (2002).

431. J. P. de Magalhaes, J. Costa, G. M. Church, An analysis of the relationship between metabolism, developmental schedules, and longevity using phylogenetic independent contrasts. *J Gerontol A Biol Sci Med Sci* **62**, 149-160 (2007).

432. J. R. Speakman, Body size, energy metabolism and lifespan. *J Exp Biol* **208**, 1717-1730 (2005).

433. J. Losa *et al.*, Perspective: a stirring role for metabolism in cells. *Mol Syst Biol* **18**, e10822 (2022).

434. M. J. Forlenza, G. E. Miller, Increased serum levels of 8-hydroxy-2'-deoxyguanosine in clinical depression. *Psychosom Med* **68**, 1-7 (2006).

435. M. Irie, S. Asami, M. Ikeda, H. Kasai, Depressive state relates to female oxidative DNA damage via neutrophil activation. *Biochem Biophys Res Commun* **311**, 1014-1018 (2003).

436. S. Schiavone *et al.*, Involvement of NOX2 in the development of behavioral and pathologic alterations in isolated rats. *Biol Psychiatry* **66**, 384-392 (2009).

437. G. Patki, N. Solanki, F. Atrooz, F. Allam, S. Salim, Depression, anxiety-like behavior and memory impairment are associated with increased oxidative stress and inflammation in a rat model of social stress. *Brain Res* **1539**, 73-86 (2013).

438. G. Patki *et al.*, Grape powder intake prevents ovariectomy-induced anxiety-like behavior, memory impairment and high blood pressure in female Wistar rats. *PLoS One* **8**, e74522 (2013).

439. C. Vollert *et al.*, Exercise prevents sleep deprivation-associated anxiety-like behavior in rats: potential role of oxidative stress mechanisms. *Behav Brain Res* **224**, 233-240 (2011).

440. L. Wang *et al.*, Psychological stress-induced oxidative stress as a model of sub-healthy condition and the effect of TCM. *Evid Based Complement Alternat Med* **4**, 195-202 (2007).

441. D. Lowe, S. Horvath, K. Raj, Epigenetic clock analyses of cellular senescence and ageing. *Oncotarget* **7**, 8524-8531 (2016).

442. C. Minteer *et al.*, Tick tock, tick tock: Mouse culture and tissue aging captured by an epigenetic clock. *Aging Cell*, (2022).

443. S. Bork *et al.*, DNA methylation pattern changes upon long-term culture and aging of human mesenchymal stromal cells. *Aging Cell* **9**, 54-63 (2010).

444. A. S. Zannas, O. Kosyk, C. S. Leung, Prolonged Glucocorticoid Exposure Does Not Accelerate Telomere Shortening in Cultured Human Fibroblasts. *Genes* **11**, 1425 (2020).

445. M. Picard *et al.*, Progressive increase in mtDNA 3243A>G heteroplasmy causes abrupt transcriptional reprogramming. *Proceedings of the National Academy of Sciences* **111**, E4033-E4042 (2014).

446. L. Boucret *et al.*, Deep sequencing shows that oocytes are not prone to accumulate mtDNA heteroplasmic mutations during ovarian ageing. *Hum Reprod* **32**, 2101-2109 (2017).

447. N. L. Bray, H. Pimentel, P. Melsted, L. Pachter, Near-optimal probabilistic RNA-seq quantification. *Nature Biotechnology* **34**, 525-527 (2016).

448. C. Soneson, M. I. Love, M. D. Robinson, Differential analyses for RNA-seq: transcript-level estimates improve gene-level inferences. *F1000Research* **4**, 1521 (2016).

449. M. I. Love, W. Huber, S. Anders, Moderated estimation of fold change and dispersion for RNA-seq data with DESeq2. *Genome Biology* **15**, (2014).

450. S. Rath *et al.*, MitoCarta3.0: an updated mitochondrial proteome now with sub-organelle localization and pathway annotations. *Nucleic Acids Research* **49**, D1541-D1547 (2021).

451. S. A. Ware *et al.*, An automated, high-throughput methodology optimized for quantitative cell-free mitochondrial and nuclear DNA isolation from plasma. *Journal of Biological Chemistry* **295**, 15677-15691 (2020).

452. J. Lin *et al.*, Analyses and comparisons of telomerase activity and telomere length in human T and B cells: Insights for epidemiology of telomere maintenance. *Journal of Immunological Methods* **352**, 71-80 (2010).

453. R. M. Cawthon, Telomere measurement by quantitative PCR. *Nucleic Acids Research* **30**, 47e-47 (2002).

454. M. J. Aryee *et al.*, Minfi: a flexible and comprehensive Bioconductor package for the analysis of Infinium DNA methylation microarrays. *Bioinformatics* **30**, 1363-1369 (2014).

455. J. T. Leek, W. E. Johnson, H. S. Parker, A. E. Jaffe, J. D. Storey, The sva package for removing batch effects and other unwanted variation in high-throughput experiments. *Bioinformatics* **28**, 882-883 (2012).

456. D. Bates, M. Mächler, B. Bolker, S. Walker, Fitting Linear Mixed-Effects Models Using lme4. *Journal of Statistical Software* **67**, 1-48 (2015).

457. A. Kuznetsova, P. Brockhoff, R. Christensen, lmerTest Package: Tests in Linear Mixed Effects Models. *Journal of Statistical Software* **82**, 1-26 (2017).

458. R. G. Shulman, F. Hyder, D. L. Rothman, Baseline brain energy supports the state of consciousness. *Proc Natl Acad Sci U S A* **106**, 11096-11101 (2009).

459. T. S. Kraft *et al.*, The energetics of uniquely human subsistence strategies. *Science* **374**, eabf0130 (2021).

460. D. C. Wallace, Bioenergetics, the origins of complexity, and the ascent of man. *Proc Natl Acad Sci U S A* **107 Suppl 2**, 8947-8953 (2010).

461. S. Cohen, M. L. M. Murphy, A. A. Prather, Ten Surprising Facts About Stressful Life Events and Disease Risk. *Annu Rev Psychol* **70**, 577-597 (2019).

462. B. S. McEwen, Protective and damaging effects of stress mediators: central role of the brain. *Dialogues Clin Neurosci* **8**, 367-381 (2006).

463. B. Niebel, S. Leupold, M. Heinemann, An upper limit on Gibbs energy dissipation governs cellular metabolism. *Nat Metab* **1**, 125-132 (2019).

464. X. Yang *et al.*, Physical bioenergetics: Energy fluxes, budgets, and constraints in cells. *Proc Natl Acad Sci U S A* **118**, (2021).

465. H. Pontzer, Energy Constraint as a Novel Mechanism Linking Exercise and Health. *Physiology (Bethesda)* **33**, 384-393 (2018).

466. J. F. Thayer, E. Sternberg, Beyond heart rate variability: vagal regulation of allostatic systems. *Ann N Y Acad Sci* **1088**, 361-372 (2006).

467. M. Picard, D. C. Wallace, Y. Burelle, The rise of mitochondria in medicine. *Mitochondrion* **30**, 105-116 (2016).

468. N. Lane, *Transformer: The Deep Chemistry of Life and Death*. (WW Norton, New York, 2022).

469. P. Kaufmann *et al.*, Natural history of MELAS associated with mitochondrial DNA m.3243A>G genotype. *Neurology* **77**, 1965-1971 (2011).

470. G. S. Gorman *et al.*, Mitochondrial diseases. *Nat Rev Dis Primers* **2**, 16080 (2016).

471. M. Picard, Energy transduction and the mind–mitochondria connection. *The Biochemist* **44**, 14-18 (2022).

472. G. F. Koob, M. Le Moal, Drug addiction, dysregulation of reward, and allostasis. *Neuropsychopharmacology* **24**, 97-129 (2001).

473. A. M. Makarieva *et al.*, Mean mass-specific metabolic rates are strikingly similar across life's major domains: Evidence for life's metabolic optimum. *Proc Natl Acad Sci U S A* **105**, 16994-16999 (2008).

474. A. Damasio, *The strange order of things: Life, feeling and the making of cultures*. (Vintage Books, New York, 2018).

475. H. Weiner, *Perturbing the Organism: The Biology of Stressful Life Experience*. (University of Chicago Press, Chicago, 1992).

476. S. E. Taylor *et al.*, Biobehavioral responses to stress in females: tend-and-befriend, not fight-or-flight. *Psychol Rev* **107**, 411-429 (2000).

477. S. S. Dickerson, M. E. Kemeny, Acute stressors and cortisol responses: a theoretical integration and synthesis of laboratory research. *Psychol Bull* **130**, 355-391 (2004).

478. J. F. Brosschot, S. Pieper, J. F. Thayer, Expanding stress theory: prolonged activation and perseverative cognition. *Psychoneuroendocrinology* **30**, 1043-1049 (2005).

479. K. Bredemeier, H. Berenbaum, Intolerance of uncertainty and perceived threat. *Behav Res Ther* **46**, 28-38 (2008).

480. K. Friston, The free-energy principle: a unified brain theory? *Nat Rev Neurosci* **11**, 127-138 (2010).

481. H. F. Nijhout, F. Sadre-Marandi, J. Best, M. C. Reed, Systems Biology of Phenotypic Robustness and Plasticity. *Integr Comp Biol* **57**, 171-184 (2017).

482. J. F. Brosschot, B. Verkuil, J. F. Thayer, Exposed to events that never happen: Generalized unsafety, the default stress response, and prolonged autonomic activity. *Neurosci Biobehav Rev* **74**, 287-296 (2017).

483. T. Nunez-Villaveiran, M. Sanchez, P. Millan, A. Garcia-de-Lorenzo, Systematic review of the effect of propanolol on hypermetabolism in burn injuries. *Med Intensiva* **39**, 101-113 (2015).

484. T. L. Sourkes, On the energy cost of mental effort. *J Hist Neurosci* **15**, 31-47 (2006).

485. L. Sokoloff, Relation between physiological function and energy metabolism in the central nervous system. *J Neurochem* **29**, 13-26 (1977).

486. M. E. Raichle, The brain's default mode network. *Annu Rev Neurosci* **38**, 433-447 (2015).

487. J. W. Mink, R. J. Blumenschine, D. B. Adams, Ratio of central nervous system to body metabolism in vertebrates: its constancy and functional basis. *Am J Physiol* **241**, R203-212 (1981).

488. Z. Wang *et al.*, Specific metabolic rates of major organs and tissues across adulthood: evaluation by mechanistic model of resting energy expenditure. *Am J Clin Nutr* **92**, 1369-1377 (2010).

489. M. E. Raichle, M. A. Mintun, Brain work and brain imaging. *Annu Rev Neurosci* **29**, 449-476 (2006).

490. R. G. Shulman, F. Hyder, D. L. Rothman, Insights from neuroenergetics into the interpretation of functional neuroimaging: an alternative empirical model for studying the brain's support of behavior. *J Cereb Blood Flow Metab* **34**, 1721-1735 (2014).

491. V. Careau *et al.*, Energy compensation and adiposity in humans. *Curr Biol*, (2021).

492. H. Pontzer *et al.*, Daily energy expenditure through the human life course. *Science* **373**, 808-812 (2021).

493. E. Morava, T. Kozicz, Mitochondria and the economy of stress (mal)adaptation. *Neurosci Biobehav Rev* **37**, 668-680 (2013).

494. C. Thurber *et al.*, Extreme events reveal an alimentary limit on sustained maximal human energy expenditure. *Sci Adv* **5**, eaaw0341 (2019).

495. P. Marchetti, Q. Fovez, N. Germain, R. Khamari, J. Kluza, Mitochondrial spare respiratory capacity: Mechanisms, regulation, and significance in non-transformed and cancer cells. *FASEB J* **34**, 13106-13124 (2020).

496. D. Querstret, M. Cropley, Exploring the relationship between work-related rumination, sleep quality, and work-related fatigue. *J Occup Health Psychol* **17**, 341-353 (2012).

497. J. F. Gillooly, J. H. Brown, G. B. West, V. M. Savage, E. L. Charnov, Effects of size and temperature on metabolic rate. *Science* **293**, 2248-2251 (2001).

498. J. A. Green, The heart rate method for estimating metabolic rate: review and recommendations. *Comp Biochem Physiol A Mol Integr Physiol* **158**, 287-304 (2011).

499. J. Nauman, I. Janszky, L. J. Vatten, U. Wisloff, Temporal changes in resting heart rate and deaths from ischemic heart disease. *JAMA* **306**, 2579-2587 (2011).

500. F. Guo *et al.*, Prospective Study on Energy Expenditure in Patients With Severe Burns. *JPEN J Parenter Enteral Nutr* **45**, 146-151 (2021).

501. S. S. Urlacher *et al.*, Constraint and trade-offs regulate energy expenditure during childhood. *Sci Adv* **5**, eaax1065 (2019).

502. A. Shechter, R. Rising, J. B. Albu, M. P. St-Onge, Experimental sleep curtailment causes wake-dependent increases in 24-h energy expenditure as measured by whole-room indirect calorimetry. *Am J Clin Nutr* **98**, 1433-1439 (2013).

503. S. S. Urlacher *et al.*, Tradeoffs between immune function and childhood growth among Amazonian forager-horticulturalists. *Proc Natl Acad Sci U S A* **115**, E3914-E3921 (2018).

504. G. Sturm *et al.*, OxPhos Dysfunction Causes Hypermetabolism and Reduces Lifespan in Cells and in Patients with Mitochondrial Diseases. *bioRxiv*, 2021.2011.2029.470428 (2021).

505. E. L. Pearce, M. C. Poffenberger, C. H. Chang, R. G. Jones, Fueling immunity: insights into metabolism and lymphocyte function. *Science* **342**, 1242454 (2013).

506. J. J. Iliff *et al.*, A paravascular pathway facilitates CSF flow through the brain parenchyma and the clearance of interstitial solutes, including amyloid beta. *Sci Transl Med* **4**, 147ra111 (2012).

507. D. Brunetti, W. Dykstra, S. Le, A. Zink, A. Prigione, Mitochondria in neurogenesis: Implications for mitochondrial diseases. *Stem Cells* **39**, 1289-1297 (2021).

508. B. Schumacher, J. Pothof, J. Vijg, J. H. J. Hoeijmakers, The central role of DNA damage in the ageing process. *Nature* **592**, 695-703 (2021).

509. F. Abascal *et al.*, Somatic mutation landscapes at single-molecule resolution. *Nature* **593**, 405-410 (2021).

510. L. K. M. Han *et al.*, Accelerating research on biological aging and mental health: Current challenges and future directions. *Psychoneuroendocrinology* **106**, 293-311 (2019).

511. E. Puterman *et al.*, Lifespan adversity and later adulthood telomere length in the nationally representative US Health and Retirement Study. *Proc Natl Acad Sci U S A* **113**, E6335-E6342 (2016).

512. E. Mick *et al.*, Distinct mitochondrial defects trigger the integrated stress response depending on the metabolic state of the cell. *Elife* **9**, (2020).

513. R. Sharma *et al.*, Circulating markers of NADH-reductive stress correlate with mitochondrial disease severity. *J Clin Invest* **131**, (2021).

514. J. K. Kiecolt-Glaser *et al.*, Psychosocial modifiers of immunocompetence in medical students. *Psychosom Med* **46**, 7-14 (1984).

515. J. Walburn, K. Vedhara, M. Hankins, L. Rixon, J. Weinman, Psychological stress and wound healing in humans: a systematic review and meta-analysis. *J Psychosom Res* **67**, 253-271 (2009).

516. J. K. Kiecolt-Glaser, P. T. Marucha, W. B. Malarkey, A. M. Mercado, R. Glaser, Slowing of wound healing by psychological stress. *Lancet* **346**, 1194-1196 (1995).

517. I. R. Kleckner *et al.*, Evidence for a Large-Scale Brain System Supporting Allostasis and Interoception in Humans. *Nat Hum Behav* **1**, (2017).

518. C. Boeck *et al.*, Inflammation in adult women with a history of child maltreatment: The involvement of mitochondrial alterations and oxidative stress. *Mitochondrion* **30**, 197-207 (2016).

519. A. M. Gumpp *et al.*, Childhood maltreatment is associated with changes in mitochondrial bioenergetics in maternal, but not in neonatal immune cells. *Proc Natl Acad Sci U S A* **117**, 24778-24784 (2020).

520. C. Boeck *et al.*, The association between cortisol, oxytocin, and immune cell mitochondrial oxygen consumption in postpartum women with childhood maltreatment. *Psychoneuroendocrinology* **96**, 69-77 (2018).

521. L. E. Gyllenhammer *et al.*, Prospective association between maternal allostatic load during pregnancy and child mitochondrial content and bioenergetic capacity. *Psychoneuroendocrinology* **144**, 105868 (2022).

522. D. Lindqvist *et al.*, Circulating cell-free mitochondrial DNA, but not leukocyte mitochondrial DNA copy number, is elevated in major depressive disorder. *Neuropsychopharmacology* **43**, 1557-1564 (2018).

523. M. Picard, Blood mitochondrial DNA copy number: What are we counting? *Mitochondrion* **60**, 1-11 (2021).

524. S. Rausser *et al.*, Mitochondrial phenotypes in purified human immune cell subtypes and cell mixtures. *Elife* **10**, (2021).

525. J. Brasanac *et al.*, Cellular specificity of mitochondrial and immunometabolic features in major depression. *Mol Psychiatry* **27**, 2370-2371 (2022).

526. P. D. Loprinzi, E. Frith, Protective and therapeutic effects of exercise on stress-induced memory impairment. *J Physiol Sci* **69**, 1-12 (2019).

527. L. M. Redman *et al.*, Metabolic Slowing and Reduced Oxidative Damage with Sustained Caloric Restriction Support the Rate of Living and Oxidative Damage Theories of Aging. *Cell Metab* **27**, 805-815 e804 (2018).

528. J. Schulkin, Social allostasis: anticipatory regulation of the internal milieu. *Front Evol Neurosci* **2**, 111 (2011).

529. P. Sterling, Allostasis: a model of predictive regulation. *Physiol Behav* **106**, 5-15 (2012).

530. N. Snyder-Mackler *et al.*, Social determinants of health and survival in humans and other animals. *Science* **368**, (2020).

531. R. M. Sapolsky, The influence of social hierarchy on primate health. *Science* **308**, 648-652 (2005).

532. D. E. Saxbe, L. Beckes, S. A. Stoycos, J. A. Coan, Social Allostasis and Social Allostatic Load: A New Model for Research in Social Dynamics, Stress, and Health. *Perspect Psychol Sci* **15**, 469-482 (2020).

533. B. M. Culbert, K. M. Gilmour, S. Balshine, Social buffering of stress in a group-living fish. *Proc Biol Sci* **286**, 20191626 (2019).

534. J. P. Mortola, Social interaction and the thermogenic response of chicken hatchlings. *Physiol Behav* **232**, 113317 (2021).

535. K. J. Millidine, N. B. Metcalfe, J. D. Armstrong, Presence of a conspecific causes divergent changes in resting metabolism, depending on its relative size. *Proc Biol Sci* **276**, 3989-3993 (2009).

536. J. A. Hall, A. J. Merolla, Connecting Everyday Talk and Time Alone to Global Well-Being. *Human Communication Research* **46**, 86-111 (2019).

537. J. R. Speakman *et al.*, A standard calculation methodology for human doubly labeled water studies. *Cell Rep Med* **2**, 100203 (2021).

538. E. De Waele, J. Jonckheer, P. E. Wischmeyer, Indirect calorimetry in critical illness: a new standard of care? *Curr Opin Crit Care* **27**, 334-343 (2021).

539. H. Benson, R. F. Steinert, M. M. Greenwood, H. M. Klemchuk, N. H. Peterson, Continuous measurement of O2 consumption and CO2 elimination during a wakeful hypometabolic state. *J Human Stress* **1**, 37-44 (1975).

540. R. K. Wallace, H. Benson, A. F. Wilson, A wakeful hypometabolic physiologic state. *Am J Physiol* **221**, 795-799 (1971).

541. A. Tyagi, M. Cohen, Oxygen Consumption Changes With Yoga Practices: A Systematic Review. *J Eviden Based Compliment Altern Med* **18**, 290-308 (2013).

542. R. S. Lazarus, S. Folkman, *Stress, appraisal, and coping*. (Springer, New York, 1984).

543. S. S. Dickerson, T. L. Gruenewald, M. E. Kemeny, When the social self is threatened: shame, physiology, and health. *J Pers* **72**, 1191-1216 (2004).

544. T. L. Gruenewald, M. E. Kemeny, N. Aziz, J. L. Fahey, Acute threat to the social self: shame, social self-esteem, and cortisol activity. *Psychosom Med* **66**, 915-924 (2004).

545. S. S. Dickerson, P. J. Mycek, F. Zaldivar, Negative social evaluation, but not mere social presence, elicits cortisol responses to a laboratory stressor task. *Health Psychol* **27**, 116-121 (2008).

546. F. Hollis *et al.*, Mitochondrial function in the brain links anxiety with social subordination. *Proc Natl Acad Sci U S A* **112**, 15486-15491 (2015).

547. A. Strasser, L. Xin, R. Gruetter, C. Sandi, Nucleus accumbens neurochemistry in human anxiety: A 7 T (1)H-MRS study. *Eur Neuropsychopharmacol* **29**, 365-375 (2019).

548. M. D. Filiou, C. Sandi, Anxiety and Brain Mitochondria: A Bidirectional Crosstalk. *Trends Neurosci* **42**, 573-588 (2019).

549. I. M. Morella, R. Brambilla, L. More, Emerging roles of brain metabolism in cognitive impairment and neuropsychiatric disorders. *Neurosci Biobehav Rev*, 104892 (2022).

550. D. S. Goldstein, B. McEwen, Allostasis, homeostats, and the nature of stress. *Stress* **5**, 55-58 (2002).

551. T. E. Seeman, B. H. Singer, J. Rowe, R. I. Horwitz, B. McEwen, Price of adaptation - allostatic load and its health consequences. *Arch Intern Med* **157**, 2259-2268 (1997).

552. T. M. Beckie, A systematic review of allostatic load, health, and health disparities. *Biological research for nursing* **14**, 311-346 (2012).

553. P. Kerr, S. Kheloui, M. Rossi, M. Desilets, R. P. Juster, Allostatic load and women's brain health: A systematic review. *Front Neuroendocrinol* **59**, 100858 (2020).

554. P. C. Ng, E. F. Kirkness, Whole genome sequencing. *Methods Mol Biol* **628**, 215-226 (2010).

555. D. Muruzabal, A. Collins, A. Azqueta, The enzyme-modified comet assay: Past, present and future. *Food Chem Toxicol* **147**, 111865 (2021).

556. J. Lin, D. L. Smith, K. Esteves, S. Drury, Telomere length measurement by qPCR - Summary of critical factors and recommendations for assay design. *Psychoneuroendocrinology* **99**, 271-278 (2019).

557. I. Torrecilla *et al.*, Isolation and detection of DNA-protein crosslinks in mammalian cells. *Nucleic Acids Res*, (2023).

558. M. Coradin, K. R. Karch, B. A. Garcia, Monitoring proteolytic processing events by quantitative mass spectrometry. *Expert Rev Proteomics* **14**, 409-418 (2017).

559. L. G. Rezende, T. T. Tasso, P. H. S. Candido, M. S. Baptista, Assessing Photosensitized Membrane Damage: Available Tools and Comprehensive Mechanisms. *Photochem Photobiol* **98**, 572-590 (2022).

560. J. Campisi, J. Vijg, Does damage to DNA and other macromolecules play a role in aging? If so, how? *J Gerontol A Biol Sci Med Sci* **64**, 175-178 (2009).

561. L. A. Esposito, S. Melov, A. Panov, B. A. Cottrell, D. C. Wallace, Mitochondrial disease in mouse results in increased oxidative stress. *Proceedings of the National Academy of Sciences* **96**, 4820-4825 (1999).

562. M. Dittrich, S. Hayashi, K. Schulten, On the mechanism of ATP hydrolysis in F1-ATPase. *Biophys J* **85**, 2253-2266 (2003).

563. F. Scialo, D. J. Fernandez-Ayala, A. Sanz, Role of Mitochondrial Reverse Electron Transport in ROS Signaling: Potential Roles in Health and Disease. *Front Physiol* **8**, 428 (2017).

564. M. P. Murphy *et al.*, Guidelines for measuring reactive oxygen species and oxidative damage in cells and in vivo. *Nature Metabolism* **4**, 651-662 (2022).

565. S. Suzen, H. Gurer-Orhan, L. Saso, Detection of Reactive Oxygen and Nitrogen Species by Electron Paramagnetic Resonance (EPR) Technique. *Molecules* **22**, (2017).

566. M. Oparka *et al.*, Quantifying ROS levels using CM-H(2)DCFDA and HyPer. *Methods* **109**, 3-11 (2016).

567. M. N. Hoehne *et al.*, Spatial and temporal control of mitochondrial H(2) O(2) release in intact human cells. *EMBO J* **41**, e109169 (2022).

568. V. V. Pak *et al.*, Ultrasensitive Genetically Encoded Indicator for Hydrogen Peroxide Identifies Roles for the Oxidant in Cell Migration and Mitochondrial Function. *Cell Metabolism* **31**, 642-653.e646 (2020).

569. B. Halliwell, A. Adhikary, M. Dingfelder, M. Dizdaroglu, Hydroxyl radical is a significant player in oxidative DNA damage in vivo. *Chem Soc Rev* **50**, 8355-8360 (2021).

570. J. S. Chang *et al.*, Ultra performance liquid chromatography-tandem mass spectrometry assay for the quantification of RNA and DNA methylation. *J Pharm Biomed Anal* **197**, 113969 (2021).

571. C. L. Hawkins, M. J. Davies, Detection, identification, and quantification of oxidative protein modifications. *J Biol Chem* **294**, 19683-19708 (2019).

572. H. Esterbauer, R. J. Schaur, H. Zollner, Chemistry and biochemistry of 4-hydroxynonenal, malonaldehyde and related aldehydes. *Free Radic Biol Med* **11**, 81-128 (1991).

573. G. L. Milne, E. S. Musiek, J. D. Morrow, F2-isoprostanes as markers of oxidative stress in vivo: an overview. *Biomarkers* **10 Suppl 1**, S10-23 (2005).

574. H. J. Shields, A. Traa, J. M. Van Raamsdonk, Beneficial and Detrimental Effects of Reactive Oxygen Species on Lifespan: A Comprehensive Review of Comparative and Experimental Studies. *Front Cell Dev Biol* **9**, 628157 (2021).

575. C. Borza *et al.*, in *Lipid Metabolism*. (InTech, 2013).

576. M. J. Birket *et al.*, A reduction in ATP demand and mitochondrial activity with neural differentiation of human embryonic stem cells. *J Cell Sci* **124**, 348-358 (2011).

577. A. Silvestrini, E. Meucci, B. M. Ricerca, A. Mancini, Total Antioxidant Capacity: Biochemical Aspects and Clinical Significance. *Int J Mol Sci* **24**, (2023).

578. Z. Haida, M. Hakiman, A comprehensive review on the determination of enzymatic assay and nonenzymatic antioxidant activities. *Food Sci Nutr* **7**, 1555-1563 (2019).

579. M. Katerji, M. Filippova, P. Duerksen-Hughes, Approaches and Methods to Measure Oxidative Stress in Clinical Samples: Research Applications in the Cancer Field. *Oxid Med Cell Longev* **2019**, 1279250 (2019).

580. A. Azqueta *et al.*, DNA repair as a human biomonitoring tool: Comet assay approaches. *Mutat Res Rev Mutat Res* **781**, 71-87 (2019).

581. N. A. Owiti, Z. D. Nagel, B. P. Engelward, Fluorescence Sheds Light on DNA Damage, DNA Repair, and Mutations. *Trends Cancer* **7**, 240-248 (2021).

582. M. Elgendy, Assessment of Modulation of Protein Stability Using Pulse-chase Method. *Bio Protoc* **7**, e2443 (2017).

583. N. Hristozova, P. Tompa, D. Kovacs, A Novel Method for Assessing the Chaperone Activity of Proteins. *PLoS One* **11**, e0161970 (2016).

584. T. Sato, K. Sako, J. Yamaguchi, Assay for proteasome-dependent protein degradation and ubiquitinated proteins. *Methods Mol Biol* **1072**, 655-663 (2014).

585. A. T. Melvin, G. S. Woss, J. H. Park, M. L. Waters, N. L. Allbritton, Measuring activity in the ubiquitin-proteasome system: from large scale discoveries to single cells analysis. *Cell Biochem Biophys* **67**, 75-89 (2013).

586. A. D. Blazek, B. J. Paleo, N. Weisleder, Plasma Membrane Repair: A Central Process for Maintaining Cellular Homeostasis. *Physiology (Bethesda)* **30**, 438-448 (2015).

587. C. A. Elverson, M. E. Wilson, Cortisol: Circadian Rhythm and Response to a Stressor. *Newborn and Infant Nursing Reviews* **5**, 159-169 (2005).

588. S. Ranabir, K. Reetu, Stress and hormones. *Indian J Endocrinol Metab* **15**, 18-22 (2011).